

**Faculty of Science and Engineering**  
**Department of Chemical Engineering**

**Application of Nanotechnology in Chemical Enhanced Oil Recovery and  
Carbon Storage**

**Sarmad Foad Jaber Al-Anssari**

**This thesis is presented for the Degree of  
Doctor of Philosophy  
of  
Curtin University**

**June 2018**

## DECLARATION OF ACADEMIC INTEGRITY

To the best of my knowledge and belief this thesis contains no material previously published by any other person except where due acknowledgment has been made. This thesis contains no material which has been accepted for the award of any other degree or diploma in any university.

A handwritten signature in black ink, consisting of several overlapping strokes. The signature is written on a yellow rectangular background. The name 'Sarmad Al-Anssari' is written in small letters below the main signature.

Signature: \_\_\_\_\_ (Sarmad Al-Anssari)

Date: \_\_\_\_\_ 22/06/2018 \_\_\_\_\_

## **COPYRIGHT**

I warrant that I have obtained, where necessary, permission from copyright owners to use any third-party copyright material reproduced in the thesis, or to use any of my own published work (e.g. journal articles) in which the copyright is held by another party (e.g. publisher, co-author).

A handwritten signature on a yellow sticky note. The signature consists of a stylized, cursive script. Above the main line of the signature, the letters 'S S S' are written. Below the main line, the name 'Sarmad Al-Anssari' is written in a smaller, more legible font.

Signature: \_\_\_\_\_ (Sarmad Al-Anssari)

Date: \_\_\_\_\_ 22/06/2018 \_\_\_\_\_

## **DEDICATION**

I would like to dedicate my thesis to all honourable and poor Iraqi people who are source of my motivation

To soul of my mother who passed away during my studying overseas

To my father for his enormous love and support

To soul of my in-law who passed away during my studying overseas

To my family, Rashaa, Deyar, and Raya for shearing years of alienation difficulties.

To the department of chemical engineering, college of engineering, university of Baghdad.

To them who suffering in life, but every time stood strong and altered every challenge into a strength.

## ACKNOWLEDGMENT

I would like to express my most deep gratitude to my principle supervisor, Prof Stefan Iglauer. Stefan is the most rigorous and learned scholar I have ever dealt with. He is so humble and modest and is always ready to stop his work in hand for discussion with me on my results and confusions. He supervised me how to structure and format the manuscript, and address the reviews' critical comments during my PhD study without reservation. I would not have these publications if here were no his continuous inputs to my manuscripts. The meetings with Stefan have motivated me to create many new ideas. Prof Iglauer's great guidance and passion for research have been and will be profoundly influencing my whole life.

I am grateful to my co-supervisor, Dr Ahmed Barifcani, for his encouragement and support to pursue my PhD degree. He led me to and has guided me adventuring in the fantastic world full of academic and scientific unknowns.

Equally, I owe my enthusiastic gratitude to my co-supervisor, Prof Shaobin Wang for his encouragement and support. Prof Wang who supervised me how to design the experiment and solve many of research problems.

I am thankful to Prof Maxim Lebedev for providing the excellent atomic force microscopy (AFM) measurement to support my results for the insightful mechanistic studies.

A sincere vote of thanks also is devoted to Prof Moses Tade, the chairperson of this research. Moses was the person who initiates this fruitful collaboration between chemical engineering and petroleum engineering departments to implement this study.

I would like to acknowledge petroleum engineering department at Curtin University, not only for hosting the experimental part of the study through providing all the required materials, devices, and room but also for showing the best kind of hospitality for a Ph.D. student from the chemical engineering department.

I want to appreciate Bob Webb, the Technical Officer, for the fruitful discussions and for his company in numerous nights and weekends. Bob provided me with help in all aspects of my study. Without his precious support, it would be impossible to conduct this research. Thank you progressive friend for everything.

I want to appreciate Muhammad Arif, my trusted friend, who always shearing his thoughts and new ideas with me. I also want to thank my colleague Lezorgia Nwidee, my supportive friend, who is always there to help me go through my hard time overseas.

I am also thankful to my friends and colleagues who showed me the real meaning of diversity. Thank you, I cannot imagine the life without you.

Last, but not least, I would like to express my deepest love to my family, Father, Rasha, Deyar and Raya. I truly thank you for your unconditional love and supports. I cannot go so far without your constant and eternal encouragement. The faith to make you be proud has guided me to go through such changeling and depressing time. I love you all dearly.

## ABSTRACT

Nanotechnology is rapidly gaining increased importance in all fields of science and industry. This includes nanofluids (i.e. nanoparticles dispersed in a base-fluid), which have remarkable potential in a broad range of applications, including pharmaceutical, medical, water treatment, soil decontamination, geothermal extraction, carbon capture and storage, and enhanced oil recovery (EOR). EOR, the focus of this work, augments oil recovery after conventional recovery methods have been exhausted. However, successful implementation of EOR techniques require understanding of the underlying controlling mechanisms that affect the distribution and displacement of the fluids in the porous rocks, including the rock's wettability. Wettability is typically quantified via contact angle measurements, which effectively measure the affinity of the mineral surface to water or oil. Thus, treatments of oil-wet surfaces, which cannot produce substantial amounts of oil mainly due to the limited spontaneous imbibition of water, with nanoparticles can potentially enhance the displacement of oil from the porous medium. Despite these excellent prospects, it is not known whether nanoparticles can work efficiently at reservoirs conditions (i.e. at high-pressure, temperature and salinity).

Thus, in this study the ability of nanoparticles to alter the wettability of oil-wet surfaces towards water-wet at reservoir conditions was systematically examined using several nano-silica dispersions (e.g. silica nanoparticles dispersed in DI-water, brine, surfactant, or brine-surfactant formulations). Sodium dodecylsulfate (SDS) and Hexadecyltrimethylammonium Bromide (CTAB) were used as anionic and cationic surfactant, respectively. Furthermore, a critical analysis of interfacial tension (IFT), wettability, nanoparticles adsorption, and nanofluid stability was performed to optimize nanofluids for EOR and carbon storage applications.

Moreover, the synergistic effect of nanoparticle-surfactant combinations on nanofluid interfacial properties and nanofluid stability were mechanistically demonstrated. Clearly, a significant surface modification was achieved via nano-treatment. Thus, this study not only presents novel nanofluid formulations for wettability alteration purposes but also introduced the first insight into nanoparticle-surfactant interactions in saline environments. In summary, this study significantly improves the understanding of subsurface nanotechnology applications, thus leading to better energy security and a cleaner environment.

## PUBLICATIONS BY THE AUTHOR

### Published Papers forming part of thesis:

1. **Al-Anssari, Sarmad**, Ahmed Barifcani, Shaobin Wang, Maxim Lebedev, and Stefan Iglauer. 2016. "Wettability alteration of oil-wet carbonate by silica nanofluid." *Journal of Colloid and Interface Science* 461:435-442. doi: <http://dx.doi.org/10.1016/j.jcis.2015.09.051>. (Cited by 8)
2. **Al-Anssari, Sarmad**, Shaobin Wang, Ahmed Barifcani, and Stefan Iglauer. 2017. "Oil-water interfacial tensions of silica nanoparticle-surfactant formulations." *Tenside Surfactants Detergents* 54 (4):334-341. doi: <https://doi.org/10.3139/113.110511>. (Cited by 64)
3. **Al-Anssari, Sarmad**, Shaobin Wang, Ahmed Barifcani, Maxim Lebedev, and Stefan Iglauer. 2017. "Effect of temperature and SiO<sub>2</sub> nanoparticle size on wettability alteration of oil-wet calcite." *Fuel* 206:34-42. doi: 10.1016/j.fuel.2017.05.077. (Cited by 9)
4. **Al-Anssari, Sarmad**, Muhammad Arif, Shaobin Wang, Ahmed Barifcani, Maxim Lebedev, and Stefan Iglauer. 2017. "CO<sub>2</sub> geo-storage capacity enhancement via nanofluid priming." *International Journal of Greenhouse Gas Control* 63:20-25. doi: 10.1016/j.ijggc.2017.04.015. (Cited by 6)
5. **Al-Anssari, Sarmad**, Muhammad Arif, Shaobin Wang, Ahmed Barifcani, and Stefan Iglauer. 2017. "Stabilising nanofluids in saline environments." *Journal of Colloid and Interface Science* 508:222-229. doi: 10.1016/j.jcis.2017.08.043. (Cited by 2)
6. **Al-Anssari, Sarmad**, Muhammad Arif, Shaobin Wang, Ahmed Barifcani, Lebedev Maxim, and Stefan Iglauer. 2018. "Wettability of nanofluid-modified oil-wet calcite at reservoir conditions." *Fuel* 211:405-414. doi: <https://doi.org/10.1016/j.fuel.2017.08.111>. (Cited by 4)

### Published Papers not forming part of thesis:

7. **Al-Anssari, Sarmad**, Muhammad Arif, Shaobin Wang, Ahmed Barifcani, Maxim Lebedev, and Stefan Iglauer. 2017. "Wettability of nano-treated calcite/CO<sub>2</sub>/brine systems: Implication for enhanced CO<sub>2</sub> storage potential." *International Journal of Greenhouse Gas Control* 66:97-105. doi: <https://doi.org/10.1016/j.ijggc.2017.09.008>. (Cited by 1)

8. Nwideo, Lezorgia N., **Sarmad Al-Anssari**, Ahmed Barifcani, Mohammad Sarmadivaleh, Maxim Lebedev, and Stefan Iglauer. 2017. "Nanoparticles influence on wetting behaviour of fractured limestone formation." *Journal of Petroleum Science and Engineering* 149:782-788. doi: <http://dx.doi.org/10.1016/j.petrol.2016.11.017>. (Cited by 14)

Conference papers:

1. **Al-Anssari, Sarmad**, Haider Abbas Shanshool, Shaobin Wang, Ahmed Barifcani, and Stefan Iglauer. 2017. "Oil-water interfacial tensions and critical micelles concentration of anionic surfactant-silica nanoparticle formulations." *7<sup>th</sup> Scientific Engineering and the 1<sup>st</sup> international conference-IEEE-Iraqi section*, Baghdad-Iraq.
2. **Sarmad Al-Anssari**, Lezorgia. N. Nwideo, Muhammad Ali, Jitendra S. Sangwai, Shaobin Wang, Ahmed Barifcani, and Stefan Iglauer. 2017. "Retention of Silica Nanoparticles in Limestone Porous Media." *SPE/IATMI Asia Pacific Oil & Gas Conference and Exhibition*, Bali, Indonesia, 17-19 October 2017. (Cited by 1)
3. **Sarmad Al-Anssari**, Lezorgia. N. Nwideo, Muhammad Arif, Shaobin Wang, Ahmed Barifcani, Maxim Lebedev, and Stefan Iglauer. 2017. "Wettability alteration of carbonate rocks via nanoparticle-anionic surfactant flooding at reservoirs conditions." *SPE Symposium: Production Enhancement and Cost Optimisation*, Kuala Lumpur, Malaysia, 7-8 November 2017.
4. **Sarmad Al-Anssari**, Shaobin Wang, Lezorgia. N. Nwideo, Ahmed Barifcani, and Stefan Iglauer. "Synergistic Effects of Cationic Surfactant and Silica Nanoparticles on Hydrocarbon Production from Carbonate Reservoirs" *The First MoHESR and HCED Iraqi Scholars Conference in Australasia*, Melbourne, Australia, 5-6 December 2017.
5. **Sarmad Al-Anssari**, Shaobin Wang, Ahmed Barifcani, and Stefan Iglauer. "Physiochemical Properties of Nanoparticle-surfactant Formulation at Harsh Salinity" *One Curtin International Postgraduate Conference (OCPC) 2017* Miri, Sarawak, Malaysia, December 10 – 12, 2017
6. Nwideo, Lezorgia N., **Sarmad Al-Anssari**, Ahmed Barifcani, Mohammad Sarmadivaleh, and Stefan Iglauer. 2016. "Nanofluids for Enhanced Oil Recovery Processes: Wettability Alteration Using Zirconium Oxide." *Offshore Technology Conference Asia*, Kuala Lumpur, Malaysia, 2016/3/22/. (Cited by 11)

Refereed conference presentations:

1. **Al-Anssari, Sarmad**, Shaobin Wang, Lezorgia. N. Nwideo, Ahmed Barifcani, Stefan Iglauer. "Nano-modification of oil-wet calcite at reservoirs conditions." *7<sup>th</sup> International Colloids Conference*, Sitges, Barcelona, Spain 18-21 June 2017.
2. **Al-Anssari, Sarmad**, Shaobin Wang, Ahmed Barifcani, Stefan Iglauer. "Effect of salt and nanoparticle concentration on the stability and agglomeration of silica nanoparticles Suspensions" *7<sup>th</sup> International Colloids Conference*, Sitges, Barcelona, Spain 18-21 June 2017.

## TABLE OF CONTENTS

DECLARATION OF ACADEMIC INTEGRITY.....	I
COPYRIGHT.....	II
DEDICATION.....	III
ACKNOWLEDGMENT.....	IV
ABSTRACT.....	VI
PUBLICATIONS BY THE AUTHOR.....	VII
TABLE OF CONTENTS.....	X
LIST OF FIGURES.....	XVI
LIST OF TABLES.....	XXI
Chapter 1 Introduction and Overview of Thesis Objectives.....	1
1.1 Background.....	1
1.2 Nanomaterial Applications in the Oil Industry.....	2
1.3 Characteristics of Nanoparticles.....	4
1.4 Motivation and Objectives of Thesis.....	5
1.5 Significance of the study.....	5
1.6 Scope of the study.....	6
1.7 Thesis organisation.....	6
Chapter 2 Literature Review.....	9
2.1 Introduction.....	9
2.2 Characterisation of Oil Reservoirs.....	12
2.2.1 Wettability.....	12
2.2.2 Wettability Measurements.....	14
2.2.3 Interfacial Tension (IFT).....	21
2.2.4 Permeability.....	22
2.2.5 Capillary and Gravitational Forces.....	23
2.3 Enhanced Oil Recovery (EOR).....	26
2.3.1 Thermal Methods.....	29
2.3.2 Gas Injection.....	29
2.3.3 Chemical Methods.....	29

2.4	Wettability Alteration .....	30
2.4.1	Interaction of Hydrocarbon/Aqueous Phase/Rock in Oil Reservoirs ..	31
2.4.2	Mechanisms of Wettability Alteration.....	32
2.4.3	Wettability Alteration by Chemical Methods .....	33
2.5	Nanoparticles: Synthesis, Types, Applications and Challenges.....	38
2.5.1	Nanoparticle Synthesis.....	38
2.5.2	Nanoparticle Types.....	38
2.5.3	Nanofluid formulation .....	40
2.5.4	Applications of Nanofluids .....	40
2.5.5	Nanoparticle and Nanofluid Applications in Chemical Enhanced Oil Recovery .....	44
2.5.6	Efficiency of Wettability Alteration by Nanofluids .....	44
2.5.7	Interfacial Tension Reduction by Nanoparticles .....	48
2.5.8	Effect of Nano-treatment on Oil-water Relative Permeability.....	49
2.5.9	Nano-treatments at High Temperatures .....	49
2.5.10	Nano-treatment at High Pressures .....	51
2.5.11	Stability of Nanofluids .....	51
2.5.12	Opportunities and Challenges .....	54
2.6	Conclusions .....	55
Chapter 3	Experimental Methodology.....	57
3.1	Research Strategy and Justifications.....	57
3.2	Experimental Task Assessment .....	58
3.3	Materials.....	58
3.3.1	Silicon Dioxide Nanoparticles.....	58
3.3.2	DI-water and Brines.....	59
3.3.3	Surfactants.....	59
3.3.4	Calcite samples.....	60
3.3.5	Decane.....	61
3.3.6	Oil-wet surface modification agents .....	62
3.3.7	Nitrogen Gas (N <sub>2</sub> ).....	63
3.3.8	Carbone dioxide Gas (CO <sub>2</sub> ) .....	64
3.3.9	Cleaning agents .....	64
3.4	Instruments and measurement devices.....	64

3.4.1	Ultrasonic homogeniser .....	64
3.4.2	Magnetic stirrer .....	65
3.4.3	Electronic balance.....	66
3.4.4	Plasma.....	67
3.4.5	Vacuum Drying Oven (VDO).....	67
3.4.6	High-P/T goniometric setup.....	68
3.4.7	Conductivity meter .....	72
3.4.8	pH meter.....	72
3.4.9	Scanning Electron Microscopy (SEM) .....	73
3.4.10	Energy Dispersive X-ray Spectroscopy (EDS) .....	73
3.4.11	Atomic Force Microscope (AFM).....	73
3.4.12	Dynamic light scattering .....	73
3.4.13	Zetasizer (ZS).....	73
3.5	Fluid formulations .....	74
3.5.1	Pre-equilibration of DI-water with calcite .....	74
3.5.2	Brine formation .....	74
3.5.3	Nanoparticle dispersion (silica nanofluid) .....	75
3.5.4	Surfactant formulations.....	75
3.5.5	Nanoparticle-surfactant suspensions .....	75
3.6	Calcite surface preparation.....	75
3.7	Modification of pure calcite to an oil-wet state.....	76
3.7.1	Surface modification with stearic acid.....	76
3.7.2	Surface modification with silanes (silanisation) .....	77
3.8	Nano-treatment of Oil-wet Calcite with Different Nanofluids .....	78
3.8.1	Nano-treatment at ambient conditions .....	78
3.8.2	Nano-treatment under reservoir conditions (high P and T) .....	78
Chapter 4 Oil-Water Interfacial Tensions of Silica Nanoparticle-Surfactant Formulations* .....		79
4.1	Introduction .....	79
4.2	Experimental Methodology.....	81
4.2.1	Materials.....	81
4.2.2	Nanofluid preparation .....	81
4.2.3	Critical micelle concentration (CMC) measurements .....	82

4.2.4	Interfacial tension measurements .....	82
4.3	Results and Discussion .....	83
4.3.1	Critical micelle concentration and the effect of nanoparticles .....	83
4.3.2	Synergistic effect of nanoparticles and NaCl on CMC of SDS .....	84
4.3.3	Nanofluid-oil interfacial tensions .....	85
4.3.4	Dynamic interfacial tension measurements .....	86
4.3.5	Interfacial tensions of decane/ SDS-nanofluid systems.....	87
4.3.6	Interfacial tensions of decane/CTAB-nanofluid systems .....	89
4.3.7	Interfacial tensions of decane-SDS-nanofluid-salt formulations .....	90
4.3.8	Effect of temperature on $\gamma$ .....	91
4.4	Conclusions .....	92
Chapter 5	Wettability alteration of oil-wet carbonate by silica nanofluid.....	93
5.1	Introduction .....	93
5.2	Experimental Methodology.....	95
5.2.1	Materials.....	95
5.2.2	Calcite surface preparation.....	96
5.2.3	Nanofluid Preparation.....	98
5.2.4	Surface modification with nanofluid (Nano-modification) and Contact angle measurements .....	99
5.3	Results and discussion .....	99
5.3.1	SEM-EDS and AFM analysis .....	100
5.3.2	Effect of exposure time on contact angle.....	102
5.3.3	Adsorption characteristics: reversible versus irreversible adsorption	103
5.3.4	Effect of electrolyte concentration on contact angle .....	104
5.3.5	Effect of nanoparticle concentration in nanofluid .....	106
5.3.6	Nanofluid-rock re-equilibration processes.....	106
5.4	Conclusions .....	107
Chapter 6	Effect of temperature and SiO <sub>2</sub> nanoparticle size on wettability alteration of oil-wet calcite.....	109
6.1	Introduction .....	109
6.2	Experimental Methodology.....	111
6.2.1	Materials.....	111
6.2.2	Calcite surface preparation.....	112

6.2.3	Contact angle measurements .....	112
6.2.4	Calcite modification with stearic acid .....	112
6.2.5	Nanofluid preparation .....	114
6.2.6	Zeta potential measurements and stability of nanofluids.....	114
6.2.7	Calcite wettability modification with silica nanofluid (nano- modification) .....	114
6.3	Results and discussions.....	115
6.3.1	Zeta potential of nanofluids .....	115
6.3.2	SEM-EDS and AFM analysis .....	117
6.3.3	Effect of particles size on wettability alteration.....	121
6.3.4	Effect of temperature on contact angle .....	122
6.4	Conclusions .....	125
Chapter 7	Wettability of nanofluid-modified oil-wet calcite at reservoir conditions	126
7.1	Introduction .....	126
7.2	Materials and Experimental methodology .....	128
7.2.1	Materials.....	129
7.2.2	Equilibration between calcite and brine.....	129
7.2.3	Calcite surface preparations .....	130
7.2.4	Nanofluid preparations.....	131
7.2.5	Nanofluid stability and phase behaviour.....	131
7.2.6	Nano-modification of oil-wet calcite surface at high pressure and temperature.....	132
7.2.7	Contact angle measurements.....	132
7.3	Results and discussion .....	133
7.3.1	Effect of salinity on nanofluids stability .....	134
7.3.2	AFM and SEM analyses .....	135
7.3.3	Adsorption characteristics: reversible versus irreversible adsorption	136
7.3.4	Effect of nanoparticle (Np) concentration on the wettability.....	138
7.3.5	Effect of brine salinity on wettability of nano-modified surfaces.....	139
7.3.6	Effect of exposure time on wettability alteration .....	141
7.4	Implications.....	143
7.5	Conclusions .....	144
Chapter 8	CO <sub>2</sub> geo-storage capacity enhancement via nanofluid priming .....	145

8.1	Introduction .....	145
8.2	Experimental methodology .....	145
8.2.1	Materials.....	145
8.2.2	Contact angle measurements .....	148
8.3	Results and Discussion .....	149
8.3.1	Effect of nanoparticle-treatment on wettability as a function of pressure 149	
8.3.2	Effect of temperature and salinity .....	151
8.4	Implications.....	152
8.5	Conclusions .....	153
Chapter 9	Stabilising nanofluids in saline environments.....	154
9.1	Introduction .....	154
9.2	Experimental methodology .....	155
9.2.1	Materials.....	155
9.2.2	Nanofluid formulation .....	156
9.2.3	Particle size, zeta potential and SEM measurements.....	156
9.3	Result and discussion.....	157
9.3.1	Characterization of SiO <sub>2</sub> nanoparticles.....	157
9.3.2	Zeta potential as a function of salinity .....	159
9.3.3	Surface activation of SiO <sub>2</sub> NPs by cationic surfactant .....	160
9.3.4	Interaction between NPs surface and cationic surfactant .....	161
9.3.5	Surface activation of SiO <sub>2</sub> NPs by anionic surfactant.....	162
9.3.6	Interaction between NPs surface and anionic surfactant .....	163
9.3.7	Zeta potential of SDS surfactant-brine-NPs formulation.....	164
9.3.8	Particle size distribution of surface treated NPs.....	165
9.4	Conclusions .....	166
Chapter 10	Overall Discussion.....	168
Chapter 11	Conclusions, Recommendations and Perspectives for Future Work.	173
11.1	Conclusions .....	173
11.2	Recommendations and Outlook for Future Work .....	177
	<b>References</b> .....	179
	<b>APPENDIX A</b> .....	217

## LIST OF FIGURES

Figure 1-1 Layout of thesis objectives and structure.....	8
Figure 2-1 Schematic of brine droplet on a tilted surface with $\theta_a$ and $\theta_r$ indicated (left); image of water drop on calcite surface (right).....	15
Figure 2-2 The actual contact angle ( $\theta_{\text{actual}}$ ) and the apparent contact angle ( $\theta_{\text{apparent}}$ ) on a rough surface (redrawn from Marmur (2006)). .....	16
Figure 2-3 Schematic representation of the electrical double layer existing at the interface between the rock matrix and pore water (from Al Mahrouqi et al. (2017)). .....	18
Figure 2-4 Spontaneous imbibition of water from a fracture system into the matrix where it replaces oil .....	20
Figure 2-5 A typical relative permeability curve for two-phase flow of an oil-water system. The relative permeability of water is zero at the residual water saturation ( $S_{wr}$ ) and increases until it reaches the residual oil saturation $S_{or}$ , at which point water is the only flowing phase referring to the endpoint relative permeability ( $krw_o$ ). Similarly, the relative permeability of oil is zero at $S_{or}$ and increases to $S_{wr}$ to reach the endpoint relative oil permeability ( $kro_o$ ). .....	23
Figure 2-6 Classification of enhanced oil recovery methods (reproduced after Thomas (2008)) .....	28
Figure 2-7 Potential scenarios after low salinity waterflooding: (left) release of oil droplet from clay particles anchored on the solid surface; (right) total detachment of clay particles attached to oil droplets. ....	34
Figure 2-8 Proposed impact of hydrophilic silica nanoparticles on an initially water-wet surface (from Nikolov et al. (2010)). .....	46
Figure 2-9 Proposed impact of hydrophilic silica nanoparticles on an initially oil-wet surface .....	46
Figure 2-10 Molecular structure of sodium dodecylsulfate (SDS). .....	53
Figure 2-11 Molecular structure of hexadecyltrimethylammonium bromide (CTAB) .....	53
Figure 3-1: Flow chart of the qualitative data process.....	57
Figure 3-2 Structural formula of sodium dodecylsulfate (SDS) .....	59
Figure 3-3 Structural formula of hexadecyltrimethylammonium bromide (CTAB) .	60
Figure 3-4 Optical image of calcite .....	61
Figure 3-5 Chemical structure of silane groups .....	62
Figure 3-6 Structural formula of stearic acid .....	63
Figure 3-7 Photograph of ultrasonic homogeniser (Model 300 VT Ultrasonic Homogenizer, Biologics). .....	65
Figure 3-8 Magnetic stirrer (Across International). .....	66
Figure 3-9 Photograph of electronic balance (Model BTA-623, 0.001 g, Phoenix Instruments) .....	66
Figure 3-10 Photograph of plasma unit (Model Yocto, Diener plasma) .....	67
Figure 3-11 Photograph of the vacuum drying system that included an oven (Model VO-16020) and a vacuum pump (Model TW-1A), both made by Across International. ....	68
Figure 3-12 Photograph of the high pressure/temperature setup.....	68

Figure 3-13 Photograph of the high P/T optical cell .....	69
Figure 3-14 Photograph of the high precision syringe pumps .....	70
Figure 3-15 Snapshot of Fiji Image J protocols used to measure interfacial tension (upper image) and contact angles (lower image).....	71
Figure 3-16 Photograph of the RS 180-7127 conductivity meter .....	72
Figure 3-17 Photograph of Rosemount 56 pH meter with two sensors and high-pressure reactor.....	72
Figure 3-18 Photograph of Zetasizer (Nano ZS, Malvern Instrument). .....	74
Figure 3-19 Surface dissociation and adsorption of stearic acid on a calcite surface with the potential structure of the adsorbed layer (after Mihajlovic et al. (2009)). ....	77
Figure 3-20 Experimental configuration for high pressure, high temperature nano-treatment: (1) syringe pump (liquids), (2) valve, (3) heating tape, (4) thermocouple, (5) high pressure-temperature vessel, (6) calcite substrate, (7) sample holders, (8) pressure relief and drainage valve, (9) collector, (10), stand, (11) nanofluid and flushing liquids feed system, (12) syringe pump, (13) CO <sub>2</sub> source for pressure increase.....	78
Figure 4-1 Effect of silica nanoparticle concentration on CMC values of aqueous CTAB and SDS suspensions at (23 °C and 10 <sup>5</sup> Pa in DI water). .....	84
Figure 4-2 Critical micelle concentrations of SDS as a function of nanoparticle (SiO <sub>2</sub> ) and NaCl concentration (measured at 23 °C and 10 <sup>5</sup> Pa).....	85
Figure 4-3 $\gamma$ of nanofluid (without a surfactant) against air and decane as a function of nanoparticle concentration at 23 °C.....	86
Figure 4-4 Dynamic interfacial tensions measured for different aqueous phases/decane systems (ambient conditions, 23 °C). .....	87
Figure 4-5 Interfacial tension of decane-SDS-SiO <sub>2</sub> nanoparticle-DI water formulations as a function of nanoparticle and surfactant concentrations, measured at 23 °C and 10 <sup>5</sup> Pa. ....	88
Figure 4-6 Interfacial tension of decane-CTAB-nanoparticle-DI water formulations as a function of SiO <sub>2</sub> nanoparticle and surfactant concentration (fraction of CMC), values measured at 23 °C and 10 <sup>5</sup> Pa.....	89
Figure 4-7 Interfacial tensions of decane-SDS-water-NaCl-SiO <sub>2</sub> nanoparticle formulations (0.5 CMC SDS, measured at 23 °C and 10 <sup>5</sup> Pa). .....	90
Figure 4-8 Interfacial tension as a function of temperature for various aqueous systems against decane; A-1wt% NaCl brine, B- DI water, C- 0.5wt% SiO <sub>2</sub> dispersion, D- 0.5 wt% SiO <sub>2</sub> in 1 wt% NaCl dispersion, E- 0.5cmc of SDS solution, F- 0.5cmc of SDS in 0.5 wt% SiO <sub>2</sub> dispersion, G- 0.5cmc SDS and 0.5 wt% SiO <sub>2</sub> in 1 wt% NaCl dispersion. ....	91
Figure 5-1 silylation of calcite surface (Wolthers et al. 2012) (after London et al. (2013)). .....	97
Figure 5-2 densities of various nanofluids used. ....	98
Figure 5-3 SEM images of an oil-wet calcite surface: a) before; b) after nanofluid treatment (4wt% SiO <sub>2</sub> in 5wt% NaCl brine, 1 hour exposure time); c) high resolution; and d) maximum resolution zoom-into the irreversibly adsorbed silica nanoparticles.....	101
Figure 5-4 Atomic force microscopy images of a calcite surface used in the experiments before (upper image) and after (lower image) nano-modification. The	

RMS surface roughness before nano-modification was 32 nm, which is very smooth. After nanofluid treatment (0.5wt% SiO<sub>2</sub> in 10wt% NaCl brine for 4 hr) the RMS surface roughness increased to 1300 nm. Different colours refer to variations in height (black: 0nm, white: peak height = 640nm [upper image], 1300 nm [lower image]).

Figure 5-5 Water contact angles on oil-wet calcite surface in air and n-decane as a function of exposure time to nanofluid (2wt% SiO<sub>2</sub>, 5wt% NaCl brine).

Figure 5-6 Water contact angles on: 1) oil-wet calcite surface in air and n-decane; 2) after nano-modification (2wt% SiO<sub>2</sub>, 20wt% NaCl brine, 1 hour exposure time); 3) DI water; 4) acetone; 5) 2nd acetone and water rinse.

Figure 5-7 Water contact angles on nano-modified calcite surface in air and n-decane as a function of brine salinity (2wt% SiO<sub>2</sub>, 1 hour exposure time).

Figure 5-8 Water contact angles on nano-modified calcite surface in air and n-decane as a function of SiO<sub>2</sub> concentration in the nanofluid (10 wt % NaCl, 1 hour exposure time).

Figure 5-9 Differences in water contact angle between fresh and used nanofluid (0.5wt % SiO<sub>2</sub>, 20 wt% NaCl, and 1 hour exposure time): 1)  $\theta_a$  in air, 2)  $\theta_r$  in air, 3)  $\theta_a$  in n-decane, 4)  $\theta_r$  in n-decane.

Figure 6-1 Zeta potentials of various SiO<sub>2</sub> nanofluids (0.2 wt% SiO<sub>2</sub> in different brine) at varying pH and 23 °C.

Figure 6-2 Zeta potential of various nanofluids with different particle loading (0.05, 0.1, 0.15, 0.2, 0.4 and 0.5 wt% SiO<sub>2</sub> in DI water) at varying pH and 23 °C.

Figure 6-3 SEM images of an oil-wet calcite surface: (A) before, (B) after nanofluid treatment (0.2 wt% SiO<sub>2</sub> in 1 wt% NaCl brine) at 23 °C; (C and D) effect of temperature increase on surface morphology; (E and F) maximum resolution zoom-into the irreversibly adsorbed silica agglomerates at 23° (left) and 50 °C (right), respectively.

Figure 6-4 Atomic force microscopy images of a calcite surface used in the experiment before (A) and after nano-treatment at two different temperatures: 23 °C (B) and 60 °C (C).

Figure 6-5 Water advancing contact angle on oil-wet calcite surface in n-decane as a function of exposure time to nanofluid (0.2wt % SiO<sub>2</sub>, 1wt % NaCl brine), temperature (23 and 50°C), and nanoparticle size (5 nm and 25 nm).

Figure 6-6 Advancing water contact angle on oil-wet calcite surface in n-decane after modification with nanofluid for 2 h (0.2wt% SiO<sub>2</sub>, 1wt% NaCl brine) as a function of measurement temperature. (A) Immersion temperature 23°C. (B) nano-treatment and contact angle measurement temperature were identical.

Figure 6-7 Set A: advancing water contact angle on oil-wet calcite surface in n-decane as function of exposure time to nanofluid (0.2wt % SiO<sub>2</sub>, 2wt % NaCl brine) and temperature. Immersion temperature was constant (23°C).

Figure 6-8 Set B: advancing water contact angle on oil-wet calcite surface in n-decane as a function of exposure time to nanofluid (0.2 wt% SiO<sub>2</sub>, 2 wt% NaCl brine) and temperature. Immersion temperature was the same as the temperature for contact angle measurements.

Figure 7-1 Experimental configuration for contact angle measurements; (a) syringe pump-brine, (b) two way valve, (c) temperature controller connected to the heating

source, (d) three way valve, (e) high resolution camera, (f) visualization software, (g) pressure relief valve, (h) high P/T cell, (i) joystick controls the surface tilting, (j) feed/drain system, (k) syringe pump-gas, (l) compressing gas (CO <sub>2</sub> )-source.....	133
Figure 7-2 Effect of electrolyte, and surfactant concentration (in terms of CMC) on zeta potential of nanoparticles/brine/surfactant system (0.1wt% SiO <sub>2</sub> at pH= 6) ..	134
Figure 7-3 Atomic force microscopy images of a nano-modified calcite surface with nanofluid (0.2 wt% SiO <sub>2</sub> in 2 wt% brine, 0.5 CMC of SDS at 50°C for 4 h) after exposure at 20 MPa (left) and 0.1 MPa (right). The RMS surface roughness was 838 nm at 0.1 MPa, and 704 nm at 20 MPa pressure. ....	136
Figure 7-4 SEM images of an oil-wet calcite surface after treatment with the same nanofluid (0.2 wt% SiO <sub>2</sub> in 2 wt% brine, 0.5 CMC of SDS at 50°C for 4 h) after exposure at A) 20 MPa and B) 0.1 MPa. ....	136
Figure 7-5 Water advancing ( $\theta_a$ ) and receding ( $\theta_r$ ) contact angle on different nano-treated oil-wet calcite surfaces in decane at ambient condition after treating each sample with a different nanofluid (0.01, 0.10, and 0.50 wt% Np in 0.5CMC of SDS, 5 wt% NaCl) for 1 hour and subjected to different pressures prior to the exposure to DI water, and acetone.....	137
Figure 7-6 Water advancing ( $\theta_a$ ) and receding ( $\theta_r$ ) contact angle on nano-modified calcite surface in decane and CO <sub>2</sub> as a function nanoparticle (Np, SiO <sub>2</sub> ) concentration in the base fluid (0.5CMC SDS in 5% NaCl).....	138
Figure 7-7 Impact of salinity and SiO <sub>2</sub> concentration (wt% Np) on advancing and receding contact angle of decane-brine system at reservoirs condition (15 MPa and 70°C) after 1 h of nano-treatment.....	140
Figure 7-8 Impact of salinity and SiO <sub>2</sub> concentration (wt% Np) on advancing and receding contact angle of CO <sub>2</sub> -brine system at reservoirs condition (15 MPa and 70°C) after 1 h of nano-treatment.....	140
Figure 7-9 Effect of nanoparticle concentration (SiO <sub>2</sub> wt%) in the base fluid (0.5cmc SDS, 4wt% NaCl) and immersing time (h) at reservoir conditions (20 MPa and 60°C) on advancing and receding contact angles of decane-brine system. The droplet salinity was 20% NaCl. ....	142
Figure 8-1 Atomic force microscopy images of a calcite surfaces used in the experiments. ....	147
Figure 8-2 Water advancing and receding contact angles measured on natural calcite (C1), oil-wet calcite (C2), and nanoparticle-treated natural (C3) and oil-wet (C4) calcite as a function of pressure at 50°C for CO <sub>2</sub> /DI-water system. ....	150
Figure 8-3 SEM images of A) oil-wet calcite and B) nanoparticle-treated oil-wet calcite; the silica nano-clusters are shown in white. ....	151
Figure 8-4 Water advancing and receding contact angles measured on natural calcite (C1), oil-wet calcite (C2), and nano-treated natural (C3) and oil-wet (C4) calcite surfaces as a function of temperature at 15 MPa for CO <sub>2</sub> /DI water systems. ....	151
Figure 8-5 Water advancing and receding contact angles measured on natural calcite (C1), oil-wet calcite (C2), and nanoparticle-treated natural (C3) and oil-wet (C4) calcite surfaces as a function of salinity at 50°C and 15 MPa. ....	152
Figure 9-1 SEM profile of SiO <sub>2</sub> nanoparticles, ultrasonically dispersed in DI water, after drying. ....	158

Figure 9-2 Size distribution of 0.1 wt% SiO <sub>2</sub> NPs ultrasonically dispersed in DI water (pH= 6.2) measured by dynamic light scattering (DLS) at ambient conditions. ....	158
Figure 9-3 Zeta potential of SiO <sub>2</sub> NP dispersion as function of base fluid salinity and NP concentration (at 23°C and a constant pH = 6.25).....	159
Figure 9-4 Sediment height versus CTAB concentration after 72 h, at different base fluid salinity for 0.1 wt% NP nanofluid at pH=7. ....	160
Figure 9-5 Mechanisms of cationic molecules adsorption with surfactant concentration before and after reaching the critical micelles concentration (CMC). ....	162
Figure 9-6 Sediment height versus SDS concentration after 72 h, at different base fluid salinity for 0.2 wt% NP nanofluid at pH=7. ....	163
Figure 9-7 Mechanisms of anionic molecules adsorption with surfactant concentration before and after reaching the critical micelles concentration (CMC). ....	164
Figure 9-8 Effect of electrolyte, and surfactant (SDS) concentration on zeta potential of NPs /brine/surfactant system (0.1wt% SiO <sub>2</sub> at pH= 6.25). ....	165
Figure 9-9 Compression of particle size distribution of NPs (0.1 wt%) with different surfactant concentrations (980 mg/l and 4900 mg/l of SDS) in the same base fluid (1 wt% NaCl). ....	166

## LIST OF TABLES

Table 2-1 Ranges of contact angles and respective wetting states .....	15
Table 2-2 Range of wettability indexes for the Amott and Amott-Harvey methods.	21
Table 3-1 General properties of the silicon dioxide nanoparticles used in this study	58
Table 3-2 Properties of SDS surfactant.....	59
Table 3-3 Properties of CTAB surfactant .....	60
Table 3-4 General properties of n-decane .....	61
Table 3-5 Properties of silanes used in this study .....	62
Table 3-6 General properties of stearic acid .....	63
Table 3-7 General properties of nitrogen gas .....	64
Table 4-1 properties of silicon dioxide nanoparticles used (Al-Anssari et al. 2016).	81
Table 5-1 Properties of silicon dioxide nanoparticles (Sigma Aldrich 2015).....	95
Table 5-2 Silanes used and their properties (Sigma Aldrich 2015).....	96
Table 5-3 Water contact angles on silane-modified calcite surfaces (ambient conditions). .....	97
Table 5-4 Surface composition of the oil-wet calcite substrates after modification with nanofluid (2wt% SiO <sub>2</sub> in 20wt% NaCl brine, 12 hours exposure time). .....	100
Table 6-1 Surface composition, measured by EDS, of oil-wet calcite after modification with nanofluid at 40 °C (0.2 wt% SiO <sub>2</sub> in 1 wt% NaCl brine, 1 h exposure time). .....	118
Table 6-2 Surface composition of the oil-wet calcite after modification with nanofluid at (0.2 wt% SiO <sub>2</sub> in 1 wt% NaCl brine, 1 h exposure time) at different temperatures; note that the composition given for each temperature is the average value of five measurements.....	119
Table 7-1 Highest contact angle reduction ( $-\Delta\theta^\circ$ ) of minerals after treatment with nanoparticles.....	127
Table 8-1 Sample treatment and original wettability state.....	148

# Chapter 1 Introduction and Overview of Thesis Objectives

## 1.1 Background

Over the last two decades, the scientific and industrial communities have experienced a revolution in material applications due to the transition from conventional bulk materials towards nano-size materials. This shift in material size and, consequently, surface properties, has led to innovative applications in many fields of science and industry, which have prompted tremendous investment in all fields of nanotechnology. The growing potential to manipulate matter at the nano-scale has driven nanoscience to become the core of upcoming technical innovation. Governments and multinational companies worldwide are spending billions of dollars to establish organisations and infrastructure to develop programs in nanotechnology and ride the wave of this rapidly growing field. It is not an overemphasis to say that the nanomaterial revolution, in terms of sheer interest, investment and potential applications, is one of the most significant fields of invention to occur since the beginning of modern science (Mirkin 2005). Typically, very well-organised methods of producing chemicals, materials and energy can be attained by designing, managing and controlling production systems at the same scale as natural systems. Over a billion years, organisms have developed nanoscale biological bodies for effective production of materials and energy. By simulating these systems, researchers can potentially achieve the aim of future sustainable life (Campelo et al. 2009).

Despite the recent interest in nanostructured materials, these materials are not entirely new. Nanomaterials have a short history. The concept of nanotechnology was first introduced in 1959 when physicist Richard Feynman announced a motivation to construct things at the atomic and molecular scales. However, experimental investigations on nanostructured materials did not start until 1981, when IBM scientists in Zurich, Switzerland, built the first scanning tunnelling microscope (STM). This helped to observe single atoms by using a tiny probe to scan the surface of a silicon crystal. Later on, the term *nanotechnology* became popularised by Drexler Eric K in the 1980s. Other techniques have since been developed to probe surfaces at the atomic scale, including atomic force microscopy (AFM) and magnetic resonance imaging (MRI). Thus, recent applications of nanomaterials are not exclusively the outcomes of current studies or laboratory syntheses. These nanostructures have existed for a long time, with traceable applications in the old days. However, the most interesting contribution was made in 1985, when chemists created soccer-ball-shaped molecules out of 60 carbon atoms. Further, in 1991, carbon nanotubes were produced as tiny super-strong rolls of carbon atoms. These nanotubes were six times lighter and 100 times stronger than steel.

Nanoscience and technology is an extremely multidisciplinary field that has input from chemists, physicists, biologists and engineers who study the preparation, application and impact of nanotechnologies. Moreover, the field of nanoscience and technology focuses on three streams of research: 1) the improvement of synthetic approaches and

surface analytical tools to create structures and materials, characteristically on the sub-100 nanometre scale; 2) characterization of the chemical and physical consequences of nano-scaling; and 3) application of unique properties to the design and development of innovative functional materials and devices (Mirkin 2005).

A nanomaterial is defined as a material that has a structure in which one or more of its dimensions are in the nanometre size range (1–100 nm). Such nano-scale materials are relevant to many fields of science and industry. Moreover, elements and components at the nano-size exhibit tremendous innovative potential for a wide range of applications. Nanotechnology involves the use of nano-sized materials to manipulate the structure of matter and tailor the physical and chemical properties of materials. Nanoparticles have gained attention in many processes, including drug delivery, biology, environment, catalysis, water treatment, heat transfer, electronic applications, mass transfer enhancement, energy storage, friction reduction, and subsurface applications such as geothermal extraction, soil decontamination, carbon geosequestration and enhanced oil recovery.

## **1.2 Nanomaterial Applications in the Oil Industry**

In recent centuries, the expansion of human society along with rapid industrialisation have severely increased the demand for hydrocarbons (Vatanparast et al. 2011) and, accordingly, increased greenhouse gases emissions (IPCC 2005). The recent issues, including energy resources and global warming, have triggered worldwide concerns. In the last decade; however, nanotechnology has introduced promising solutions to many scientific, industrial and environmental problems.

Enhanced oil recovery (EOR) involves hydrocarbon production from limestone reservoirs, which contain more than half of the known remaining oil reserves in the world (Vatanparast et al. 2011, Sharma and Mohanty 2013). These reservoirs are typically mixed-wet or oil-wet and fractured (Gupta and Mohanty 2010). Consequently, conventional water-flooding techniques are inefficient and have low productivity. Mainly, oil from fractures is produced since water does not spontaneously imbibe into the oil-wet rock matrix (Mason and Morrow 2013); however, most oil is stored in this matrix (Gupta and Mohanty 2010) and, as a result, only 10–30% of the oil is recovered (Wu et al. 2008). The industrial and domestic use of power, which mainly comes from fossil fuels, has increased dramatically due to heavy industries and human population growth. Nevertheless, many limestone reservoirs are considered depleted although they still contain around 70% of their oil.

One mechanism that can significantly improve oil production is to render the oil-wet or mixed-wet carbonate surfaces water-wet, so that water spontaneously imbibes into the rock and displaces the oil (Rostami Ravari et al. 2011). Furthermore, water-wet formations are also favourable for carbon capture and storage (CCS; Iglauer et al. (2015c). Characteristically, structural (Iglauer et al. 2015b) and residual (Rahman et al. 2016) trapping capacities are significantly lower in oil-wet formations. It is thus desirable to render oil-wet reservoirs water-wet to optimize CCS projects.

Carbon geo-sequestration (CGS), or carbon capture and storage (CCS) in underground formations has been identified as a promising technology for mitigating global warming (Lackner 2003). Anthropogenic CO<sub>2</sub> captured from large emitters (e.g. coal-fired power plants) is injected deep underground into geological formations for storage. Deep saline aquifers (Bikkina 2011) and depleted oil reservoirs (Rahman et al. 2016) are possible storage places where carbon can be trapped the mechanisms of mineral trapping, dissolution trapping, structural trapping and residual trapping (Iglauer et al. 2011a, Iglauer et al. 2011b, Arif et al. 2016d, Rahman et al. 2016). Carbon geo-sequestration in deep saline aquifers and depleted oil reservoirs comprises chemical and transport processes that are controlled by the wettability of the solid phase in contact with injected CO<sub>2</sub> and in situ native brines. The availability of all the required infrastructure, including seismic survey equipment, makes depleted oil reservoirs a significant candidate for carbon storage (Cook 2014). Moreover, some EOR processes inject CO<sub>2</sub> into oil reservoirs (Eide et al. 2015), and it is logical to combine carbon sequestration directly with CO<sub>2</sub>-driven EOR. However, even depleted oil reservoirs are oil-wet (Wu et al. 2008, Gupta and Mohanty 2010); meanwhile, pre-scale residual trapping of carbon dioxide has been proven to work only in clean sandstone (Iglauer et al. 2011a) and carbonate (Andrew et al. 2014). Thus, the carbonate surface should be water-wet or strongly water-wet to enhance hydrocarbon production and carbon storage. The economic feasibility of such processes ultimately depends on carbon taxes and oil prices (Suebsiri et al. 2006).

On the other hand, researchers never stop competing to develop state-of-the-art technologies to provide less expensive oil and effective carbon storage to deal with climate change. In regard to enhanced oil recovery, several chemical methods have been suggested: surfactant flooding (Wu et al. 2008, Mason and Morrow 2013), polymer flooding (Ding et al. 2010, Guo et al. 2013), nanoparticle-stabilised emulsions (Shen and Resasco 2009), various nanoparticle surfactants (Cui et al. 2009, Zargartalebi et al. 2014, Zargartalebi et al. 2015, Al-Anssari et al. 2017e, Nwidee et al. 2017b), nanoparticle polymers (Al-Manasir et al. 2009, Zhu et al. 2014), nanoparticle-surfactant-polymer formulations (Sharma et al. 2014a, Sharma et al. 2014b), and nanofluids (Ju et al. 2006, Ju and Fan 2009, Suleimanov et al. 2011, Hendraningrat et al. 2013, Al-Anssari et al. 2016, Nwidee et al. 2017a). Among the techniques mentioned above, nanofluids are one of the most efficient approaches that can rapidly alter oil-wet and strongly oil-wet surfaces to become water-wet (Al-Anssari et al. 2016, Zhang et al. 2016).

Nanoparticles and, particularly, silica nanoparticles have attracted intensive attention in recent decades due to their superb capability to alter wettability. In a typical EOR, oil production can be greatly increased by rendering the rocks, particularly carbonate surfaces, water-wet (Ju and Fan 2009, Onyekonwu and Ogolo 2010, Alotaibi et al. 2011, Karimi et al. 2012b, Hendraningrat et al. 2013) and injecting silica nanofluid can increase oil production by 15% (Zhang et al. 2016). In this case, a higher ratio of oil can be displaced from pore spaces owing to water imbibition into the rock matrix (Rostami Ravari et al. 2011).

In the meantime, the harsh conditions found in oil reservoirs, including high pressures, temperatures and salinity, require a full understanding of nanofluid behaviour and

stability in such critical conditions. The use of silica nanoparticles as smart materials in the fields of EOR and CGS may open up a bright avenue for using depleted oil reservoirs as hydrocarbon sources and safe anthropogenic carbon stores.

### 1.3 Characteristics of Nanoparticles

Nanoscale particles exhibit exceptionally different behaviours compared with their bulk form equivalents. Nanoparticles have a broad range of unique properties including quantum confinement, superparamagnetism, superior catalytic activity, intrinsic reactivity, great adsorption affinity and dispersibility (Hashemi et al. 2014, Perez 2007). The uniqueness of nanomaterial characteristics has been known for several centuries. The oldest historical example of controlled nanotechnology used for optical devices was the metallic lustre decoration of glazed ceramics, which was performed in Mesopotamia during the 9<sup>th</sup> century AD before spreading throughout Egypt, Persia and Spain. Typically, the optical properties of these lustres are mainly related to the metallic nanoparticles that are dispersed in the outermost layers of the glaze by empirical chemical means (Philippe Sciau 2009). Progressively over the last two or three decades, nanostructured materials have become widely used due to their unique rheological, thermal, chemical and physical properties. Properties including particle size, particle size distribution, purity, particle grain boundaries, and the surface area per unit volume are examples of the characteristic properties of nanoparticles. Remarkably, the surface properties of nanoparticles can be designed and modified (Sharma et al. 2014b) for different applications, including subsurface industries.

The distinctly differing physicochemical characteristics presented by metal particles at the nano-size, as compared to their bulk material counterparts, is one of the main reasons for the prompt development of the nanoparticle field. However, the high surface energies and the large surface areas of nanoparticles results in unstable behaviour. Typically, nanoparticles act as very active agents, yet they are thermodynamically unstable. Mechanistically, separated nanoparticles tend to agglomerate again to a larger nano- or micro-aggregate due to the interaction forces between bare nanoparticles, leading to loss of the unique properties of nanoparticles. The production of stable nanoparticles requires the termination of particle growing reactions. Characteristically, the very high ratio of nanoparticle surface to volume makes their interactions dominated by short-range forces including the surface repulsive force and van der Waals attraction force (Quemada and Berli 2002). As a consequence, nanoparticles remain together if van der Waals attraction force is greater than the repulsive force that prevents nanoparticles from sticking to each other (Paik et al. 2005). Thus, electrostatic repulsion is preferred to achieve stable nanoparticles. Naturally, however, nanoparticles in suspension experience two scenarios; reaction limit aggregation (RLA) and diffusion limit aggregation (DLA). In RLA, many collisions take place before two particles can stick together and produce small aggregates (Lin et al. 1990). While in DLA, when the repulsive forces between nanoparticles are weak, the rate of aggregation is only limited by the time between

collisions of clusters due to their diffusion and Brownian motion (Elaissari and Pefferkorn 1991).

#### **1.4 Motivation and Objectives of Thesis**

This research study aims to develop a novel and stable nanofluid for wettability alteration of oil-wet carbonate surfaces that can be used in EOR and CGS applications. Meanwhile, this research is also dedicated to providing the first insight into the intrinsic mechanisms of nanoparticle adsorption over solid surfaces. To this end, comprehensive studies integrating deliberate fluid nanoparticle characterisation, nanofluid preparation, nanofluid density, nanofluid stability and nanoparticle deposition are implemented. This will involve advanced instrumentation including scanning electron microscopy, atomic force microscopy and use of Zetasizers. The specific objectives of this study are as follows.

1. Preparation of different nanofluids, silica-nanoparticles dispersed in base fluid (brine, deionised (DI) water, and surfactant) by changing the concentrations of SiO<sub>2</sub> and composition of the base fluid.
2. Employing the nanofluids for oil/water interfacial tension reduction and wettability alteration of oil-wet calcite surfaces, and characterising wettability alteration by contact angle measurements.
3. Studying the effects of harsh conditions, including high pressure, high temperature and salinity on nanofluid stability and wettability alteration efficiency.
4. Probing the mechanism of surface modification by investigating the intrinsic influence of silica deposition on calcite surfaces using an atomic force microscopy (AFM), scanning electron microscope (SEM), and energy dispersive X-ray (EDS).
5. Testing the potential synergistic effects of nanoparticles and surfactant molecules in terms of oil-water interfacial tension and wettability alteration.
6. Investigating the effect of immersion duration on calcite surface properties.
7. Identifying the optimum composition of nanofluid that assures the most significant reduction in contact angle and shows the most stable behaviour.

#### **1.5 Significance of the study**

The modification of surface properties with nanoparticles at high pressures, temperatures and salinity is new topic. Only a limited number of studies have previously investigated the effects of nano-priming on the contact angle of oil-wet carbonate surfaces. Further, previous studies were conducted at ambient conditions or within a limited range of temperature changes using nanoparticles dispersed in DI-water. Moreover, the majority of surface nano-modification studies have been conducted on quartz surfaces (representing sandstone formations), while carbonate

formations with complicated microstructures have rarely been investigated. Understanding the wettability of carbonate formations is a complex practice, and controlling the surface affinity to oil and water via surface modification with nanoparticles is even more complicated. In addition, the stable behaviour of nanoparticles in subsurface formations is crucial and very difficult to control. We believe this study will considerably improve the understanding of surface wetting preferences, which is a key factor for oil production applications and will accelerate the implementation of nanoparticle applications for enhanced oil recovery and carbon capture and storage at industrial scales.

## **1.6 Scope of the study**

This study focuses on the modification of interfacial properties utilising hydrophilic nanoparticles and investigates the stability of these fine particles under subsurface conditions. The qualitative part of this study provides an in-depth analysis of oil-water interfacial tension, contact angles, and nanoparticle affiliation and stability for oil recovery and carbon storage applications. The experimental work was conducted using silica nanoparticles in the form of a metal oxide ( $\text{SiO}_2$ ). Silica nanoparticles were chosen for this study due to their low cost of fabrication and surface modification, which makes them very popular in the oil industries. Several formulations of silica nanoparticles with different chemicals, including anionic (SDS), cationic (CTAB) surfactant and sodium chloride (NaCl) brine were ultrasonically formulated and their interfacial and wetting properties systematically tested. The influence of nanoparticles, salt, and surfactant concentrations on suspension stability and the liquid-liquid and liquid-solid interfacial properties were investigated in terms of pressure, temperature and contact time to mimic all the potential scenarios in the real process. A wide range of formulations was thoroughly tested and analysed to address the current lack of data on liquid-liquid and liquid-solid interfaces in complex nanoparticle-brine-surfactant-oil systems.

## **1.7 Thesis organisation**

The thesis consists of eleven chapters including an introduction, literature review, materials and experimental methodology, results and discussion with implication of the measured data (Chapter 4 - Chapter 9), an overall discussion and, finally, conclusions and directions for future studies. Figure 1-1 gives a layout of the thesis objectives and structure. It designates the framework of the aforementioned thesis objectives and relates them to the chapters.

***Chapter 1 – Introduction*** – A brief introduction to the background, common issues and treatment solutions concerning nanoparticles, especially relating to chemical-

enhanced oil recovery and carbon storage. This chapter also includes the objectives of the research and structure of the thesis.

**Chapter 2 – Literature Review** – Comprehensively summarises the various EOR techniques and chemical strategies of enhanced oil recovery, including emerging nanotechnology methods. Moreover, this chapter covers the types, synthesis methods and applications of different nanoparticles.

**Chapter 3 – Experimental Methodology** – Provides comprehensive explanations of the materials, instruments, software and methods used to achieve the goals of this research. The study is based on experimental research but also has a qualitative component.

**Chapter 4 – Oil-Water Interfacial Tensions of Silica Nanoparticle-surfactant Formulations.** (*Tenside Surfactants Detergents 2017; 54, 334-341*) – Investigates the improvement of surfactant ability in terms of interfacial tension reduction by addition of silicon dioxide nanoparticles at different temperatures and salinity.

**Chapter 5 – Wettability Alteration of Oil-wet Carbonate by Silica Nanofluid.** (*Journal of Colloid and Interface Science 2016; 461, 435-442*) – Examines how silica-based nanofluids can induce a wettability shift on oil-wet and mixed-wet calcite substrates. We found that silica nanoparticles have the ability to alter the wettability of such calcite surfaces.

**Chapter 6 – Effect of Temperature and SiO<sub>2</sub> Nanoparticle Size on Wettability Alteration of Oil-wet Calcite.** (*Fuel 2017; 206, 34-42*) – Investigates the effects of temperature, exposure time and particle size on wettability alteration of oil-wet calcite surfaces and examines the stability of nanofluids.

**Chapter 7 – Wettability of Nanofluid-modified Oil-wet Calcite at Reservoir Conditions.** (*Fuel 2018; 211, 405-414*) – Quantifies the performance of hydrophilic silica nanoparticles as surface property modifiers at high pressures, temperatures and salinity to mimic hydrocarbon production scenarios.

**Chapter 8 – CO<sub>2</sub> Geo-storage Capacity Enhancement via Nanofluid Priming.** (*International Journal of Greenhouse Gas Control 2017; 63, 20-25*) – Examines the role of silica nanoparticles on both structural and residual CO<sub>2</sub> trapping capacities of oil-wet carbonate formations under storage conditions.

**Chapter 9 – Stabilising Nanofluids in Saline Environments.** (*Journal of Colloid and Interface Science 2017; 508, 222-229*) – Measures and quantifies nanofluid stability

for a wide range of nanofluid formulations in terms of salinity, nanoparticle content and various additives, and we investigated how this stability can be improved.

**Chapter 11 – Overall Discussion** – Briefly discusses all the results and their potential implications for the oil industry.

**Chapter 11 – Recommendations and Outlook for Future Work** – Highlights the major findings of this study and suggests further research directions in the field.

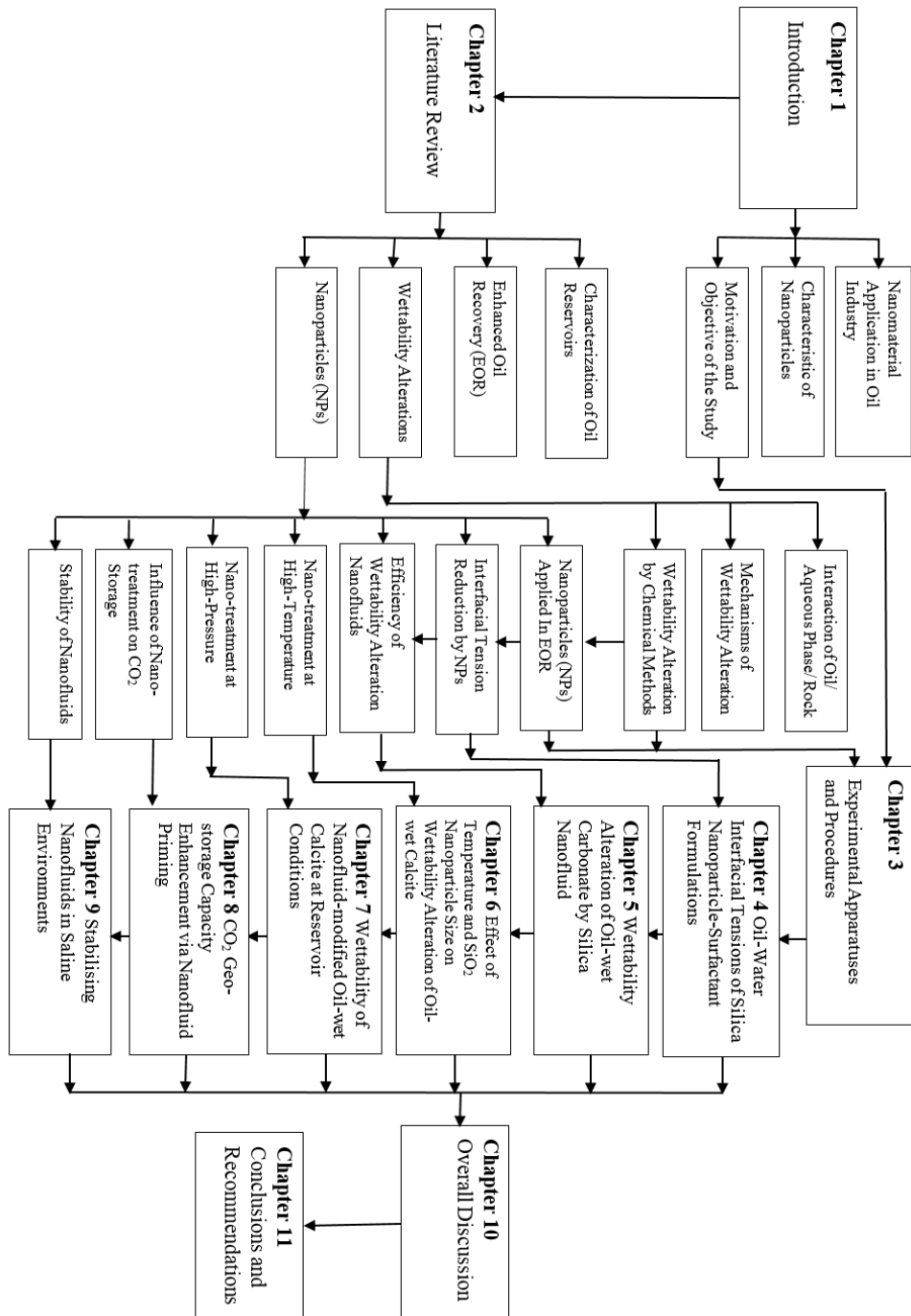


Figure 1-1 Layout of thesis objectives and structure.

## Chapter 2 Literature Review

### 2.1 Introduction

In recent decades, hydrocarbon demand has grown rapidly due to rapid industrialisation and population growth, leading to shortages of energy sources and severe climate change due to increased anthropogenic greenhouse gas emissions. The lack of energy has exacerbated rapidly and the serious global warming has become far beyond the self-balancing capacity of nature. It threatens to break the harmonious balance between humans and nature that has existed for thousands of years. Carbonate reservoirs contain more than half of the known oil in the world and are the main source of crude oil. They are also strong candidates for injection of carbon dioxide for storage and incremental oil recovery. However, most carbonate reservoirs are naturally fractured oil-wet or mixed-wet reservoirs, which significantly decreases their potential for hydrocarbon production and increases the riskiness of carbon storage projects. Many techniques have been applied to change the wettability of oil-wet reservoirs to water-wet and reduce the interfacial tension (IFT) between oil and injected water, thus enhancing oil recovery. In addition to the two traditional methods used for wettability alteration—thermal and chemical—nanoparticles have newly emerged as an application for wettability alteration projects. Recently, nanomaterials have demonstrated extensive applications in a wide spectrum of fields, particularly in subsurface projects including enhanced oil recovery (EOR) and carbon geo-storage (CGS) owing to their drastic ability to render oil-wet rocks water-wet when injected into depleted oil reservoirs.

In terms of hydrocarbon sources and EOR, only approximately one-third of the original oil in place (OOIP) can be recovered by the primary and secondary recovery process. One of the main challenges is oil production from limestone reservoirs, which contain around 50% of the known remaining hydrocarbon reserves in the world (Sharma and Mohanty 2013). These reservoirs are typically fractured and mixed-wet or oil-wet (Gupta and Mohanty 2010); thus, conventional water-flooding techniques are ineffective and oil productivity is low. Hydrocarbon is mainly produced from fractured formations since water does not spontaneously imbibe into the oil-wet rock matrix (Mason and Morrow 2013); however, most oil is stored in this matrix (Gupta and Mohanty 2010) and, consequently, only 10-30% of crude oil is recovered (Wu et al. 2008).

One mechanism that can effectively improve oil production is to change the oil-wet or mixed-wet carbonate surfaces to being water-wet; thus, water can spontaneously imbibe into the matrix and displace the oil (Rostami Ravari et al. 2011). Also, water-wet reservoirs are favourable for carbon capture projects (Andrew et al. 2014, Iglauer et al. 2015c).

Carbon geosequestration (CGS), or carbon capture and storage in underground formations, has been identified as a promising technology for mitigating global warming (White et al. 2003). In this process, CO<sub>2</sub> is captured from large emitters (e.g. coal-fired power plants) and injected deep underground into geological formations for storage. The wettability of the solid phase that is in contact with native in situ brines

and injected carbon, controls the chemical and transport processes of carbon geostorage. Deep saline aquifers (Bikkina 2011) and depleted oil reservoirs (Cook 2014, Rahman et al. 2016) are a possible storage places where carbon can be trapped by four mechanisms: mineral trapping, dissolution trapping, structural trapping and residual trapping (Iglauer et al. 2011a, Iglauer et al. 2011b, Arif et al. 2016a, Rahman et al. 2016). In this context, some EOR processes inject CO<sub>2</sub> into oil reservoirs (Eide et al. 2015), and it is logical to combine carbon sequestration directly with CO<sub>2</sub>-driven EOR despite the oil-wet nature of these reservoirs. However, CO<sub>2</sub>-water wetting phenomena in oil-wet surfaces differ greatly from that in water-wet surfaces (Li and Fan 2015). Structural (Iglauer et al. 2015c, Arif et al. 2016a) and residual (Rahman et al. 2016) trapping are the key mechanisms of carbon storage and they both work significantly better in water-wet rocks. Thus, both EOR and CGS applications require water-wet reservoirs, which can be created using nanoparticles (Ju and Fan 2009, Onyekonwu and Ogolo 2010, Alotaibi et al. 2011, Karimi et al. 2012a, Hendraningrat et al. 2013, Al-Anssari et al. 2016, Zhang et al. 2016, Nwideo et al. 2016a).

Chemical methods have been used to enhance oil recovery from low-productivity oil reservoirs. Interfacial tension reduction, and alteration of oil-wet carbonate surface wettability to being water-wet, are the key techniques for recovering oil from such reservoirs (Gupta and Mohanty 2010). Surfactant flooding, for example, is one of the chemical techniques that has been tested for increasing oil recovery from such low productivity reservoirs. Cationic (Standnes and Austad 2000), anionic (Wu et al. 2008), and non-ionic (Xie et al. 2005) surfactants have been identified as wettability alteration agents of originally oil-wet carbonate reservoirs. Mechanistically, surfactants alter the wettability of rock surfaces by solubilizing adsorbed hydrophobic components from surfaces, leading to higher hydrocarbon production, e.g., more than 60% of OOIP (Gupta and Mohanty 2010) from initially oil-wet reservoirs. However, surfactant adsorption on rock surfaces (e.g. adsorption of anionic surfactant on calcite mineral in carbonate reservoirs) can reduce the efficiency of surfactant flooding and make the process unfeasible (Ma et al. 2013). Nanoparticles have shown promising abilities to render oil-wet carbonate surfaces water-wet. Moreover, the combination of surfactants and nanoparticles (Ravera et al. 2006, Lan et al. 2007, Ma et al. 2008) can improve the capabilities of these agents to enhance oil recovery through the effect of surfactants on nano-suspension stability (Kvítek et al. 2008, Whitby et al. 2009). Nanoparticles, on the other hand, can reduce the loss of surfactant by adsorption on reservoir minerals (Zargartalebi et al. 2015) and by improving the efficiency of surfactants in terms of IFT reduction (Esmailzadeh et al. 2014).

Nanoparticles with uniquely-designed properties are elegant solutions for many industrial problems. They show promise for application in numerous fields including medicine (Lohse and Murphy 2012), biomedicine (Rubilar et al. 2013), drug delivery (Tong et al. 2012), biology (De et al. 2008, Baeckkyoung et al. 2015), environment (Garner and Keller 2014) and pollution (Wu et al. 2013a, Sarkheil and Tavakoli 2015), water treatment (Syed et al. 2011, Wang et al. 2012), food production (Fischer et al. 2013, Rajauria et al. 2015, van Dijk et al. 2015), polymer composites (ShamsiJazeyi et al. 2014), stable emulsions (Whitby et al. 2009, Qiao et al. 2012), heat transfer (Ghadimi et al. 2011, Branson et al. 2013), corrosion protection (Winkler et al. 2011), conductive materials (Chakraborty and Padhy 2008), heterogeneous catalysis (Balaji

et al. 2011), and subsurface applications including drilling (Ponmani et al. 2015), carbon geosequestration (Al-Anssari et al. 2016) and enhanced oil recovery (Suleimanov et al. 2011, Sharma et al. 2014b, Zhang et al. 2014, Al-Anssari et al. 2016, Zhang et al. 2016). Deposition of (functionalised) nanoparticles on solid surfaces is a promising technique for controlling the wettability of these surfaces.

The efficiency of nanoparticles, in terms of the wettability alteration of solid surfaces, depends on several factors, including, particularly, the nanoparticle type (Bayat et al. 2014b, Moghaddam et al. 2015) and solid surface chemistry (Täuber et al. 2013). Also, operating conditions such as pressure, temperature nanofluid composition and contact time have significant effects on such surface modifications (Zhang et al. 2015, Al-Anssari et al. 2016, Al-Anssari et al. 2018). In this context, silica nanoparticles have shown promising properties for subsurface applications.

Silica nanoparticles in a metal oxide form (silica oxide;  $\text{SiO}_2$ ) are widely used, as non-metal nanoparticles, owing to their low cost of fabrication and surface modification. Chol (1995) was the first to call the suspension of nano-sized particles (5–100 nm) dispersed in a base liquid a *nanofluid*. Nanoparticles are dispersed in the liquid phase (DI water, brine, polymer or surfactant solutions) by an ultrasonic homogenisation process (Mahdi Jafari et al. 2006, Leong et al. 2009, Al-Anssari et al. 2016). The ultrasonic homogeniser is more efficient at producing a stable dispersion than other techniques such as high shear mixers (Petzold et al. 2009) and magnetic stirrers (Mahdi Jafari et al. 2006). The high dispersion efficiency of the ultrasonic homogeniser is due to its high-density energy, which actively breaks up nano-agglomerates (Leong et al. 2009). However, after sonication, individual nanoparticles tend to agglomerate owing to their interaction forces, particularly in the presence of an electrolyte. Although at high salt concentrations the collapse of the electrical double layer of nanoparticles leads to the formation of fractal aggregates in the nanosuspension, silica dispersions have been of prominent interest in colloidal science because of their unusual aggregation behaviour. Brownian motion makes nanoparticles come into contact with each other. According to the classical DLVO (Deriaguin-Landau-Verwey and Overbeek) theory, colloidal suspension stability in a dielectric medium is determined by repulsive electrostatic interaction energy and attractive van der Waals energy (Yotsumoto and Yoon 1993, Paik et al. 2005). Thus, nanoparticles will remain together if van der Waals attraction force is greater than the repulsive force (Paik et al. 2005). During the early period of coagulation, the collision of nanoparticles experiences two scenarios, reaction limit aggregation (RLA) and diffusion limit aggregation (DLA). In RLA, a large number of collisions takes place before two particles stick together and produce a small aggregate (Lin et al. 1990). While in DLA, the rate of aggregation is only limited by the time between the collisions of clusters due to their diffusion (Elaissari and Pefferkorn 1991). In nanofluids, the very high ratio of surface to volume makes all particle-particle interactions dominated by short-range forces such as the surface repulsive force and van der Waals attraction force (Quemada and Berli 2002, Zhang et al. 2015). Electrostatic repulsion is preferred for achieving a stable nanosuspension. However, the high salinity of reservoirs can significantly suppress these repulsive forces and accelerate the aggregation process of silica nanoparticles, producing an unstable suspension. Mechanistically, electrolytes can dramatically

eliminate the surface charges of nanoparticles, leading to dramatic reductions in the electrostatic repulsive forces between the nanoparticles in the suspension.

Surfactants, particularly ionic surfactants, can improve the stability of silica nanofluids by modifying the surface charge of nanoparticles and, consequently, increasing the electrostatic repulsion forces between nanoparticles (Zheng et al. 2003, Kvítek et al. 2008). The performance of surfactants as stabilising agents is controlled by their adsorption on silica nanoparticle surfaces (Ahualli et al. 2011). Moreover, in terms of oil transport and recovery, oil penetration into the hydrocarbon chains of surfactant monolayers is a key factor affecting the self-curvature of the oil-water interface and, thus, the phase behaviour in micro-emulsions (McKenna et al. 2000). Consequently, the combination of ionic surfactants and nanoparticles can potentially play a major role in EOR projects.

Sodium dodecylsulfate (SDS), and hexadecyltrimethylammonium bromide (CTAB) are very popular examples of anionic and cationic surfactants, respectively, that are widely used in industry, particularly in oil recovery (Bera et al. 2013), to reduce oil-water interfacial tension. Moreover, recent studies have revealed synergistic effects between nanoparticles and surfactant molecules in terms of IFT reduction and nanofluid stability.

## **2.2 Characterisation of Oil Reservoirs**

### **2.2.1 Wettability**

*Wettability* is defined as the tendency of one fluid to adhere to or spread on a solid surface in the presence of another immiscible fluid (Craig 1971). The desired surface wetness may be hydrophilic (water-wet) or hydrophobic (oil-wet) according to project requirements. Enhanced oil recovery (EOR) and carbon geosequestration, for instance, require hydrophilic surfaces. While hydrophobicity; in contrast, is useful for self-cleaning materials. For water-oil systems, wettability is the tendency for the rock to preferentially attract water, oil, or both to different degrees. The importance of wettability is related to its control of the location, flow and distribution of fluids within reservoir rocks (Anderson 1986). In water-wet conditions, the aqueous phase is retained by the capillary forces in the smaller pores and on the walls of the larger pores, while the oleic phase occupies the centre of the larger pores and forms globules, which might extend along many pores. Different degrees of wettability have been reported in the literature. *Neutral wettability* refers to the condition when there is no clear preference for oil or water. *Fractional wettability* has been widely defined in the literature and represents the variations in wettability that are due to the different surface chemistries and adsorption properties of the many minerals that form reservoir rocks (Wolthers et al. 2008, Ma et al. 2013). *Mixed wettability* is very common in oil reservoirs, particularly carbonate reservoirs (Gupta and Mohanty 2010). A mixed-wet porous medium has formation brine occupying its hydrophilic small pores and an oleic phase occupying the hydrophobic large pores. Moreover, within the same pore, different minerals may be wet by different fluids (Wolthers et al. 2008). Originally,

the natural rock is strongly water-wet before hydrocarbon migration. However, due to oil migration, the oleic phase expels the aqueous phase, especially from the larger pores, but it never enters the small pores owing to capillary forces. Moreover, the oleic phase tends to wet the surfaces of large pores, making them oil-wet. This is the basic principle for mixed-wet reservoirs. Conversely, *oil-wet rock* refers to the condition when the oleic phase overcomes the capillary forces and occupies the small pores as well as coating the walls of the larger pores, displacing the aqueous phase to the centre of the large pores. Some sources (Jarrell et al. 2002) argue that the expressions *oil-wet* and *mixed-wet* are substitutable because all oil-wet formations are, in reality, mixed-wet, since the oleic phase does not enter the small pores. Carbonate reservoirs that contain more than 50% of the remaining oil are mainly oil-wet (Ma et al. 2013), while sandstone reservoirs are generally water-wet (Chilingar and Yen 1983) unless they contain a considerable ratio of clay, which makes them oil-wet.

### 2.2.1.1 Wettability of Carbonate Reservoirs

Carbonate rocks are considered to be among the most reactive minerals on Earth, which complicates the interaction of rocks and underground fluids in carbonate reservoirs. From a chemical point of view, complexes of carbonate ions  $CO_3^{2-}$  and cations including  $Ca^{2+}$ ,  $Mg^{2+}$  and  $Fe^{2+}$ , as well as less-common cations such as  $Mn^{7+}$ ,  $Zn^{2+}$  and others can be found in the structures of carbonate rocks. The dominant minerals in carbonate formations are calcite ( $CaCO_3$ ), which forms limestone, and dolomite ( $Ca, Mg(CO_3)_2$ ). Calcite is a common mineral, comprising approximately 40% of the Earth's crust (Al Mahrouqi et al. 2017). Surface reactions of calcite in underground formations play a major role in many environmental and geochemical systems, as well as some subsurface industries, including  $CO_2$  geostorage and hydrocarbon recovery. The oil-wetting state of carbonate oil-reservoirs is related to the acid number, which determines the amount of carboxylic acid groups in the oleic phase (Xie et al. 2010). Owing to the positive charges of carbonate surfaces, hydrocarbons with higher acidic numbers are further activated to alter the wettability of carbonate rocks to being oil-wet (Legens et al. 1999). Although some earlier studies (Buckley et al. 1989, Buckley et al. 1998a, Buckley et al. 1998b, Buckley 1999) have announced that asphaltenes in crude oil are the main reason for wettability alteration (rather than high acidity), Austad and Standnes (2003) noticed no direct influence of asphaltenes in hydrocarbons on carbonate wetness. Furthermore, many other studies have demonstrated that treating calcite surfaces with stearic acids is a useful process in oil-wet carbonate reservoirs (Hansen et al. 2000, Hoiland et al. 2001, Morse and Arvidson 2002, Hamouda and Gomari 2006, Shi et al. 2010).

### **2.2.1.2 Wettability of Sandstone Reservoirs**

The negative charges of sandstone help to adsorb the basic components from crude oil rather than acids (Anderson 1986). Thus, the acid number may not be as important as the condition of the carbonate (Buckley et al. 1989). Four mechanisms have been suggested to explain the effect of crude oil on the wettability of sandstone: polar interaction, surface precipitation, acid/base interaction, and ion binding (Buckley et al. 1998b). Hydrocarbons with high base numbers and low acid numbers can render the wettability of sandstone surfaces by acid/base interaction. Meanwhile, hydrocarbons with high acidic numbers and low base numbers may alter the wettability due to ion-binding interactions. Precipitation is responsible for wettability alteration of sandstone via the high asphaltene content in crude oil. According to (Denekas et al. 1959), the molecular weight of crude oil is the key parameter for wettability change in sandstone. The molecular weight of the oil-fraction in contact with the rock controls its wetness state. Typically, the strongest oil-wet condition can be reached under the effect of heavier components.

The effect of clay content in sandstone is another potential cause of oil-wet conditions. Tang and Morrow (1999) revealed that wettability alteration of sandstone is mainly caused by clay. Further, it is well agreed that sandstone with higher clay content is more oil-wet (Schembre et al. 2006). Mechanistically, adsorption of surface-active components from oil onto rock surfaces is the main reason for wettability change. Multi-divalent ions, in high salinity formations, reduce the negative surface charges of clay and, consequently, minimise the repulsive force (Vledder et al. 2010).

In conclusion, acid number is the crucial factor for shifting the wettability of carbonate formations via crude oil. Higher acid numbers give the strongest oil-wettability. In sandstone, asphaltene content, API, and clay content are the major factors that control changes in wettability via crude oil. Several techniques can be used to measure the wettability and wettability alteration of surfaces.

### **2.2.2 Wettability Measurements**

Dependable wettability alteration measurement devices are required to accurately measure the effectiveness of wettability alteration. However, there is a standard test for wettability measurement (Rao 1999). Consequently, it is important to consider all the proposed techniques that are normally used for wettability measurements. Although spontaneous imbibition tests are the most popular way to assess the wetness of core samples, additional techniques, particularly contact angle measurement, are very reliable for wettability measurement before and after surface treatment. In this regard, Anderson (1986) introduced a review of different tools of measurement. Each type of measuring device can accurately monitor the process of wettability alteration from a different perspective. Thus, we provide below a summary of common wettability alteration tests.

### 2.2.2.1 Contact Angle

Contact angle is the contact point of oil and water interfaces on a solid surface. Water contact angle is used to analyse wettability alteration of surfaces before and after surface treatment, since it can give a general qualitative indication of the wetting tendencies of the surface in a continuous manner (Al-Sulaimani et al. 2012). The value of the contact angle provides a direct indication of the wettability condition of the rock (Anderson 1986).

Table 2-1 Ranges of contact angles and respective wetting states

	Water-wet	Natural-wet	Oil-wet
Contact angle (minimum)	0°	60° to 75°	105° to 120°
Contact angle (maximum)	60° to 75°	105° to 120°	180°

Although many researchers have used contact angle measurements to study the alteration of surface wettability, there is no universal protocol that limits the performance of this test. Alotaibi et al. (2011) demonstrated that contact angle measurements are usually applied by using small pieces of rock and two immiscible fluids. To avoid any hysteresis issues, contact angle tests can be simply applied on rock minerals such as mica, calcite or quartz; otherwise, the rock surface should be smoothed and well-polished (Alotaibi et al. 2011).

It is generally agreed that water contact angles below 90° are indicative of water-wet surfaces and water contact angles greater than 90° are indicative of oil-wet surfaces. Moreover, intermediate surfaces are indicated by contact angles around 90°. There are two types of contact angle usually used to demonstrate the wetness status: *advancing* and *receding* contact angles (Marmur 2006). However, advancing contact angles are more often used to evaluate the wettability of surfaces (Treiber and Owens 1972).

Advancing ( $\theta_a$ ) and receding ( $\theta_r$ ) contact angles can be directly measured at the same time using the tilted plate technique (Lander et al. 1993, Extrand and Kumagai 1995). Technically, a droplet of liquid (DI water or brine) at an average volume of  $\mu\text{L} \pm 1 \mu\text{L}$  is dispensed on to a substrate placed on the tilted base (Figure 2-1).

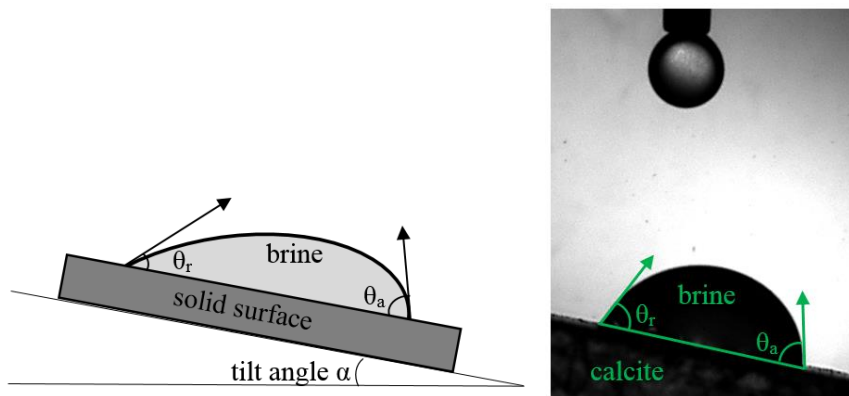


Figure 2-1 Schematic of brine droplet on a tilted surface with  $\theta_a$  and  $\theta_r$  indicated (left); image of water drop on calcite surface (right).

Increasing the water contact angle on a solid surface refers to a change in wettability towards being more oil-wet. Rock surfaces are turned oil-wet by aging in crude oil or treatment with chemicals including silanes (Grate et al. 2012) or fatty acids including stearic acid (Hansen et al. 2000, Hoeiland et al. 2001, Morse and Arvidson 2002, Hamouda and Gomari 2006, Shi et al. 2010). Measurements of advancing and receding contact angles may be conducted at ambient or reservoir conditions. Arif et al. (2016a) assessed the advancing and receding contact angles on quartz samples for a wide range of temperatures (23 to 70 °C) and pressures (0.1 to 20 MPa). Further, Rao (1999) has measured the receding contact angle at temperatures as high as 200 °C.

Many limitations on using contact angle as a method of wettability alteration measurement have been reported. Mainly, contact angle values are very sensitive to contamination (Iglauer et al. 2014). Moreover, high contact angle hysteresis is a crucial challenge for accurate measurement of surface wettability (Alotaibi et al. 2011). In this case, repeating the measurement several times to minimise errors is a common practice to reduce the limitations of contact angle measurement. In addition, there is no international agreement about whether it is more representative to apply contact angle measurements on porous rock plates or mineral plates. For example, calcite is used to represent carbonate, while quartz is used in place of sandstone. However, these pure minerals will not accurately represent the mineralogy of the rock during contact angle measurement. In this context, Sharma and Mohanty (2013) revealed that contact angle doesn't accurately reflect the effect of some chemicals on surface wettability. They explained that chemicals that have the ability to shift the wettability of a calcite substrate failed to spontaneously imbibe into reservoir core samples. Thus, it is crucial to find a representative surface that has the ability to properly capture the actual properties of reservoir rock. In short, contact angle is a fast and economical method for evaluating the wetness state and effect of treatment on surface wettability. Other tests such as zeta potential, surface imaging and, particularly, spontaneous imbibition tests, can be used to confirm the results. Although using porous rock seems to be more realistic, heterogeneity of rock surfaces (Figure 2-2) may also affect the accuracy of the measurements (Marmur 2006).

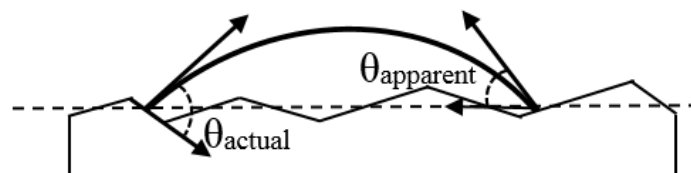


Figure 2-2 The actual contact angle ( $\theta_{\text{actual}}$ ) and the apparent contact angle ( $\theta_{\text{apparent}}$ ) on a rough surface (redrawn from Marmur (2006)).

### 2.2.2.2 Zeta potential test

The zeta potential of natural surfaces plays a major role in many subsurface applications since it is a unique measure of electrical potential at mineral surfaces. The magnitude and sign of zeta potential govern the electrostatic interactions between rock mineral surfaces and polar species in both aqueous- (Al Mahrouqi et al. 2017) and non-aqueous-phase liquids (Hirasaki and Zhang 2004). Alroudhan et al. (2016) reported measurements of the zeta potential on limestone samples and found a correlation between an increasingly negative zeta potential and increasing oil recovery due to the increased alteration of wettability towards water-wet status. Further, in nanofluid flooding applications in carbonate reservoirs, zeta potential and surface charge are the key parameters influencing nanoparticle adsorption on reservoir rock and, thus, the potential alteration of wettability towards being more water-wet.

#### 2.2.2.2.1 Zeta potential and the electric double layer of calcite surfaces

The invasion of an aqueous solution into reservoir rocks leads to separation of electrical charge at the aqueous phase-mineral interface. In this context, the excess of charges at the mineral surface is balanced by an area of equivalent (equal but opposite) charge in the nearby solution. This charge-balancing region is called the *electrical double layer* (EDL, (Glover and Jackson 2010, Al Mahrouqi et al. 2017). Calcite surfaces, for example, form seven ions ( $CO_3H^0$ ,  $CaO^{-+}$ ,  $CO_3Ca^+$ ,  $CaOH^0$ ,  $CaCO_3^-$ ,  $CaOH_2^+$ , and  $CO_3^-$ ) after immersion in an aqueous solution (Pokrovsky and Schott 2002). The relative concentrations of these ions are controlled by the pH of the fluid (Glover and Jackson 2010). The decrease in co-ion (ions with the same charge as the surface) concentration and the increase in counter-ion (ions with the opposite charge as the surface) concentration in the nearby solution act to balance the surface charge of the mineral. The seven ions are formed from the outer region of calcite mineral that faces the aqueous solution (see Figure 2-3). Further, the hydrolysis layer which connects the chemi-bonded  $H^+$  and  $OH^-$  ions into bulk ions (Stipp 1999), connects the mineral surface to the EDL in the nearby aqueous solution.

The region of the aqueous phase that is directly adjacent to the hydrolysis layer is typically termed the *Stern layer*, while the outer layer is named the *diffuse layer*. Both the Stern layer and the diffuse layer form the EDL. In addition, the Stern layer contains two sub-layers (the inner and outer Stern layers; Figure 2-3). The inner Stern layer is the area where the ions that closely approach the mineral surface are attached to surface sites. The outer Stern layer is the area between the inner Stern layer and the diffuse layer. Although ions in the outer Stern layer are hydrated ions and cannot enter the inner stern layer, they are, however, well-attached to the mineral surface (Bard et al. 1980).

In most cases, the charge in the Stern layer cannot really equilibrate the mineral surface charge. Consequently, this unbalanced surface charge gives rise to the diffuse layer, which holds the remaining additional charge in the solution that is necessary to ensure the electrical neutrality of the EDL (Lee et al. 2016, Al Mahrouqi et al. 2017). However, despite the ionic conditions in the Stern layer, the co- and counter-ions in the diffuse layer are not attached to the mineral surface. Moreover, the thickness of the

diffuse layer depends on the aqueous phase concentration and can be several microns in low-concentration solutions. In this case, the small pores of the rocks will be fully occupied by aqueous fluid in the form of the diffuse layer, rather than as bulk fluid (Glover and Jackson 2010).

The decrease in the electrical potential (which is equivalent to the charge distribution), with distance from the mineral surface follows different trends depending on the layer in the aqueous solution. The decrease is linear through the Stern layers; however, it becomes exponential through the diffuse layer and falls to zero in the uncharged solution (i.e. free electrolyte region, Al Mahrouqi et al. (2017)). Zeta potential is measured at the shearing plane separating the regions of attached and unattached ions (e.g. the stagnant and moving fluid).

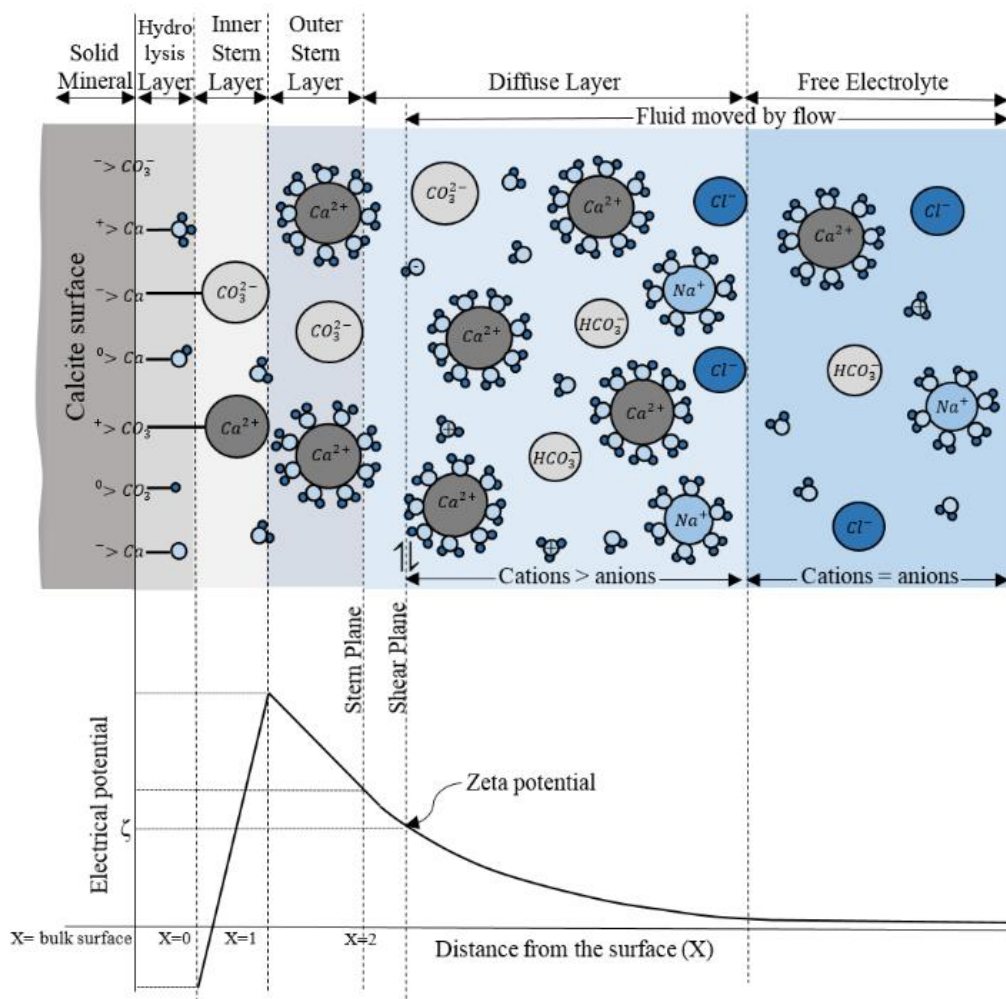


Figure 2-3 Schematic representation of the electrical double layer existing at the interface between the rock matrix and pore water (from Al Mahrouqi et al. (2017)).

### 2.2.2.3 Surface Imaging Tests

Surface imaging techniques, including atomic force microscopy (AFM), scanning electron microscopy (SEM), and nuclear magnetic resonance (NMR) can probe changes in the characteristics of rock surfaces that occur due to wettability alteration treatments. Many studies have performed AFM measurements on treated substrates to elucidate wettability changes (Al-Sulaimani et al. 2012, Al-Anssari et al. 2016, Arif et al. 2016d). On the other hand, Schembre et al. (2006) used SEM images to demonstrate the mechanisms of wettability alteration sandstone from oil-wet to water-wet at high temperatures. Al-Anssari et al. (2016) probed the adsorption of silica nanoparticles on calcite surfaces in a study using nanofluid as a wettability alteration agent.

### 2.2.2.4 Spontaneous Imbibition (SI)

*Imbibition* is the process of oil displacement by water. Meanwhile, *spontaneous imbibition* is imbibition that occurs due to capillary action and/or gravity when a core sample or matrix block is immersed or surrounded with brine (Hirasaki and Zhang 2004). The displacement of the non-wetting phase by the wetting phase under stationary conditions can be measured via a spontaneous imbibition test (SI). Wettability of the rock surface controls the relationship between wetting phase saturation and capillary pressure. In water-wet systems, oil is easily displaced by water due to the positive capillary pressure of the water-wet system (Figure 2-4). In contrast, capillary pressure is negative in oil-wet systems, which leads to strong adhesion of oil to the rock surface. Thus, water does not imbibe into an oil-wet porous medium and no displacement of oil occurs.

The spontaneous imbibition test exhibits the influence of gravity and capillary forces through wettability alteration (Li and Horne 2006). The SI test is conducted experimentally by immersing an oil-saturated solid core into water (brine or any treatment fluid) using a graduated cell. An imbibition curve is used to determine the wettability of the rock sample and is evaluated by plotting displaced hydrocarbons versus time. In addition to wetting properties, SI tests can also be used to investigate the influence of operating conditions on oil displacement. Moreover, SI tests can give some other visual information, such as the contribution of the side of the rock sample to oil production. For example, Høgnesen et al. (2006) used an imbibition cell to examine the hydrocarbons produced from the top surface of a rock sample by gravitational forces and the oil produced from the side surface due to capillary forces. Owing to all these factors, SI tests are considered one of the most dependable measures of wettability alteration.

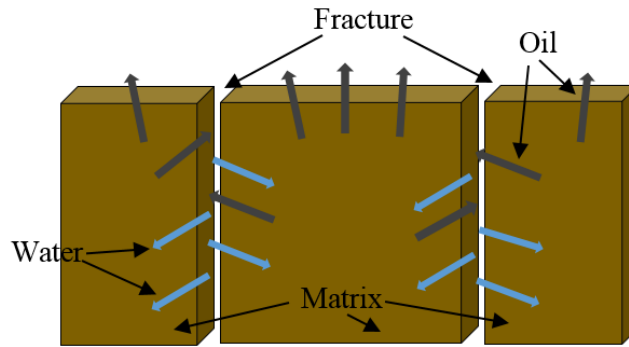


Figure 2-4 Spontaneous imbibition of water from a fracture system into the matrix where it replaces oil

Spontaneous imbibition tests provide a dynamic measurement of wettability. They are superior to static tests of wettability such as contact angle. The dynamic nature of the SI test enables it to estimate alterations in wettability over time under the same or different conditions. For instance, Mohammed and Babadagli (2014) reported SI data for two oil-wet carbonate cores immersed in different aqueous phases (i.e. DI water and 1.0 wt% CTAB solution). Their results revealed that no significant displacement of oil by DI water was recorded owing to the oil-wet nature of the core sample that prevents the spontaneous imbibition of water to the porous medium. They also demonstrated that the very low ratio ( $\leq 2\%$  PV) of oil displaced by water was related to the gravitational forces that are firmly repelled by negative capillary forces. On the other hand, for the first 10 days after immersion in CTAB, the core sample showed a similar trend to being immersed in water with a higher oil displacement (2.5–3.5% PV). This slow recovery was also driven by gravity and the relatively high oil-displacement (compared to DI water) was related to the limited contribution from capillary imbibition. However, after 10 days, a sudden acceleration of oil displacement was observed due to the alteration of wettability by surfactant, which improves the capillary imbibition intake. Thus, the wettability of the core sample changed with time, leading to increased spontaneous imbibition. The dynamic nature of SI test helps to recognise the trend of wettability alteration at different stages of immersion in the displacing fluid. Despite the potential advantages of SI tests, some limitations can affect the accuracy of the measurements. The recovered oil, for example, is certainly not reported at the exact time of displacement. Experimentally, additional time is probably required for droplets that are displaced from the porous medium to detach from the surface of the core.

#### 2.2.2.4.1 Amott Method

The Amott method (Amott 1959) was the first quantitative measurement of rock core wettability. It used a sequence of imbibition and forced displacement tests with the following steps

- 1) Centrifuge of the core under brine to obtain the residual oil saturation
- 2) Spontaneous imbibition of oil to reduce the volume of brine displaced
- 3) Forced displacement of brine by oil under centrifuge to evaluate the volume of brine displaced

- 4) Spontaneous imbibition of brine to measure the volume of oil recovered
- 5) Forced displacement of oil by brine by centrifuging to record the volume of oil displaced

The ratio of the displaced volume by spontaneous imbibition ( $\delta_o$ ) and forced displacement ( $\delta_w$ ) provides an indication of core wettability.

$$\delta_o = \frac{V_{wsp}}{V_{wt}}$$

where  $V_{wsp}$  is the brine volume that is displaced by spontaneous imbibition and  $V_{wt}$  is the brine volume displaced by both oil imbibition and forced displacement.

$$\delta_w = \frac{V_{osp}}{V_{ot}}$$

where  $V_{osp}$  is the oil volume that is displaced by spontaneous imbibition and  $V_{ot}$  is the oil volume displaced by both water imbibition and forced displacement.

One problem with the Amott method is its insensitivity near neutral wettability, which makes it necessary to apply a modification to the method. The Amott-Harvey method is a modified Amott method that overcomes this weakness and introduces a wettability index ( $I_{a-h}$ ) that combines  $\delta_o$  and  $\delta_w$ .

$$I_{a-h} = \delta_w - \delta_o = \frac{V_{osp}}{V_{ot}} - \frac{V_{wsp}}{V_{wt}}$$

Table 2-2 Range of wettability indexes for the Amott and Amott-Harvey methods

	Water-wet	Neutral-wet	Oil-wet
Amott wettability index displacement by water ratio	> 0	0	0
Amott wettability index displacement by oil ratio	0	0	> 0
Amott-Harvey wettability index	$0.3 \leq I_w \leq 1.0$	$-0.3 \leq I_w \leq 0.3$	$-1.0 \leq I_w \leq -0.3$

### 2.2.3 Interfacial Tension (IFT)

The interfacial tension (IFT) between oil and water is one of the key factors that controls the capillary forces acting on trapped oil within reservoir rocks. The basic requirement of EOR processes is to achieve ultralow IFT, since the difficulty of emulsifying oil into the aqueous phase is the main cause of the low displacement efficiency of hydrocarbon (Chen and Zhao 2015). Thus, many EOR methods rely on reducing the oil-water IFT to extremely low values (e.g.  $\leq 10^{-4}$  dyne/cm) to overcome

the capillary forces that trap the residual oil (Curbelo et al. 2007). Shah et al. (1977) investigated interfacial tension behaviour in oil and aqueous phases and reported that oil recovery is fundamentally dependent on the miscibility mobility control of the oil/water/rock interface. It is well known that the addition of surfactant significantly decreases the interfacial tension between crude oil and formation water. This lowers the capillary forces and facilitates the mobilisation of oil and, thus, enhances oil recovery. A synergistic IFT effect takes place between the ionized acid species produced from crude oil and surfactant introduced during surfactant flooding (Zhang et al. 2002, Chu et al. 2004).

#### **2.2.4 Permeability**

Permeability is a fundamental property of porous media (rock) and can broadly be defined as the ability of fluid (gas/liquid) to flow through porous media. Many early engineering and geological studies investigated the reduction in permeability (e.g. formation damage) resulting from the exposure of reservoir formations to relatively fresh water, i.e. water with salinity lower than that of the connate water (Jones Jr 1964, White et al. 1964, Mungan 1965). This is a major issue in the oil industry, since fresh water is used very often during the drilling, completion and production stages. Jones Jr (1964) revealed that ultimate productivity could dramatically decrease when the formation damage is severe, particularly at low pressures. Moreover, the reduction in permeability increases the operation costs due to the increase in the injection pressure and the time required for waterflooding. Mechanistically, formation damage is the result of the obstruction of flow channels by clays or other mineral fines dispersed by water (Jones Jr 1964, Tavenas et al. 1983, Anderson 1986, Anderson 1987a, b, Sharma and Yortsos 1987). Thus, the potential implementation of nanofluids in the oil industry adds challenges to permeability loss in porous media since nanoparticles ( $\geq 100$  nm) can accumulate and block the small passages. Permeability is a characteristic of a single-phase flow in porous media; however, in the case of multi-phase flow, the term *relative permeability* must be used.

##### **2.2.4.1 Relative Permeability**

Relative permeability is the direct measure of a porous system's ability to conduct one fluid in the presence of one or more other fluids. This flow property is the composite influence of wettability, pore geometry, fluid distribution and saturation history (Anderson 1987b). Wettability has a significant impact on relative permeability, because it is key to controlling the flow, location and spatial distribution of oil and liquid in porous media (Craig 1971). Mechanistically, for strongly water-wet cores, the wetting phase (water) occupies the small pores and forms a thin layer (film) over the rock surface. Meanwhile, oil (the non-wetting phase) occupies the centres of the larger pores. This is the most energetically favourable fluid distribution in the case of water-wet cores. Thus, any oil located in the small pores will be displaced by spontaneous water imbibition into the centre of the larger pores, which occurs due to lowering of the energy of the system (Anderson 1987b).

Under single-phase flow at Reynolds numbers less than 1.0, the volumetric flux ( $u$ ) of a fluid flowing in a permeable medium follows Darcy's law:

$$u = -\frac{k}{\mu} \nabla \Phi \quad \text{Eq. 2-1}$$

Darcy's law is modified for multiphase flow in permeable media by adding a relative permeability term ( $k_{rj}$ ) defined in terms of the effective permeability of each phase  $j$ :

$$k_j = k_{rj} k \quad \text{Eq. 2-2}$$

$$u_j = \frac{k_{rj} k}{\mu_j} \nabla \Phi_j \quad \text{Eq. 2-3}$$

Under two-phase flow, the relative permeability of phase  $j$  is a function of its own saturation (Figure 2-5). The shape of the relative permeability curves depends on the pore morphology, wettability and interfacial tension.

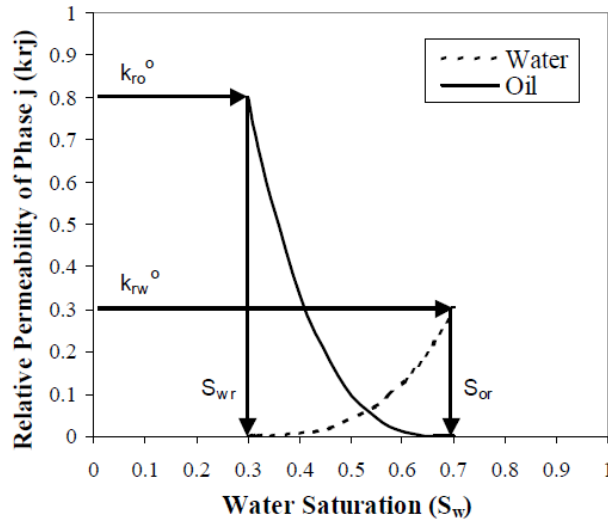


Figure 2-5 A typical relative permeability curve for two-phase flow of an oil-water system. The relative permeability of water is zero at the residual water saturation ( $S_{wr}$ ) and increases until it reaches the residual oil saturation ( $S_{or}$ ), at which point water is the only flowing phase referring to the endpoint relative permeability ( $k_{rw}^o$ ). Similarly, the relative permeability of oil is zero at  $S_{or}$  and increases to  $S_{wr}$  to reach the endpoint relative oil permeability ( $k_{ro}^o$ ).

### 2.2.5 Capillary and Gravitational Forces

In porous media, the displacement of fluids is communally controlled by capillary forces ( $F_{capillary}$ ), gravity forces ( $F_{gravity}$ ), and viscous forces ( $F_{viscous}$ ). The rate of hydrocarbon production from oil reservoirs is determined by the interaction between these forces.

$$F_{capillary} = \frac{2\gamma_{ow} \cos \theta_c}{r} \quad \text{Eq. 2-4}$$

$$F_{gravity} = \Delta\rho gh \quad \text{Eq. 2-5}$$

Where  $\gamma_{ow}$  is the interfacial tension between oil and water,  $r$  is the pore radius, and  $\theta_c$  is the water contact angle. Two parameters,  $\gamma_{ow}$  and  $\theta_c$ , should be modified to improve the capillary forces.

The relationship between these forces can be described by the capillary number ( $CN$ ) and inverse bond number ( $BN^{-1}$ ).

$$CN = \frac{F_{viscous}}{F_{capillary}} \quad \text{Eq. 2-6}$$

$$BN^{-1} = \frac{F_{gravity}}{F_{capillary}} \quad \text{Eq. 2-7}$$

The dominant force in Eqs. 2-6 and 2-7 is the capillary force. Factors including oil-water interfacial tension, water contact angle and pore radius control the value and direction of the capillary force. In water-wet formations, capillary number is the major determinant of hydrocarbon production, while viscous forces determine the dynamics of oil displacement. Increased capillary number due to the reduction of capillary forces is crucial for higher recovery rates, since it decreases the amount of residual oil. Capillary forces decrease with oil-water interfacial tension. For mixed-wet, oil-wet and, particularly, naturally fractured carbonate reservoirs, the fracture volume is low and the high pore volume matrix shows extremely low permeability. Thus, high viscous forces cannot be applied effectively and viscous displacement is insufficient. In this case, the fluid dynamics are dominated by gravity and hydrocarbon recovery is controlled by the inverse bond number ( $BN^{-1}$ ).

It is clear that capillary forces can be positive or negative, and can change from one sign to another depending on the contact angle and, thus, the wettability of the reservoir. For water-wet rock, the contact angle should be  $> 90^\circ$  ( $\cos\theta_c \geq 0$ ), consequently, capillary forces initiate and continue water imbibition leading to movement of oil in a counter-current pattern. In contrast, for oil-wet samples, the contact angle is higher than  $90^\circ$  ( $\cos\theta_c \leq 0$ ) and, thus, no capillary imbibition will occur.

Surface wettability ( $\cos\theta_c$ ) and oil-water interfacial tension ( $\gamma_{ow}$ ) control the value and direction (sign) of capillary forces. Lower contact angles are favourable for efficient capillary imbibition; however, interfacial tension must be kept at the highest value. Wettability alteration processes in oil reservoirs are complicated, since surface wettability and oil-water interfacial tension are dependent factors, and many wettability modifier agents reduce the oil-water interfacial tension as they act to change the wettability towards a more water-wet status. This complicated interaction can be demonstrated by Young's equation, which measures the contact angle from oil-solid, oil-water and water-solid interfacial tensions.

$$\cos\theta_c = \frac{\gamma_{os} - \gamma_{ws}}{\gamma_{ow}} \quad \text{Eq. 2-8}$$

Where  $\gamma_{os}$  is the oil-solid interfacial tension,  $\gamma_{ws}$  is the water-solid interfacial tension, and  $\gamma_{ow}$  is the oil-water interfacial tension. Considering the capillary force equation

and Young's equation shows that the reduction in oil-water interfacial tension will directly reduce capillary forces. However, at the same time, this reduction in oil-water interfacial tension will reduce the water contact angle according to Young's equation and thus increase the capillary forces. Also, lower  $\theta_c$  can be achieved via decreasing the  $(\gamma_{os} - \gamma_{ws})$  value, and this is can be done by increasing the affinity of rock to water rather than to oil.

Reduction of oil-water interfacial tension, which reduces capillary forces, facilitates the displacement of oil by gravity. Many studies have investigated the process of capillary imbibition, which is mainly driven by both wettability and interfacial tension at different values of the inverse bond number ( $BN^{-1}$ ). Schechter et al. (1994) tested the effect of different oil-water interfacial tension values on the capillary imbibition process. Their results revealed that at high  $\gamma_{ow}$  values (38 mN/m), an early counter-current imbibition process can occur, and oil was displaced from the lateral sides of the core sample. In the case of intermediate values of  $\gamma_{ow}$  (1 mN/m), production of oil was noticed from all sides of the sample, which is indicative of the collaborative effects of capillary and gravitational forces on hydrocarbon displacement. A probable enhancement in oil production was recorded compared to the case with high  $\gamma_{ow}$ . Meanwhile, at low  $\gamma_{ow}$  (0.1 mN/m), greater oil recovery was recorded but at a slower rate compared to the other two cases. Thus, higher oil recovery is acquired at lower interfacial tension owing to the reduction of residual oil.

Fluids flow in porous media at low interfacial tensions as determined by gravity; thus, oil production can be increased by increasing the gravitational forces. Moreover, reduction of  $\gamma_{ow}$  reduces residual oil and, thus, enhances oil recovery. Al-Lawati and Saleh (1996) discussed the decrease in residual oil when the interfacial tension is lower. They explained that the relative permeability of oil/water is low for the duration of the counter-current flow, and both oil and water repel each other's flow. However, with gravitational imbibition, the flow is of the co-current type with high relative permeability of oil and water. In this case, fluid flow is governed by the permeability of the core and the difference in fluid densities. Thus, at intermediate values of  $\gamma_{ow}$ , both gravitational (in a co-current manner) and capillary forces contribute to the imbibition process. This phenomenon explains the higher rate of imbibition at intermediate interfacial tensions despite the higher final amount of oil recovered at low interfacial tension (Morrow and Mason 2001).

Greater reduction in interfacial tension may support or reduce spontaneous imbibition subject to the influence of gravity. This contribution can accelerate the rate of imbibition; however, the total displaced oil in this case will be significantly less than that for low interfacial tension (Morrow and Mason 2001). Thus, there is a critical interfacial tension ( $\gamma_{ow_{critical}}$ ) below which a considerable amount of trapped hydrocarbon can be released from the porous medium (Saleh and Graves 1993). Mechanistically, when the interfacial tension of the oil/aqueous phase system is  $\leq \gamma_{ow_{critical}}$ , hydrocarbon drops can elongate and divide into smaller drops. This deformation in the shape and size of hydrocarbon drops facilitates the releasing and flowing out of these drops through even smaller pore throats. In line with this, Morrow and Mason (2001) revealed that higher ultimate oil recovery can be achieved with

lower interfacial tension. Thus, using surfactant solutions can enhance  $\gamma_{ow}$  reduction, thus allowing the displacing solution to reach the inaccessible parts of the matrix.

The above discussion states that gravitational forces can contribute to oil production at intermediate and low oil-water interfacial tensions. The strength of gravity is determined by the difference in fluid density ( $\Delta\rho$ ). Thus, in heavy and extra heavy oils, gravity forces will be quite low due to small differences in the densities of crude oil and formation fluid. Meanwhile, the gravity force is the dominant mechanism for fluid flow during ionic surfactant flooding (Høgnesen et al. 2006). On the other hand, Al-Hadhrami and Blunt (2000) revealed that gravitational forces can contribute in displacing oil from the lower parts of a reservoir during the thermal treatment of carbonate reservoirs. In this case, the gravitational force in the top part of the oil reservoir is not sufficient for the spontaneous displacement of oil. Thus, the activation of capillary forces is essential for enhancing oil recovery and can be supported by thermal treatment due to viscosity reduction.

Ionic surfactants have been studied as enhanced oil recovery agents. Cationic and anionic surfactants adopt different mechanisms to improve hydrocarbon displacement. The main role of cationic surfactants in oil recovery is to change surface wettability towards being more water-wet, which supports spontaneous capillary imbibition (Standnes and Austad 2000). On the other hand, anionic surfactants act to reduce, but not eliminate, the negative capillary forces by reducing the oil-water interfacial tension, which eventually enhances gravitational imbibition (Hirasaki and Zhang 2004). Many factors determine the optimisation of cationic and anionic surfactants for higher hydrocarbon production from carbonate reservoirs. Further, it is essential to understand the suitable mechanism that leads to higher oil production depends on the type of oil (i.e. heavy or light), and reservoir characteristic (i.e. permeability, size of matrix, current wettability status, and boundary conditions).

Boundary conditions, for example, can significantly affect the contribution of gravity and capillary forces on incremental oil recovery. Also, differences in oil and water densities can limit the contribution of gravitational forces. Høgnesen et al. (2006), as stated before, declared that for heavy and extra heavy oil where the difference in densities is almost zero, the gravitational force should not be overestimated. In such cases, the density must be reduced first to activate the contribution of gravitational force. In addition, capillary forces can be enhanced by viscosity reduction via thermal treatment of oil reservoirs. However, the synergy of capillary and gravitational forces should be evaluated under the effect of increased temperature.

### **2.3 Enhanced Oil Recovery (EOR)**

Enhanced oil recovery processes aim to recover large amounts of trapped hydrocarbons in reservoirs after primary and secondary oil recovery methods have been used. Thomas (2008) reported that nearly  $2.0 \times 10^{12}$  barrels of conventional oil and  $5.0 \times 10^{12}$  barrels of heavy oil will remain in reservoirs worldwide after primary and secondary oil recovery (traditional) methods have been exhausted. Primary oil

recovery is the process of extracting oil from natural rises of hydrocarbons to the surface or via pumps and other artificial instruments. However, this technique is very limited in productivity potential, since only around 5–15% of the oil in place can be recovered by primary methods. This limitation in oil recovery depends on the reservoir pressure increase needed for secondary oil recovery, which involves the injection of gas or water to displace the oil and force it to travel from its resting place to the surface. Secondary oil recovery is typically successful in recovering an additional 30% of the oil in place, and no more oil can be recovered from these reservoirs without applying additional enhanced oil recovery techniques. Enhanced oil recovery offers many different options since each reservoir is unique in its degree of complexity. Moreover, regulatory and economic limitations are also unique to particular geographical regions and specific sets of operational conditions. Enhanced oil recovery implies the mobilisation of retained oil in porous media by thermal or non-thermal methods, mainly gas injection and chemical techniques. In addition, there are other less applicable methods (Figure 2-6). The challenge of identifying the most applicable process for maximising hydrocarbon recovery can be achieved by considering geological knowledge and the inherent benefits of each EOR process (Buenaventura et al. 2014). Thus, the required EOR techniques vary considerably depending on different hydrocarbons (e.g. light or heavy oils) and reservoir characterisations, e.g. reservoir geology and fluid properties (Babadagli 2003). A general classification of these techniques is listed in Figure 2-6. Thus, the optimisation and combination of methods depend on many technological and economic considerations (Thomas 2008).

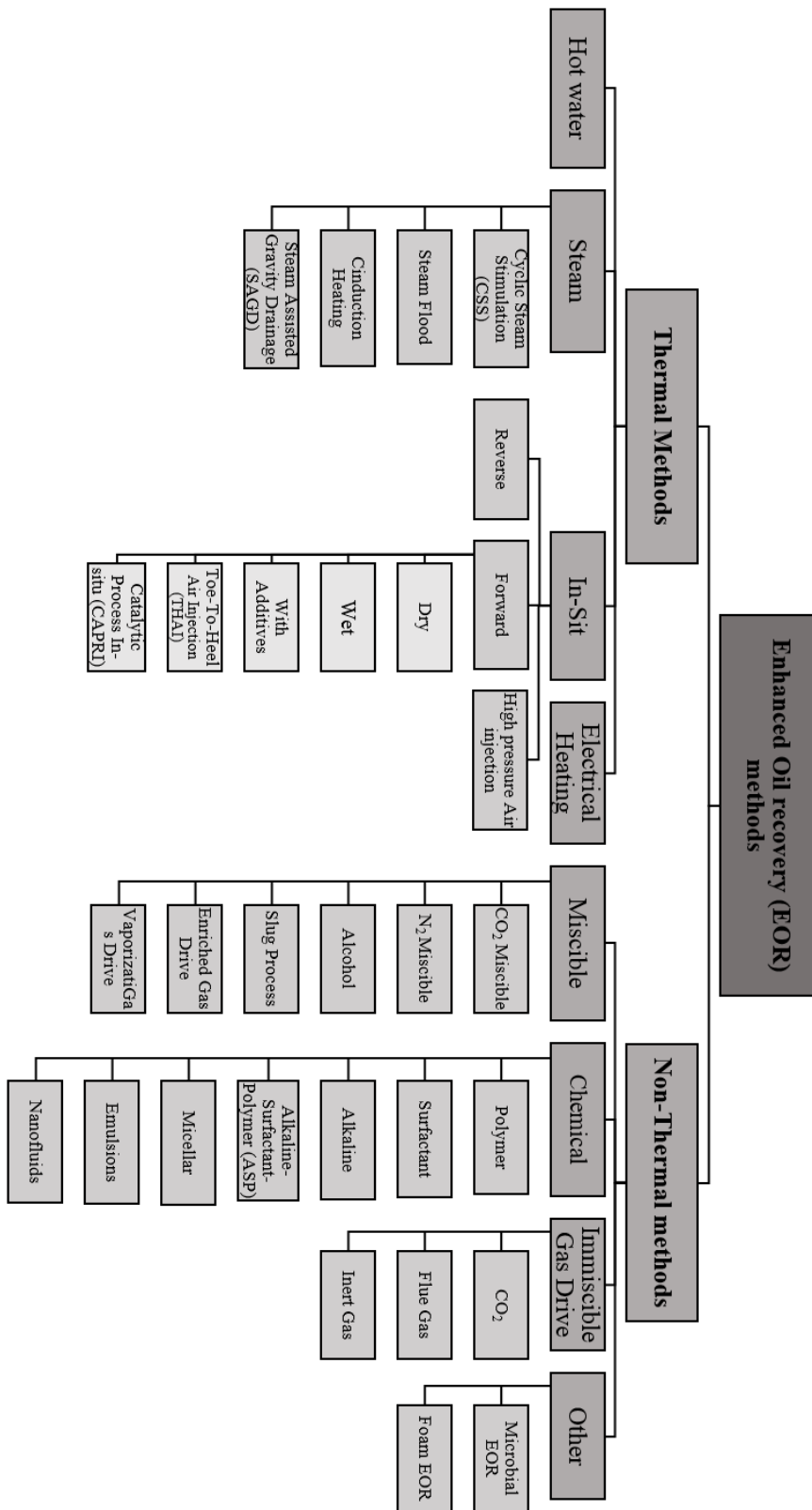


Figure 2-6 Classification of enhanced oil recovery methods (reproduced after Thomas (2008))

### **2.3.1 Thermal Methods**

Thermal EOR techniques supply heat to hydrocarbon reservoirs to reduce the viscosity of the crude oil, allowing easier flow of hydrocarbons to the surface. Steam is commonly introduced into oil reservoirs, which heats the crude oil. In some cases, fire flooding or in-situ burning are used to heat the rest of the oil (Hart 2014). These techniques are mainly used for heavy oils and tar sands; however, thermal treatments are also applicable to light oils in certain circumstances. Among the thermal techniques, steam-based methods are more commercially feasible than others. These techniques have been widely applied in Canada, the USA, Venezuela, Indonesia and other countries (Thomas 2008).

### **2.3.2 Gas Injection**

Gas injection is an EOR method that involves injecting gas, mainly carbon dioxide (CO<sub>2</sub>) or, less commonly, nitrogen and some inert gases, via an injection well to displace remaining oil after primary and secondary methods have been used. It is essential to distinguish between gas injection, which is an EOR technique, and gas lift, which is a type of artificial lifting during primary oil recovery. Practically, the most favourable process, technically and financially, consists of injecting CO<sub>2</sub> gas to increase the pressure of the oil reservoir. Although generalised miscibility is unlikely to occur due to low reservoir pressure, it is found that CO<sub>2</sub> can achieve multiple contact miscibility in some parts of reservoirs. Moreover, the injected gas can help to change the flow path of oil by contact with new oil (Buenaventura et al. 2014).

### **2.3.3 Chemical Methods**

Chemical EOR techniques involve rock wettability alteration and reduction of oil-water interfacial tension (IFT). Moreover, there are other potential EOR techniques such as mobility, which is controlled by a high viscosity agent, and thermal treatments that reduce the viscosity of oil by increasing the reservoir temperature. In addition, the use of microbes for oil recovery from depleted reservoirs is another example of a chemical EOR application. Tertiary oil recovery can include one or more EOR techniques. Rendering oil-wet rocks water-wet is the key to accelerating oil recovery and improving the recovery factor (Wu et al. 2008, Gupta and Mohanty 2010), which can be accomplished in several ways. The success of EOR and carbon capture projects requires the use of reliable, scalable and economical approaches in harsh subsurface conditions and, particularly, at high salinities, noting that the salinity of reservoirs varies significantly and can reach very high levels (Dake 1978, Krevor et al. 2016).

Thus, for incremental hydrocarbon production from oil-wet reservoirs, several steps should be systematically followed:

1. Understand the mechanisms that have caused the oil-wet condition of the reservoir.
2. Evaluate the characteristics of the reservoir, including the current wetness condition and permeability.
3. Determine the characteristics of the fluid, including density and viscosity.
4. Investigate the interplay between all the potential forces in the reservoir conditions, including gravity, viscosity and capillary forces.
5. Specify the properties that need to be changed, such as wettability, density, viscosity, etc.
6. Examine wettability alteration techniques considering the type of formations and the mechanisms that have altered the original water-wet condition to being mixed- or oil-wet.
7. Optimise the mechanisms of wettability alteration.

## 2.4 Wettability Alteration

Wettability alteration, in the subsurface industry, is the procedure of rendering oil-wet formations water-wet. The purpose of this rendering modification is to recover the remaining oil during primary and secondary (waterflooding) recovery processes. Previous well-established studies have declared that the restoration of rock wetness to being water-wet enhances the ratio of oil recovered (Rostami Ravari et al. 2011). Similarly, in gas condensate reservoirs, wettability shifts from oil-wet to water-wet prompts an increase in relative gas permeability, leading to higher deliverability from the gas well (Kewen and Abbas 2000).

The major effect of rock wetness on hydrocarbon recovery techniques, including waterflooding, was addressed early on (Wagner and Leach 1959). Moreover, waterflooding techniques during secondary oil recovery are entirely controlled by the wettability of the reservoir. Basically, previous studies have reported that hydrocarbon recovery during waterflooding from an oil-wet reservoir is around 15% lower than that recovered from water-wet reservoirs (Wagner and Leach 1959). However, strongly water-wet or even water-wet oil reservoirs are uncommon. Typically, the majority of reservoirs show some degree of oil-wetness. Practically, wettability can be considered neutral if the rock has a similar affinity for water and oil. In addition, when the formation exhibits heterogeneity in water or oil wetness, the reservoir is defined as a *mixed-wet reservoir* (Salathiel 1973).

Despite general agreement about the favourable alteration of strongly oil-wet reservoirs to water-wet formations for incremental oil production, there is no certainty about the optimal degree of alteration for hydrocarbon recovery. Salathiel (1973), for example, stated that mixed-wet reservoirs could produce more oil during waterflooding than that produced from water-wet reservoirs, depending on field production data. Furthermore, Jadhunandan and Morrow (1995) revealed that

optimum oil recovery during water injection was achieved from neutral-wet formations rather than strongly water-wet ones.

Alteration of wettability from strongly oil-wet to neutral and then water-wet changes the balance of capillary and gravitational forces in a porous medium. Enhanced oil recovery by wettability shifting can be achieved by different mechanisms. For instance, by shifting wettability to neutral-wet in order to reduce and then eliminate capillary forces. Thus, gravitational forces can play a crucial role in oil displacement for neutral-wet formations. Here, the contact angle decreases to a smaller value (but not below  $90^\circ$ ) and wettability alteration has no direct influence on hydrocarbon displacement. Mechanistically, wettability shifting reduces negative capillary pressure and thus helps to enhance oil recovery by the effect of gravity. Further shifting of wettability towards being strongly water-wet promotes capillary imbibition. Thus, both capillary and gravitational forces potentially contribute to oil displacement in cases where the contact angle is less than  $90^\circ$ .

#### **2.4.1 Interaction of Hydrocarbon/Aqueous Phase/Rock in Oil Reservoirs**

It is common knowledge that oil reservoirs were initially occupied by formation brine prior to later relocation by oil. However, owing to the water-wet state of common minerals that form reservoir rock, including carbonate and silica, invasion of oil to a porous medium only partially displaces the water (Abdallah et al. 2007). Thus, the rock surface is covered with a thin layer of water that isolates the formation from oil. Consequently, the final wetness state of the reservoir depends totally on the preservation of this brine film. Destabilisation of the water layer due to interactions between solid surfaces, hydrocarbon and brine leads to changes in reservoir wettability to oil-wet conditions (Buckley et al. 1989). Mechanistically, when the attractive forces between brine/rock and brine/hydrocarbon interfaces overcome the repulsive forces, oil will consequently come into contact with the rock surface owing to the collapse of the water layer. In EOR, wettability alteration of reservoirs is the reverse of the technique used to restore original hydrophilic wetness. Consequently, the first step of any successful wettability alteration process is to understand the mechanisms of the initial alteration of wettability to oil-wet status.

It is well agreed that rock surfaces can adsorb some components from heavy oil, which reverts the wettability of such rocks from the original water-wet status to oil-wet or strongly oil-wet status (Buckley et al. 1998b, Gomari and Hamouda 2006). Rock mineralogy controls which component of heavy oil can be adsorbed onto a rock surface and, thus, the degree of wettability shifting. Carbonate surfaces are positively charged under reservoir conditions (Alroudhan et al. 2016); thus, they can adsorb acidic components (Wolthers et al. 2008) including naphthenic acid (Hoeiland et al. 2001, Wu et al. 2008) or carboxylic acids (Buckley et al. 1998b) when they come into contact with crude oil. Silica surfaces, on the other hand, are negatively charged under reservoir conditions and can only adsorb basic components from crude oil. Anderson (1986) demonstrated that a reservoir can have homogeneous wetness that may be water-wet, intermediate-wet and oil-wet, or may be at an in-between wetness status

depending on the brine/rock/oil interactions. However, it is also possible for the reservoir to exhibit mixed-wet states. In this case, different parts of oil reservoirs can have different states of wettability (Salathiel 1973).

#### 2.4.2 Mechanisms of Wettability Alteration

Responses of oil reservoirs to waterflooding depend on their wettability state. It is well known that the recovery rate declines when reservoirs are oil-wet. Thus, most EOR projects improve hydrocarbon production via alteration of the wetness to a water-wet state. Several thermal and chemical EOR techniques have been proposed to shift the wettability of oil reservoirs to being more oil-wet. Extension of wettability shifting by different techniques depends on the impact of each technique on the hydrocarbon/brine/rock properties. Also, it is important to know that the interactions between crude oil, rock and brine depend on the composition of formation brine and crude oil, as well as the rock mineralogy and other reservoir properties. Thus, to change the wetting state of oil-wet rock to being more water-wet, it is essential to understand the mechanisms that altered the original water-wet rock to being oil-wet.

Chemical agents known as *wettability modifiers* can be used in the EOR process in oil-wet reservoirs according to two mechanisms: *cleaning* and *coating* (Giraldo et al. 2013). Normally, cleaning mechanisms are associated with surfactant-derived wettability alteration. For example, cationic surfactants desorb the oil layer from an oil-wet surface, rendering the rock water-wet. Coating is a method of coating an oil-wet surface with water-wet materials after displacing the oil layer. For instance, Al-Anssari et al. (2016) demonstrated that hydrophilic silicon dioxide nanoparticles can be adsorbed on oil-wet rock to form a nano-texture that coats the oil-wet surfaces. Thermal EOR techniques are another example of cleaning mechanisms, where oil-wet fines are detached from an oil-wet surface by the effect of high temperature (Schembre et al. 2006). Further, both cleaning and coating mechanisms can synergistically act on the EOR process when a suspension of nanoparticles and surfactant are used to alter the wettability of an oil-wet surface (Sharma et al. 2014b, Sharma et al. 2015b).

Optimisation of chemical EOR processes mainly depends on the mechanism that is suitable for each formation type. Anionic surfactants, for instance, are typically used in sandstone reservoirs as wettability modifiers, while cationic surfactants are more frequently used with carbonate surfaces. In general, wettability alteration process in oil-wet reservoirs is important process for all type of oil reservoirs. However, this process is crucial and key in naturally fractured carbonate reservoirs (NFCRs) that contain more than half of the known remaining oil in the world. Characteristically, most of the NFCRs are intermediate (neutral) or oil-wet. Thus, primary and secondary recovery techniques (conventional waterflooding) usually fail to displace oil, and their productivity is low due to high capillary pressure. Typically, NFCRs are composed of a low permeability matrix and fracture system. The majority of the hydrocarbon is tightly locked inside the matrix by high capillary pressure. Thus, only oil from the fractures is produced as water does not spontaneously imbibe into the oil-wet matrix (Al-Anssari et al. 2016). Wettability alteration towards being more water-wet can

promote the imbibition process, which is the best natural way to displace retained hydrocarbon from the matrix.

Knowledge of how the formation became oil-wet can help to restore the reservoir. Therefore, all potential mechanisms of crude oil/brine/rock interaction are considered precisely. Moreover, understanding how the principal forces, i.e., capillary, gravity, and viscosity forces, contribute to the wettability alteration process is key to designing an EOR project. Thus, we have briefly discussed the interactions among these forces. In addition, chemical alteration methods, i.e., surfactants, high and low pH solutions, low salinity water and particularly nanofluids were reviewed. Furthermore, opportunities and challenges in wettability alteration were discussed. We also reported the results of wettability alteration experiments in which silica nanoparticles were used to formulate a nanosuspension and modify the wetness state of oil-wet calcite surfaces.

Surface hydrophobicity can be increased or decreased using different wettability alteration techniques, such as by increasing surface roughness (Andreas et al. 2007) or coating surfaces with low surface energy materials, which is useful for changing surfaces to a super-hydrophobic state (Feng et al. 2002).

### **2.4.3 Wettability Alteration by Chemical Methods**

Several chemical methods have been proposed to render the wettability of oil-wet reservoirs to water-wet status. Low salinity water, alkaline solutions, smart water, cationic and anionic surfactants, and nanofluids are examples of the chemical techniques used in EOR. The optimisation of these techniques depends on reservoir and fluid characterisations. Below, we briefly discuss the application of these methods.

#### **2.4.3.1 Low Salinity Water**

Flooding with low salinity brine is the lowest-cost EOR method. Wettability alteration is an effective mechanism in low salinity injection applications, and leads to higher hydrocarbon recovery. Early studies revealed that injecting low salinity water enhances spontaneous imbibition, consequently leading to higher hydrocarbon recovery (Tang and Morrow 1996, Tang and Morrow 1999, Tang and Morrow 2002). Nine years later, Morrow and Buckley (2011) confirmed that intermediate-wet small particles, which are potentially responsible for the oil-wet condition of reservoirs, can be detached from surfaces by low salinity water injection. Earlier, Vledder et al. (2010) observed the same effect of low salinity water and showed that despite the increase in pH values during low salinity water injection owing to ion exchange, the increase in oil recovery is mainly related to the effect of low salinity water. Also, Berg et al. (2010) reported that the amount of oil displaced from clay surfaces using low salinity water (2 g/L) was higher than that displaced by high salinity water (25.95 g/L). They designed an open flow model to monitor the displacement of oil drops that were attached to clay after flooding with water of different salinities. They argued that the capability of water to minimise the adhesion forces between oil droplets and solid particles increases as salinity decreases. According to their visual observations, Berg

et al. (2010) suggested two potential scenarios for oil detachment from solid surfaces (Figure 2-7). The principle of their experiments demonstrated that oil droplets attach to clay particles that anchor on the solid substrate under high salinity conditions. Flowing of low salinity water will shift the wettability status, leading to detachment of oil droplets due to breaking of the bonds between oil and clay. The second potential scenario is the release of clay layer(s) together with oil droplets. They also argued that this is a wettability alteration phenomenon, since a more hydrophilic surface was left behind. Moreover, the total detachment of clay particles attached to oil droplets left a more hydrophilic surface (Figure 2-7, right).

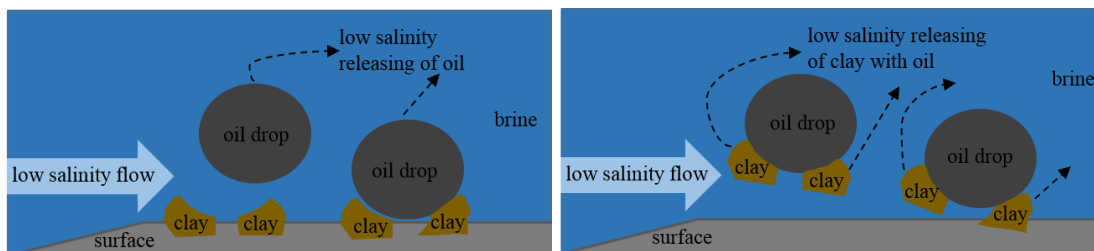


Figure 2-7 Potential scenarios after low salinity waterflooding: (left) release of oil droplet from clay particles anchored on the solid surface; (right) total detachment of clay particles attached to oil droplets.

Spontaneous imbibition tests by Morrow and Buckley (2011) with water of various salinities showed that, in addition to a higher recovery rate, ultimate hydrocarbon recovery was also greater with low salinity water. Similarly, results of a study by RezaeiDoust et al. (2009) showed the same effect of low salinity water on both recovery rate and ultimate oil recovery. Mechanistically, lowering the salt concentration of water increases the solubility of organic components and, thus, accelerates the detachment of these materials from rock surfaces into the aqueous phase (Tang and Morrow 1999). Moreover, injection of low salinity water decreases the zeta potential of solid surfaces, which reduces the attractive forces between the acidic components of the oil and the rock surface (Nasralla et al. 2013). Thus, the composition of oil, in addition to rock mineralogy, can significantly affect the efficiency of wettability change by low salinity water.

A field-scale study was conducted by Vledder et al. (2010) to investigate the effect of low salinity water (river water with a salinity around 0.2 mg/L) on oil recovery from a sandstone reservoir. They stated that up to 15% incremental hydrocarbon recovery can be reached in sandstone formations after low salinity water injection. Carbonate reservoirs, however, have stronger adhesion forces between rocks and adsorbed materials, and the injection of low salinity water is insufficient to alter the wettability of oil-wet carbonate reservoirs.

#### 2.4.3.2 Smart Water

Water with a customised composition that has specific properties and serves particular applications is called *smart water* (Strand et al. 2008, RezaeiDoust et al. 2009, Fathi et al. 2011). In the oil industry, smart water refers to the pumping of water with

regulated acidity and brine composition to modify the wettability of oil reservoirs towards a more water-wet status. The pioneering study by Yildiz and Morrow (1996) showed that the ionic composition of injected brine significantly influences oil recovery. Moreover, Strand et al. (2006) demonstrated that the addition of different salts, acids or basic chemicals can successfully and efficiently change the wettability of sandstone reservoirs. Many other studies have demonstrated that the modification of injected water properties can enhance oil recovery by wettability alteration, even from carbonate reservoirs (Webb et al. 2005, Lager et al. 2007, RezaeiDoust et al. 2009). Mechanistically, the strength of the adhesion forces of the adsorbed material on the solid surface determines the required composition of water used for wettability alteration. In sandstone, the adsorbed materials weakly stick to rock surfaces, thus, low salinity water can efficiently detach organic materials and transfer them to the aqueous phase (Yildiz and Morrow 1996). For carbonate, in contrast, owing to the stronger adhesion forces of the adsorbed materials, a different composition of injected water is required to alter the wetness of the limestone reservoir (Zhang et al. 2007b, RezaeiDoust et al. 2009, Fathi et al. 2011).

The concentrations of multi-divalent ions, including calcium, sulfate, and magnesium ions, determine the efficiency of injected water for wettability alteration. Calcium ions, for example, can alter or change the wettability of limestone reservoirs towards being more water-wet. Magnesium and sulfate ions, in contrast, cannot significantly modify the wettability of carbonate formations. However, according to Gupta and Mohanty (2010), a combination of these two ions with calcium ions can enhance water-wetness. Moreover, (Zhang et al. 2007b) revealed that calcium ions can be replaced by magnesium ions. In line with this, using molecular modelling, Sakuma et al. (2014) stated that substitution of  $Ca^{+2}$  by  $Mg^{+2}$  promotes the desorption process of organics from carbonate formations, as does the replacement of  $CO_3^{-2}$  by  $SO_4^{-2}$ . Mechanistically, injection of high salinity seawater into limestone formations will increase the amount of calcium and sulfate ions, leading to higher adsorption of sulfate ions into rock surfaces. Positive sites on carbonate can consequently be minimised, which increases the repulsive forces between carbonate and crude oil. Eventually, sulfate ions will detach carboxylic acids from the carbonate surface, resulting in a more water-wet state.

Previous studies have reported that oil recovery by seawater injection is 40% higher than that by brine solution injection (Zhang et al. 2007b, RezaeiDoust et al. 2009), and sulfate ions play the major role in this enhancement (Strand et al. 2006). In line with this, and according to Strand et al. (2008), oil recovery by multi-divalent ion solutions can be reduced by 15% in the absence of sulfate ions. However, owing to the precipitation of sulfate ions during chemical reaction with calcium ions, formation brine in carbonate reservoirs only has a low concentration of sulfate ions. In a field scale study, Yousef et al. (2012) reported that the residual oil saturation was significantly lower when smart waterflooding was applied instead of conventional seawater flooding. Thus, smart water containing a high sulfate ion concentration is crucial for high oil recovery.

#### 2.4.3.3 Alkaline Solutions (High pH Solutions)

Alkaline flooding can increase hydrocarbon production from both sandstone (Ehrlich and Wygal Jr 1977) and carbonate reservoirs (Seethepalli et al. 2004). The history of alkaline injection dates back to the early 1920s, with origins in the combination of chemistry and reservoir engineering (Leach et al. 1962, Mayer et al. 1983). Wettability shifting, in addition to the creation of in situ-surface active materials, are examples of potential mechanisms for increasing oil recovery (Nelson et al. 1984). Mechanistically, the reaction between an aqueous caustic solution and the acids in crude oil controls the formation of the surface active materials that affect both rock wettability and oil-water interfacial tension (Ehrlich and Wygal Jr 1977). Relative permeability measurements have revealed a significant change in sandstone core wettability—from oil to intermediate and then water-wet status—as a result of flooding with alkaline solution. Moreover, Ehrlich and Wygal Jr (1977) showed that flooding with sodium hydroxide solution enhances hydrocarbon production.

Regulation of acidity was proposed as a method for altering the wetness of oil-wet limestone reservoirs to water-wet status. Originally, carbonate surfaces are water-wet; however, the positive surface charge of carbonate at pH less than 9 (Alroudhan et al. 2016) supports the adhesion of the negative acidic materials in crude oil to the surfaces, which makes them oil-wet. Mechanistically, changing the acidity to neutralize or alter the positive charges of carbonate surfaces will increase the detachment of adsorbed organic components from them due to increased repulsive forces.

Many studies have previously investigated the effect of alkaline flooding on oil recovery. Zhang et al. (2008), for example, studied the influences of several high pH solutions on carbonate reservoirs. Their results indicated that high pH NaOH solutions are very efficient in improving oil recovery. Najafabadi et al. (2008) studied the effect of alkali injection after waterflooding in limestone reservoirs and showed that it can change the wettability of oil-wet limestone to water-wet status. They also demonstrated that the sign of capillary forces transformed to positive; thus, both capillary and viscous forces contribute to oil recovery. Later, in their study of spontaneous imbibition in siliceous shale, Takahashi and Kovscek (2010a) stated that a high pH solution followed by a low pH solution provides the highest efficiency in rendering oil-wet surfaces water-wet. They also reported no influence of neutral pH solutions on wetting status. In a different study by the same authors (Takahashi and Kovscek 2010b), zeta potential measurements on siliceous shale showed no effect of neutral pH solutions on surface wettability. They revealed that the water film of neutral pH solutions is not stable, while high pH solutions can maintain the water layer and thus shift the wetness status towards being more strongly water-wet.

Leach et al. (1962) conducted a practical reservoir trial in the Harrisburg Muddy Oil Reservoir to investigate the feasibility of alkaline flooding for hydrocarbon production. A 2% NaOH solution was injected into several wells prior to waterflooding. The reported data showed gradual increases in oil recovery in many tested wells, which indicates alteration of wettability to water-wet conditions. The researchers also pointed out that restoration of water-wet conditions in oil-wet reservoirs at the early stages of development, before waterflooding, can decrease the residual hydrocarbon to a degree close to that of an originally water-wet reservoir.

#### 2.4.3.4 Surfactants

Surfactant solutions mainly act to reduce oil-water interfacial tension from moderate or low to ultra-low values, and can alter the wettability of oil reservoirs. Surfactants can form different types of microemulsions when mixed with oil and water. The solubility of each phase in the other determines the type of emulsion. Moreover, the salinity of oil/water/surfactant systems can control the type of microemulsion (Kunieda and Aoki 1996), which is very crucial in EOR projects.

The charges of surfactant monomers and rock surfaces determine the spreading of surfactant on the solid surface, which consequently controls the rock wettability. Cationic surfactants contain a hydrophobic tail and a positive hydrophilic head. In contrast, anionic surfactants contain a negative head group, while non-ionic surfactants have no charge. It is well agreed that the injection of surfactant in oil-wet formations can reduce the oil-water interfacial tension and make the wettability more water-wet. Interfacial tension reduction reduces the adhesive forces that hold oil by capillarity action, while shifting of wettability to a more water-wet state can activate the capillary imbibition of water. Previous studies have introduced two mechanisms of wettability alteration, including the formation of a water-wet layer over an oil-wet layer, and displacement of an oil-wet coating so that the original water-wet surface of the rock can be reached (Standnes and Austad 2000).

Despite the efficient role of surfactants in achieving good hydrocarbon production, their activity in modifying the wettability of oil-wet surfaces seems to occur very slowly. Stoll et al. (2008) revealed that, at the field scale, wettability alteration of oil-wet rock by surfactants might require several hundred years, based on the results of lab-based spontaneous imbibition studies conducted over several months. Moreover, other limitations, including surfactant diffusion in the porous medium and losses by adsorption on solid surfaces, can limit the economic viability of using surfactants as sole wettability alteration agents (Zargartalebi et al. 2015).

Adsorption of surfactants on rock surfaces is a crucial challenge for applying surfactants in EOR projects. There is disagreement about the effect of rock surface types (sandstone and carbonate) on the adsorption behaviour of surfactants (cationic and anionic) during surfactant flooding applications. (Ahmadall et al. 1993) reported that losses of anionic surfactants due to adsorption on carbonate rocks are higher than those of cationic surfactants with similar-length hydrophilic chains. Seethepalli et al. (2004) stated that addition of alkaline chemicals can decrease the loss of anionic surfactants on carbonate substrates. In line with this, Alroudhan et al. (2016) demonstrated that an increase in pH changes the surface charge of carbonate from positive to negative, which promotes the repulsive forces between surfactant molecules and the carbonate surface. In contrast, Schramm (2000) suggested that chalk surfaces have only a limited ability to adsorb anionic surfactants. Despite these controversial results, it is agreed that the adsorption of surfactant increases with concentration and can reach a maximum at the critical micelles concentration. However, Zargartalebi et al. (2015) reported that the presence of nanoparticles in a surfactant formulation can significantly reduce surfactant adsorption on reservoir

rocks. Thus, it may be beneficial to modify surfactant formulations with materials such as nanoparticles.

#### **2.4.3.5 Nanoparticles**

Hydrophilic nanoparticles such as silicon dioxide have drastic abilities to change the wettability of oil-wet surfaces to water-wet. The efficiency of such particles in changing the wettability of surfaces is determined by several factors such as nanoparticle type and hydrophilicity, the original wetness status of the surface, and the operational conditions. Thus, nanofluid injections should be adjusted according to the characteristics of oil reservoirs, the type and load of nanoparticles in the injected nanofluid, and the expected range of surface wettability and interfacial tension. Nanoparticles are injected into oil reservoirs as a *nanofluid*—a dispersion of nanoparticles in a base fluid. Thus, it is essential to understand the formation, stability and efficiency of such nanofluids in terms of wettability alteration.

### **2.5 Nanoparticles: Synthesis, Types, Applications and Challenges**

#### **2.5.1 Nanoparticle Synthesis**

Modern manufacturing technology allows the production of materials at the nanometre scale. The synthesis and organisation of nanoparticles are complementary tools of nanotechnology. Although the conventional techniques for the preparation of metal sols, known since the time of Michael Faraday, still use metal nanoparticles for synthesis, drastic developments and modifications in synthesis techniques have been achieved that allow better control over the size, shape, surface charge and other characteristics of nanoparticles (Saravanan et al. 2008). Nanoparticles can be synthesised by chemical, biological and physical methods. Typically, the synthesis technique depends on the nature of the materials and the chemical reactions occurring during the preparation process. Thermal spraying, spray pyrolysis, chemical precipitation, chemical vapour deposition and microemulsions are common techniques used in the chemical synthesis of nanoparticles. Alternatively, physical synthesis methods include mechanical grinding and the inert gas condensation method.

#### **2.5.2 Nanoparticle Types**

Nanoparticles are categorised as *metallic* (e.g. platinum, gold, silver), *non-metallic* (e.g. carbon-based nanomaterials), *magnetic* (e.g. iron, cobalt), and metal oxide (e.g. oxides of silicon, titanium and aluminium), which are the most popular type. Silicon dioxide (SiO<sub>2</sub>) nanoparticles exhibit unique structures and surface properties, which make them common materials for EOR applications. Characteristically, the efficiency

of these fine materials in different applications depends mainly on their synthesis methods, which determines their surface properties.

#### **2.5.2.1 Metallic Nanoparticles**

The unique properties of metallic nanoparticles, such as their shape selectivity and large surface-to-volume ratio, makes them suitable for use in a wide range of high-accuracy applications, such as analytical instruments and sensors. Typically, the adsorption of an analyte on the surfaces of metallic particles creates a detectable shift in their electric field (White et al. 2009). This phenomenon is defined as *surface plasma adsorption*. It naturally happens as nanoparticles decrease in size below the 100 nm threshold, and frequently generates a colour in the visible region. Moreover, metallic nanoparticles exhibit high thermal conductivity and can be used as heat carriers in heat transfer fluids. Chol (1995) reported the potential benefits of using copper nanoparticle materials in heat transfer fluid to enhance heat transfer efficiency.

#### **2.5.2.2 Non-Metallic Nanoparticles**

The unique physical and chemical properties of non-metallic nanoparticles are of critical prominence in the production of multifunctional drug delivery system. Carbon-based nanofibers and mesoporous silica nanoparticles are important examples of nanomaterial that combine diagnostic and therapy for cancer treatment (Yu-Cheng et al. 2013).

#### **2.5.2.3 Magnetic nanoparticles**

Magnetic nanoparticles display exclusive nanoscale properties due to the magnetic element in their structure. Their potential applications in various magnetic processes are of high interest. Heterostructured magnetic nanoparticles, for example, are considered next-generation agents owing to their improved magnetism and potential multifunctionality. The magnetic characteristics of nanoparticles mainly depend on their particles size. These nanoparticles, for example, become extremely superparamagnetic at particle sizes below a threshold value (normally  $\leq 50$  nm, (Pastrana-Martínez et al. 2015).

#### **2.5.2.4 Metal Oxide Nanoparticles**

Metal oxide nanoparticles are commonly used in a wide range of processes, particularly in the oil and gas industries, due to their low cost of fabrication and the ability to modify their surfaces for a particular usage. Moreover, the unique chemical and physical properties exhibited by metal oxide materials, as well as their diverse structures and compositions, make these nanoscale materials attractive in subsurface applications (Al-Anssari et al. 2017d). Furthermore, metal oxide nanostructures also have high thermal conductivity, i.e., the amount of heat conducted by the material. The presence of metal oxide nanoparticles in a base fluid can increase its heat transfer by up to 12% (Branson et al. 2013). Metal oxide nanoparticles also exhibit an exceptional degree of stability. However, this mainly depends on the synthesis method and

dispersant used (Costa et al. 2006). Fedele et al. (2011) compared the stability of metal oxide nanoparticles according to preparation methods that included sonication, high-pressure homogenisation, and ball milling. Ultrasonic homogenisation was the most efficient technique for producing stable nanoparticles. Recently, metal oxide nanoparticles (e.g. SiO<sub>2</sub> nanoparticles) have been suggested as an efficient agent for subsurface projects, as they can be potentially transported through micro-structured porous media to enhance oil displacement (Al-Anssari et al. 2018, Roustaei and Bagherzadeh 2014).

### 2.5.3 Nanofluid formulation

A nanofluid is a dispersion of nanoparticles in a base fluid. Chol (1995) was the first to call the suspension of metallic nanoparticles in conventional heat transfer fluids *nanofluids*. These were first proposed as an innovative new class of heat transfer fluids with enhanced thermal conductivity that could achieve significant reductions in heat transfer pumping power. Typically, there are two approaches for nanofluid production: the *one-step method* and the *two-step method* (Ramakoteswaa et al. 2014). In the one-step method, the synthesis of nanoparticles and the dispersion of these particles in the base liquid are performed together in one process. The common *direct evaporation* one-step method, for example, is based on the direct solidification of nanoparticles from a gas phase inside the base fluid (Eastman et al. 2001). The main disadvantage of one-step methods is that these techniques are not efficient for mass production, which limits their commercialisation (Yu et al. 2008). The two-step techniques, on the other hand, require two separate steps. The first is the production of nanoparticles and the second, which can be done at a different time and place, is the efficient dispersion of nanoparticles in a base fluid (Ramakoteswaa et al. 2014). Although it is more suited to mass production than the one-step method, the main drawback of the two-step technique is the formation of nanoparticle clusters during the formulation of nanofluid (Yu et al. 2008). The creation of these nano- or micro-aggregates can prevent the proper dispersion of nanoparticles inside the base fluid. Consequently, despite the commercial aspects of nanofluid production, the one-step method is better for formulating characteristically stable nanofluids.

### 2.5.4 Applications of Nanofluids

The main challenge for nanotechnology applications is in enhancing the performance and running costs of the materials, processes and devices used in the industry with innovative solutions. Nanofluids were initially used to enhance heat transfer and power efficiency in a wide range of thermal applications. At the early stage, most of the research in the field of nanofluids was done in academia and government laboratories. In recent times, however, growing numbers of international companies have been developing nanofluids for particular medical and industrial applications.

#### **2.5.4.1 Biomedical Applications (Drug Delivery and Antibacterial Activities)**

In the past half-century, colloidal drug delivery systems have been investigated and developed. These aim to enhance the effectiveness and specificity of medications. Recently, developments in the nanotechnology field, particularly the ability to prepare highly engineered nano-scale particles of any size, shape, solubility and surface properties, has allowed the creation of new biomedical agents. The unique properties of nanoparticles facilitate interactions with complex cellular functions in new scenarios (Srikant et al. 2009). Gold nanoparticles, for example, are calcified as non-toxic carriers for drug delivery. Moreover, zirconium oxide nanofluid at concentrations below 10 mM causes complete inhibition of bacterial growth due to the intracellular accretion of nanoparticles (Jones et al. 2008). Further, these ZnO nanofluids show antibacterial behaviour due to their bacteriostatic activity on microorganisms (Zhang et al. 2007a). According to extensive electrochemical measurements, these antibacterial activities are potentially controlled by the size of the ZnO particles and the existence of visible light

#### **2.5.4.2 Heat Transfer Fluids (Thermal Management of Shrinking Devices)**

Nanofluids are a novel type of nanotechnology-based heat transfer fluids designed by suspending nanoparticles in traditional coolant fluid. Apparently, the last five decades have been dominated by the semiconductor revolution, which has driven the development of space technology, biotechnology and nuclear reactor technology. The great progress in these fields was mainly based on innovations in electronic hardware. These have resulted in a wide range of applications in the field of information technology, such as the smartphones and digital tablets of today. The backbone of these innovations was size reduction—packing many components into a compact circuit board. However, these ultra-thin technologies are limited by the thermal issue. Typically, designing compact devices with powerful processors causes rapidly elevated heat flux. In general, generation of a few watts in a sub-microprocessor of nano-scaled dimensions can create heat flux equivalent to that of the sun. Consequently, thermal management of mini devices is the key constraint in the nano-age (Rohrer 1995). The previous thermal challenges demand a heat transfer medium with high thermal conductivity, which is key for efficient heat transfer. However, traditional cooling fluids such as water, oils and ethylene glycol have low thermal conductivity compared to solids. Characteristically, the thermal conductivity of solid metals is drastically higher than that of liquids. Thus, the thermal conductivity of traditional coolant fluids could be drastically higher if solid metallic particles were suspended in them. This technique, however, has several drawbacks, including the rapid sedimentation of micro-particles, erosion of heat transfer devices, increased pressure drops, and the potential for micro-size particles to clog the tiny tubes used in miniaturised devices. These limitations have made micrometre-sized particles suspended in cooling fluid impractical (Das and Choi 2009).

Rapidly developing nanotechnology has allowed the production of metallic nanoparticles with particle sizes  $\leq 100$  nm. The thermal, optical, electrical, mechanical,

magnetic and surface properties of nano-sized particles are better than those of equivalent bulk materials. Choi (1995) introduced the novel concept of nanofluids, and revealed that it is time to overcome their traditional constraints by means of manipulating the innovative properties of nanomaterials. Several properties of nanoparticles, including large surface-to-volume ratio and high mobility, have made them promising additives for suspension in heat transfer fluids. Nano-coolant fluids are suggested to be more conductive, more stable, have less sediment and cause less blockage than conventional coolants (Das and Choi 2009). Thus, cooling systems using nanofluids will be smaller and more efficient.

#### **2.5.4.3 Solar Absorption**

Solar energy is a perfect source of sustainable and non-polluting energy. Typically, direct-adsorption solar collectors are implemented in a wide range of applications, including heating systems. However, the feasibility of this energy source is limited by the absorption properties of the working fluids used in thermal solar collectors. The absorption rate of commercial working fluids is typically poor. In recent times, this technology has been combined with nanotechnology. Experimentally, the presence of nanoparticles in the working fluid can drastically enhance its thermodynamic properties, leading to significantly higher heat absorption rates (Zhang et al. 2007a).

#### **2.5.4.4 Energy Storage**

Thermal energy storage (TES) in the forms sensible and latent heat is a promising energy management technique, particularly in terms of the well-organised use of power and preservation of excess heat and solar energy. Typically, the specific storage capacity of phase change materials (PCMs) is key for feasible renewable thermal generation and residential heating projects. The higher thermal conductivity of PCMs can enhance the rate of thermal energy exchange with other heat transfer media (Zabalegui et al. 2014). Nanofluids have tremendous potential in thermal energy applications. In this context, nanofluids as phase changing materials exhibit drastically higher thermal conductivities than typical base fluids. Dispersion of  $\text{Al}_2\text{O}_3$  nanoparticles in DI-water, for example, can significantly improve the thermal energy storage in heating systems (Wu et al. 2013b). Mechanistically, this heat capacity enhancement is mainly related to the improved thermal properties of semi-solid layers at nanoparticle interfaces (Shin and Banerjee 2011).

#### **2.5.4.5 Friction Reduction**

Nanofluid lubrication is an innovative approach to reducing the energy wasted at sliding interfaces. Typically, lubrication is essential for friction and wear reduction in machine components. Dispersion of inorganic nanoparticles in lubrication oil has recently become a major topic of research in the field of tribology. These nano-scale additives can be mixed with engine oil to enhance the longevity of moving parts and reduce energy consumption (Bonu et al. 2016). Typically, more than 30% of the total mechanical energy is wasted as heat caused by friction (Hernández Battez et al. 2008)

making moving mechanical components such as bearings, gears or internal combustion cylinders less efficient. Mechanistically, engineered nanoparticles with appropriate properties for energy conservation in tribology applications can improve lubrication by forming tribo-film on sliding surfaces, thereby establishing a unique “nano-ball-bearing” effect (Bonu et al. 2016). Efficient rolling of nanoparticles between two sliding bodies requires high-hardness, spherical nano-structures that can convert a sliding mechanism into a rolling one. This approach can minimise the frictional energy and degradation of the base oil and thus maximise the load-carrying capability. Song et al. (2014) reported several examples of spherical nanoparticles, including ZnO, TiO<sub>2</sub>, CuO and Fe<sub>3</sub>O<sub>4</sub>. Dispersions of these nanoparticles in lubricant oil can drastically mitigate friction and wear via the rolling effect.

#### **2.5.4.6 Water treatment**

Water is the key component for biological activity. However, the quality of water sources is dramatically deteriorating due to the rapidly growing human population, urbanisation and industrialisation. The concentrations of various toxic heavy metals such as Hg, Cd, Pb and As have increased beyond safe limits in many water sources. Exposure to toxic heavy metals is a critical health threat owing to their poisonous and carcinogenic effects. Arsenic contamination in drinking water is another serious ecological issue that has recently affected humankind. Arsenic is a poison with serious side effects and high lethality. More than 100 million people are potentially at risk from using arsenic-contaminated water (Henke 2009). In general, these contaminants are also extremely hazardous for the ecosystem.

For the last half-century, various techniques have been suggested, developed and used to enhance the quality of water. These include oxidation (Gogate and Pandit 2004), zonation (Al-Anssari 2009), distillation, filtration and ultra-filtration (Fan et al. 2014), centrifugation, evaporation, extraction, flotation, reverse osmosis (Greenlee et al. 2009), ion exchange, adsorption (Shanshool et al. 2011), crystallization, precipitation and sedimentation (Fathi et al. 2006).

In the last fifteen years, nanotechnology has made tremendous advances in almost all fields of science and industry, including water treatment. Several studies developed nano-agents for water treatment and purification. Nano-sized adsorbents, for instance, have been proposed and implemented for the removal of water contaminants (Ali 2012, Kumar et al. 2014). Utilisation of nano-adsorbents in adsorption processes for water treatment is a breakthrough of emerging nanotechnology. More so, magnetic nanoparticles, such as Fe<sub>3</sub>O<sub>4</sub> have been successfully utilised to remove arsenic from water (Yavuz et al. 2006). Typically, the high selectivity and designed affinity of functionalised nanoparticles for particular water pollutants key to their efficiency in water quality improvement. Recently, engineered nanomaterials such as catalytically-energetic nanopowders, bioactive nanoparticles, and nano-structured membranes have been successfully used in water treatment. The efficiency of water treatment agents such titanium oxide, zeolite, and zirconium oxide in reducing the concentrations of heavy ions and organic matter is greater when they are used at the nano-scale than at

bulk sizes (Kumar et al. 2014). This enhancement in water-treatment efficiency is mainly related to the high surface-to-volume ratio of nanoparticles.

#### **2.5.4.7 Subsurface Applications**

Nanofluids have tremendous potential for use in subsurface applications such as aquifer pore-water treatment (Antia 2011), geothermal extraction (Sui et al. 2017), drilling (Ponmani et al. 2015), carbon geosequestration (Al-Anssari et al. 2017b, c), and enhanced oil recovery (Ju et al. 2006, Ju and Fan 2009, Sharma and Mohanty 2013, ShamsiJazeyi et al. 2014, Sharma et al. 2014b, Zargartalebi et al. 2015, Al-Anssari et al. 2016). However, the high salinity of subsurface formations can limit the performance of these nanofluids due to the instability of the nanoparticles in the suspension (Metin et al. 2011). The successful implementation of nanofluids in underground projects such as carbon geostorage and chemical EOR requires the formulation of low-cost nano-suspensions that are stable at high salinity (Al-Anssari et al. 2017a).

### **2.5.5 Nanoparticle and Nanofluid Applications in Chemical Enhanced Oil Recovery**

Nanoparticles with sizes less than 100 nanometres have been used in several applications, either as solid particles or in nanofluids. The term *nanofluid* was first used by (Choi 1995) to describe the dispersion of nanoparticles in a base fluid such as DI water, brine, ethylene glycol, or surfactant solution (Al-Anssari et al. 2016). Properties of the prepared nanofluids can be controlled to fit a specific application. Moreover, nanofluids are characterised by the concentration, hydrophilicity and initial size of the nanoparticles, as well as the properties of the base fluid such as electrolyte composition and pH value.

In the oil industry, nanoparticles have several promising applications, such as drilling fluid (Ponmani et al. 2015), controlling the viscosity of heavy oil (Li et al. 2007), reduction of oil-water interfacial tension (Al-Anssari et al. 2017e), and wettability alteration of oil-wet reservoirs (Nwidee et al. 2017a). Adsorption of fictionalized nanoparticles on solid surfaces is a unique technique for regulating surface wettability.

### **2.5.6 Efficiency of Wettability Alteration by Nanofluids**

Surface contact angle measurement is often used to assess the efficiency of nanoparticles as wettability modifiers. This technique provides a fast, direct and efficient way to assess the type, hydrophobicity and concentration of nanoparticles in terms of their effectiveness in altering surface wetness. Further, after narrowing the suggested nanoparticles list, an imbibition or coreflooding test for original reservoir plug or oil-saturated outcrop can monitor the efficiency of the nominated nanofluids

under reservoir conditions. Two valuable statistics—recovery rate and ultimate hydrocarbon recovery—can be obtained from a graph of recovery versus time (via an imbibition test) or recovery versus pore volume (via a coreflooding test). Prey and Lefebvre (1978) showed that the effect of capillary imbibition is observed in the early period, while gravitational influences can be detected at a later time. Moreover, the tested cores can be a source of further information by using advanced visualisation methods. Micro-computerised tomography (micro-CT) scans, for example, can probe the distribution of fluids and nanoparticles during imbibition or coreflooding tests (Zhang et al. 2016).

The implementation of nanoparticles in wettability alteration applications is quite novel. Several studies have reported that different nanoparticle dispersions can efficiently change sandstone (Ju and Fan 2009, Maghzi et al. 2011) and carbonate (Karimi et al. 2012a) from being oil-wet to water-wet. Mechanistically, adsorption of hydrophilic nanoparticles on rock surfaces forms a nano-texture that coats the rock and changes the wetness status to being more water-wet (Al-Anssari et al. 2016). Several types of nanoparticles, including alumina, silica, nickel, zirconium, cerium and carbon have been studied individually and comparatively to evaluate their activity in altering the wettability of different surfaces. The pioneering work of Ju et al. (2006) was the first to test the influence of nanofluids on sandstone wetness. It revealed that lipophilic and hydrophilic polysilicon (LHP) can render oil-wet sandstone as water-wet. Further, by using mathematical models and numerical simulation to mimic the application of these nanoparticles in a sandstone oilfield, Ju and Fan (2009) discovered that the water-phase permeability of nano-treated sandstone was increased. However, the absolute permeability decreased due to the adsorption of nanoparticles on pore surfaces and potential accumulation of nanoparticles at pore throats. Since then, further studies (Maghzi et al. 2011, Hendraningrat et al. 2013, Ehtesabi et al. 2014, Sharma et al. 2014b) have been conducted to confirm the ability of nanoparticles to alter the wettability of oil-wet sandstone.

Limited information is available on the capability of nanoparticles to change the wetting status of oil-wet carbonate surfaces, since research in this field has only started recently. Karimi et al. (2012a) tested the effect of  $ZrO_2$  nanoparticles on the wetness status of carbonate surfaces using contact angle measurements. Their results revealed that zirconium nanofluid could efficiently render strongly oil-wet carbonate water-wet. In a comparative study, Bayat et al. (2014b) studied the influence of different nanoparticle types, such as aluminium oxide ( $Al_2O_3$ ), titanium oxide ( $TiO_2$ ), and silicon dioxide ( $SiO_2$ ) on the wettability of limestone rocks. They reported that silica nanoparticles were more efficient than the other tested nanoparticles in terms of wettability alteration. Moghaddam et al. (2015) also established that silica nanoparticles are more effective for wettability alteration and oil recovery than other types, including alumina, magnesium, titanium, cerium and carbon nanotubes.

Silica nanoparticles, as the metal oxide ( $SiO_2$ ), are widely used in industry due to their low cost of fabrication and ability to control their hydrophobicity by surface modification with specific chemicals. Moreover, according to wettability alteration studies, silica nanofluid is a favourable candidate for EOR applications due to its ability to drastically reduce water contact angles.

Nikolov et al. (2010) were the first to test the influence of silica nanoparticles on the wetting properties of solid surfaces. They revealed that self-structuring of nanoparticles in a nanofluid film formed between a solid surface and oil droplets acts to change the wettability of the surface. Further, they demonstrated that the nano-film might be composed of one or more layers of particles depending on the size and concentration of the nanoparticles in the nanofluid. Moreover, (Wasan et al. 2011) demonstrated that the activation of structural disjoining pressure is based on the presence of in-between wedge between the oil and the solid surface (Figure 2-8).

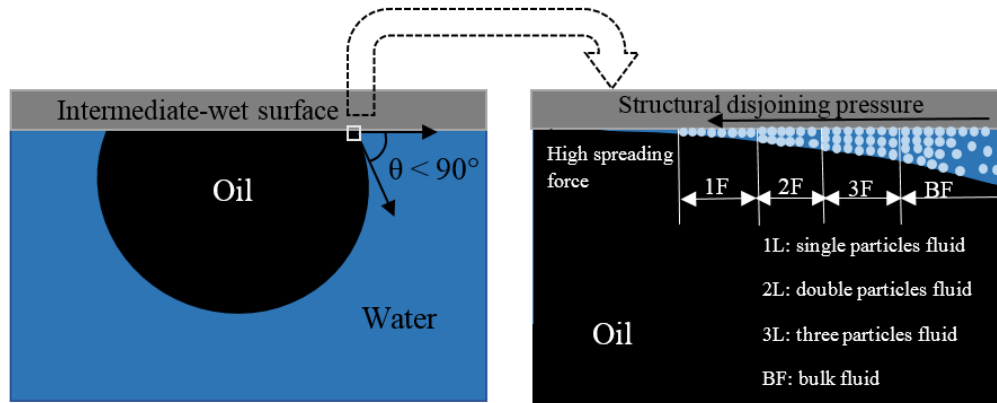


Figure 2-8 Proposed impact of hydrophilic silica nanoparticles on an initially water-wet surface (from Nikolov et al. (2010)).

Recently, based on their experimental data on contact angles and spontaneous imbibition, Al-Anssari et al. (2017d) confirmed that the structural disjoining pressure and, thus, the spreading effect of nanoparticles, mainly acts in water-wet conditions or, less efficiently, in intermediate-wet ones. In addition, nanoparticles can also act as wettability modifiers on strongly oil-wet surfaces; however, such surfaces first become intermediate-wet; for example, by the effect of surfactant monomers. Mechanistically, the in-between wedge between oil and a solid surface can only occur when the water contact angle is lower than  $90^\circ$  (Figure 2-9).

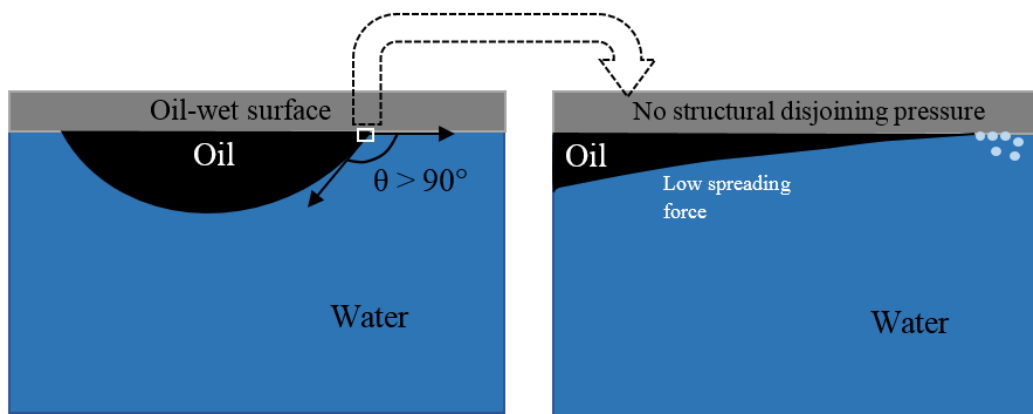


Figure 2-9 Proposed impact of hydrophilic silica nanoparticles on an initially oil-wet surface

In the last decade, several studies have investigated the role of silica nanoparticles as wettability modifiers. Maghzi et al. (2011) investigated the role of silica nanoparticles on the wettability alteration of porous surfaces. In addition to a 10% enhancement in oil recovery during polymer flooding, they also revealed that nanotreatment with silica nanofluid changes the oil-wet surface into a strongly water-wet one. Amraei et al. (2013) tested the effect of relatively high-concentration silica nanofluid (8 wt% SiO<sub>2</sub>) on the contact angle of an oil-wet carbonate surface and the interfacial tension of decane/water. They found that concentrated silica nanofluid can significantly alter the wettability of oil-wet carbonate to a water-wet state, and the presence of silica nanoparticles may cause a reduction in interfacial tension. Bayat et al. (2014b) were the first to investigate the influence of temperature on carbonate surfaces treated with silica nanofluid. Their results revealed that the effectiveness of silica nanoparticles in shifting the wettability of carbonate towards a more water-wet state increases with temperature. Li and Cathles (2014) investigated the effect of brine concentration on silica nanofluid's ability to change the wetting properties of carbonate surfaces. Despite a negative effect on nano-suspension stability, the presence of an electrolyte (e.g. NaCl) supported the adsorption of silica nanoparticles on carbonate surfaces, which altered wettability. Roustaei and Bagherzadeh (2014) conducted nanofluid-flooding experiments and contact angle measurements to determine that the optimum concentration of silica nanofluid for oil recovery from carbonate reservoirs was 0.4 wt%. Approximately, one pore volume (PV) of nanofluid has injected into a carbonate core sample after regular waterflooding. In the same year, Sharma et al. (2014b) studied the effect of a silica nanoparticle, surfactant and polymer combination in the presence of NaCl on oil recovery under reservoir conditions (13.6 MPa, 90 °C). After nano-flooding, they observed oil recovery to increase by 23%, and argued that this was related to the effect of the combination on the interfacial tension and wettability of the porous medium. Moghaddam et al. (2015) tested the effect of several nanoparticles (including silica) on wettability and spontaneous imbibition in carbonate rocks. Results of contact angle and spontaneous imbibition measurements confirmed the major role of SiO<sub>2</sub> nanoparticles in enhancing oil recovery. They also proposed that a structural disjoining pressure gradient is potentially responsible for wettability alteration. Al-Anssari et al. (2016) were the first to investigate the effect of silica nanoparticles on oil-wet calcite surfaces that were used to mimic carbonate oil reservoirs. They studied the effects of nanofluid composition (brine and nanoparticle concentrations), immersion time and reversibility of nanoparticle adsorption on the contact angle of an initially oil-wet surface. Their results showed that in lab conditions, silica nanoparticles can render the strongly oil-wet calcite surfaces water-wet. More recently, Zhang et al. (2016) conducted contact angle measurements and core flooding experiments with silica nanofluid under ambient conditions. High-resolution X-ray microtomography (micro CT) was used to image oil and brine distributions in the core before and after nanofluid flooding. Their results confirmed the effect of silica nanoparticles on surface wettability and demonstrated that approximately 15% more oil can be produced by using a silica nanofluid.

Silica nanoparticles, in addition, are environmentally friendly materials. The dispersion of such nanoparticles in DI water forms a relatively stable suspension. Costa et al. (2006) demonstrated that silica nanoparticles have exceptional colloidal stability

even in the presence of an electrolyte. However, for subsurface applications, high salinity can directly affect fluid chemistry and, thus, stability (Amiri et al. 2009, Tantra et al. 2010, Li and Cathles 2014). Instability of nanofluids due to reservoir temperature and salinity, for instance, can narrow the range of nanofluids that are appropriate. Thus, thermal stability tests should be performed in parallel with zeta potential measurements to determine the best compositions for nano-suspensions. Importantly, the stability of displacement fluids must be examined under real operating conditions (Hirasaki and Zhang 2004).

### **2.5.7 Interfacial Tension Reduction by Nanoparticles**

Reduction of interfacial tension is one of the key factors for EOR. Once the surfactant concentration within a solid matrix exceeds the critical micelles concentration, a microemulsion is formed depending on the salinity and presence of oil. The IFT can be reduced to very low values depending on the amount of solubilised oil. Moreover, the capillary pressure can be shifted to values close to zero owing to the reduction of IFT.

Several techniques, including chemical, microbial and thermal flooding, have been suggested for reducing the IFT values of oil-water systems in oil reservoirs. Surfactants, surfactant-polymers, and surfactant-nanoparticle formulations are promising chemical techniques that reduce the IFT between oil and water. Mechanistically, the adsorption of surface-active species such as surfactants or nanoparticles at the oil/water interface acts to lower the surface energy of the liquid phases, thereby reducing interfacial tension (Hendraningrat et al. 2013).

A number of studies have investigated the effect of silica nanoparticles on IFT (Okubo 1995, Dong and Johnson 2003, Vignati et al. 2003, Saleh et al. 2005, Blute et al. 2009). However, the results are inconclusive and somewhat contradictory. Although Dong and Johnson (2003) and Blute et al. (2009) reported that IFT decreases as nanoparticle concentration increases, Saleh et al. (2005) demonstrated that silica nanoparticles have no significant effect on IFT. On the other hand, Hendraningrat et al. (2013) showed that low concentrations of silica nanoparticles are enough to reduce IFT by 60%, which is a significant reduction.

Further, it has been well established that combinations of nanoparticles and surfactants can enhance IFT reduction (Ma et al. 2008, Mandal and Bera 2012b, Esmaeilzadeh et al. 2014, Zargartalebi et al. 2014). Ma et al. (2008), for example, demonstrated that hydrophilic silica nanoparticles enhance the efficiency of anionic surfactant (e.g. sodium dodecyl sulfate, SDS) in reducing IFT. Moreover, Mandal and Bera (2012a) showed that IFT can be considerably reduced—by 3–4 orders of magnitude—in polyethylene glycol-silica nanoparticle formations. Similarly, Esmaeilzadeh et al. (2014) and Zargartalebi et al. (2014) have investigated various surfactant-nanoparticle combinations and reported that the presence of nanoparticles improves the efficiency of surfactants in reducing IFT. Recently, Al-Anssari et al. (2017e) investigated the effect of nanoparticles on critical micelle concentration (CMC). Their results revealed

that hydrophilic silica nanoparticles have significant effects on the CMC of anionic surfactants (e.g. SDS).

### **2.5.8 Effect of Nano-treatment on Oil-water Relative Permeability**

Nanofluid flooding can directly affect the relative permeability of oil reservoirs. It was suggested in 1965 that reductions in permeability can be caused the accumulation of small particles, including cementation materials, dispersed clays and other fine materials, that block small passages in the rock (Mungan 1965). Despite numerous studies having investigated the use of nanoparticles in EOR from carbonate and sandstone oil reservoirs, only a limited amount of work has investigated the effect of nanoparticles on oil-water relative permeability in porous media. The pioneering work of Ju et al. (2006) investigated the influence of nanoparticles on various physical and chemical characteristics of oil reservoirs. They revealed that both the porosity and permeability of porous media are reduced after nanofluid injection; however, the reduction in permeability is greater than that of porosity (Ju and Fan 2009). Further, increased nanoparticle concentration decreases the relative permeability of water and increases the relative permeability of oil (Liu et al. 2012a). Recently, using crude oil and real carbonate reservoir rock samples, Amedi and Ahmadi (2016) investigated the effect of the nanoparticle concentration of injection fluid on oil-water relative permeability and hydrocarbon production. Their results demonstrated that, despite decreased residual oil saturation, increased silica nanoparticle concentration dramatically decreases water permeability and increases oil permeability. Thus, the nanofluid-flooding enhancement of oil recovery of up to 5–20% (Ju and Fan 2009, ShamsiJazeyi et al. 2014, Zhang et al. 2016) was attributed to altered wettability of the porous medium, rather than the effect of nanoparticles on oil-water relative permeability. This finding is supported by the study of Ju et al. (2006) who reported that an optimal nanoparticle concentration must be carefully chosen to optimise the effects on rock wettability and oil-water relative permeability (Ju and Fan 2009, ShamsiJazeyi et al. 2014).

### **2.5.9 Nano-treatments at High Temperatures**

Temperature has significant effects on the properties of rock, and nanofluid chemistry and stability. Moreover, the adsorption of nanoparticles on reservoir rocks and, consequently, their efficiency as wettability alteration agents, is a function of temperature (Bayat et al. 2014b). Thus, temperature can influence the effect of nano-treatment on wettability alteration.

It is well documented that thermal operations enhance hydrocarbon recovery via various mechanisms, including fluid/fluid and fluid/rock interactions (Hjelmeland and Larrondo 1986, Gupta and Mohanty 2010). In this content, Rao (1999) reported that carbonate surfaces become water-wet at elevated temperatures. Mechanistically, high temperatures prompt  $CaCO_3$  precipitation from formation brine into carbonate. Also,

oil-wet carbonate surfaces become water-wet when covered with calcium carbonate. Moreover, detachment of fine organic molecules, which are responsible for the oil-wet state, from rock at elevated temperature may be another reason for the effect of temperature on reservoir wettability (Schembre et al. 2006). In this context, Gupta and Mohanty (2010) confirmed that temperature increases in oil-wet reservoirs shifts wettability towards the water-wet state due to changes in the solubility of surface-active materials. Further, temperature increases can also increase the spontaneous imbibition of ionic solutions into limestone samples. Gupta and Mohanty (2010) attributed the enhancement of spontaneous imbibition to increased gravitational forces caused by viscosity reduction at higher temperatures. Enhanced spontaneous water imbibition at elevated temperatures was reported by Al-Hadhrami and Blunt (2000) to provide 27—35% OOIP incremental oil recovery. Their model for imbibition and heat transport in a rock matrix estimated that around 30% OOIP was recovered during 100 weeks of hot waterflooding, compared to 2% produced via natural reservoir drive. The authors attributed this increase in oil recovery to wettability alteration at elevated temperatures, since there was no imbibition under normal reservoir conditions (Al-Hadhrami and Blunt 2000).

Hamouda and Gomari (2006) studied the effect of temperature on the wettability of carbonate reservoirs using interfacial tension, zeta potential and contact angle measurements. They observed that both contact angle and interfacial tension followed the same trend at high temperatures. A significant reduction in contact angle, from 92° to 60°, was a stark indication that wettability was restored to water-wet status. Moreover, they revealed that temperature increases reduce the positive charges on calcite surfaces, leading to a higher repulsive force between calcite and the adsorbed organic components. This effect of temperature on carbonate surface charge is crucial for nanofluid-mediated wettability alteration of carbonate reservoirs.

Despite the direct impact of elevated reservoir temperatures on nanofluid stability and rock wettability, nanoparticles, particularly silica, are acknowledged as being more stable than surfactants and polymers at elevated temperatures (Bayat et al. 2014b). Earlier, Zhang et al. (2009) demonstrated that the addition of 1 mg/L natural organic matter will increase the negative surface charge of nanoparticles (e.g. ZnO, NiO, TiO<sub>2</sub>, FeO<sub>3</sub> and SiO<sub>2</sub>) and, consequently, their tendency to aggregate can be reduced. Further, they revealed that SiO<sub>2</sub> nanoparticles exhibit unique stability under various harsh subsurface conditions, even without surface modification. The alteration of oil reservoir wettability by nano-modification is based on the adsorption of nanoparticles by the porous medium. Charge differences between nanoparticles and rock surfaces are the prime driver of that adsorption. Carbonate reservoirs, for example, are positively charged at moderate and low temperatures ( $\leq 55$  °C). Within this range of temperatures, negatively charged nanoparticles can be adsorbed on carbonate surfaces. However, increased temperatures can invert carbonate surface charges to negative, which impedes the adsorption of negatively charged nanoparticles and consequently reduces the impact of nanoparticles on surface wettability.

### **2.5.10 Nano-treatment at High Pressures**

It is well established that at different oil reservoir injection depths, a broad range of pressures may be encountered (Dake 1978). High pressure has significant effects on rock surface properties (Bikkina 2011), nanofluid phase behaviour and, subsequently, the adsorption of nanoparticles onto solid surfaces (Hamouda and Gomari 2006, Murshed et al. 2008). Although some studies have suggested that high pressure only has slight effects on contact angle and rock wettability (Wang and Gupta 1995, Hansen et al. 2000, Alotaibi et al. 2011), recent studies have reported a significant increasing in contact angle with pressure, particularly with carbon dioxide pressure (Siemons et al. 2006, Yang et al. 2007, Espinoza and Santamarina 2010, Bikkina 2011, Ameri et al. 2013, Chaudhary et al. 2013, Farokhpoor et al. 2013, Sarmadivaleh et al. 2015, Arif et al. 2016a, Arif et al. 2016c). Moreover, pressure can directly affect the zeta potential of mineral surfaces and, thus, the electrostatic interactions between rock surfaces and polar species in adjacent fluid due to the effect of pressure, particularly CO<sub>2</sub> pressure, on the ionic strength and pH of the aqueous electrolyte. Further, these effects can also extend to the stability and adsorption behaviour of nanoparticles from the injected nanofluid. It has been previously demonstrated that adsorption of nanoparticles on solid surfaces as single or multiple layers is the main cause of changes to wettability following nanofluid treatment (Hendraningrat et al. 2013, Roustaei and Bagherzadeh 2014, Al-Anssari et al. 2016, Nwidee et al. 2017a). Mechanistically, negatively charged hydrophilic silica nanoparticles (Metin et al. 2011, Metin et al. 2012b) adsorb on positively charged calcite surfaces (Wolthers et al. 2008, Ma et al. 2013) owing to strong bonds between silica nanoparticles and calcium ions. Thus, any change in the surface charges of reservoir rocks or silica nanoparticles due to pressure changes can reduce the adsorption of nanoparticles onto rock surfaces, leading to an insignificant effect of nano-flooding on the wetness status of the reservoir.

### **2.5.11 Stability of Nanofluids**

The greatest challenge for nanofluid implementation in the oil industry, particularly in subsurface applications, concerns the stability of the nanoparticles dispersed in the fluid. Maintaining high repulsive forces between the suspended nanoparticles by supercharging their surfaces is the key to a stable nanofluid. To accomplish this, different techniques are used, including surface modification (e.g. with silane), addition of ionic surfactants (e.g. cationic and anionic surfactants), controlling pH, and using high strength ultrasonic vibration.

Ultrasonic homogenisation processes are very efficient at producing stable nano-suspensions (Mondragon et al. 2012). Their high dispersion efficiency is related to the high-density energy of the ultrasonic homogeniser that is used to break up nano-agglomerates and produce nano-dispersions with small particle sizes (Leong et al. 2009). However, despite the power and duration of the ultrasonic homogenisation process, bare nanoparticles that are dispersed in liquid will tend to re-agglomerate after some time owing to interactions between contiguous particles. Gradually, particle

interactions result in flocculation, aggregation and, eventually, phase separation of the nanofluid.

The instability of bare nanoparticle dispersions is related to the lack of an energy barrier preventing the collision and coalescence of individual particles (Jarvie et al. 2009). According to the classic Deriaguin-Landan-Verway and Overbeek (DLVO) theory; the stability of colloidal suspensions is determined by repulsive electrostatic interaction energy and attractive van der Waals energy (Yotsumoto and Yoon 1993, Paik et al. 2005). When the van der Waals attractive force is greater than the electrostatic repulsive force, nanoparticles stick together after colliding, leading to larger particles (Paik et al. 2005). Williams et al. (2006) applied ultrasonic vibration for more than 12 h to formulate nanofluids from zirconium and alumina nanoparticles. They reported that the sonicated nanoparticles tended to agglomerate directly after preparation of the nanofluid. They also stated that controlling the pH of the suspension could increase the repulsive forces between particles and thus enhance stability. Generally, higher absolute zeta potential ( $|\xi|$ ) values refer to higher repulsive forces between nanoparticles and, consequently, higher stability (Tantra et al. 2010). In such cases of high repulsive forces, only limited collisions between particles can occur. This will keep nanoparticles individually suspended at their smaller size, leading to a stable nanosuspension. Further, Ahualli et al. (2011) showed that the addition of surfactants can supercharge particle surfaces and thus increase the repulsive forces between adjusted nanoparticles. Recently, Hamedi Shokrlu and Babadagli (2014) used polymers to enhance the stability of a nickel nanodispersion. In line with this, ShamsiJazeyi et al. (2014) confirmed the positive effect of polymers on nanosuspension stability. Even more recently, Sharma et al. (2015a) used a combination of surfactant and polymer to formulate a stable nanosuspension with increased wettability alteration activity.

#### **2.5.11.1 Effect of Anionic Surfactant on Nanofluid Stability**

Anionic surfactants (e.g. sodium dodecylsulfate, SDS; Figure 2-10) with a negative head group (Dutkiewicz and Jakubowska 2002) can partially adsorb onto a silica surface from their tail group, despite the similar negative charges of the surfactant head group and the nanoparticle surface (Ahualli et al. 2011). Mechanistically, adsorption of negative SDS molecules on silica particles from the tail group can supercharge silica nanoparticles, producing higher electrostatic repulsion forces between nanoparticles, which improves colloidal stability (Iglesias et al. 2011). Lately, Nooney et al. (2015) successfully implemented SDS molecules to stabilise fluorescent silica nanoparticles in a phosphate buffer saline phase. However, the increase in SDS concentration ( $\geq$  CMC) decreases its ability to stabilise nano-suspensions. This is related to the formation of micelles by surfactant monomers before reaching the nanoparticle surfaces.

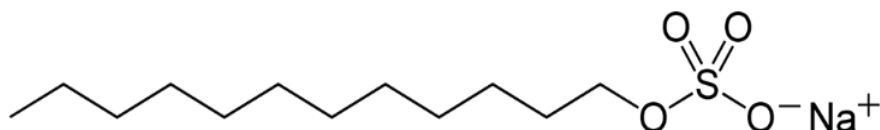


Figure 2-10 Molecular structure of sodium dodecylsulfate (SDS)

At low surfactant concentrations ( $< \text{CMC}$ ), SDS monomers can adsorb onto the surfaces of hydrophilic nanoparticles by their hydrophobic tail, leading to super negatively charged nanoparticles that repel each other strongly. However, at higher SDS concentration ( $\geq \text{CMC}$ ), surfactant monomers can join from their hydrophilic tail group rather than be adsorbed to similarly charged nanoparticles. The formation of these micelles can increase the repulsive forces between surfactant micelles and nanoparticles, and the overlapping of this repulsive force (osmotic pressure) on the nanoparticle depletion zone gradually causes nanoparticles to flocculate. Tadros (2006) demonstrated this osmotic depletion phenomenon, which decreases the stabilising performance of concentrated SDS surfactants.

#### 2.5.11.2 Effect of Cationic Surfactants on Nanofluid Stability

Cationic surfactants (e.g. hexadecyltrimethylammonium bromide, CTAB; Figure 2-11) with its positive (hydrophilic) head group, can be adsorbed strongly onto oppositely charged hydrophilic silica nanoparticles. Consequently, the surface charges of nanoparticles gradually turn from negative to zero and then become positively charged. This phenomenon leads to a decreased affinity of these particles to the water phase, leading to a rapid coagulation process between nanoparticles (Liu et al. 2013a). Mechanistically, CTAB monomers adsorb from their hydrophobic head onto the nanoparticle surfaces, decreasing the hydrophobic nature of nanoparticles and thus their affinity to the water phase. Further increases in CTAB concentration lead other free surfactant monomers to adhere to the already adsorbed monomers from the tail group and subsequently alter the nanoparticles to become positively charged.

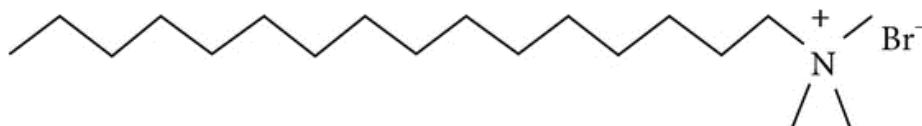


Figure 2-11 Molecular structure of hexadecyltrimethylammonium bromide (CTAB)

At cationic surfactant concentrations higher than the CMC, micelles are formed before adsorption into nanoparticles, leading to the same change in nanoparticle

hydrophobicity. Thus, the positively charged nanoparticles adsorb other free hydrophilic nanoparticles, forming an interconnected network of nanoparticles.

### **2.5.12 Opportunities and Challenges**

Wettability alteration of oil-wet reservoirs is essential to improving displacement behaviour and oil recovery efficiency. Several methods, including surface treatment with nanofluids, have been suggested in the literature for achieving that goal. However, the nano-modification of subsurface formations has certain limitations and challenges that must be extensively researched. According to the type and conditions of the proposed reservoir, some nanofluids may be more favourable than others. Moreover, in several studies, nanoparticles were introduced as primary or secondary wettability modifying agents in combination with other materials such as a surfactant, polymer, or surfactant-polymer mixture. In such cases, one of the agents will be the main wettability modifier, while a secondary agent may be used to stabilise, control or improve the efficiency of the primary agent. The impact of nanoparticles as wettability modification agents in combination with other agents is still under debate. Zargartalebi et al. (2014), for example, stated that nanoparticles have no significant effect on interfacial properties when combined with an anionic surfactant. However, they reported a significant reduction in the surfactant adsorption onto carbonate surfaces, leading to reduced losses of surfactant molecules and increased EOR efficiency. Similarly, the flooding experiments of Zargartalebi et al. (2015) demonstrated that nanoparticles can efficiently enhance surfactant performance and considerably increase oil displacement. Sharma et al. (2015b) investigated the effect of silica surfactant-polymer-silica nanoparticles on the oil recovery process. Their results revealed that the addition of nanoparticles to a surfactant-polymer combination had limited influence on hydrocarbon recovery. However, the nanoparticles significantly reduced the effect of temperature on the viscosity of the surfactant-polymer mixture, thus ensuring a stable mobility ratio during EOR. Recently Al-Anssari et al. (2017e) reported that a low nanoparticle concentration in an anionic surfactant solution can significantly reduce the critical micelles concentration (CMC) of the surfactant, and the oil/water interfacial tension. However, these nanoparticles had no noticeable effect on oil/water or air/water interfacial tension when they were the only addition to the suspension. On the other hand, Binks et al. (2007) suggested that nanoparticles and surfactant compete to alter contact angle and interfacial tension. Properties of the solution, including pH and particle concentration, determine the activity of nanoparticles as interface modifiers.

Some studies, in contrast, have proposed nanoparticles to be the primary EOR agent when combined with another modifier. Sharma et al. (2016), for instance, demonstrated that SiO<sub>2</sub> nanofluids dramatically increase oil recovery when formulated with standard oilfield polymers, particularly at high temperatures. That significant

enhancement in oil recovery was, according to the authors, mainly due to the wettability condition changing to being strongly water-wet due to the effect of silica nanoparticles. In addition to their impacts on surface wettability, nanoparticles can reduce the effects of high temperatures on fluid viscosity (Sharma et al. 2016), leading to stable mobility ratios.

Despite the advantages of combining nanoparticles with other modifiers, using mono-agents (i.e. nanoparticles alone) is preferred to minimise project costs. However, suspensions of bare nanoparticles are unstable in long-term applications, particularly under subsurface conditions. For example, in wettability alteration fluids, nanoparticles can agglomerate and precipitate on rock surfaces during the early stages of injection. Such precipitation can change the unique properties of the dispersion and cause a heterogeneous distribution of nanoparticles in the part of the reservoir close to the injection well.

Different methods for stabilising nanoparticles have been reported in the literature. It is generally agreed, based on DLVO theory, that nanofluids can be stabilised by keeping the repulsive forces between nanoparticles higher than the attractive forces. The surface charges of nanoparticles and, thus, their stability in a suspension, depend on the particle type. Surface-modified nanoparticles, with silane for example, are more stable in nano-suspension due to their higher zeta potential. Moreover, parameters such as nanoparticle size and concentration, and base fluid composition, directly impact the stability of nanoparticles in suspension. Larger nanoparticles, for example, can agglomerate and precipitate faster than smaller particles due to lower repulsive forces and gravitational effects. In addition, high nanoparticle concentrations lead to faster agglomeration and precipitation of nanoparticles. Increased nanoparticle concentrations have higher densities, resulting in an increased rate of particle collisions and more coalescence. This scenario will consequently lead to larger aggregates. In addition, electrolytes in the base fluid have screening effects on particle surface charges and, thus, the repulsive forces between particles. On the other hand, controlling the pH of the base fluid can lead to a stable suspension even in the presence of an electrolyte. Thus, optimising the nanoparticle load, type and initial size, as well as customising the fluid's properties and using efficient preparation techniques (e.g. an ultrasonic homogeniser) are vital for achieving stable nanofluids for feasible wettability alteration applications.

## **2.6 Conclusions**

Wettability is a key characteristic of solid-fluid systems. Nanofluids are a promising technology for altering the wettability type of carbonate rocks from oil-wet to water-wet. This can facilitate higher oil production and increase the containment security of CO<sub>2</sub> storage projects. Silicon dioxide nanoparticles have the ability to favourably modify the wettability of calcite. Alteration of wettability by nano-flooding can increase hydrocarbon recovery via gravitational or capillary forces. However, it should be noted that concentrated nanofluids can have negative impacts on reservoirs by increasing interfacial tension and causing permeability damage. Moreover, dispersions

of nanoparticles in DI-water or brine are unstable under harsh subsurface conditions such as those with high salinity and temperature. Electrolytes can screen the repulsive forces between suspended nanoparticles, lead to increased rates of collisions and coalescence. Consequently, supercharging the surfaces of nanoparticles is critical for creating stable nanofluids under reservoir conditions. Surfactants, particularly anionic surfactants, are potential candidates for use as stabilisers in hydrophilic silica nanofluid. Moreover, surfactant-nanoparticle combinations can enhance oil recovery by altering wettability and reducing interfacial tension. Moreover, high-pH nanofluids are one of the most feasible wettability alteration agents. Increased pH will increase the absolute value of the zeta potential, thus increasing the surface charges and creating higher repulsive forces between nanoparticles, which produces a stable nanosuspension. Further, high-pH solutions, even without nanoparticles, are successful wettability modifiers for carbonate and sandstone reservoirs. However, the kinds and concentrations of alkaline additives used must be carefully considered to avoid their rapid adsorption into formations. We conclude that nano-treatment can significantly improve oil recovery and carbon storage in underground formations.

## Chapter 3 Experimental Methodology

This chapter provides a comprehensive explanation of the materials, instruments and methods used to achieve the goals of this research. The study is based on experimental research while also having a qualitative aspect.

### 3.1 Research Strategy and Justifications

The research plan implemented in this study is mainly based on its aims and objectives. The qualitative part of the study was adopted for analysis of EOR and carbon capture and storage (Figure 3.1). It considers the effects of interfacial tension, wettability and nanoparticles.

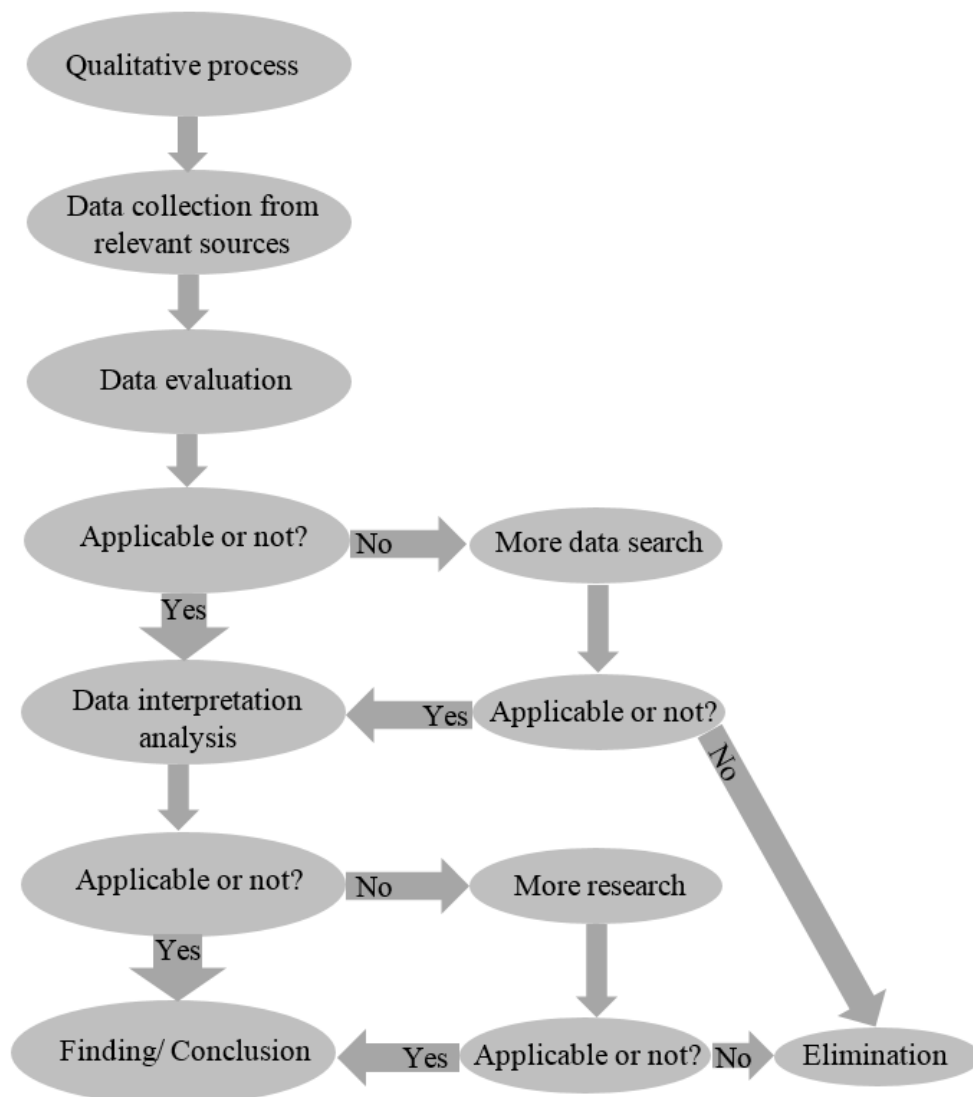


Figure 3-1: Flow chart of the qualitative data process

The quantitative part of the study comprises laboratory experiments that aim to accomplish the objectives of this research. It constitutes the main part of this work.

## 3.2 Experimental Task Assessment

Many experiments were conducted on calcite samples under ambient and reservoir conditions. The experimental work started with the selection of a relevant model oil and chemicals that can efficiently modify the wetness of pure carbonate samples from their original hydrophilic condition to a stable hydrophobic state, thereby mimicking the scenario in oil reservoirs. Subsequently, nanofluid formulations, nanoparticle surface treatments and an extensive series of contact angle and interfacial tension measurements were conducted.

## 3.3 Materials

### 3.3.1 Silicon Dioxide Nanoparticles

Porous sphere silicon dioxide ( $\text{SiO}_2$ ) nanoparticles were purchased from Sigma Aldrich Australia and used to formulate nanofluids. The purity of the nanoparticles was 99.5 wt% and they were used “as is” without any further purification or treatment. Two different sizes (5–10 nm and 20–25 nm) of hydrophilic silica nanoparticles were used to separately formulate various suspensions of silica nanoparticles dispersed in various base fluids. The general properties of the silica nanoparticles are listed in Table 3-1.

Table 3-1 General properties of the silicon dioxide nanoparticles used in this study

Formula	$\text{SiO}_2$
Purity [wt%]	99.5
Density [ $\text{kg/m}^3$ ]	(2200–2600)
Boiling point [K]	2503
Melting point [K]	1873
Molecular mass [g/mol]	60.08
Colour	White
Appearance	Powder
Hydrophilicity	Hydrophilic
Solubility in water	Insoluble

### 3.3.2 DI-water and Brines

Ultrapure water (conductivity = 0.02 mS/cm) from David Gray was used as a base fluid for nanoparticle dispersions, and to formulate brine and surfactant solutions. A wide range of brines (up to 20 wt%) was prepared by dissolving sodium chloride (NaCl  $\geq$  99.5 mol%, from Scharlan) in water under magnetic stirring.

### 3.3.3 Surfactants

Two different types of ionic surfactant, anionic and cationic, were used to prepare the surfactant solutions. Detailed information about the surfactants is given below.

#### 3.3.3.1 Anionic surfactant

Sodium dodecylsulfate (SDS, from Sigma Aldrich, Australia) was used as the anionic surfactant (Figure 3-2). Its general properties are listed in Table 3-2.

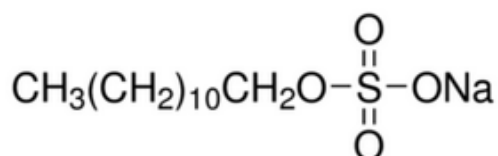


Figure 3-2 Structural formula of sodium dodecylsulfate (SDS)

Table 3-2 Properties of SDS surfactant

Linear formula	C <sub>12</sub> H <sub>25</sub> NaO <sub>4</sub> S
Purity [mol%]	98.5
CMC [mg/l]	2450
Relative density [g/cm <sup>3</sup> ]	0.37
Flashpoint [K]	443
Melting point [K]	477
Molecular weight [g/mol]	288.38
Colour	White
Appearance	Powder
pH	9.1 at 10g/l
Solubility in water	Soluble

### 3.3.3.2 Cationic surfactant

Hexadecyltrimethylammonium bromide (CTAB, from Sigma Aldrich, Australia) was used as the cationic surfactant (Figure 3-3). Its general properties are listed in

Table 3-3.

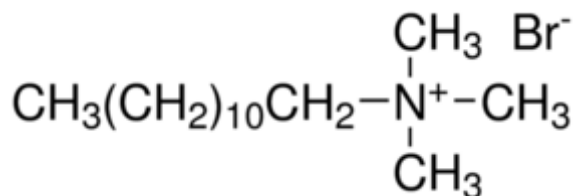


Figure 3-3 Structural formula of hexadecyltrimethylammonium bromide (CTAB)

Table 3-3 Properties of CTAB surfactant

Linear formula	$\text{CH}_3(\text{CH}_2)_{11}\text{N}(\text{Br})(\text{CH}_3)_3$
Purity [mol%]	98.5
CMC [mg/l]	350
Relative density [ $\text{g}/\text{cm}^3$ ]	0.37
Flashpoint [K]	517
Molecular weight [g/mol]	364.45
Colour	White
Appearance	Solid
pH	5–7 at 36.4 g/L
Solubility in water	Soluble

### 3.3.4 Calcite samples

Iceland spar samples (pure calcite, from Ward's Natural Science) were used as carbonate substrates. Calcite was used as received from the supplier without any further polishing (see Figure 3-4). All samples were very smooth with root mean square (RMS) surface roughness  $\geq 32$  nm. Calcite is mainly composed of calcium and carbonate and was strongly water-wet (water contact angle  $\approx 0^\circ$ ). Consequently, calcite samples were treated with chemicals (stearic acid or silanes) to achieve a wide range of wetness types (intermediate, oil-wet and strongly oil-wet). These various wettability types helped to simulate the conditions of carbonate rocks in real oil reservoirs.

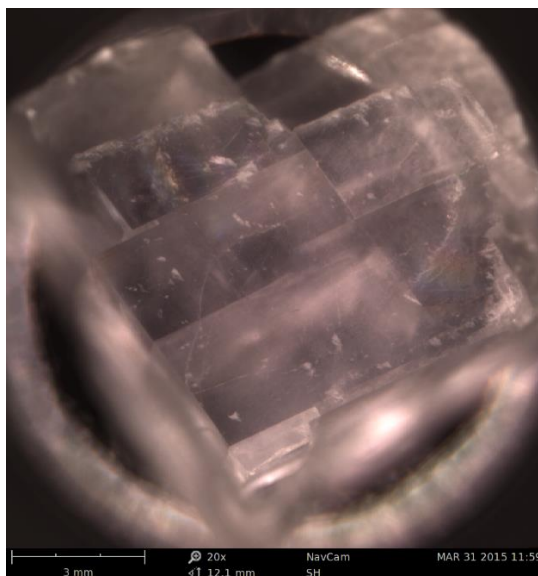


Figure 3-4 Optical image of calcite

### 3.3.5 Decane

N-decane ( $C_{10}H_{22}$ , Sigma Aldrich) was used as a model oil for interfacial tension and contact angle measurements, and as a solvent with stearic acid to formulate 0.01 M stearic acid. The general properties of n-decane are listed in Table 3-4.

Table 3-4 General properties of n-decane

Linear formula	$CH_3(CH_2)_8CH_3$
Purity [%]	$\geq 99$
Density [g/mol]	0.73
Boiling point [K]	574.1
Refractive index ( $n_D$ )	1.411–1.412
Molecular weight [g/mol]	142.28
Specific heat capacity [C]	$315.46 \text{ J K}^{-1} \text{ mol}^{-1}$
Colour	Colourless
Appearance	Liquid

### 3.3.6 Oil-wet surface modification agents

#### 3.3.6.1 Silanes

Three types of silanes (hexamethyldisilazane, HMDS, dodecyltriethoxysilane, and (3-aminopropyl) triethoxysilane) were separately used to achieve various degrees of surface wetness (Figure 3-5). The general properties of the three silane types are listed in Table 3-5.

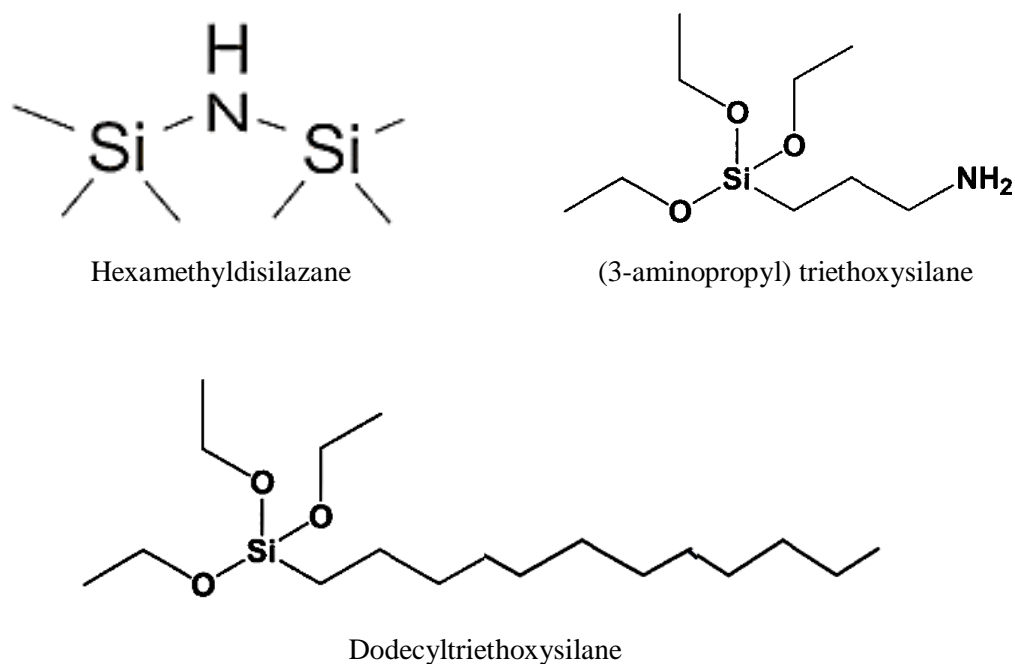


Figure 3-5 Chemical structure of silane groups

Table 3-5 Properties of silanes used in this study

Property	Silane		
	Hexamethyldisilazane	Dodecyltriethoxysilane	(3-aminopropyl) triethoxysilane
Chemical formula	$(\text{CH}_3)_3\text{SiNHSi}(\text{CH}_3)_3$	$\text{C}_{18}\text{H}_{40}\text{O}_3\text{Si}$	$\text{H}_2\text{N}(\text{CH}_2)_3\text{Si}(\text{OC}_2\text{H}_5)_3$
Molecular mass [g/mol]	161.39	332.59	221.37
Boiling point [K]	398	538.4	490
Density [kg/m <sup>3</sup> ]	770	875	946

### 3.3.6.2 Stearic acid

Stearic acid (C<sub>18</sub>H<sub>36</sub>O<sub>2</sub>, Sigma Aldrich, Figure 3-6) was also used to shift the wettability of pure calcite samples from strongly water-wet to oil-wet. The general properties of stearic acid are listed in

Table 3-6. Basically, 0.01 M stearic acid solution was prepared by dissolving 0.2845 g of solid stearic acid in 100 ml of n-decane using a magnetic stirrer.

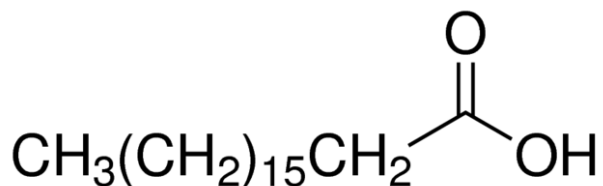


Figure 3-6 Structural formula of stearic acid

Table 3-6 General properties of stearic acid

Linear formula	CH <sub>3</sub> (CH <sub>2</sub> ) <sub>16</sub> COOH
Purity [%]	≥ 98.5
Density [g/mol]	0.73
Melting point [K]	343
Flashpoint [K]	386
Boiling point [K]	574.1
Molecular weight [g/mol]	284.48
Relative density [g/cm <sup>3</sup> ]	0.845
Colour	White
Appearance	Solid

### 3.3.7 Nitrogen Gas (N<sub>2</sub>)

Ultrapure nitrogen gas (BOC, Australia) was used as a drying agent. Using nitrogen instead of compressed air for drying is beneficial for avoiding any potential

contamination that could dramatically influence the accuracy of contact angle measurements. The general properties of the nitrogen gas used are listed in Table 3-7.

Table 3-7 General properties of nitrogen gas

Chemical symbol	N <sub>2</sub>
Purity [%]	99.999
Density [g/L]	1.251
Melting point [K]	63.15
Boiling point [K]	77.355
Impurities	CO <sub>2</sub> ≤ 1 ppm, hydrocarbon (e.g. methane) ≤ 1 ppm, O <sub>2</sub> ≤ 2 ppm, moisture ≤ 2 ppm
Reactivity	Non-reactive
Colour	Colourless
Appearance	Gas

### 3.3.8 Carbene dioxide Gas (CO<sub>2</sub>)

Food grade carbon dioxide (99.9 mol%, liquid phase, BOC, gas code-082) was used to increase the pressure in the contact angle measurement cell when required.

### 3.3.9 Cleaning agents

Several chemicals such as n-hexane (> 95mol %, Sigma-Aldrich), acetone and methanol (> 99.9 mol%, Rowe Scientific) were used as cleaning agents. These materials were used to clean samples before and after each treatment and measurement step.

## 3.4 Instruments and measurement devices

### 3.4.1 Ultrasonic homogeniser

Ultrasonic homogenizers use sound waves to agitate mixtures and disperse fine solid particles in a liquid phase. Consequently, an ultrasonic homogeniser (300 VT Ultrasonic Homogenizer, Biologics) was used to efficiently disperse nanoparticles in

base fluids. Sonication time and power were varied according to the load of nanoparticles and the size and composition of the formulated fluid. The instrument was composed of generator and transducer sections (Figure 3-7) connected to each other by a power cord. The generation parts contained a control port with indicators and a regulator to control the power and duration of sonication processes. The transducer part was composed of a solid tip that transforms electric power to ultrasonic waves. The tip was fabricated from titanium and could be handheld or mounted inside a soundproof box (Figure 3-7).

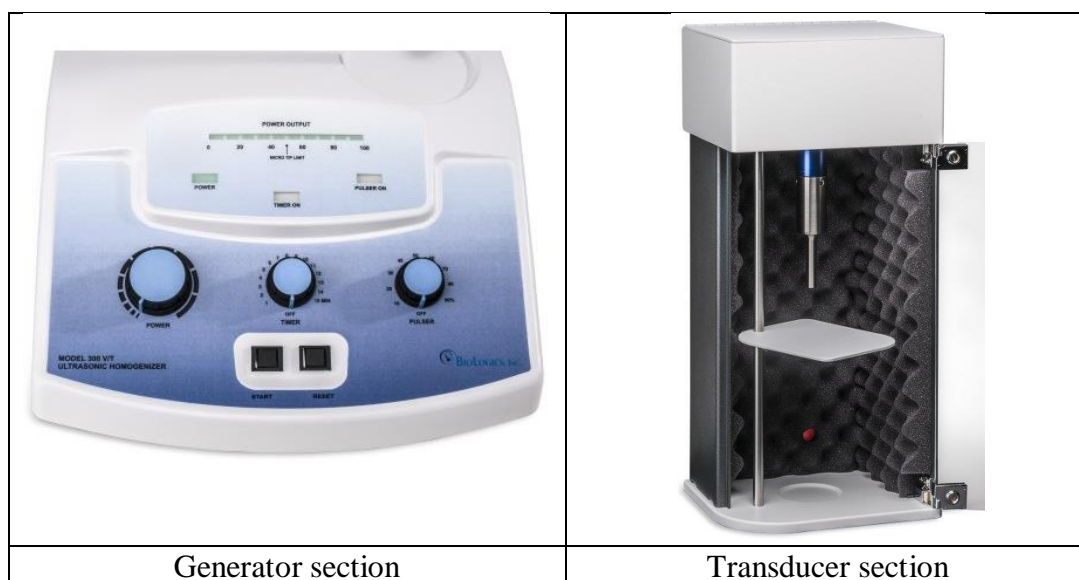


Figure 3-7 Photograph of ultrasonic homogeniser (Model 300 VT Ultrasonic Homogenizer, Biologics).

Specifically, a titanium microtip with a 9.5 mm diameter was used to prepare different batches of nanofluid using a sonication power of 240 W. Typically, after extended use, the titanium tip will corrode due to intensive cavitation, leading to gradual decreases in ultrasonic energy. The titanium tip is a replaceable part and must be changed when advanced erosion causes undue degradation of sonication efficiency.

### 3.4.2 Magnetic stirrer

A magnetic stirrer (1500 RPM, Across International) was used to formulate the brine and surfactant solutions (Figure 3-8). The magnetic mixer is an electrical device that employs a rotating magnetic field to rapidly spin a stirring bar that is immersed in the liquid and vigorously stirs it. Magnetic stirrers are commonly used in chemistry experiments for their high efficacy, compact size and easy cleaning.

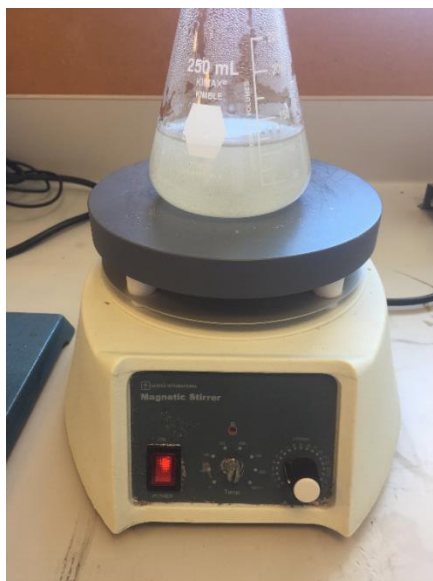


Figure 3-8 Magnetic stirrer (Across International).

### 3.4.3 Electronic balance

An electronic analytical balance (BTA-623, 0.001 g, Phoenix Instruments) was used to accurately weigh the nanoparticles, salt, surfactants and stearic acid required to prepare different formulations.

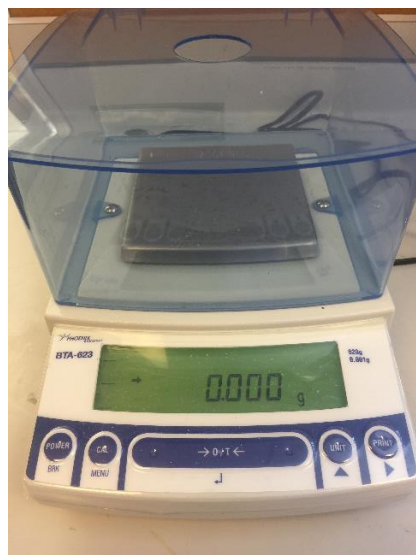


Figure 3-9 Photograph of electronic balance (Model BTA-623, 0.001 g, Phoenix Instruments)

### 3.4.4 Plasma

Electronic plasma (Model Yocto, Diener plasma-surface-technology) was used for the treatment of calcite surfaces (Figure 3-10). Plasma was mainly used for surface cleaning and activation. The unit was composed of a generator (frequency: 100 kHz, power 30 W), and a vacuum pump (suction power: 0.75 m<sup>3</sup>/h). The automatic treatment time was 4 minutes.



Figure 3-10 Photograph of plasma unit (Model Yocto, Diener plasma)

### 3.4.5 Vacuum Drying Oven (VDO)

A vacuum drying oven (Model VO-16020, Across International) with a vacuum pump (Model TW-1A, Across International) was used for drying and heating purposes (Figure 3-11). The oven included a stainless steel chamber containing two wire shelves on which to place samples and solutions with containers over them. The oven was used to increase the temperature during salinisation and ageing with stearic acid, while the vacuum drying system was used to dry the samples after cleaning and receiving different treatments.



Figure 3-11 Photograph of the vacuum drying system that included an oven (Model VO-16020) and a vacuum pump (Model TW-1A), both made by Across International.

### 3.4.6 High-P/T goniometric setup

A high pressure/temperature goniometric setup (Figure 3-12) was used for contact angle and interfacial tension measurements, and was composed of several instruments.

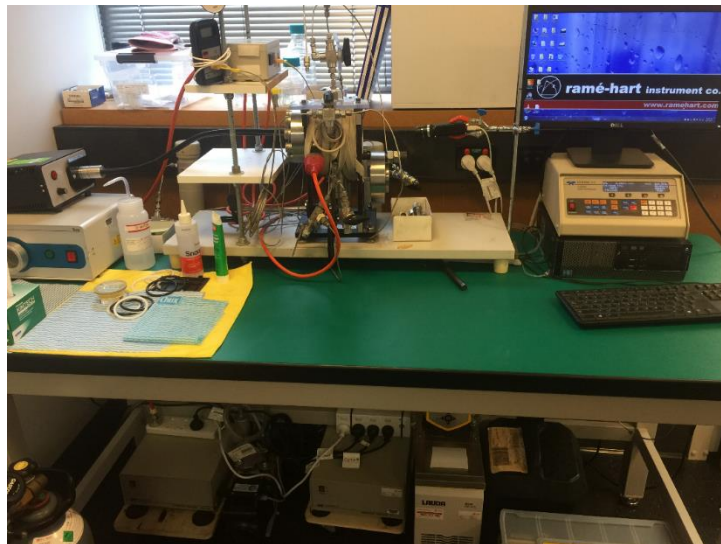


Figure 3-12 Photograph of the high pressure/temperature setup

#### 3.4.6.1 High P/T optical cell

The stainless steel optical cell (Figure 3-13) was designed to work under typical reservoir conditions (pressure, temperature and salinity).

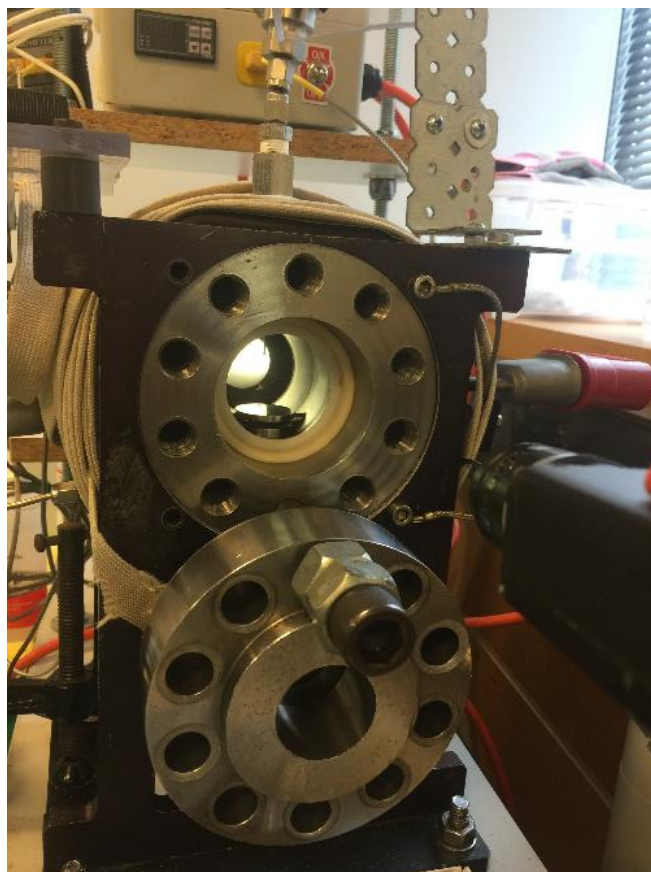


Figure 3-13 Photograph of the high P/T optical cell

During experiments, after increasing the pressure and temperature to the desired values and achieving stable conditions inside the cell, a droplet of degassed liquid with an average volume of  $6 \mu\text{L} \pm 1 \mu\text{L}$  was allowed to flow at  $0.4 \text{ mL/min}$  through a needle inside the cell. The droplet was kept hanging for IFT measurement or allowed to dispense onto the substrate for contact angle measurements. The stainless steel sample base inside the vessel, where the samples were placed, was tilted at an angle of  $17^\circ$  to allow direct measurement of advancing and receding contact angles. The cell was heated by an industrial heating tape. Moreover, the inside of the cell was connected to the high-pressure pumps via Swagelok fittings, pipes and valves.

#### **3.4.6.2 Heating tape and thermocouple**

Industrial heating tape (240 W, HTS/Amptek) was used to heat the measurement cell to the desired temperature. The temperature was controlled using a digital temperature controller (model TTM-002, TOHO) and surface thermocouple (model SA1XL, Omega, Figure 3-13).

#### **3.4.6.3 High precision syringe pumps**

Two high precision syringe pumps were used in this system (Figure 3-14). The first pump (Model 500D syringe pump, Teledyne) was used to increase the pressure inside the measurement cell by injecting  $\text{CO}_2$  gas. Meanwhile, the second pump

(Model 260D syringe pump, Teledyne) was used to follow the de-gassed liquid into the cell. The pressure accuracy for these pumps was 0.1% FS (full scale).



Figure 3-14 Photograph of the high precision syringe pumps

#### 3.4.6.4 Microscope Camera

A high-resolution microscope camera (Basler scA 640–70 fm, pixel size = 7.4  $\mu\text{m}$ ; frame rate = 71 fps; Fujinon CCTV lens: HF35HA-1B; 1:1.6/35 mm) was used to monitor the whole process and record movement inside the optical cell. Moreover, a white light (model Microlight LED, Fibreoptic Lightguides) was used to light the optical cell.

#### 3.4.6.5 Software

The software Fiji Image J was used to analyse images extracted from the video recordings of the process to measure the interfacial tension and contact angle values. The software was installed on the same computer (Desktop, Dell) that was connected to the microscope camera in order to achieve direct measurements.

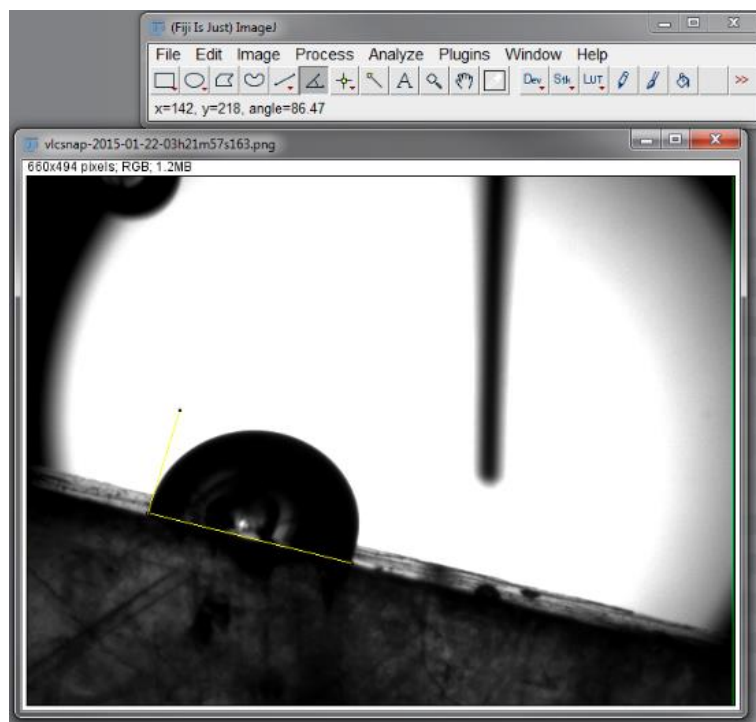
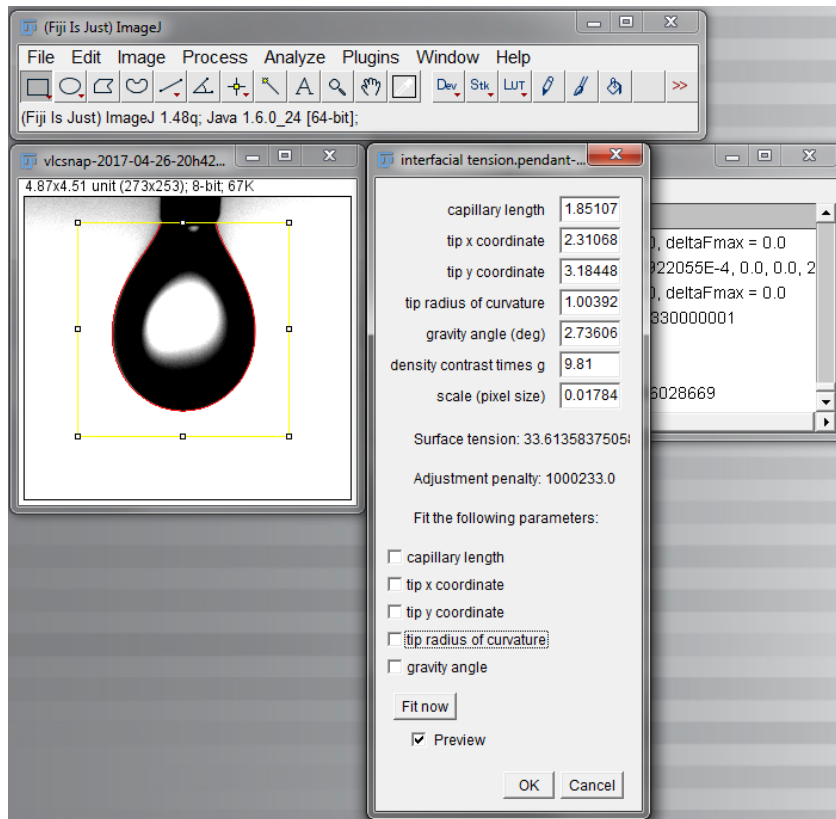


Figure 3-15 Snapshot of Fiji Image J protocols used to measure interfacial tension (upper image) and contact angles (lower image).

### 3.4.7 Conductivity meter

A conductivity meter (RS 180-7127) was used to measure the conductivity of the surfactant and nanoparticle-surfactant formulations (Figure 3-16) at ambient conditions. The device included a wide automatic temperature compensation range of 0°C–60°C. The electrode was made of carbon. The device also included a button to change the measurement units from  $\mu\text{S}$  (microSiemens) to  $\text{mS}$  (milliSiemens).



Figure 3-16 Photograph of the RS 180-7127 conductivity meter

### 3.4.8 pH meter

An advanced dual input analyser (Rosemount 56, Emerson) was used to measure the pH of different formulations under various conditions. The pH measurement device ranged from 0 to 14 with an accuracy  $\pm 0.01$  pH. The device supports continuous measurement of analytical inputs from one or two sensors.



Figure 3-17 Photograph of Rosemount 56 pH meter with two sensors and high-pressure reactor.

### **3.4.9 Scanning Electron Microscopy (SEM)**

A scanning electron microscope (SEM, model Zeiss Neon 40EsB FIBSEM) was used for site-specific analyses of sample surfaces and subsurfaces in two and three-dimensional images. The instrument was a double beam focussed ion beam scanning electron microscope (FIBSEM) equipped with a field emission gun and liquid metal  $Ga^+$  ion source.

### **3.4.10 Energy Dispersive X-ray Spectroscopy (EDS)**

An energy dispersive X-ray spectroscope (EDS, Oxford X-act SSD X-ray detector) with Inca and Aztec software was used to analyse the surface elements of the samples. Atomic weight and stoichiometric concentrations were deduced from these measurements.

### **3.4.11 Atomic Force Microscope (AFM)**

An atomic force microscope (AFM, DSE 95-200, Semilab) was used to measure the surface roughness of different solid samples.

### **3.4.12 Dynamic light scattering**

A Mastersizer 3000 (Malvern Instrument, UK) was used to measure particle sizes, effective particle sizes and the particle size distribution of nano-suspensions.

### **3.4.13 Zetasizer (ZS)**

A Zetasizer (Nano ZS, Malvern Instrument, UK, Figure 3-18) was used to measure the zeta potential of different suspensions.



Figure 3-18 Photograph of Zetasizer (Nano ZS, Malvern Instrument).

### 3.5 Fluid formulations

#### 3.5.1 Pre-equilibration of DI-water with calcite

Calcite surfaces can dramatically dissolve in DI-water or formulated brines, leading to significant changes in surface morphology. Moreover, the formation brine in carbonate oil reservoirs is naturally in equilibration with carbonate surfaces and any in-situ  $\text{CO}_2$ . Consequently, it is critical to pre-equilibrate all the used fluids (e.g. DI-water, brine, nanoparticles dispersions, surfactant formulations, and nanoparticle-surfactant suspensions) with calcite. The DI-water that was used to formulate all the previously mentioned fluids was initially equilibrated with calcite to achieve pre-equilibrated fluids.

Experimentally, offcut calcite was immersed in water and the pH was continuously monitored during the immersion process. Initially, pH will increase due to the dissolution of calcite and the consequent formation of hydroxide ions  $[\text{OH}^-]$ . A later decrease in pH, however, is related to the formation of bicarbonate ions  $[\text{HCO}_3^-]$ . Equilibrium conditions were achieved when no more changes in pH were recorded, meaning that no more calcite was dissolving (Vinogradov and Jackson 2015).

#### 3.5.2 Brine formation

A wide range of brine was formulated by dissolving sodium chloride in pre-equilibrated DI water using a magnetic stirrer at room temperature. The mixing period

was varied depending on the amount of dissolving salt (i.e., concentration of prepared brine). Further, the formulated NaCl solutions were degassed using a vacuum pump to avoid the potential effects of dissolved air, particularly for the brine used to form liquid droplets for interfacial tension and contact angle measurements.

### **3.5.3 Nanoparticle dispersion (silica nanofluid)**

Various silica nanodispersions were formulated to evaluate their behaviour, stability, and effectiveness in terms of interfacial tension reduction and wettability alteration. These suspensions were prepared by ultrasonic homogenisation of different amounts of silicon dioxide nanoparticles in the base fluid (DI water or brine). The required time and power of the ultra-sonication process depended on the load of nanoparticles in the formulated fluid. Further, in some circumstances, a cooling bath was used to avoid any unfavourable increases in temperature, particularly during the preparation of relatively concentrated nanofluids.

### **3.5.4 Surfactant formulations**

Various surfactant solutions with different surfactant concentrations and types (cationic or anionic), and different salinities (NaCl concentration) were formulated. Various surfactant amounts in powder form were mixed with DI water or brine using a magnetic stirrer. The critical micelles concentration (CMC) of each formulation was measured after preparation.

### **3.5.5 Nanoparticle-surfactant suspensions**

Various nanoparticle-surfactant suspensions were prepared by adding a range of nanoparticle amounts to the pre-formulated surfactant solutions and sonicating them. A cooling bath was used during sonication processes to avoid dramatic impacts of raised temperature on surfactant properties.

## **3.6 Calcite surface preparation**

It is essential to sufficiently clean calcite samples before any treatment process, as even minor contaminants can cause large systematic errors. Consequently, the calcite samples were first blown with air to remove any dust or off-cut pieces. Then, samples were cleaned with DI water (pre-equilibrated with calcite) and rinsed with toluene to remove any organic contaminants that were potentially present on the surfaces. Then, calcite samples were pre-dried in the oven at 40 °C for 10 min and subsequently exposed to air plasma to remove any residual contamination.

### 3.7 Modification of pure calcite to an oil-wet state

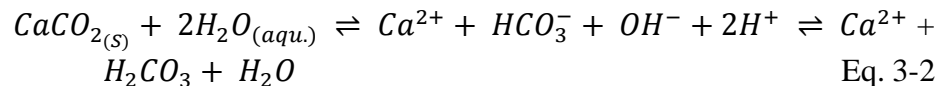
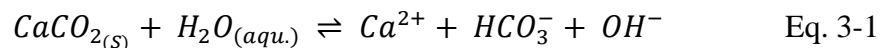
Two different techniques were separately used to shift the wettability of calcite to an oil-wet state to mimic the wetting properties of rock found in oil reservoirs.

#### 3.7.1 Surface modification with stearic acid

Stearic acid, a long fatty acid, can efficiently be adsorbed onto calcite surfaces, changing their wetness status from strongly water-wet to strongly oil-wet (Hansen et al. 2000, Mihajlovic et al. 2009, Shi et al. 2010). In the experiments, 0.01 M stearic acid solution was initially formulated by dissolving 0.285g of solid stearic acid in 100 ml n-decane using a magnetic stirrer at 40 °C for 2 h. A closed flask was used for the mixing process to avoid any potential evaporation and consequent changes in stearic acid concentration.

Before treating them with the prepared stearic acid, calcite samples were first immersed in a low-pH aqueous solution (pH = 4) for 30 min to allow water to diffuse into the lattice of the calcite samples. A fixed calcite-to-aqueous phase weight ratio of 1:5 was used to assure consistent modification conditions for all the modified samples. The acidity of the aqueous solution was controlled by adding drops of HCl or NaOH. After 30 min of immersion, calcite surfaces were carefully blown with ultrapure nitrogen gas to remove excess water. Subsequently, calcite samples were directly immersed in the 0.01 M stearic acid solution and aged for 24 h at ambient conditions. After removing them from the stearic acid, calcite samples were washed with n-hexane and flushed with methanol, acetone and water to remove any excess stearic acid adhered to the surfaces. Finally, the contact angle of the modified surfaces was measured in air and decane to evaluate their surface wettability.

Mechanistically, carbonate ions [ $Ca^{2+}$ ] are the primary sites for stearic acid adsorption (Figure 3-19). Consequently, the chemisorption of stearic acid on calcite surfaces and, thus, wettability modification, is controlled by the dissociation reaction of calcite (Eq. 3-1), which leads to increased hydroxyl ions on the surface due to the effects of pH and dissolved  $CO_2$ . The mechanisms of surface dissociation and adsorption of stearic acid are based on  $H^+$  ions moving to the surface (Eq. 3-2), and carbonate ions  $CO_3^-$  and stearine ions chemisorbing on the surface sites of  $Ca^{2+}$  ions (Eq. 3-4). The  $-Ca^+$  centres that result from calcite surface dissociation will be available for chemisorption.



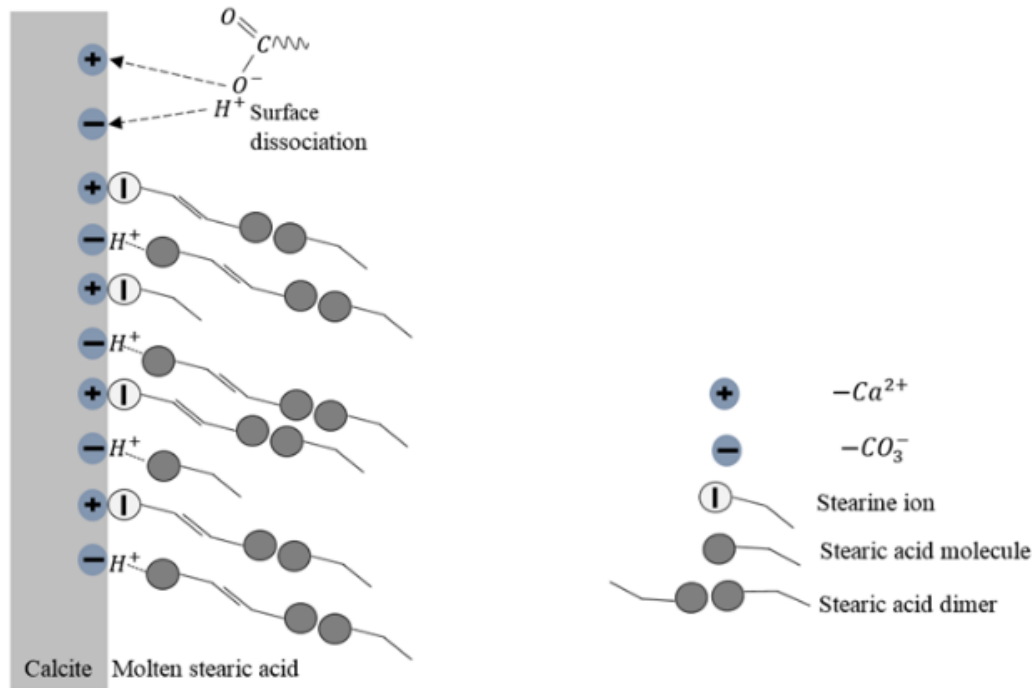
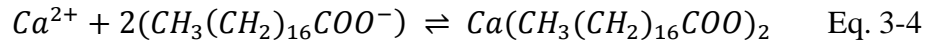
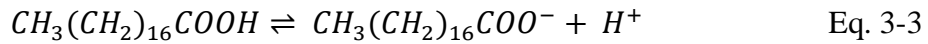


Figure 3-19 Surface dissociation and adsorption of stearic acid on a calcite surface with the potential structure of the adsorbed layer (after Mihajlovic et al. (2009)).

### 3.7.2 Surface modification with silanes (silanisation)

Although different silanes have different tendencies for switching water-wet surfaces into oil-wet ones, the procedure of surface salinisation was identical for all the three used silanes. In the experiments, clean and dry calcite samples were placed in a glass bottle with an airtight cover. Subsequently, silane was gradually pipetted to fully submerge the sample inside the bottle. A constant calcite-to-silane weight ratio (1:5) was used to assure the complete immersion of the sample and identical modification conditions for all samples. The glass bottle was then firmly covered to avoid any evaporation or sample contamination. Then, the sealed glass container was heated to 90 °C for 24 h in an oven. After removal from the silane bottle, the modified calcite sample was washed with different cleaning agents such as n-hexane, methanol and acetone to remove excess silane from the surfaces, which were then dried with ultrapure nitrogen.

### 3.8 Nano-treatment of Oil-wet Calcite with Different Nanofluids

#### 3.8.1 Nano-treatment at ambient conditions

Oil-wet calcite surfaces were treated with silica nanofluids in glass containers at ambient conditions. Specifically, calcite samples were laid vertically in the treatment container and entirely submerged in nanofluid. A constant weight ratio of calcite to nanofluid was used for all treatment experiments. The glass container was kept away from heat and light during nano-treatment to prevent any potential degradation. After the prescribed nano-treatment period, calcite samples were removed from the nanofluid and rinsed with DI water and acetone to remove excess and irreversibly adsorbed nanoparticles. Subsequently, the treated samples were dried with ultrapure nitrogen gas prior to measuring their surface contact angle.

#### 3.8.2 Nano-treatment under reservoir conditions (high P and T)

A high pressure and temperature vessel was used to treat calcite samples with nanofluids under reservoir conditions (Figure 3-20). To accomplish this, each clean calcite sample (pure or oil-wet) was placed vertically in the nano-treatment vessel and submerged in a specific nanofluid for a certain duration at a designated pressure and temperature. A constant immersion ratio of 10 g nanofluid for each 1 g of calcite was used to achieve a duplicated treatment environment. Further, the pressure inside the nano-treatment vessel was increased using the syringe pump (Teledyne D-500) to the desired value (0.1, 10, 20 MPa) and the temperature of the system was set at fixed values (23, 50 or 70 °C).

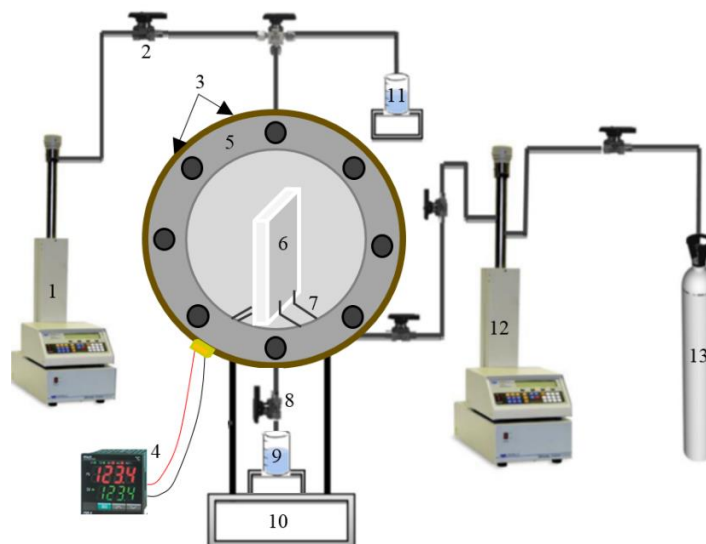


Figure 3-20 Experimental configuration for high pressure, high temperature nano-treatment: (1) syringe pump (liquids), (2) valve, (3) heating tape, (4) thermocouple, (5) high pressure-temperature vessel, (6) calcite substrate, (7) sample holders, (8) pressure relief and drainage valve, (9) collector, (10) stand, (11) nanofluid and flushing liquids feed system, (12) syringe pump, (13) CO<sub>2</sub> source for pressure increase.

## Chapter 4 Oil-Water Interfacial Tensions of Silica Nanoparticle-Surfactant Formulations\*

### Abstract

The implementation of nanotechnology in all industries is one of most significant research fields. Nanoparticles have shown promising applications in subsurface fields. On the other hand, various surfactants have been used in the oil industry to reduce oil/water interfacial tension and also widely used to stabilize the nano-suspensions. The primary objective of this study was to investigate the improvements of surfactants ability in term of interfacial tension ( $\gamma$ ) reduction utilizing addition of silicon dioxide nanoparticles at different temperatures and salinity. The pendant drop technique has used to measure  $\gamma$  and electrical conductivity has used to measure the critical micelle concentration (CMC). The synergistic effects of surfactant-nanoparticles, salt-nanoparticles, and surfactant-salt-nanoparticles on  $\gamma$  reduction and the critical micelles concentration of the surfactants have been investigated. Extensive series of experiments for  $\gamma$  and CMC measurements were performed. The optimum condition for each formulation is shown. We conclude that nanoparticles-surfactant can significantly reduce  $\gamma$  if correctly formulated.

**Keywords** Nanoparticles, Silicon dioxide, Surfactant, Interfacial tension

### 4.1 Introduction

Nanofluids have become a major topic in colloid science as they are an elegant solution for many industrial processes, ranging from drug delivery (Tong et al. 2012), medicine (Baeckkyoung et al. 2015, Lohse and Murphy 2012), polymer composites (ShamsiJazeyi et al. 2014), lubrication (Lu et al. 2014), and metal ion removal (Wang et al. 2012) to carbon geosequestration and enhanced oil recovery (Al-Anssari et al. 2016, Nwidee et al. 2016a). Typically, thermodynamic properties of the base fluids are significantly modified by the suspended nanoparticles; thus specific and attractive properties can be tailored, including viscosity, rheology (Lu et al. 2014), thermal conductivity (Chakraborty and Padhy 2008, Branson et al. 2013) and interfacial tension (Wu et al. 2013a). We examine here the interfacial tension of aqueous nanofluids versus oil ( $\gamma$ ), which is a key factor in many applications including heat transfer (Taylor et al. 2013), production of biofuels (Fan et al. 2011), and hydrocarbon recovery from geological formations (Iglauer et al. 2009, 2010, Hendraningrat et al. 2013).

Silica nanoparticles, as metal oxide form ( $\text{SiO}_2$ ), are widely used owing to their low cost of fabrication and surface modification. Chol (1995) was the first who called the suspension of nano-sized particles (5-100 nm) in base liquid (DI water, brine, polymer or surfactant solutions) as nanofluid. Previously a number of researchers have investigated the effect of silica nanoparticles on oil/water interfacial tension ( $\gamma$ ) (Okubo 1995, Dong and Johnson 2003, Vignati et al. 2003, Saleh et al. 2005, Blute et

al. 2009); however, results are inconclusive and partially contradict each other. For example, Dong and Johnson (2003) have shown that, as silica nanoparticle concentration increases,  $\gamma$  first decreases and then increases to value even higher than that without nanoparticles. Contrary to this, Saleh et al. (2005) demonstrated that bare silica nanoparticles do not affect  $\gamma$  values. Meanwhile, Blute et al. (2009) reported that the highest possible reduction in  $\gamma$  can be achieved by increasing nanoparticle concentration.

Furthermore, the previous tests were limited to relatively low nanoparticle concentrations (<0.05 wt%), which, however, is too small for some applications, e.g. enhanced oil recovery (EOR) (Al-Anssari et al. 2016), CO<sub>2</sub> absorption (Kim et al. 2008) or water-based drilling fluids (Ponmani et al. 2016). For instance, Hendraningrat et al. (2013) have studied the effect of silica nanoparticles on EOR regarding  $\gamma$  reduction. They showed that adding small amounts (0.01-0.05 wt%) of SiO<sub>2</sub> nanoparticles to water can reduce  $\gamma$  of crude oil/ water system from 20 to 8 mN.m<sup>-1</sup>, which is a significant reduction.

Surfactants are widely used in industry and particularly oil production to reduce oil-water interfacial tension (Vatanparast et al. 2011, Wang and Mohanty 2014, Bera et al. 2014). The effect of sodium dodecylsulfate (SDS) as an anionic surfactant and hexadecyltrimethylammonium Bromide (CTAB) as a cationic surfactant on  $\gamma$  is extensively investigated regarding their significant influence on oil/water interfacial tension (Bera et al. 2013). Moreover, it has been reported that nanoparticles can significantly enhance the  $\gamma$  lowering by the effect of surfactants, e.g. Ma et al. (2008) showed that hydrophilic silica nanoparticles increase the efficiency of sodium dodecylsulfate with regards to  $\gamma$  reduction, and Mandal and Bera (2012a) demonstrated that  $\gamma$  can be substantially reduced, by up to 3-4 orders of magnitude in polyethylene glycol-silica nanoparticle formations. This is supported by Esmailzadeh et al. (2014) and Zargartalebi et al. (2014) results for various surfactant-nanoparticle combinations. Biswal et al. (2016) investigated the influence of negatively charged silica nanoparticles on the interfacial tension of n-hexane-water systems for different cationic, anionic and non-ionic surfactant concentration. They observed a reduction in interfacial tension with the increasing cationic and anionic surfactant concentration; however, an increase in interfacial tension was observed when the non-ionic surfactant concentration increased.

Although both electrolytes and temperature significantly affect the properties of nanofluids (Cai et al. 1996, Al-Sahhaf et al. 2005, Hamouda and Karoussi 2008, Bera et al. 2014, Sharma et al. 2015a), these effects were not systematically tested. All surfactant-nanoparticle  $\gamma$  studies used distilled water or a single brine concentration and only tested at room temperatures. Moreover, no previous study has investigated the effect of nanoparticles on the critical micelle concentration (CMC). However, some applications, particularly subsurface applications contain harsh conditions including high temperature and salinity. Moreover, adsorption of surfactant molecules on the solid surface can significantly reduce its concentration in the suspension.

This study thus focuses on the effects of temperature, salinity of the base fluid, and concentration of both surfactant and nanoparticle on  $\gamma$  of decane/surfactant-

nanoparticles formulations. Moreover, the impacts of nanoparticle on CMC of surfactant were also studied.

## 4.2 Experimental Methodology

### 4.2.1 Materials

Two silicon dioxide nanoparticle sizes (porous spheres, Sigma Aldrich, 5 and 25nm) were used to prepare nanofluids with different initial particle size; the nanoparticle properties are tabulated in Table 4-1. n-decane (> 99 mol% purity, from Sigma-Aldrich) was used as a model oil, and acetone (> 99.9 mol% purity, from Rowe Scientific) was used as a cleaning agent. Deionized (DI) water (Ultrapure from David Gray; conductivity = 0.02 mS.cm<sup>-1</sup>) was used to prepare NaCl (≥99.5 mol% purity, from Scharlan) brine, nanofluids and surfactant solutions (two surfactants, one anionic [Sodium Dodecylsulfate, SDS, Sigma Aldrich, ≥ 98.5 mol%, Mol.wt= 288.38 g.mol<sup>-1</sup>, CMC= 2450 mg.L<sup>-1</sup> (8.49x10<sup>-3</sup> mol.L<sup>-1</sup>)] and one cationic [Hexadecyltrimethylammonium Bromide, CTAB, Sigma-Aldrich, ≥ 98 mol%, Mol.wt= 364.45 g.mol<sup>-1</sup>, CMC= 350 mg.L<sup>-1</sup> (9.6x10<sup>-4</sup> mol.L<sup>-1</sup>)].

Table 4-1 properties of silicon dioxide nanoparticles used (Al-Anssari et al. 2016).

Surface area [m <sup>2</sup> .g <sup>-1</sup> ]	140
Purity [wt%]	≥ 99.50
Density [ kg.m <sup>-3</sup> ]	(2200-2600)
Molecular mass [g.mol <sup>-1</sup> ]	60.08
Boiling point [°C]	2230
Zeta potential [mV]	-32.15
Solubility in water	Insoluble

### 4.2.2 Nanofluid preparation

Various 100 mL surfactant solutions with varying surfactant (based on the CMC: 0.001, 0.010, 0.100, 0.500, 0.750, 1.000, 1.250, 1.500 and 2.000 CMC) and NaCl (0, 0.1, 0.5, 1.0, 1.5, 2.0, 2.5, 3.0 and 4.0 wt%) concentration were prepared by adding the

surfactant powder to brine and mixing with magnetic stirrer. Note that the measured CMCs are 2380 and 355 mg.L<sup>-1</sup> for SDS (Atkin et al. 2003, Zargartalebi et al. 2015) and CTAB (Lan et al. 2007), respectively.

Subsequently, different amounts of silica dioxide nanoparticles (0.05, 0.10, 0.50, 1.00, 1.25, 1.50 and 2.00 g) were mixed with aqueous phase (brine, DI water or surfactant solution) and sonicated (with a 300 VT Ultrasonic Homogenizer/ BIOLOGICS instrument) for 60 min to homogenize the fluid (Mahdi Jafari et al. 2006, Petzold et al. 2009, Shen and Resasco 2009, Mondragon et al. 2012). A micro titanium tip with a 9.5 mm diameter was used to prepare the nanofluids with a 240 W sonication power. Each batch solution was sonicated for four periods of 15 min followed by 5 min rest to avoid overheating. In addition, a cooling bath was used to prevent any undesirable increase in temperature (Al-Anssari et al. 2016). The phase stability was then checked under the experimental conditions, and all nanofluids were stable during testing periods; note that the pH was kept at 5 for all suspension by adding drops of HCl or NaOH since silica nano-suspensions are stable against agglomeration and sedimentation when the pH of the suspension is around 4 to 5 even with the presence of salt (NaCl) at concentration  $\leq 6$  wt%. However, these suspensions with such salinity can be coagulated if the pH value exceeds 6 (Franks 2002, Amiri et al. 2009, Mondragon et al. 2012).

#### **4.2.3 Critical micelle concentration (CMC) measurements**

Owing to the high electrical conductance of both, aqueous CTAB and SDS, the electrical conductivity method (Roger et al. 2008, Marcolongo and Mirenda 2011, Zendehboudi et al. 2013) was selected to measure CMC, and the effect of nanoparticle concentration; on micelles formation was measured. The measurements were conducted with a RS 180-7127 conductivity meter at 23 °C and ambient pressure.

#### **4.2.4 Interfacial tension measurements**

Interfacial tensions between n-decane and the aqueous fluids (surfactant, surfactant-nanofluid and nanofluid formulations), and air and the aqueous fluids were measured using the pendant drop method as it is convenient and flexible (Adamson and Gast 1967, Susnar et al. 1994). Here, a liquid droplet is allowed to hang from one end of a dispensing needle in the presence of another smaller density fluid (air or decane). At static condition, the balance between gravity and surface force adjusts the shape of liquid droplet. The  $\gamma$  values were obtained using Young-Laplace equation of capillarity (Arif et al. 2016a). The density of the nanofluid was considered for  $\gamma$  measurements (instead of the base fluid (Ma et al. 2008)) to generate more accurate results.

$$\gamma = \frac{\Delta\rho g}{(\beta k_{apex})^2} \quad \text{Eq. 4-1}$$

Where  $\Delta\rho$  is the density difference between decane or air and nano-suspension,  $g$  is the gravitational acceleration,  $\beta$  is the dimensionless shape parameter, and  $k_{apex}$  denotes the interface curvature at the apex point of the drop (Georgiadis et al. 2010).

All experiments were performed under atmospheric pressure. An optical cell positioned on a vibration-free desk (Arif et al. 2016a) was filled with decane and heated with a heating jacket to a pre-set temperature (23, 30, 40, 50, 60 °C). Subsequently, a drop of aqueous fluid was introduced into the cell through a needle with a high precision HPLC pump (KNAUER P 4.1 S). A high-resolution camera (Basler scA 640–70 fm, pixel size = 7.4  $\mu\text{m}$ ; frame rate = 71 fps; Fujinon CCTV lens: HF35HA-1B; 1:1.6/35 mm) was used to capture the images of the droplets. The extracted images were analysed to determine  $\gamma$  (Alvarez et al. 2009). Each measurement was repeated for three drops under the same condition, and the standard deviation of measurements was  $\pm 3 \text{ mN}\cdot\text{m}^{-1}$ .

### 4.3 Results and Discussion

Limited data are available for the interfacial tension of oil/aqueous surfactant-nanoparticle suspensions. Hence we measured  $\gamma$  at various temperatures and base fluid salinities. First, experiments have examined the effect of particle size (not shown), and the preliminary results revealed that there is absolutely no effect of particle sizes within the studied sizes (5 and 25 nm) on the measurements. Thus, all experiments were applied using 5 nm silicon dioxide nanoparticles.

#### 4.3.1 Critical micelle concentration and the effect of nanoparticles

The critical micelle concentration (CMC); the concentration at which surfactant solutions forms micelles in large amounts (Hoff et al. 2001), was measured for aqueous CTAB and SDS. The measured CMCs were 360 and 2450  $\text{mg}\cdot\text{L}^{-1}$  for CTAB and SDS respectively. These results are consistent with that available in the literature (Atkin et al. 2003, Zargartalebi et al. 2014, Biswal et al. 2016) and from the supplier (Sigma Aldrich) with no more 0.4% error range.

Subsequently, the effect of silica nanoparticle on CMCs of both surfactant was measured, Figure 4-1.

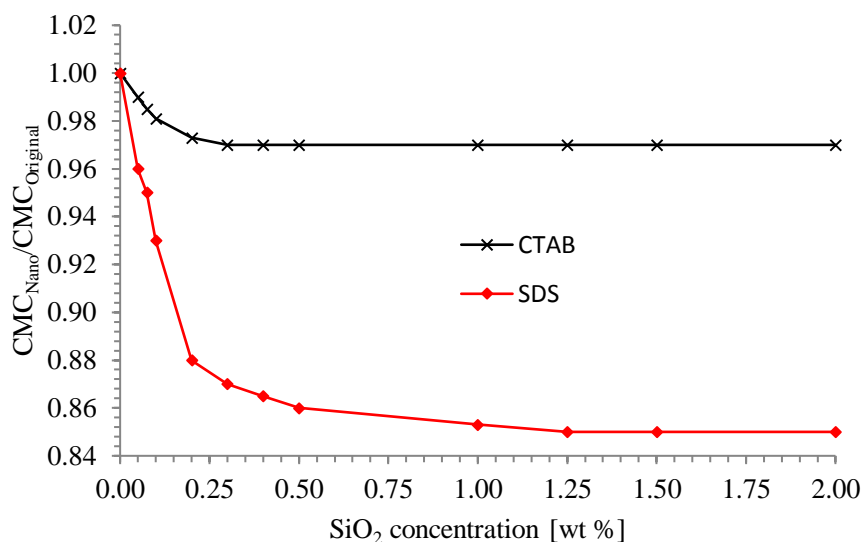


Figure 4-1 Effect of silica nanoparticle concentration on CMC values of aqueous CTAB and SDS suspensions at (23 °C and 10<sup>5</sup> Pa in DI water).

Results show that the CMCs of CTAB and SDS decreased as the concentration of nanoparticles was increased; however, the change in the CMCs for SDS was much more significant when compared to the only slight change for CTAB.

This phenomenon demonstrates that different surfactant molecule-nanoparticle interactions are active. For the SDS-nanoparticle suspension, the increase in solution hydrophilicity due to the increase in (hydrophilic) nanoparticle concentration renders the bulk phase more unfavourable for the hydrophobic tail of the surfactant (Zargartalebi et al. 2015) and thus promotes their affinity to form micelles. Furthermore, the increase in electrostatic repulsion owing to the negative charge on both, the nanoparticle surface and surfactant head group, also promotes micelle formation. Consequently, the formation of micelle aggregates takes place at a lower surfactant concentration, and the CMC is reduced. The opposite electrical charges of CTAB molecule and nanoparticle surface leads to surfactant adsorption on the nanoparticle surfaces (Lan et al. 2007), which has only a minor effect on CMC. At high nanoparticle concentrations, a constant CMC is reached as all surfactant molecules have been already aggregated.

#### 4.3.2 Synergistic effect of nanoparticles and NaCl on CMC of SDS

The synergistic effect of silica nanoparticles in combination with NaCl on CMC values of SDS is shown in Figure 4-2.

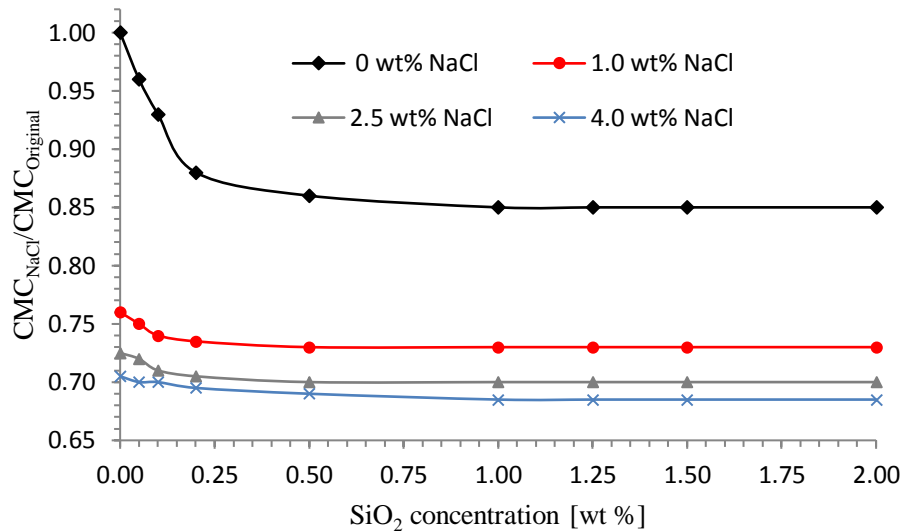


Figure 4-2 Critical micelle concentrations of SDS as a function of nanoparticle (SiO<sub>2</sub>) and NaCl concentration (measured at 23 °C and 10<sup>5</sup> Pa).

In general, the presence of NaCl reduces the CMC, consistency with the literature data (Zhao et al. 2006). When nanoparticles were absent, CMC was reduced by 25% when the NaCl concentration increased from 0 to 1 wt%. CMC was further reduced with a further increase in NaCl concentration, but to a smaller extent. Mechanistically, salt reduces the surfactant solubility by deionizing the surfactant molecules, which leads to the formation of micelles at lower surfactant concentrations (Zhang et al. 2002).

It also can be seen from Figure 4-2 that the efficiency of nanoparticles to reduce CMC of SDS decreases as NaCl concentration increases and at higher salinities the influence of nanoparticles on CMC was relatively insignificant, in particular, above 2.5 wt% NaCl concentrations. Several reports have shown that salts including NaCl can destabilize nanoparticle dispersions by compressing the electrical double layer and screening the electrostatic repulsion force among nanoparticles (Bayat et al. 2014a, Bayat et al. 2014b) resulting in lower zeta potentials and leading to aggregation of nanoparticles in the bulk fluid. This result in a reduced effect of nanoparticles on surfactant tendency to form micelles.

### 4.3.3 Nanofluid-oil interfacial tensions

As mentioned above, the reduction of  $\gamma$  strongly depends on the adsorption of surface active materials at the interface between the two immiscible fluids. It is thus interesting to see whether SiO<sub>2</sub> nanoparticles alone undergo such an adsorption, resulting in a change in  $\gamma$ .

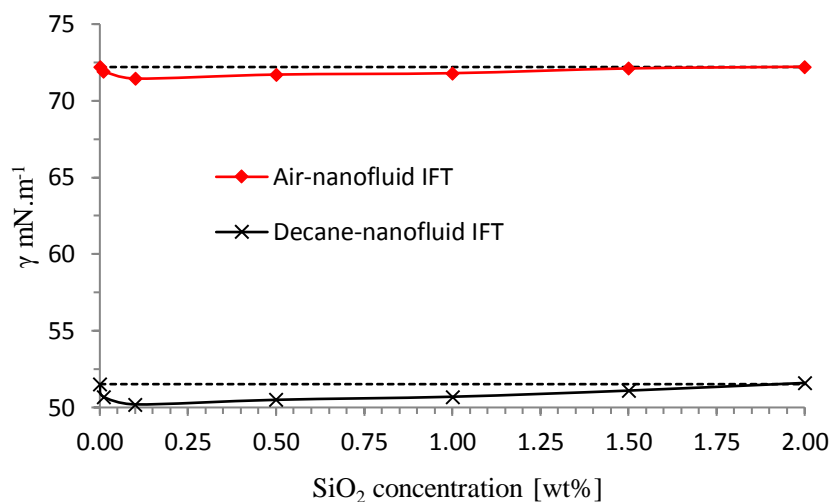


Figure 4-3  $\gamma$  of nanofluid (without a surfactant) against air and decane as a function of nanoparticle concentration at 23 °C.

We thus tested low nanoparticle concentrations ( $\leq 2$  wt%), since these are economically more viable, and clearly the presence of sole nanoparticles did not significantly influence the (air-water or oil-water) interfacial tension (Figure 4-3) This is related to the hydrophilic nature of those particles: they have a high affinity to the water phase and remain in the water bulk phase (Okubo 1995), away from the interface (Ravera et al. 2008). However, some nanoparticles can reach the oil-water interface due to Brownian motion especially at low nanoparticle concentration as demonstrated by dynamic light scattering (Amiri et al. 2009); and this leads to the slight reduction in  $\gamma$  when nanoparticles are added (cp. Figure 4-3). Moreover, agglomeration of nanoparticles at higher concentrations suppresses the motions of these particles (Liu et al. 2012b) and reduces their ability to reach the interface (Mondragon et al. 2012, Lu et al. 2014).

#### 4.3.4 Dynamic interfacial tension measurements

Dynamic  $\gamma$  was measured for several selected fluid systems as shown in Figure 4-4. The dynamic  $\gamma$  of DI-water/decane slightly decreased (by -3%), most likely due to adsorption of some surface active materials (impurities) at the interface although the high purity of the used materials. This reduction was barely noticeable but continuous with time, consistent with Gaonkar (1992) who showed that  $\gamma$  between two immiscible fluids decreases with time. However, the dynamic  $\gamma$  of the nanofluid/decane systems showed a stronger  $\gamma$  reduction (by 5%), which is mainly driven by the adsorption of nanoparticles at the aqueous suspension/oil interface (Zargartalebi et al. 2015).

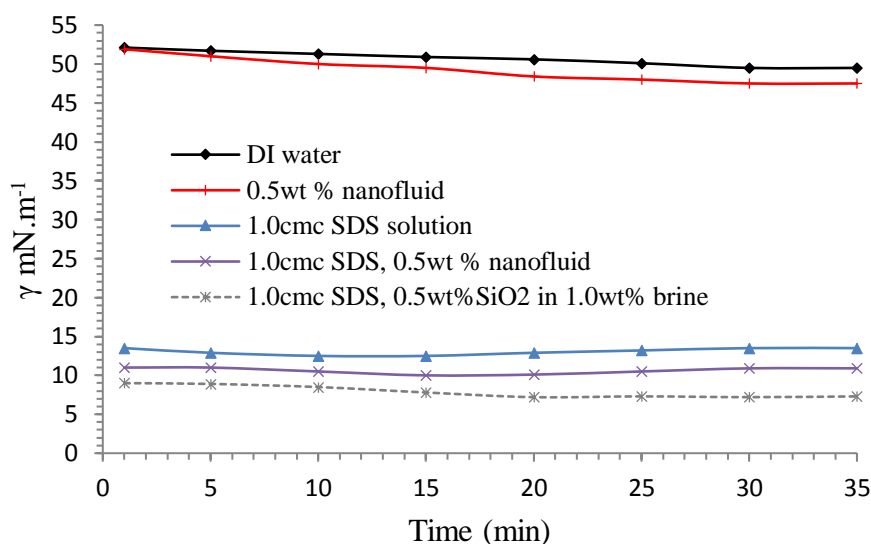


Figure 4-4 Dynamic interfacial tensions measured for different aqueous phases/decane systems (ambient conditions, 23 °C).

The  $\gamma$  of the surfactant formulation was significantly lower as expected (13.5 mN.m<sup>-1</sup>, a 74.1% reduction), elucidating that the surfactant has a much more dominating effect than the SiO<sub>2</sub> nanoparticles with respect to  $\gamma$  reduction (Vashisth et al. 2010). Moreover, an essentially constant  $\gamma$  value was measured (within experiment uncertainty), as surfactant molecules already adsorb at the interface. This finding was unexpected and suggested that contaminants do not significantly change  $\gamma$  which is inconsistent with the results reported by Biswal et al. (2016) who measured a decrease in interfacial tension with time. This inconsistency may be due to the different surfactant concentrations, materials purity, and/or the different cleaning strategies for the measurement equipment (Iglauer et al. 2014).

The addition of nanoparticles further reduced  $\gamma$  to 11.6 mN.m<sup>-1</sup> (Biswal et al. 2016) and particularly when salt was added to the system, which is consistent with the previous observations (Sharma et al. 2015b) and the lowest  $\gamma$  (10 mN.m<sup>-1</sup>) was reached, Figure 4-4. The significant decrease in  $\gamma$  with time in the salt-water-surfactant-nanoparticle-decane system was caused by the salt, which reduced the surfactant solubility in the aqueous phase, thus enhancing surfactant adsorption at the interface (Chu et al. 2004, Zhao et al. 2006).

#### 4.3.5 Interfacial tensions of decane/ SDS-nanofluid systems

The interfacial behaviour of oil-water-nanoparticle-surfactant systems is quite complicated; different surfactant concentrations tend to exhibit dissimilar behavioural patterns in the presence of nanoparticles.

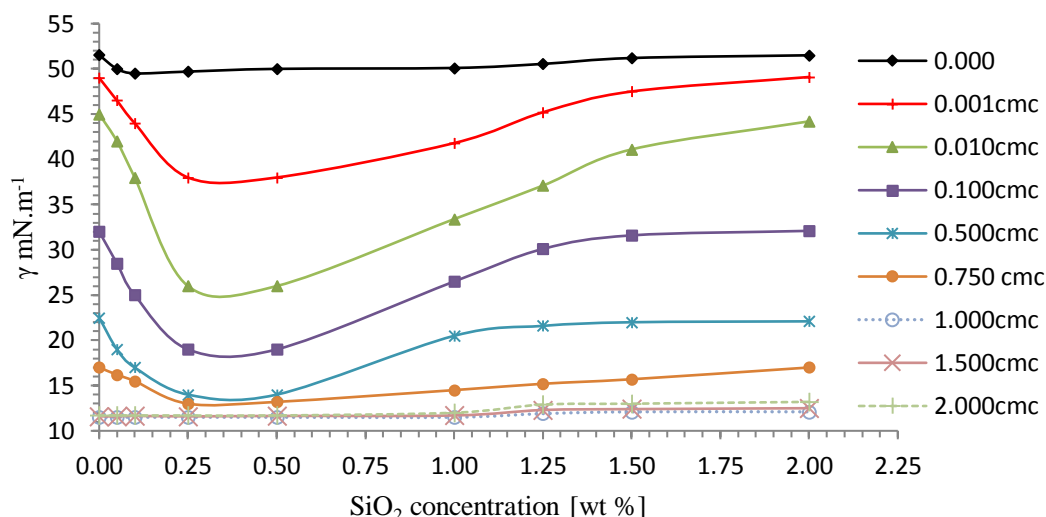


Figure 4-5 Interfacial tension of decane-SDS-SiO<sub>2</sub> nanoparticle-DI water formulations as a function of nanoparticle and surfactant concentrations, measured at 23 °C and 10<sup>5</sup> Pa.

Bare silica nanoparticles at low concentrations (0.05-0.25 wt%) have only a slight effect ( $\sim -4\%$ ) on  $\gamma$  in the absence of surfactant. However, at a higher solid content,  $\gamma$  again reaches the same value as without nano-additives.

The  $\gamma$  pattern of water-decane-SDS-nanoparticle systems is more complex (Figure 4-5). For such systems, surfactant molecules and nanoparticles exist at the interface, which leads to a minimum in  $\gamma$ . At higher surfactant concentrations ( $\geq 0.75$  CMC) however, the surfactant molecules entirely occupy the interface, thus no synergistic effect is observed. The synergistic effect of a surfactant-nanoparticle mixture is related to surface charge (Whitby et al. 2009). The surfactant surface activity increases when the interaction between nanoparticles and surfactant is repulsive (same electrical charge), and this repulsion increases with the increasing nanoparticle concentration (if nanoparticles concentration is  $\leq 0.5$  wt%) (Ma et al. 2008). However, an increase in nanoparticle concentration to  $\geq 1.25$  wt% increases the collisions and agglomerations between nanoparticles, which significantly mitigate the Brownian motion (Amiri et al. 2009). These observations are consistent with both Metin et al. (2012a) and Sharma et al. (2015a) who have studied the effect of high nanoparticle concentration ( $\geq 1$  wt%) on  $\gamma$ .

Specifically, at low surfactant (0.5 CMC) and nanoparticle ( $\leq 0.5$  wt%) concentrations, the reduction in  $\gamma$  is related to both the surfactant molecules and, with a lesser extent, to the solid nanoparticles (Figure 4-5).

### 4.3.6 Interfacial tensions of decane/CTAB-nanofluid systems

The effect of silica nanoparticles on the interfacial tension of a cationic surfactant (e.g. CTAB)-water-decane system is more complex (Figure 4-6) than that of analogue anionic surfactant (e.g. SDS) system, due to the attractive forces between positively charged surfactant molecules and negatively charged nanoparticles (Lan et al. 2007).

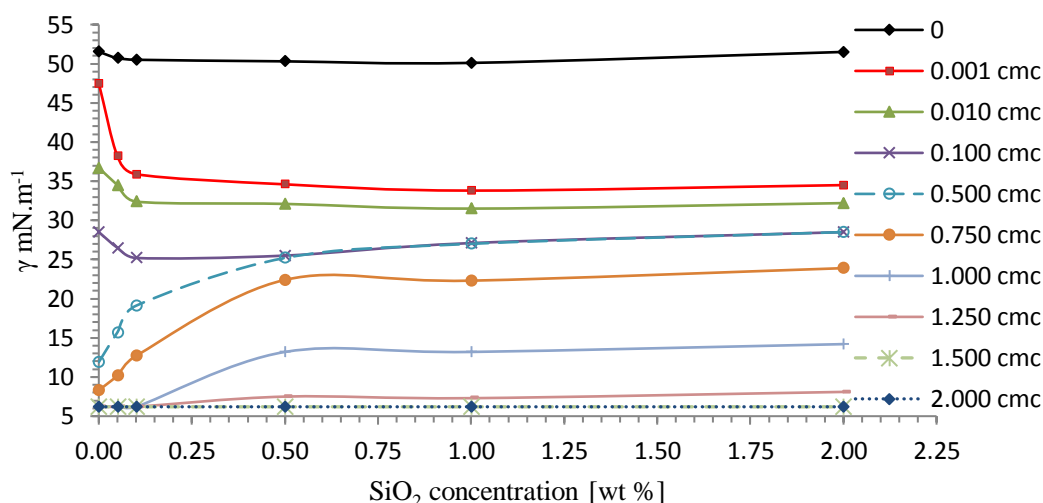


Figure 4-6 Interfacial tension of decane-CTAB-nanoparticle-DI water formulations as a function of SiO<sub>2</sub> nanoparticle and surfactant concentration (fraction of CMC), values measured at 23 °C and 10<sup>5</sup> Pa.

Results show that, specifically, the addition of small amounts (0.05-0.1 wt%) of silica nanoparticles at low cationic surfactant concentrations ( $\leq 0.1$ cmc) led to significant reduction in  $\gamma$ . In contrast, when the surfactant concentration ranged between 0.5 to 1 CMC,  $\gamma$  increased with increasing nanoparticle concentration, which means that the amount of adsorbed surfactant at the interface decreased. Mechanistically, the potential of negative surface charge for silica nanoparticles decrease due to the adsorption of positively charged CTAB molecules. Here, nanoparticles work as carriers to surfactant molecules into the interface direction owing its Brownian motion, and this explains the reduction in  $\gamma$ . However, the increase in cationic surfactant concentration accelerates the reduction of nanoparticles negative surface charge until it reaches the point of zero charges before reversing positive. Consequently, nanoparticles will allow traveling to the interface direction and displacing surfactant molecules. However, any competition between surfactant and nanoparticles for space at the oil-water interface cause  $\gamma$  to increase because surfactant molecules are displaced from the interface (Vashisth et al. 2010). Further, nanoparticles near the interface can form a nanoparticle layer (Zargartalebi et al. 2014), which prevent the cationic molecules from reaching the interface.

### 4.3.7 Interfacial tensions of decane-SDS-nanofluid-salt formulations

To the best of our knowledge, this is the first time that the effect of salt concentration on the interfacial tension of oil-surfactant- aqueous nanofluid systems has been investigated. In industrial applications, salinities can reach high values, e.g. in oil recovery up to maximum values (Xu et al. 2008) or in medical applications up to physiological concentrations (Alam et al. 2015).

Note that increased salinity increases decane/water  $\gamma$  (without surfactant or nanoparticles) (Cai et al. 1996). This is consistent with our measurements, where we measured  $\gamma$  increase by  $4 \text{ mN}\cdot\text{m}^{-1}$  (8.25% from 51 to 55  $\text{mN}\cdot\text{m}^{-1}$ ) upon an increase in NaCl concentration from 0 to 5 wt%.

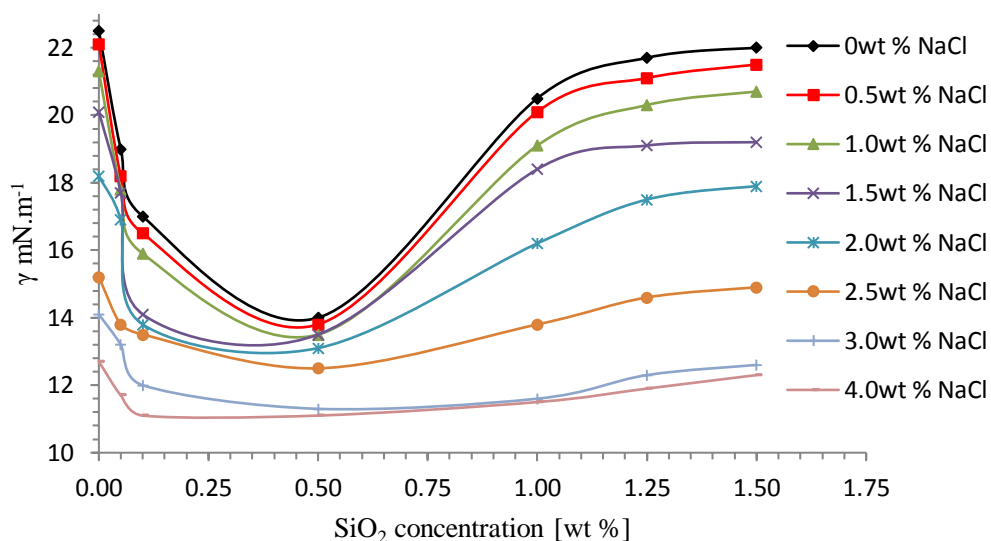


Figure 4-7 Interfacial tensions of decane-SDS-water-NaCl-SiO<sub>2</sub> nanoparticle formulations (0.5 CMC SDS, measured at 23 °C and 10<sup>5</sup> Pa).

The interfacial tensions measured for the decane-SDS-nanoparticles-brine formulations are shown in Figure 4-7. Again, we observed a minimum  $\gamma$  at 0.5 wt% SiO<sub>2</sub> concentration, and this minimum was much more pronounced at lower salinities. Apparently, there is a sweet spot at 0.5 wt% nanoparticle concentration owing to the critical particle concentration (CPC), which is the highest concentration of nanoparticles in brine before the starting of nanoparticles agglomeration due to the effect of salt (Amiri et al. 2009). Mechanistically, the effect of salt ions on  $\gamma$  is related to the influence of such ions on the surface charges of the surfactant molecules.

Overall, the addition of salts further reduced the  $\gamma$  of SDS formulations owing mainly to the existence of electrostatic contribution (electric double layer) (Zhang et al. 2002, Al-Sahhaf et al. 2005, Gurkov et al. 2005). This effect is caused by decreased

surfactant ionization (due to salt addition), which promotes surfactant adsorption at the oil-water interface (Chu et al. 2004, Zhao et al. 2006).

The presence of nanoparticles can significantly influence this  $\gamma$  reduction. At relatively low nanoparticle concentrations ( $\leq 0.5$  wt%  $\text{SiO}_2$ ), a gradually increasing of  $\text{SiO}_2$  concentration leads to a severe  $\gamma$  reduction, particularly at low salt concentrations ( $\leq 2$  wt%  $\text{NaCl}$ ). This phenomenon is again caused by the synergistic effect of nanoparticles and surfactants. Most surfactant but also some nanoparticles adsorb at the interface. At higher nanoparticle concentration ( $> 1$  wt%) the effect of the nanoparticles is, however, neutralized again due to nanoparticles agglomeration (Amiri et al. 2009).

#### 4.3.8 Effect of temperature on $\gamma$

Temperature has a significant effect on the decane-water interfacial tension (Jennings Jr 1967);  $\gamma$  is reduced with increasing temperature, and this influence starkly increases with the presence of salts (Gaonkar 1992, Al-Sahhaf et al. 2005). However, no data for decane-water-salt-SDS-nanoparticles are currently available.

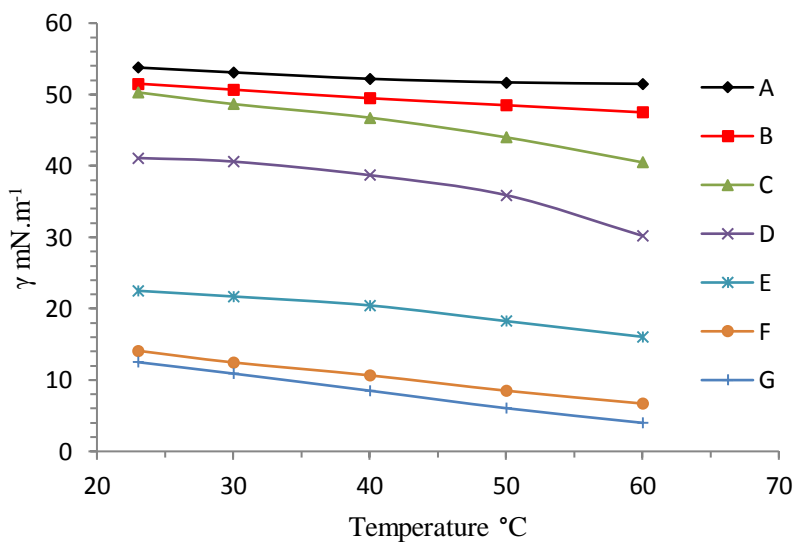


Figure 4-8 Interfacial tension as a function of temperature for various aqueous systems against decane; A-1wt%  $\text{NaCl}$  brine, B- DI water, C- 0.5wt%  $\text{SiO}_2$  dispersion, D- 0.5 wt%  $\text{SiO}_2$  in 1 wt%  $\text{NaCl}$  dispersion, E- 0.5cmc of SDS solution, F- 0.5cmc of SDS in 0.5 wt%  $\text{SiO}_2$  dispersion, G- 0.5cmc SDS and 0.5 wt%  $\text{SiO}_2$  in 1 wt%  $\text{NaCl}$  dispersion.

We thus measured  $\gamma$  for various decane-nanofluid systems at different temperatures, Figure 4-8. For systems without nanoparticles, our results are consistency with literature data (Zeppieri et al. 2001, Vashisth et al. 2010, Bera et al. 2013). For the nanofluids, the temperature influence was even more pronounced, especially at higher temperatures ( $\geq 50$  °C). Moreover, the presence of salt in the nano-suspensions increased the temperature effect. Further, a similar  $\gamma$  decrease, albeit at nominally lower  $\gamma$  values, was observed when a surfactant was added to the system owing to the

change in surfactant solubility and nanoparticle behaviour, see above (Handy et al. 1983, Anderson 1986, Gupta and Mohanty 2010).

#### 4.4 Conclusions

In this study, the synergistic effect between silica nanoparticles and anionic surfactant has been explicitly addressed for the first time. The effect of nanoparticles on the interfacial tension of decane-water, decane-brine, decane-surfactant-water, and decane-surfactant-brine system was investigated. Two different (one cationic and one anionic) surfactants were screened to evaluate the best surfactant concerning  $\gamma$  reduction. The effect of salt was also investigated using eight different concentrations (0 to 4 wt% NaCl) and the optimum salt and nanoparticle concentrations were identified.

The results of this study help to specify the optimum nanoparticle concentration that leads to significant reduction in oil/water interfacial tension.

While nanoparticles on their own had only little influence on  $\gamma$ , consistent with Mondragon et al. (2012) results, the addition of anionic surfactant led to significant synergistic effects, again consistent with literature data (Whitby et al. 2009): a sweet spot (minimum  $\gamma$ ) was identified at 0.5 wt% SiO<sub>2</sub> nanoparticle concentration for surfactant concentrations  $\leq 1$  CMC. The CMC itself was strongly influenced by salt concentration as expected (Zhang et al. 2002, Zhao et al. 2006) but CMC was only slightly affected by nanoparticles. Consistent with the effects on CMC and results reported by Bera et al. (2014),  $\gamma$  was also significantly reduced at higher salinities for all systems. However, no synergistic effect was observed between cationic surfactant and silica nanoparticles.

Furthermore, increasing the temperature generally reduced  $\gamma$ , for all formulations due to its effect on the decane solubility in water (Al-Sahhaf et al. 2005, Vashisth et al. 2010, Bera et al. 2013).

Overall, we conclude that nanoparticles have a significant ability to reduce the CMC of SDS systems; however, an increase in NaCl concentration in the base fluid can mitigate this influence. Moreover, the presence of a relatively small concentration of nanoparticles ( $\leq 0.5$  wt %) can increase the efficiency of surfactant to reduce  $\gamma$ , especially when NaCl concentrations are  $\leq 2$  wt%. This is caused by a synergistic effect of nanoparticles formulated with surfactant; both particles and surfactant can migrate to the oil-water interface and reduce  $\gamma$  (Lan et al. 2007, Wang et al. 2008). However, no nanoparticle influence on surfactant's efficiency was observed at or above CMC.

## Chapter 5 Wettability alteration of oil-wet carbonate by silica nanofluid

### Abstract

Changing oil-wet surfaces towards higher water wettability is of key importance in subsurface engineering applications. This includes petroleum recovery from fractured limestone reservoirs, which are typically mixed or oil-wet, resulting in poor productivity as conventional waterflooding techniques are inefficient. A wettability change towards more water-wet would significantly improve oil displacement efficiency, and thus productivity. Another area where such a wettability shift would be highly beneficial is carbon geo-sequestration, where compressed CO<sub>2</sub> is pumped underground for storage. It has recently been identified that more water-wet formations can store more CO<sub>2</sub>.

We thus examined how silica based nanofluids can induce such a wettability shift on oil-wet and mixed-wet calcite substrates. We found that silica nanoparticles have an ability to alter the wettability of such calcite surfaces. Nanoparticle concentration and brine salinity had a significant effect on the wettability alteration efficiency, and an optimum salinity was identified, analogous to that one found for surfactant formulations. Mechanistically, most nanoparticles irreversibly adhered to the oil-wet calcite surface (as substantiated by SEM-EDS and AFM measurements). We conclude that such nanofluid formulations can be very effective as enhanced hydrocarbon recovery agents and can potentially be used for improving the efficiency of CO<sub>2</sub> geo-storage.

### 5.1 Introduction

The unique properties of designed nanoparticles have shown promising applications in a diverse range of fields, spanning from medicine (Lohse and Murphy 2012), drug delivery (Tong et al. 2012), biology (De et al. 2008), food additives (Rajauria et al. 2015), polymer composite (ShamsiJazeyi et al. 2014), metal ions removal (Wang et al. 2012), corrosion protection (Winkler et al. 2011), heterogeneous catalysis (Balaji et al. 2011), and improved surface properties (Wilson et al. 2006) to enhanced oil recovery (ShamsiJazeyi et al. 2014, Zhang et al. 2014), on which we focus here.

In enhanced oil recovery (EOR), one of the main challenges is hydrocarbon production from fractured limestone reservoirs. These reservoirs contain more than half of the known remaining oil reserves in the world (Sharma and Mohanty 2013), and they are typically intermediate-wet or oil-wet (Gupta and Mohanty 2010). Secondary recovery (conventional waterflooding techniques) is inefficient and productivity is low: mainly oil from the fractures is produced as water does not spontaneously imbibe into the oil-wet rock matrix (Mason and Morrow 2013); however, most oil is stored in the matrix (Gupta and Mohanty 2010), and as a result only 10-30% of the oil is recovered (Wu et al. 2008).

One mechanism, which can significantly improve oil production, is to render the oil- (or intermediate-) wet carbonate surfaces water-wet, so that water spontaneously imbibe into the rock and displaces the oil from the matrix pore space (Rostami Ravari et al. 2011). Several methods have been suggested: surfactant flooding (Wu et al. 2008, Mason and Morrow 2013), polymer flooding (Ding et al. 2010, Guo et al. 2013), nanoparticle stabilized emulsions (Shen and Resasco 2009), various nanoparticle-surfactant-polymer formulations (Al-Manasir et al. 2009, Cui et al. 2009, Sharma et al. 2014b, Zhu et al. 2014, Zargartalebi et al. 2015), and nanofluids (Ju et al. 2006, Ju and Fan 2009, Suleimanov et al. 2011, Hendraningrat et al. 2013). Surfactant EOR has been tested at field scale, but efficiency proved to be poor (Maerker and Gale 1992). However, when polymer was used as co-surfactant, oil recovery was enhanced significantly (Maerker and Gale 1992). The other techniques have not been used at industrial scale as far as we are aware.

Furthermore a wettability change towards more water-wet would be greatly beneficial to Carbon Geo-Storage (CCS) projects, where oil-wet rock surfaces lead to dramatically reduced storage capacity and containment security (Iglauer et al. 2015a, Iglauer et al. 2015c). Specifically, higher water wettability has been shown to increase residual trapping capacities, at the reservoir scale (Iglauer et al. 2015c), and at the core- or pore-scale (e.g. Spiteri et al. (2008), (Iglauer et al. 2011a, Iglauer et al. 2012) versus Chaudhary et al. (2013)). Moreover, higher structural trapping capacities are predicted for strongly water-wet systems (Iglauer et al. 2015c).

It is thus highly desirable to render such hydrophobic mineral surfaces strongly water-wet; the key to successful EOR and improved CCS is therefore to find formulations, which are very efficient in wettability alteration at very low concentrations (because of economical cost). The economic viability of these processes depends on crude oil prices and carbon tax.

Nanoparticle formulations can meet these requirements as they are active at low concentrations (e.g. compare Mahbubul et al. (2014)), and can migrate through the pore space of the reservoir and penetrate into even the smallest pores (Zargartalebi et al. 2015) – note that rock matrix pore sizes in limestone vary between 0.01-100  $\mu\text{m}$  (Arns et al. 2005). However, the efficiency of such formulations is a complex function of several factors, including the size and type of nanoparticles, nanofluid preparation and stability, the nature of the porous medium, thermo-physical and geological conditions and dwell time in the reservoir (Petosa et al. 2010, Zhang et al. 2015). Despite the vital importance for limestone reservoirs globally, previous studies focused on sandstone formations (Ju et al. 2006, Ju and Fan 2009, Maghzi et al. 2011, Hendraningrat et al. 2013, Sharma et al. 2014b), and only limited information is available for carbonate reservoirs: Roustaei and Bagherzadeh (2014) conducted coreflood tests and they demonstrated that nanofluid-EOR can increase oil production by 9-17% depending on ageing time, and Zhang et al. (2015) have investigated the adsorption behaviour of silica nanoparticles on calcite powder.

We thus examine the wettability alteration efficiency of silica nanofluids on oil-wet and intermediate-wet calcite surfaces and how various factors influence this efficiency.

All experiments were conducted at ambient conditions. At reservoir conditions, however, significantly higher pressures and elevated temperatures prevail, and as pressure and particularly temperature can affect nanofluid properties (Hendraningrat et al. 2013), nanofluid efficiency at reservoir conditions may be different to that measured at ambient conditions; furthermore, nanofluid efficiency is probably also influenced by rock heterogeneity, which determines nanofluid flow and distribution (ShamsiJazeyi et al. 2014, Skaug et al. 2015) throughout the formation.

## 5.2 Experimental Methodology

### 5.2.1 Materials

N-decane (> 99mol %, from Sigma-Aldrich) was used as a model oil. N-hexane (> 95mol %, from Sigma-Aldrich), nitrogen (> 99.99mol%, from BOC), acetone and methanol (> 99.9mol%, from Rowe Scientific) were used as cleaning agents. Deionized (DI) water (Ultrapure from David Gray; conductivity = 0.02 mS/cm) and sodium chloride ( $\geq 99.5$  mol%, from Scharlan) were used to prepare brines (0-20 wt% NaCl).

Silicon dioxide nano-powder (porous spheres, Sigma Aldrich) was used to prepare the nanofluids (general properties are listed in Table 5-1).

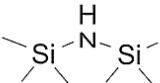
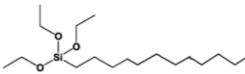
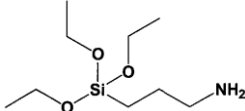
Table 5-1 Properties of silicon dioxide nanoparticles (Sigma Aldrich 2015).

Particle size [nm]	5-15
Purity [wt%]	99.5
Density [kg/m <sup>3</sup> ]	(2200-2600)
Boiling point [°C]	2230
Melting point [°C]	1600
Molecular mass [g/mol]	60.08
Solubility in water	Insoluble

Iceland spar samples (pure calcite, from WARD'S Natural Science) were used as substrates; the surface topography of the calcite samples was measured with an atomic force microscope (model DSE 95-200), Figure 4, as surface roughness influences wettability (Marmur 2006) and adsorption rate of nanoparticles (Munshi et al. 2008). Prior to nano-treatment, all calcite samples were very smooth with root mean square (RMS) surface roughness between 18-32 nm.

Pure calcite, however, is strongly water-wet (Wu et al. 2008, Espinoza and Santamarina 2010). This was confirmed by our contact angle measurements on clean substrates (the water contact angle  $\theta$  was  $0^\circ$ ). We note that in the literature slightly higher contact angles were reported, probably due to insufficient cleaning (Iglauer et al. 2014). Consequently, it was necessary to render the calcite surface oil-wet to simulate an oil (or  $\text{CO}_2$  storage) reservoir. To accomplish this, the calcite surfaces were treated with a range of silanes (Kallury et al. 1994, Grate et al. 2012): hexamethyldisilazane (HMDS), dodecyltriethoxysilane and (3-aminopropyl) triethoxysilane (Table 5-2). We note that previously some researchers used naphthenic acids or crude oil for wettability alteration, however, such a wettability change is unstable and leads to only weakly water-wet or intermediate-wet surfaces (Wu et al. 2008), rather than clearly oil-wet surfaces.

Table 5-2 Silanes used and their properties (Sigma Aldrich 2015).

Silane	Chemical Formula	Chemical Structure	Molecular mass [g/mol]	Boiling point [K]	Density [ $\text{kg/m}^3$ ]
Hexamethyldisilazane	$(\text{CH}_3)_3\text{SiNHSi}(\text{CH}_3)_3$		161.39	398	770
Dodecyltriethoxysilane	$\text{C}_{18}\text{H}_{40}\text{O}_3\text{Si}$		332.59	538.4	875
(3-aminopropyl) triethoxysilane	$\text{H}_2\text{N}(\text{CH}_2)_3\text{Si}(\text{OC}_2\text{H}_5)_3$		221.37	490	946

## 5.2.2 Calcite surface preparation

The calcite surfaces were flushed with DI water and rinsed with toluene to remove any organic contaminants. Subsequently, the samples were dried for 10 min at  $40^\circ\text{C}$  and exposed to air plasma (Iglauer et al. 2014, Sarmadivaleh et al. 2015) for 40 min to remove any residual contaminants. It is important to properly clean the samples' surfaces as residual contaminations can lead to dramatic systematic errors (Love et al. 2005, Mahadevan 2012, Iglauer et al. 2014). Silanization started directly after surface preparation to minimize any contamination.

### 5.2.2.1 Surface modification with silanes

Three different silanes were used to render the calcite surfaces to oil wet (Table 2). Each cleaned calcite substrate was placed in a separate small glass bottle and silane was pipetted gradually over the sample surface until the substrate was fully immersed

in silane. The bottle was then tightly sealed to prevent any evaporation or sample contamination. Subsequently, the bottles were placed in an oven and heated at 363 K for 24 h. Finally, the calcite surfaces were washed with n-hexane and methanol in order to remove excess silane and finally flushed with DI water before drying with pure nitrogen. During this process the silyl groups of the silane reacted with the hydroxyl groups on the surface forming siloxane bonds (Figure 5-1; London et al. (2013)). As a result, alkyl (or aminoalkyl) groups were chemically bonded to the surface, which rendered the surface more oil-wet. The alkyl groups are more representative of lighter oil, while the amino-alkyl, with its heteroatom nitrogen, mimics more medium density oil with significant resin contents (Pedersen et al. 2014). We quantified the degree of wettability alteration by dispensing a drop of water onto the surfaces in air or n-decane (Table 5-3) using the tilted plate method (Lander et al. 1993), see below.

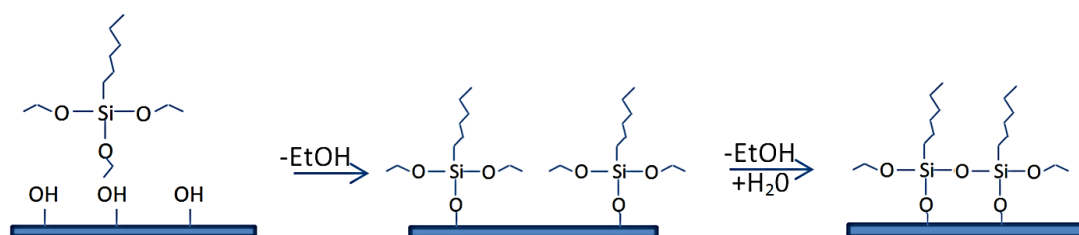


Figure 5-1 silylation of calcite surface (Wolthers et al. 2012) (after London et al. (2013)).

Hexamethyldisilazane and dodecyltriethoxysilane were very effective in terms of increasing the water contact angle  $\theta$ . Water advancing contact angles  $\theta_a$  (which are relevant for the water imbibition process into the small rock capillaries) reached  $\sim 130$ - $140^\circ$ . The 3-aminopropyltriethoxysilane was less effective, and mixed-wet substrates were obtained ( $\theta \sim 70^\circ$ ), probably due to the higher polarity of the terminal amine group. We note that the measured water contact angles were significantly higher in n-decane than in air, and we conclude that tests should be conducted with oil as this is more relevant. As dodecyltriethoxysilane altered the surface to the most oil-wet state, we selected this silane for all subsequent studies.

Table 5-3 Water contact angles on silane-modified calcite surfaces (ambient conditions).

Silane	n-decane		air	
	advancing	receding	advancing	receding
	$\theta_a$ [°]	$\theta_r$ [°]	$\theta_a$ [°]	$\theta_r$ [°]
Hexamethyldisilazane	129	120	76	71
Dodecyltriethoxysilane	141	129	93	88
(3-aminopropyl) triethoxysilane	73	66	47	39

### 5.2.3 Nanofluid Preparation

Various nanofluids were tested for their ability to render oil-wet calcite surfaces water-wet. These fluids were formulated by homogenizing the silicon dioxide nanoparticles (properties are listed in Table 5-1) in brine with an ultrasonic homogenizer (300 VT Ultrasonic Homogenizer/ BIOLOGICS) for 120 min (Shen and Resasco 2009). We note that magnetic stirring is insufficient to homogenize such fluids (Mahdi Jafari et al. 2006). Specifically, a titanium micro tip with a 9.5mm diameter was used to prepare 100 mL batches of nanofluid using a sonication power of 240W. Each batch was sonicated for 8 periods of 15 minutes with 5 minutes rest to avoid overheating. After sonication, the nanofluid was stored in a dark and cool environment for 2 hours to ensure stability and homogeneity. Different nanoparticle concentrations (0.5- 4wt%) and brine salinities (0-20wt% NaCl) were tested; nanofluid and brine densities were measured at room conditions (Figure 5-2) with an Anton Paar DMA 4500 densitometer (accuracy  $\pm 0.0001 \text{ g/cm}^3$ ).

The phase behaviour of the nanofluids was monitored by taking photos of the test tubes every 30 min in the first 6 hours and every 6 hours over 6 weeks. During this time all nanofluids with  $\text{SiO}_2$  concentrations above 0.5wt% showed stable behaviour. At lower nanoparticle concentration, however, and especially at high salinities ( $\geq 15 \text{ wt}\%$ ), instabilities (i.e. nanoparticle flocculation within hours) were observed; this is related to the screening effect of electrolytes on the electrostatic repulsion forces between the nanoparticles: high electrolyte concentration reduces this repulsive forces (Li and Cathles 2014), which leads to accelerated coalescence and sedimentation of nanoparticles after homogenization, particularly at low nanoparticle concentration.

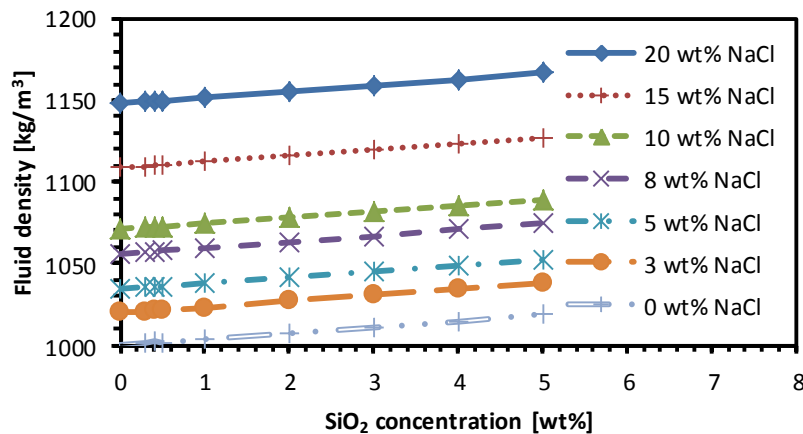


Figure 5-2 densities of various nanofluids used.

#### **5.2.4 Surface modification with nanofluid (Nano-modification) and Contact angle measurements**

In order to test the efficiency of the nanofluids in terms of wettability alteration, the oil-wet calcite substrates were immersed in the nanofluid at room conditions for prescribed exposure times (1-100 h). Subsequently, contact angles were again measured.

Specifically, advancing and receding water contact angles were measured using the tilted plate technique (Lander et al. 1993). Generally, 6-7 $\mu$ L water drops were dispensed onto the substrate (Munshi et al. 2008), which was placed on a metal platform at an inclination angle of 17°. The water contact angles were measured just before the drop started to move following the procedure described by Al-Yaseri et al. (2015a). The whole process was recorded with a high resolution video camera (Basler scA 640–70 fm, pixel size = 7.4  $\mu$ m; frame rate = 71 fps; Fujinon CCTV lens: HF35HA-1B; 1:1.6/35 mm) and  $\theta$  was measured on images extracted from these movies with Image J software. The standard deviation for the  $\theta$  measurements was  $\pm 3^\circ$  based on replicate measurements. The water advancing contact angle is associated with the imbibing water front in a reservoir or individual capillary, and  $\theta_a$  is thus most important for the applications described in this study. We note that  $\theta_a$  is a key variable in pore-scale fluid dynamics models (Sheppard et al. 2005, Gharbi and Blunt 2012); with which oil production curves or CO<sub>2</sub> spreading behaviour in rock can be calculated.

### **5.3 Results and discussion**

A shift in rock surface wettability from oil-wet to water-wet is expected to significantly increase oil production particularly from fractured formations where spontaneous imbibition of water is the prime production mechanism (Wu et al. 2008, Ju and Fan 2009). Furthermore, significantly higher CO<sub>2</sub> trapping capacities have been predicted for carbon geo-storage projects, if the rock is strongly water-wet (Iglauer et al. 2015a, Iglauer et al. 2015c). This is true for the structural trapping capacity, where a lower water contact angle raises the capillary entry pressure of the caprock, and thus significantly increases the column height of CO<sub>2</sub>, which can be permanently immobilized beneath the caprock (Iglauer et al. 2015c). And it is also true for the capillary trapping capacity of CO<sub>2</sub> (Iglauer et al. 2011b), where lower water contact angles lead to more frequent snap-off and trapping of CO<sub>2</sub> bubbles (which are trapped in the pore network of the rock matrix by capillary forces; cp. Iglauer et al. (2011a) versus Chaudhary et al. (2013)). Here we discuss how application of nanofluids can achieve a substantial wettability change, and the effect of different parameters on this change.

### 5.3.1 SEM-EDS and AFM analysis

Surface modification was probed with a scanning electron microscope (SEM, Zeiss Neon 40EsB FIBSEM) and energy dispersive x-ray spectroscope (EDS, Oxford X-act SSD x-ray detector with Inca and Aztec software). Significant silicon concentrations were detected on five points on the sample surface after nano-modification (Table 5-4), which indicates that nanoparticles were rather homogeneously distributed on the surface, consistent with previous studies on glass and silicon substrates (Nikolov et al. 2010, Winkler et al. 2011). The slight variation of silica concentration is related to small perturbations in the nanofluid's homogeneity and the surface roughness of the substrate (Täuber et al. 2013, Zhang et al. 2015).

Table 5-4 Surface composition of the oil-wet calcite substrates after modification with nanofluid (2wt% SiO<sub>2</sub> in 20wt% NaCl brine, 12 hours exposure time).

Point	Calcium [wt%]	Silicon [wt%]	Oxygen wt%
1	33.4	1.9	64.7
2	35.2	2.3	62.5
3	32.6	3.3	64.1
4	33.4	1.9	64.7
5	35.2	2.3	62.5

The SEM images revealed significant adsorption of nanoparticles onto the calcite surface; and these adsorbed particles partially agglomerated into larger clusters (Figure 5-3). While the original calcite surface was very flat (except a crystal layer edge, in the images of 10 µm), exposure to nanofluid changed the surface morphology significantly, and an irregularly spreaded coating was visible. On all SEM images the irreversibly adsorbed fraction was imaged (i.e. the substrate was exposed to different cleaning fluids, see section 5.3.3).

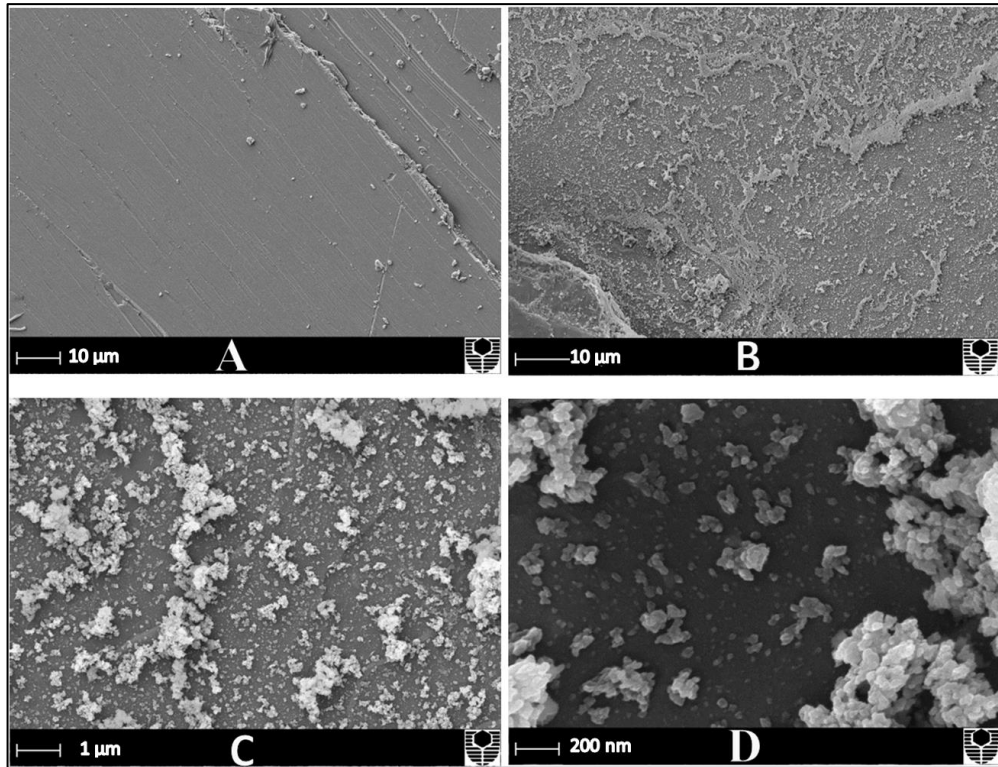


Figure 5-3 SEM images of an oil-wet calcite surface: a) before; b) after nanofluid treatment (4wt% SiO<sub>2</sub> in 5wt% NaCl brine, 1 hour exposure time); c) high resolution; and d) maximum resolution zoom-into the irreversibly adsorbed silica nanoparticles.

These results are consistent with AFM measurements performed on the nano-treated calcite substrates (Figure 5-4): Higher surface roughness was found on the nano-treated surface: the RMS surface roughness increased to 350-3000nm (from 18-32nm) and associated z-ranges (i.e. peak heights) increased to 550-5000nm (from 30-300nm). The AFM images also confirmed quasi-homogeneous spread of the adsorbed nanoparticles on the surface.

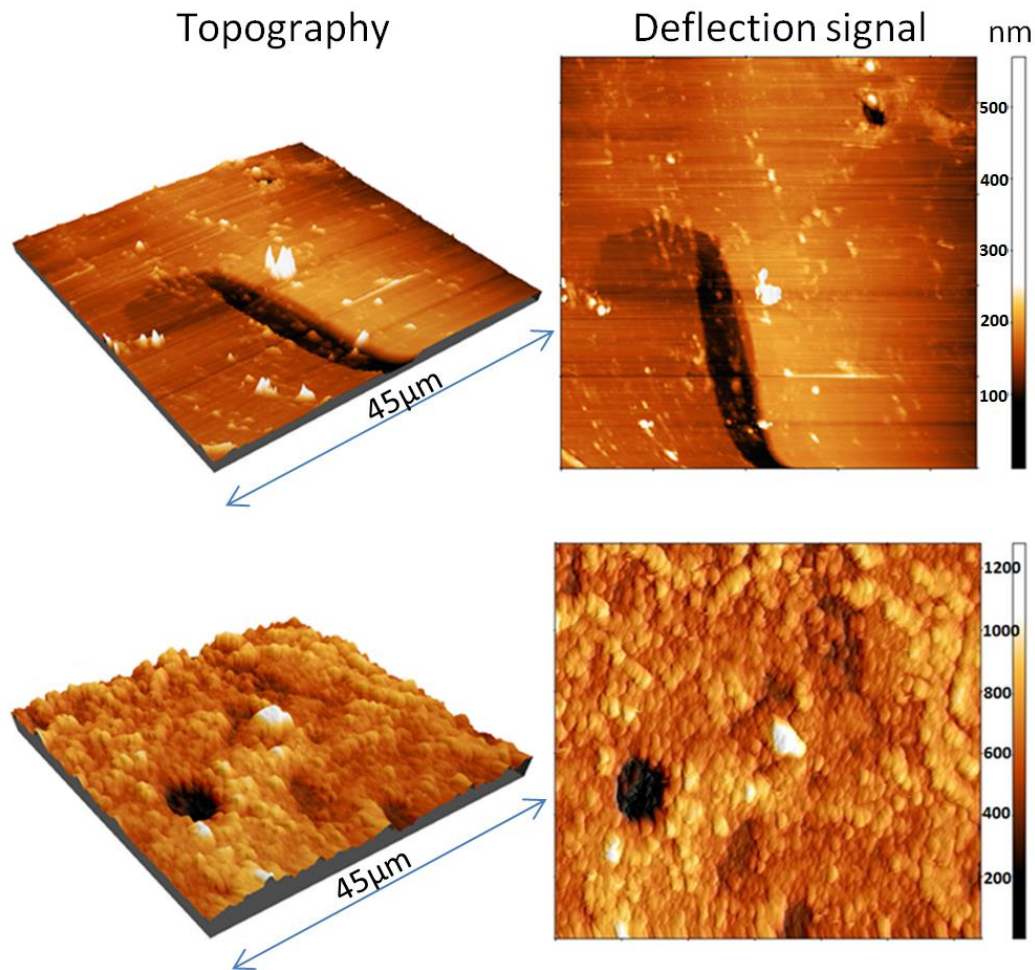


Figure 5-4 Atomic force microscopy images of a calcite surface used in the experiments before (upper image) and after (lower image) nano-modification. The RMS surface roughness before nano-modification was 32 nm, which is very smooth. After nanofluid treatment (0.5wt% SiO<sub>2</sub> in 10wt% NaCl brine for 4 hr) the RMS surface roughness increased to 1300 nm. Different colours refer to variations in height (black: 0nm, white: peak height = 640nm [upper image], 1300 nm [lower image]).

### 5.3.2 Effect of exposure time on contact angle

As the surface modification is caused by nanoparticle adsorption (see above), longer contact time leads to decreased  $\theta$  (through increased adsorption), Figure 5-5 ( $\theta$  in air decreased from 77° to 18° after 1 h and to 10° after 3 h exposure time; and  $\theta$  in n-decane decreased from 122° to 30° after 1 h and further to 18° after 3 h exposure time).  $\theta$  rapidly decreased within the first 60 minutes of exposure followed by further, but smaller, reduction in  $\theta$  (Figure 5-5). After 3h exposure time no further change in  $\theta$  was observed. We conclude that the sample reached adsorption capacity after three hours. This is consistent with the trend observed by Roustaei and Bagherzadeh (2014) on limestone and Zhang et al. (2015) who demonstrated that a smaller flow rate of

nanofluid through a calcite powder increased nano-silica adsorption (since contact time increased).

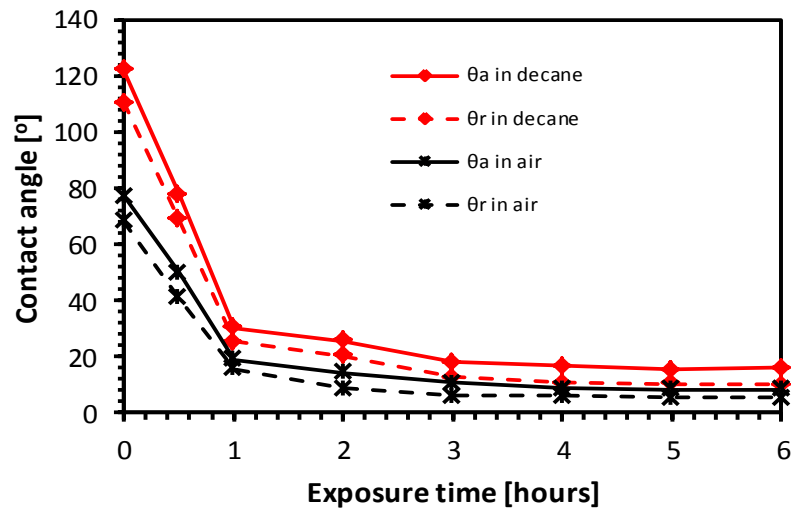


Figure 5-5 Water contact angles on oil-wet calcite surface in air and n-decane as a function of exposure time to nanofluid (2wt% SiO<sub>2</sub>, 5wt% NaCl brine).

### 5.3.3 Adsorption characteristics: reversible versus irreversible adsorption

Adsorption characteristics related to nanofluid surface modification were further studied as this fundamentally influences the success of the application. Of particular interest is the ratio between reversibly and irreversibly bonded silica, and thus the stability of nanofluid modification. We therefore exposed the nano-modified calcite surface to various solvents:

- 1- Oil-wet calcite surface [not nano-modified]
- 2- Nanofluid
- 3- Nanofluid and DI water
- 4- Nanofluid, acetone, and DI water
- 5- Procedure 4 followed by second rinsing with acetone and DI water

After each step, the substrate was dried with N<sub>2</sub> gas, and the advancing and receding contact angles were measured (Figure 5-6).

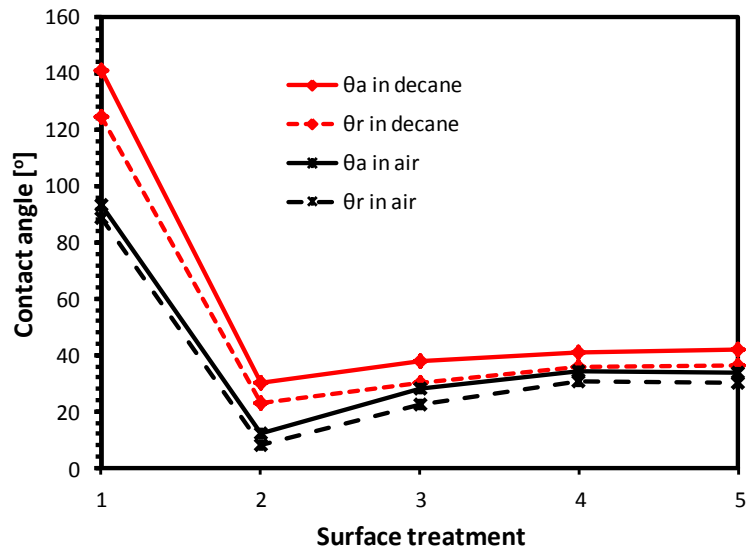


Figure 5-6 Water contact angles on: 1) oil-wet calcite surface in air and n-decane; 2) after nano-modification (2wt% SiO<sub>2</sub>, 20wt% NaCl brine, 1 hour exposure time); 3) DI water; 4) acetone; 5) 2nd acetone and water rinse.

Most nanoparticles were bonded irreversibly, which is in agreement with observations for sandstone surfaces (Ju and Fan 2009). Quantitatively, the total difference in contact angle after removal of the reversibly bonded nanoparticles was  $\sim 15^\circ$ , which is smaller than the drastic reduction caused by the nanofluid itself ( $-98^\circ$ ). Mechanistically, it is likely that the silica nanoparticles chemisorbed onto the surface (on patches which were not modified by the silane and thus contained surface silanol groups (Zhuravlev 2000); such silanol groups probably strongly interacted with the silanol groups on the silica particle surface, this has also been observed in recent formation damage studies, Al-Yaseri et al. (2015b)). These adsorption effects were observed with AFM and on SEM images, see above.

### 5.3.4 Effect of electrolyte concentration on contact angle

It is well known that the electrolyte concentration significantly influences nanofluid properties (Winkler et al. 2011, Li and Cathles 2014); and at the same time it is well established that the salinity of formation brine can vary greatly and can reach very high levels (Iglauer et al. 2012). It is thus necessary to investigate the effect of salinity on  $\theta$  and nanofluid stability.

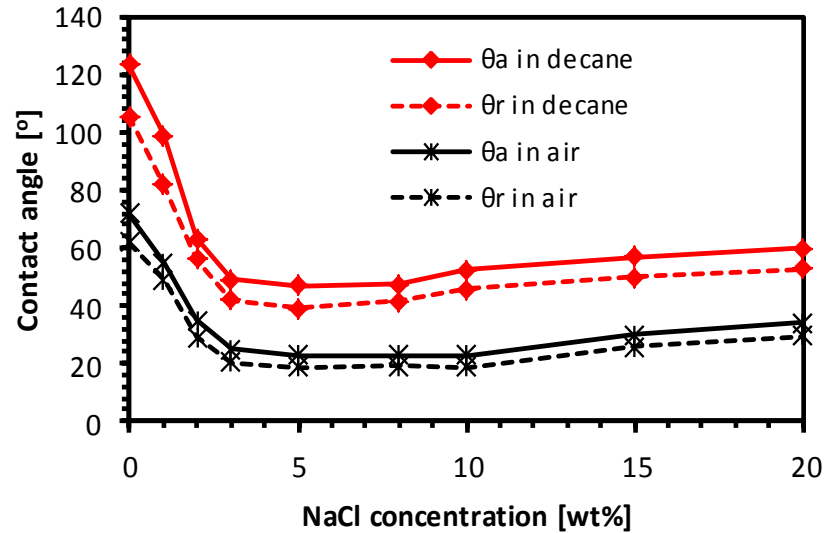


Figure 5-7 Water contact angles on nano-modified calcite surface in air and n-decane as a function of brine salinity (2wt% SiO<sub>2</sub>, 1 hour exposure time).

We therefore systematically measured  $\theta$  as a function of NaCl concentration;  $\theta$  was high for DI water (100-125° for n-decane), and much lower for all tested brines (40-50° in n-decane), Figure 5-7.  $\theta$  reached a minimum at 3wt% NaCl concentration, which implies that there is an optimum salinity similar to that found in surfactant formulations (Salager et al. 2000, Iglauer et al. 2009). In case of the 2wt% SiO<sub>2</sub> nanofluid, optimal NaCl concentrations ranged between 3-8 wt% (Figure 5-7). Salinity thus plays a crucial role in wettability alteration by nanofluid. Nanofluid treatment had a significant effect on the contact angle in DI water ( $\theta$  reduction by 17.5°), but this effect was massively enhanced when electrolytes were present (reduction of  $\theta$  by 95° in case of 3wt% NaCl brine).

This behaviour is related to the stability of the dispersed nanoparticles, which is controlled by their surface charge (note that the zeta potential for silica nanoparticles is around -45 mV for the pH range 6-10; Metin et al. (2011)). This negative surface charge creates electrostatic repulsion forces, which prevent nanoparticle agglomeration (Zargartalebi et al. 2015) and sedimentation. Electrolytes weaken the net repulsion forces between the nanoparticles and thus accelerate the precipitation of nanoparticles onto the calcite surface (Li and Cathles 2014). As a consequence, increasing nanofluid salinity increases wettability alteration efficiency. However, at high salinities (>10 wt% NaCl) the repulsion forces are dramatically reduced (Zargartalebi et al. 2015), which increases the rate of agglomeration between these particles (Winkler et al. 2011) and slightly reduces efficiency (Figure 5-7).

### 5.3.5 Effect of nanoparticle concentration in nanofluid

While higher nanoparticle concentrations are expected to be more efficient (i.e. reduce  $\theta$  more and faster, Roustaei and Bagherzadeh (2014)), it is vital from an economical perspective that costs are minimized, and typically only small amounts of additives are profitable (e.g. (Iglauer et al. 2009, 2010, Iglauer et al. 2011a)). Thus, it is necessary to determine the smallest effective nanoparticle concentration. Furthermore, high concentrations of nanoparticles (>3 wt%) may reduce reservoir permeability (ShamsiJazeyi et al. 2014), which should be avoided. In this study we found that nanoparticle concentration at 1 wt% changed the oil-wet surface (initially  $\theta = 120^\circ$ ) into a weakly water-wet state ( $\theta = 60^\circ$ ), and into a strongly water-wet state at 2wt% nanoparticle concentration ( $\theta = 45^\circ$ , versus n-decane, Figure 5-8).

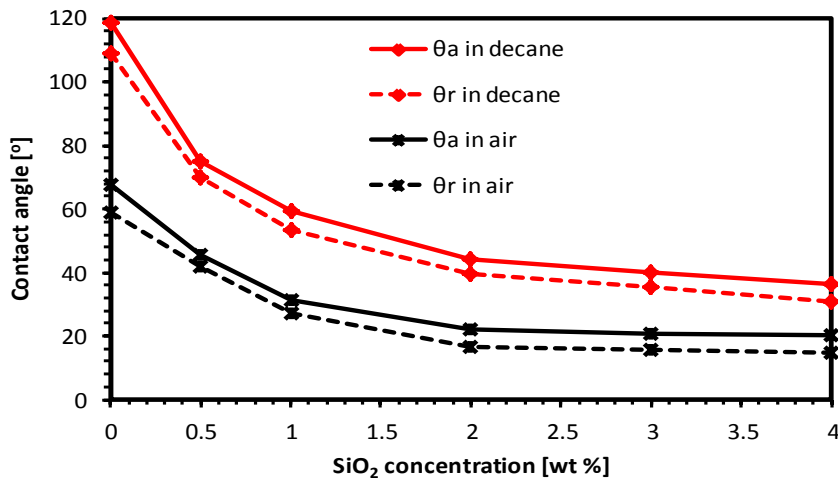


Figure 5-8 Water contact angles on nano-modified calcite surface in air and n-decane as a function of SiO<sub>2</sub> concentration in the nanofluid (10 wt %NaCl, 1 hour exposure time).

Moreover, a threshold value (~2wt% silica concentration) was observed, above which  $\theta$  did not change, consistent with data reported for silicon (Munshi et al. 2008) and glass (Nikolov et al. 2010).

### 5.3.6 Nanofluid-rock re-equilibration processes

Here we tested whether repeated nanofluid usage changes its effectiveness. Such a scenario with constantly re-equilibrating fluid-rock interactions simulates the leading edge of the nanofluid flood in the formation, and associated adsorption-desorption-transport phenomena need to be considered. No significant differences in contact angle

were observed for fresh versus used nanofluid (Figure 5-9), consistent with previous studies reported for powdered calcite (Zhang et al. 2015).

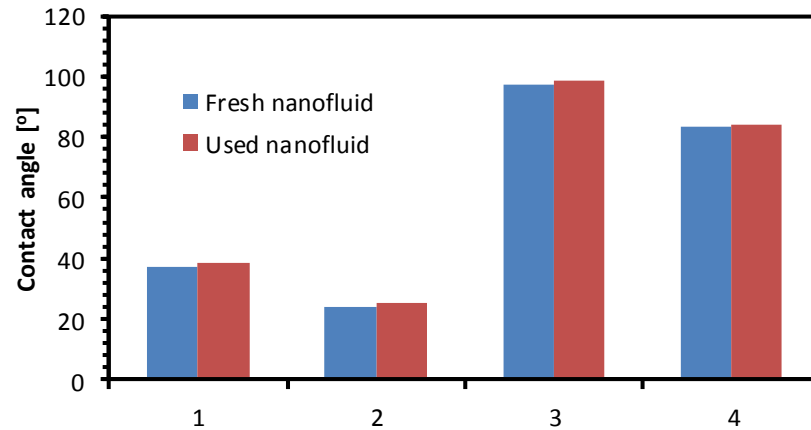


Figure 5-9 Differences in water contact angle between fresh and used nanofluid (0.5wt % SiO<sub>2</sub>, 20 wt% NaCl, and 1 hour exposure time): 1)  $\theta_a$  in air, 2)  $\theta_r$  in air, 3)  $\theta_a$  in n-decane, 4)  $\theta_r$  in n-decane.

#### 5.4 Conclusions

Hydrocarbon production from fractured, oil-wet limestone reservoirs is a big challenge as conventional recovery techniques are inefficient (Austad et al. 2012, Castro Dantas et al. 2014), mainly due to water not spontaneously imbibing into the oil-wet rock matrix. Production would, however, be dramatically increased, if the rock matrix could be rendered water-wet (so that water can spontaneously imbibe and displace oil (Wu et al. 2008)). Furthermore, it is highly desirable to change oil-wet surfaces more water-wet in carbon geo-sequestration projects to increase storage capacities and de-risk containment security (Mahbubul et al. 2014, Iglauer et al. 2015c, Iglauer et al. 2015a). Despite the vital importance for limestone reservoirs, previous studies focused on sandstone formations (Ju et al. 2006, Ju and Fan 2009, Suleimanov et al. 2011, Hendraningrat et al. 2013) and only limited information is available for carbonate reservoirs (Roustaei and Bagherzadeh 2014, Zhang et al. 2015).

It is therefore now necessary to better understand the fundamental characteristics of nanofluid-carbonate interactions and how wettability is affected; thus we investigated the wettability alteration efficiency of various nanofluids on oil-wet carbonate.

Tested parameters included nanoparticle concentration, nanofluid salinity, surface modification time, and reversibility of nanoparticle adsorption as these variables have been previously shown to affect nanofluid treatment performance (Ju and Fan 2009, Roustaei and Bagherzadeh 2014, Zargartalebi et al. 2015, Zhang et al. 2015).

We found that nanofluids can change the wettability of oil-wet calcite to strongly water-wet under condition. Exposure time played a major role, and after ~1 hour, most

of the wettability change was achieved, consistent with the results of (Roustaei and Bagherzadeh 2014). It was furthermore observed that nanoparticle adsorption was mainly irreversible, although a partially reversible behaviour was measured after washing the surface with acetone and/or DI water. The minimum effective nanoparticle concentration was 1-2wt%, consistent with data reported for clay (ShamsiJazeyi et al. 2014). Moreover, an optimum salinity range was detected (3-8wt % NaCl concentration), similar to the optimum salinity in surfactant formulations (Salager et al. 2000, Iglauer et al. 2009).

We note that pressure and particularly temperature can significantly affect nanofluid properties (Hendraningrat et al. 2013), thus nanofluid behaviour and efficiency at reservoir conditions may be different; furthermore nanofluid efficiency is also likely affected by rock heterogeneity, which influences nanoparticle transport within the solid matrix (Skaug et al. 2015).

Technically, nanofluid would be injected through the wellbore and hydraulically pressed into the fractures. From there the particles diffuse into the pore matrix (Iglauer et al. 2011b) or they are pumped deeper into the formation by the viscous pressure gradient.

Overall, we conclude that nanofluids can be very efficient in terms of wettability alteration. Thus, such formulations have a high potential in the area of enhanced oil production or CO<sub>2</sub> geo-storage.

## Chapter 6 Effect of temperature and SiO<sub>2</sub> nanoparticle size on wettability alteration of oil-wet calcite

### Abstract

Nanofluid treatment of oil reservoirs is being developed to enhance oil recovery and increase residual trapping capacities of CO<sub>2</sub> at the reservoir scale. Recent studies have demonstrated good potential for silica nanoparticles for enhanced oil recovery (EOR) at ambient conditions. Nanofluid composition and exposure time have shown significant effects on the efficiency of EOR. However, there is a serious lack of information regarding the influence of temperature on nanofluid performance; thus the effects of temperature, exposure time and particle size on wettability alteration of oil-wet calcite surface were comprehensively investigated; moreover, the stability of the nanofluids was examined. We found that nanofluid treatment is more efficient at elevated temperatures, while nanoparticle size had no influence. Mechanistically most nanoparticles were irreversibly adsorbed by the calcite surface. We conclude that such nano-formulations are potentially useful EOR agents and may improve the efficiency of CO<sub>2</sub>-storage even at higher reservoir temperatures.

**Keywords:** Wettability alteration, Carbonate reservoirs, EOR, Oil-wet, Nanoparticles, Silicon dioxide, Temperature, Zeta potential.

### 6.1 Introduction

Nanoparticles with unique designed properties are an elegant solution for many industrial problems and they have ubiquitous promising application in numerous fields ranging from medicine (Lohse and Murphy 2012) and biomedicine (Rubilar et al. 2013), drug delivery (Tong et al. 2012), biology (De et al. 2008, Baeckkyoung et al. 2015), environment (Garner and Keller 2014) and pollution (Wu et al. 2013a, Sarkheil and Tavakoli 2015), water treatment (Syed et al. 2011, Wang et al. 2012), food production (Fischer et al. 2013, Rajauria et al. 2015, van Dijk et al. 2015), polymer composite (ShamsiJazeyi et al. 2014), stable emulsions (Whitby et al. 2009, Qiao et al. 2012), heat transfer (Ghadimi et al. 2011, Branson et al. 2013), corrosion protection (Winkler et al. 2011), conductive materials (Chakraborty and Padhy 2008), heterogeneous catalysis (Balaji et al. 2011), and subsurface applications including drilling (Ponmani et al. 2015), carbon geosequestration (Al-Anssari et al. 2016) and enhanced oil recovery (Suleimanov et al. 2011, Sharma et al. 2014b, Zhang et al. 2014, Al-Anssari et al. 2016, Zhang et al. 2016). Deposition of (functionalized) nanoparticles on the solid surfaces is a promising technique to control the wettability of these surfaces.

The efficiency of nanoparticles in terms of wettability alteration of solid surfaces depends on several factors including particularly the nanoparticle type (Bayat et al. 2014b, Moghaddam et al. 2015) and solid surface chemistry (Täuber et al. 2013). Also,

operating conditions such as nanofluid composition and contact time have significant effects on such surface modifications (Zhang et al. 2015, Al-Anssari et al. 2016). A major challenge in enhanced oil recovery (EOR), on which we focus here, is hydrocarbon production from naturally fractured carbonate reservoirs; oil production here is controlled by imbibition of water into the oil-wet rock matrix. Currently, these typically oil-wet and intermediate-wet reservoirs account for more than half of the known remaining oil in the world (Shushan and Marcoux 2011, Sharma and Mohanty 2013, Roustaei and Bagherzadeh 2014). As most oil is stored in the matrix (Gupta and Mohanty 2010), water during secondary recovery can only move through fractures, resulting in the low productivity (10-30%) of oil by waterflooding (Wu et al. 2008, Amraei et al. 2013). Alteration of oil-wet carbonate surfaces to water-wet is thus a key mechanism, which can significantly increase oil production (Ju and Fan 2009, Onyekonwu and Ogolo 2010, Alotaibi et al. 2011, Karimi et al. 2012a, Hendraningrat et al. 2013, Al-Anssari et al. 2016, Zhang et al. 2016, Nwidee et al. 2016a). Once wettability is altered to water-wet, water can imbibe into the matrix of the rock and displace a significantly higher ratio of oil from the pore space (Rostami Ravari et al. 2011).

Water-wet reservoirs are also favourable to carbon capture and storage (CCS), Iglauer et al. (2015c), specifically structural (Iglauer et al. 2015b, Arif et al. 2016a) and residual (Rahman et al. 2016) trapping capacities are significantly lower in oil-wet formations. It is thus desirable to render oil-wet reservoirs water-wet to optimize CCs projects.

Previous investigations have studied the application of nanoparticles for EOR in sandstone reservoirs (Ju et al. 2006, Ju and Fan 2009, Hendraningrat et al. 2013, Ehtesabi et al. 2014, Sharma et al. 2014b); however, only limited information is available in terms of the activity of silicon dioxide nanoparticles to improve oil displacement efficiency in carbonate reservoirs. Specifically, Karimi et al. (2012a) and Nwidee et al. (2016a) have examined the role of  $ZrO_2$  nanoparticles on wettability alteration of carbonate reservoirs using contact angle ( $\theta$ ) measurements. They showed that  $ZrO_2$ -based nanofluids can significantly alter strongly oil-wet rocks to water-wet. Bayat et al. (2014b) studied the influence of several types of nanoparticles including, aluminium oxide ( $Al_2O_3$ ), titanium oxide ( $TiO_2$ ), and silicon dioxide ( $SiO_2$ ) on the production of oil from limestone reservoirs. It was found that  $SiO_2$  nanoparticles are more efficient than  $TiO_2$  and  $Al_2O_3$  regarding wettability alteration towards a more water-wet state. Similarly, Moghaddam et al. (2015) conducted a comparative study using different types of nanoparticles including magnesium oxide (MgO), cerium oxide ( $CeO_2$ ), carbon nanotubes (CNT) as well as all types previously studied by Bayat et al. (2014b). The results of contact angle, imbibition and core flooding experiments at room temperature revealed that  $SiO_2$  nanoparticles are more effective in wettability alteration and improved oil recovery. Lately, the effect of silica nanofluid on carbonate surfaces wettability was also investigated by Al-Anssari et al. (2016) concerning nanofluid composition (brine and nanoparticles concentrations), immersion time and reversibility of nanoparticle adsorption. Their results showed that at room conditions, silica nanoparticles can render the strongly oil-wet surface water-wet. Furthermore, Zhang et al. (2016) have conducted contact angle and core flooding experiments with silica nanofluid at room temperature. A high resolution X-ray microtomography

(micro CT) was used to image oil and brine distribution in the core before and after nanofluid flooding. Their results confirmed the effect of silica nanoparticles on surface wettability and demonstrated that approximately 15% more oil can be produced using silica nanofluid.

At harsh reservoirs conditions, particularly at high temperature and salinity, the fluids chemistry plays a crucial role in surfaces wettability (Gupta and Mohanty 2010, Al-Sulaimani et al. 2012, Chen and Mohanty 2014) and nanofluid stability (Amiri et al. 2009, Tantra et al. 2010, Li and Cathles 2014), leading to aggregation and sedimentation of nanoparticles owing to significant reduction in zeta potential ( $\zeta$ ). However, the effect of salinity and particularly temperature on nanofluid stability and ability to render oil-wet surfaces water-wet are only poorly understood.

In this work, we thus investigate how temperature and nanoparticle size affect nanofluid wettability alteration of intermediate-wet and oil-wet calcite surfaces. Moreover, zeta potentials for nanofluids of different compositions was measured, and the phase behaviour of the prepared nanofluid was monitored.

## 6.2 Experimental Methodology

### 6.2.1 Materials

Iceland spar (pure calcite, from WARD'S Natural Science) was used as a representative for carbonate reservoir rock. Atomic force microscopy (model DSE 95-200) was used to measure the topography of the calcite samples since wettability [56] and rate of nanoparticle adsorption are controlled by the surface roughness and nanoparticles distribution (Munshi et al. 2008). The root mean square (RMS) surface roughness ranged between 18-32 nm, which is very smooth.

n-decane (>99 mol%, Sigma-Aldrich) was used as model oil. Toluene (99mol%, Chem-supply), n-hexane (>95 mol%, Sigma-Aldrich), nitrogen (>99.99 mol%, BOC), acetone and methanol (99.9 mol%, Rowe Scientific) were used as cleaning agents. Sodium chloride ( $\geq 99.5$  mol%, Scharlan) was used to prepare brine solutions. Silicon dioxide nanoparticles (porous spherical, purity = 99.5 wt%, Sigma Aldrich) with two different sizes (5-10 nm and 20-25 nm) were used separately to prepare nanofluids with different particle sizes (Table 1). Deionized (DI) water (Ultrapure from David Gray; conductivity = 0.02 mS/cm) was used to prepare brines or nanofluid (base fluid). Calcite carbonate powder (ACS reagent,  $\geq 99.0\%$ , Sigma-Aldrich) was used to establish an accurate equilibrium between calcite mineral and surrounding electrolyte. The silica nanoparticles were sonicated with base fluid (DI water or brine) to prepare nanofluids; details about the preparation process are described by Al-Ansari et al. (2016) and Nwideo et al. (2016a).

Stearic acid ( $\geq 98.5\%$ , Sigma Aldrich) was used to render the original calcite surface (which is strongly water-wet, see below) oil-wet.

## 6.2.2 Calcite surface preparation

Cleaning steps are crucial in contact angle measurements as residual contaminations can lead to systematic errors (Iglauer et al. 2014). Therefore, the calcite samples were first flushed with ultra clean air to remove any loose calcite, followed by washing with DI water and rinsed with toluene to remove any organic and inorganic contaminants. Note that the DI water and brines used in this study was equilibrated with  $\text{CaCO}_3$  to avoid a dramatic surface dissolution (Alroudhan et al. 2016). Experimentally, different amounts of calcite carbonate powder (ACS reagent,  $\geq 99.0\%$ , Sigma-Aldrich) have been efficiently mixed with several brine samples for 2h. Then all samples had left for a week to monitor if any precipitation of calcite occur. Thus the sample with highest powder load without showing any precipitation of solid particles have been used as an equilibrated brine. Subsequently, cleaned calcite samples were dried for 60 min at  $100^\circ\text{C}$  and exposed to air plasma for 40 min (using a Diemer Yocto instrument) to further remove any residual contaminants (Iglauer et al. 2014, Al-Anssari et al. 2016). Modification of calcite surface with stearic acid (see section 6.2.4 for detailed protocol) was started immediately after surface preparation.

## 6.2.3 Contact angle measurements

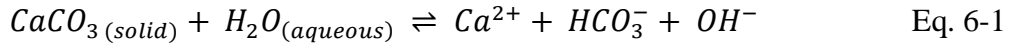
In order to investigate the efficiency of nanofluids in terms of wettability alteration, the contact angle of water droplet on a different calcite surfaces in n-decane was measured. The tilting-plate technique (Lander et al. 1993) was used to measure advancing ( $\theta_a$ ) and receding ( $\theta_r$ ) water contact angles. A 6-7  $\mu\text{L}$  water drop was dispensed onto the calcite substrate that was placed on a metal platform at an inclination angle of  $17^\circ$  (Al-Anssari et al. 2016, Arif et al. 2016a). The water contact angles were measured just before the drop started to slide. A high resolution video camera (Basler scA 640–70 fm, pixel size = 7.4  $\mu\text{m}$ ; frame rate = 71 fps; Fujinon CCTV lens: HF35HA-1B; 1:1.6/35 mm) was used to record movies of these whole processes, and  $\theta_a$  and  $\theta_r$  were measured on images extracted from the movie files. The percentage error of contact angle measurement was  $\pm 3\%$ . Initially the pure calcite surface was tested in air and  $\theta_a = \theta_r = 0^\circ$  (completely water-wet).

## 6.2.4 Calcite modification with stearic acid

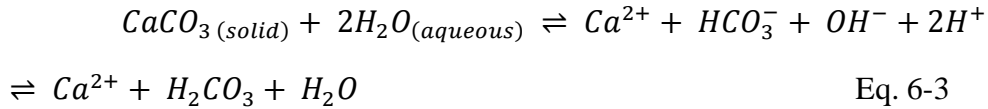
Subsequently the calcite surfaces were rendered oil-wet by following process: stearic acid ( $\text{CH}_3(\text{CH}_2)_{16}\text{COOH}$ ) was initially dissolved in n-decane to prepare a 0.01M stearic acid solution. Here, stearic acid was initially formulated by dissolving 0.285 g of stearic acid in 100 mL of n-decane ( $>99$  mol%, Sigma-Aldrich) with mixing by a magnetic stirrer for a sufficient time. Stearic acid as a long chain fatty acid can actively adsorbs on the calcite surface rendering it to oil or strongly oil-wet (Hansen et al. 2000,

Mihajlovic et al. 2009, Shi et al. 2010). The calcite substrate was first immersed in low pH aqueous solution (1 wt% NaCl, pH=4) for 30 min to allow water to diffuse into the lattice of the water-wet sample. A 1/5 weight ratio for solid sample to aqueous solution was used (Morse and Arvidson 2002); pH values of this aqueous solution were regulated with drops of HCl and NaOH. Air was then carefully blown over the calcite surface to remove the surface water film. Then, the calcite sample was immersed directly into the 0.01M stearic acid/n-decane solution and aged at ambient condition for 24 h.

A pre-coverage of calcite surface with acidic (pH  $\approx$ 4) aqueous solution, before immersing in stearic acid, supports the adsorption of acid on calcite surface (Hansen et al. 2000). The water phase over the substrate helps the dissolution of calcite and the dissociation of the stearic acid.



Ionization of carboxylic acid groups on the calcite surface depends on the pH and ionic strength of the aqueous phase (water composition, (Hoeiland et al. 2001)). The pH is the key factor limiting the reaction between the dissociated acid and calcium ions (Schramm et al. 1991). At higher acidity, eq.  $CaCO_3(solid) + H_2O(aqueous) \rightleftharpoons Ca^{2+} + HCO_3^- + OH^-$  Eq. 6-1 extends to:



Calcite surface, at low pH, becomes positively charged due to the formation of calcium ions (Ma et al. 2013). In contrast, at high pH, the calcite surface becomes negatively charged due to carbonate ions. Mechanistically, carboxylate molecules from stearic acid solution are adsorbed on the positive sites of the calcite surface. Thus, immersing calcite surface in an aqueous solution of low pH before treatment with stearic acid, produces strongly oil-wet surfaces.



Note that in all previous studies, calcite samples were directly aged in stearic acid solution after immersing in water without air drying (Hansen et al. 2000, Hamouda and Gomari 2006, Gomari and Hamouda 2006). However, we found that the presence of a notable water film on the calcite surface prior to immersion into stearic acid

solution leads to unstable  $\theta$  measurements. This phenomenon is owing to the instability of the water film covering the mineral surface (Hoeiland et al. 2001).

### 6.2.5 Nanofluid preparation

Nanofluids were formulated by sonicating silicon dioxide nanoparticles (properties are listed in Table 1) in base fluid (equilibrated DI water or brine) using an ultrasonic homogenizer (300 VT Ultrasonic Homogenizer/ BIOLOGICS) for 20 min. Considering our earlier work on nanofluids (Al-Anssari et al. 2016) and the observations from ShamsiJazeyi et al. (2014) with respect to the (detrimental) effects of high nanoparticle concentration on rock permeability, we used a low SiO<sub>2</sub> nanoparticle concentration (0.2 wt%) in a different equilibrated brines (0 - 2 wt% NaCl). The nanofluid was sonicated 4 times at 240 W for 5 min with 5 min rest to avoid overheating. Finally, the prepared nanofluid was stored in a cold and dark for 2 h to assure homogeneity and stability.

### 6.2.6 Zeta potential measurements and stability of nanofluids

Zeta potentials ( $\zeta$ ) of the nanofluids were measured using a Zetasizer Nano ZS instrument (Malvern Instruments, UK). Specifically, the zeta potential was obtained from electrophoretic mobility measurements and application of the Smoluchowski-Helmholtz equation (Eq. 6-5):

$$\zeta = \frac{\varepsilon \cdot \mu_E}{\mu} \quad \text{Eq. 6-5}$$

where  $\zeta$  is the zeta potential (mV),  $\varepsilon$  is the dielectric constant of the solution,  $\mu_E$  is the electrophoretic mobility (equal to  $V_E/E$ );  $V_E$  is the electrophoretic rate ( $s^{-1}$ ),  $E$  is the electric field ( $V \cdot m^{-1}$ ), and  $\mu$  is the fluid viscosity. The effect of fluid pH and nanofluid composition on zeta potential was measured systematically as part of this study.

### 6.2.7 Calcite wettability modification with silica nanofluid (nano-modification)

In order to investigate the effect of temperature and nanoparticle size on nanofluid efficiency in terms of wettability alteration, oil-wet calcite samples were immersed in nanofluids at different temperatures (23, 30, 40, 50, and 60°C) for different immersing times (15, 30, 45, 60, 90, 120, 180, and 240 min). Specifically, the clean oil-wet substrates were placed in a glass container and were entirely submerged in nanofluid. The calcite samples were laid vertically in the nanofluids to avoid the effect of nanoparticle deposition by gravity. Thus, changes in wettability are solely caused by

adsorption of nanoparticles onto the calcite surface. A constant immersion ratio of 5g nanofluid and 1g of calcite was used. The sample container was kept away from light to avoid any degradation effects during modification. After the prescribed immersion time, the sample was removed from the container and flushed with acetone and DI water, then dried with ultrapure nitrogen. Two sets of experiments were performed regarding the temperature effect; in the first set (A) samples were immersed at 23°C, while contact angle measurements were conducted at specified elevated temperatures. In the second set (B), both immersion and contact angle measurements were carried out at the same (elevated) temperature.

### **6.3 Results and discussions**

Oil production from fractured oil-wet carbonate formations, can be significantly increased by shifting the rock surface wettability from oil-wet to water-wet (Ju et al. 2006, Ju and Fan 2009, Roustaei and Bagherzadeh 2014). Moreover, if the rock is strongly water-wet, the trapping capacity of CO<sub>2</sub> is significantly higher (Iglauer et al. 2015b, Iglauer et al. 2015c, Arif et al. 2016a, Rahman et al. 2016). In this context it has been shown that nanofluids have a drastic ability to render oil-wet carbonate surface water-wet (Moghaddam et al. 2015, Al-Anssari et al. 2016, Nwideo et al. 2016a, Zhang et al. 2016). However, the effect of temperature and nanoparticle size has not been systematically studied yet. We thus systematically analysed the effect of these parameters on wettability alteration efficiency.

#### **6.3.1 Zeta potential of nanofluids**

The nanofluids zeta potential has a direct relationship with suspension stability as well as the adhesion and wetting phenomena (Israelachvili 2011). Nanoparticles with lower zeta potentials are electrically more unstable and thus flocculate and precipitate more rapidly (El-Sayed et al. 2012). Stability of nanofluid is an essential parameter that can limit the nanofluid application, and it depends on both the van der Waals attraction (Israelachvili 2011) and electrostatic repulsion forces among nanoparticles (Zhang et al. 2015). Hydrocarbon reservoirs usually contain relatively high salt concentrations and thus the effect of NaCl concentration on suspension stability was investigated. The percentage error of  $\zeta$  measurements was 6%.

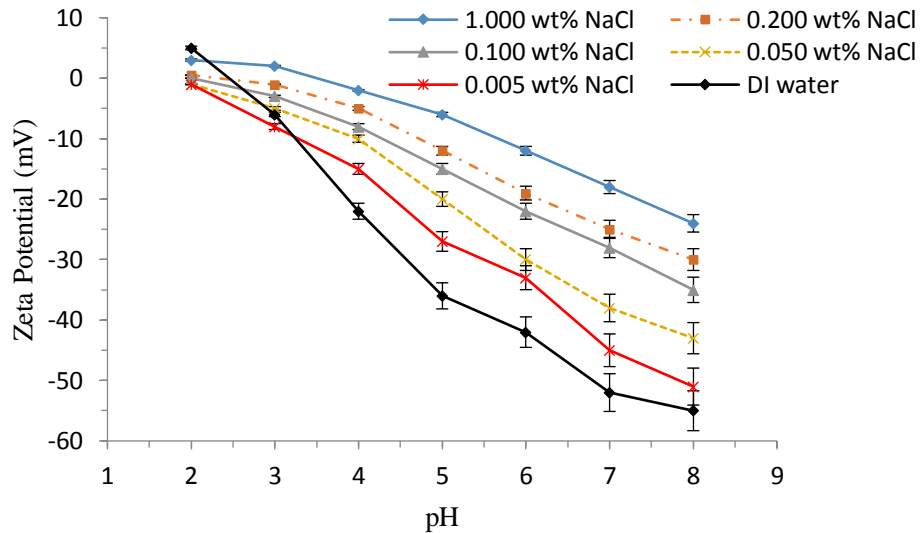


Figure 6-1 Zeta potentials of various SiO<sub>2</sub> nanofluids (0.2 wt% SiO<sub>2</sub> in different brine) at varying pH and 23 °C.

Figure 6-1 shows the variation of zeta potential with pH of silica nanoparticle suspensions at different salinity. The absolute value of zeta potential ( $\zeta$ ) increased with pH and decreased with salinity consistent with literature data for ( $\leq 0.01$  wt% NaCl) (Bayat et al. 2014b, Bayat et al. 2014a). Electrolyte ions reduce the repulsion force among nanoparticles owing to the neutralization of particle surface charges. According to DLVO (Deriaguin-Landan-Verway and Overbeek) theory, attraction and repulsion forces among particles depend on the surface electric charge; thus, the stability of colloidal suspension in a dielectric medium is determined by the repulsive electrostatic interaction energy and attraction of van der Waals energy which is affected by salt concentration. Consequently, higher ionic strength leads to nanoparticles instability due to the lower zeta potential. Note that the formation of salt bridges among silica nanoparticles (Dishon et al. 2009, Metin et al. 2011) is the main reason for the instability of nanofluid suspension.

Furthermore, particle loading affects the zeta potential, Figure 6-2

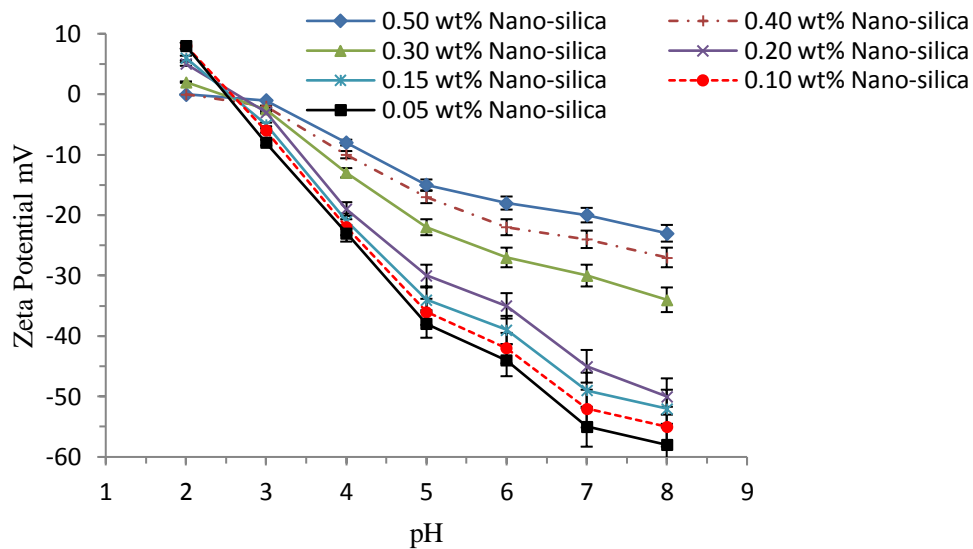


Figure 6-2 Zeta potential of various nanofluids with different particle loading (0.05, 0.1, 0.15, 0.2, 0.4 and 0.5 wt% SiO<sub>2</sub> in DI water) at varying pH and 23 °C.

The absolute value of zeta potential increased with pH and decreased as particle concentration increased. At low particle loading ( $\leq 0.2$  wt% SiO<sub>2</sub>), the increase in nanoparticle concentration had only a small influence; however, at higher particle content, the increase in particle concentration remarkably decreased the absolute value of the zeta potential. This is different to Tantra et al. (2010) who claim that only within very low zeta potential ( $10^{-2}$ - $10^{-4}$ ), the zeta potential is not a function of nanoparticle loading. Consequently, at high nanoparticle load, it is necessary to increase the pH of the suspension to keep the nanofluid far away from the isoelectric point (IEP): the point at which zeta potential of the suspension equals zero (Mondragon et al. 2012), as then the nanofluid rapidly flocculated.

The (0.2 wt% SiO<sub>2</sub> in 1 wt% NaCl) nanofluid showed stable behaviour during the investigation period. Note that Franks (2002) found that silica nano-suspensions are stable against agglomeration and sedimentation even at relatively high salt concentration ( $\leq 6$  wt % NaCl) if the pH of the solution is kept at an appropriate value. Thus, all prepared nanofluids were kept at pH 5-6 to ensure stability.

### 6.3.2 SEM-EDS and AFM analysis

The irreversibly adsorbed fraction of nanoparticles (i.e. after the nano-treated substrate was exposed to different cleaning fluids) was investigated via scanning electron microscopy (SEM, Zeiss Neon 40EsB FIBSEM), energy dispersive X-ray spectroscopy (EDS, Oxford X-act SSD X-ray detector with Inca and Aztec software), and atomic force microscopy AFM instruments (model DSE 95-200, semilab). EDS indicated a significant concentration of silicon ( $\sim 2$  wt%) on five different points on several samples (which were treated by nanofluids at various temperatures), Table 6-1

and Table 6-2. Note that values on Table 6-2 are average values for measurements taken from five different points in each sample. Although Ma et al. (2013) announced that it is challenging to determine the complicated surface charges of carbonate due to the effect of small impurities (e.g. aluminium (Al), and silicon (Si)) on zeta potential, X-ray photoelectron spectroscopy (XPS) showed that calcite samples was totally made of calcium (Ca). Surfaces charge difference between calcite and silica nanoparticle is the main motive force for nanoparticles adsorption on calcite (Zhang et al. 2015). Mechanistically, negatively-charged silica nanoparticles are strongly adsorbed onto the positively-charged calcium ions of calcite. The electrokinetic data showed that the isoelectric points of calcite were at a pH ranged from (7.8 to 10.6) depending on the ionic strength in aqueous solutions (Wolthers et al. 2008). Thus, calcite surface becomes positively charged when it came into contact with nanoparticles from stable silica nanofluid at pH=5-6 (Amiri et al. 2009) and nanoparticles were adsorbed homogeneously on all surfaces at all temperatures, consistent with previous results (Al-Anssari et al. 2016) at room temperature and other glass and silicon substrates (Nikolov et al. 2010, Winkler et al. 2011).

The calcite surface significantly changed after nanofluid exposure, nanoparticles irregularly spread on the surface (Figure 6-3 A and B) while an increase in immersion temperature changed the form and structure of the surface (Figure 6-3 C and D); e.g. a temperature increase from 23 to 50 °C increased the adsorption of nanoparticles on the solid surface and enlarged the size of silica agglomerates into larger clusters (Figure 6-3 E and F).

AFM measurements performed on the nano-modified calcite surfaces confirmed the observations (

Figure 6-4). Treating calcite with nanofluid increased the surface roughness (

Figure 6-4 B) and higher surface roughness was measured for higher immersion temperatures (Figure 5-5 C). The root-mean-square (RMS) surface roughness increased from 18-32 nm for the original calcite surface to 450-580 nm when treated at room temperature and a maximum 2100- 2700 nm when the surface was treated at higher temperature (60°C).

Table 6-1 Surface composition, measured by EDS, of oil-wet calcite after modification with nanofluid at 40 °C (0.2 wt% SiO<sub>2</sub> in 1 wt% NaCl brine, 1 h exposure time).

Point	Calcium (wt%)	Silicon (wt%)	Oxygen (wt%)
1	33.1	2.2	64.7
2	34.2	1.9	63.9
3	33.2	2.7	64.1
4	35.1	1.8	63.1
5	32.7	2.5	64.8

Table 6-2 Surface composition of the oil-wet calcite after modification with nanofluid at (0.2 wt% SiO<sub>2</sub> in 1 wt% NaCl brine, 1 h exposure time) at different temperatures; note that the composition given for each temperature is the average value of five measurements.

Sample	Temperature (°C)	Calcium (wt%)	Silicon (wt%)	Oxygen (wt%)
1	23	34.2	1.2	64.6
2	30	34.3	1.9	63.8
3	40	34.2	2.5	63.3
4	50	35.1	2.2	62.7
5	60	34.4	2.1	63.5

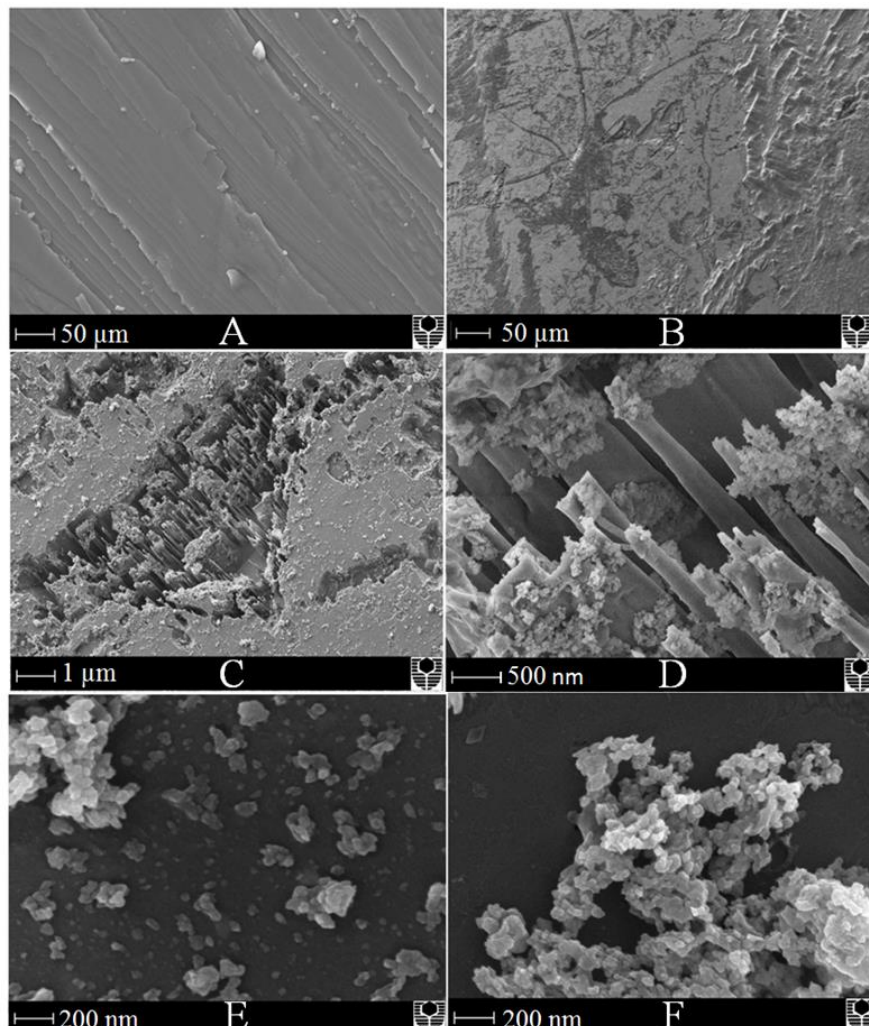


Figure 6-3 SEM images of an oil-wet calcite surface: (A) before, (B) after nanofluid treatment (0.2 wt% SiO<sub>2</sub> in 1 wt% NaCl brine) at 23 °C; (C and D) effect of temperature increase on surface morphology; (E and F) maximum resolution zoom-into the irreversibly adsorbed silica agglomerates at 23° (left) and 50 °C (right), respectively.

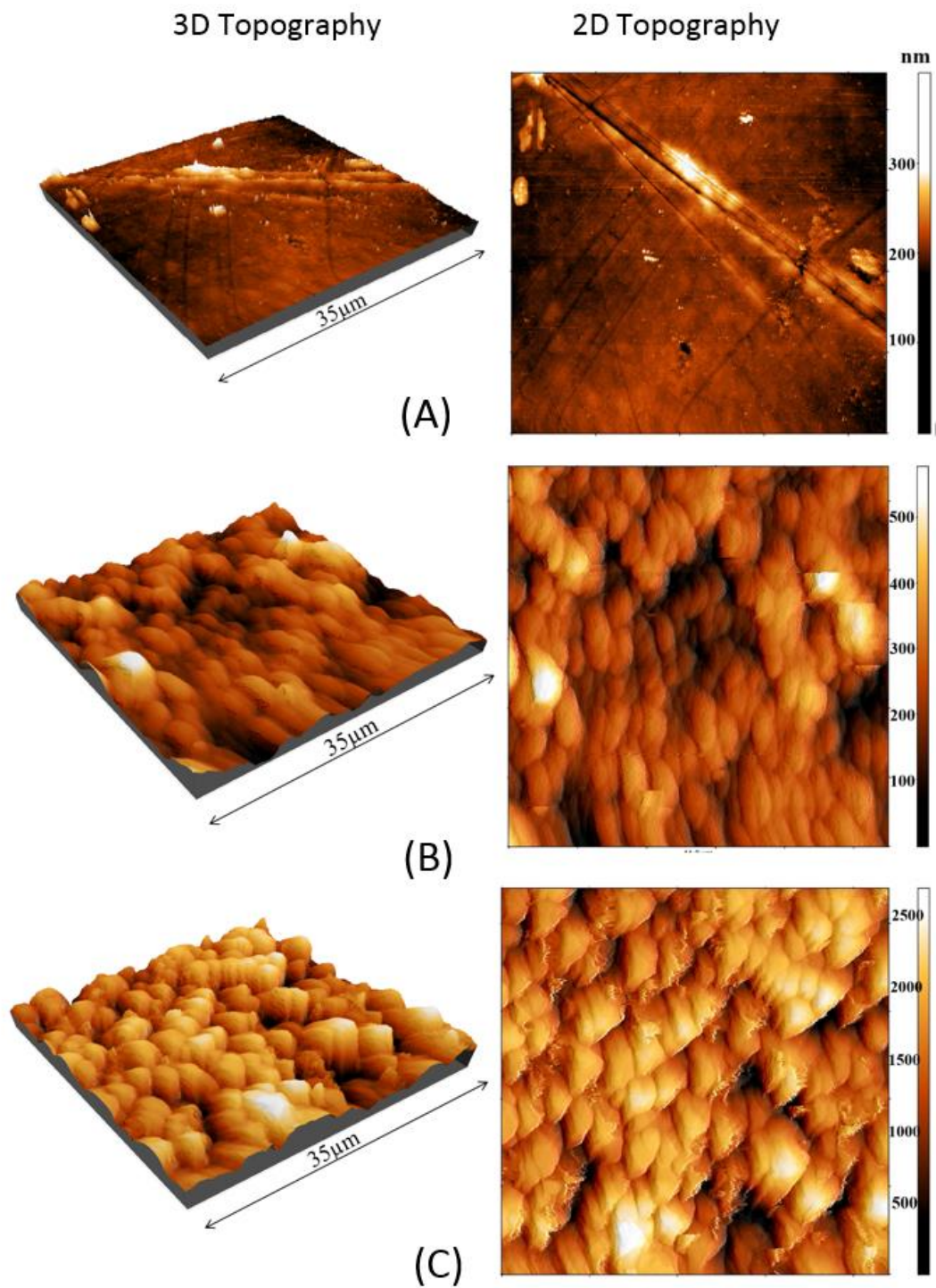


Figure 6-4 Atomic force microscopy images of a calcite surface used in the experiment before (A) and after nano-treatment at two different temperatures: 23 °C (B) and 60 °C (C).

### 6.3.3 Effect of particles size on wettability alteration.

All oil-wet samples were immersed in an equilibrated brine of the same composition as that used in nanofluid preparation, and contact angles were recorded as a base contact angle before nano-treatment. Thus,  $\theta$  reduction after treatment with nanofluid was related only to the effect of nanoparticles rather than the effect of the base fluid.

Two SiO<sub>2</sub> nanoparticle sizes (5 and 25 nm) were used to formulate two distinct nanofluids (but with the same concentration 0.2 wt% SiO<sub>2</sub> in 1wt % NaCl brine).

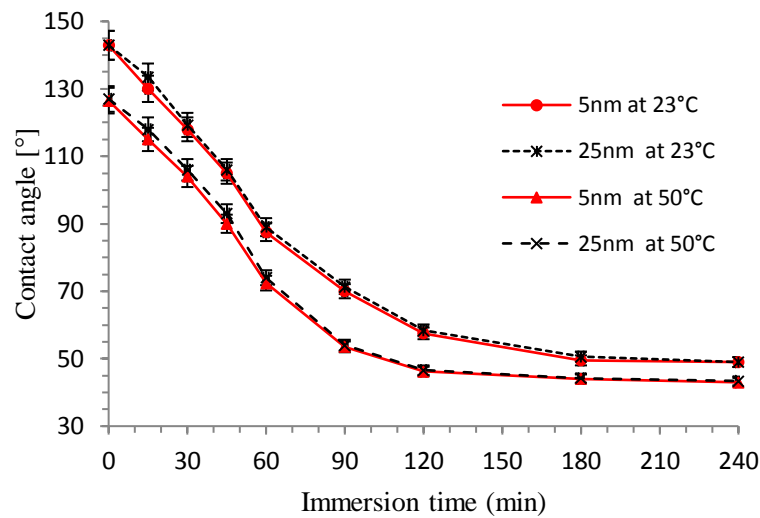


Figure 6-5 Water advancing contact angle on oil-wet calcite surface in n-decane as a function of exposure time to nanofluid (0.2wt % SiO<sub>2</sub>, 1wt % NaCl brine), temperature (23 and 50°C), and nanoparticle size (5 nm and 25 nm).

Initially the water advancing contact angles in decane at 23 °C and 50 °C measured  $\theta = 144 \pm 2^\circ$  and  $126 \pm 2^\circ$ , respectively, on the untreated surface, which indicates an oil-wet condition. After immersing the oil-wet substrate in silica nanofluid for 2 h at 23 °C and 50 °C,  $\theta$  was reduced to  $57 \pm 2^\circ$  and  $46 \pm 2^\circ$ , respectively (Figure 6-5). Thus  $\theta$  decreased with increasing immersion temperature and time, consistent with literature data (Al-Ansari et al. 2016). However, silica particle size (5 and 25 nm) had no effect on  $\theta$  reduction, consistent with Kulak et al. (2004) and Costa et al. (2006) results for 10-35 nm SiO<sub>2</sub> nanoparticles. Consequently, all subsequent measurements were based on a single particle size only (5nm).

### 6.3.4 Effect of temperature on contact angle

Temperature has a major effect on wettability alteration of solid surfaces (Gupta and Mohanty 2010, Al-Sulaimani et al. 2012, Chen and Mohanty 2014). Thus, two sets of measurements were performed to examine the effect of temperature on nanofluid wettability alteration efficiency. In the first set (A), immersion temperature was maintained constant at 23°C and contact angles were measured at elevated in-situ temperature. In the second set (B), the temperature for nanofluid treatment and contact angle measurements were the same which is more realistic in oil production application.

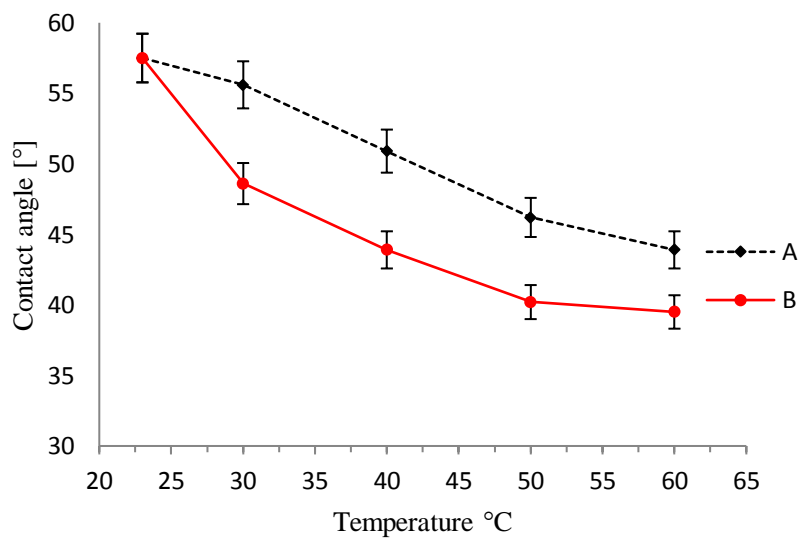


Figure 6-6 Advancing water contact angle on oil-wet calcite surface in n-decane after modification with nanofluid for 2 h (0.2wt% SiO<sub>2</sub>, 1wt% NaCl brine) as a function of measurement temperature. (A) Immersion temperature 23°C. (B) nano-treatment and contact angle measurement temperature were identical.

We found that the efficiency of nanoparticles in terms of reducing the water contact angle significantly improves as temperature increases. For test case A, the contact angle at 23°C reduced from  $\theta = 145^\circ$  to  $56^\circ$  after immersion for 2 hours at 60°C, consistent with our previous study (Al-Anssari et al. 2016). If the temperature was increased to 60°C during  $\theta$  measurement, the contact angle reduced further to  $43^\circ$ . This reduction in  $\theta$  is attributed to the influence of temperature on the spreading behaviour of the drop since the number of active Ca<sup>+2</sup> sites on the carbonate surface are reduced with increasing temperature (Hamouda and Gomari 2006, Gupta and Mohanty 2010).

Meanwhile, for test case B, the calcite samples were immersed in nanofluid for 2 h at various elevated temperatures and  $\theta$  was measured at the same temperatures. In this case at 50 °C,  $\theta$  was reduced from  $145^\circ$  to  $38^\circ$  indicating a significantly higher wettability alteration efficiency. Adhesion of particles on a surface depends on both

surfaces charges and surface roughness (Israelachvili 2011). These factors control the interaction between silica nanoparticles and carbonate surface since roughness and potential difference can increase the adhesion forces. Mechanistically, more nanoparticles adsorbed onto the limestone surface as temperature increased due to carbonate surface dissolution which increases the surface roughness consistent with EDS results (Table 6-1). However, when the immersion temperature increased from 50 °C to 60 °C, there was no additional significant influence on  $\theta$ ; which is attributed to the change in surface charge of calcite over 60°C. Zeta potential measurements of calcite surface as function of temperature (Hamouda and Gomari 2006) revealed a reduction in calcite surface charge to a less positive value at higher temperature reducing the difference in surfaces potential

Furthermore, the influence of immersion time on  $\theta$  was measured for these two test set (Figure 6-7).

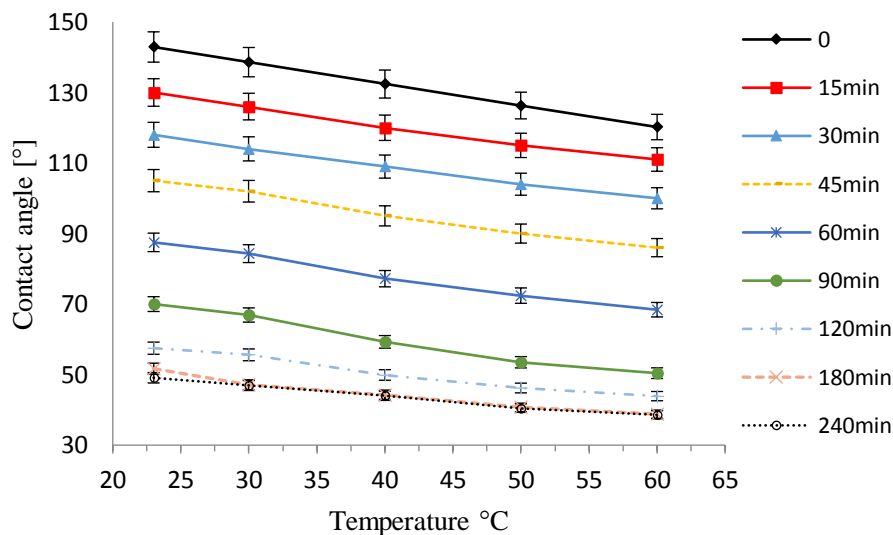


Figure 6-7 Set A: advancing water contact angle on oil-wet calcite surface in n-decane as function of exposure time to nanofluid (0.2wt % SiO<sub>2</sub>, 2wt % NaCl brine) and temperature. Immersion temperature was constant (23°C).

The contact angle decreased with increasing temperature or immersion time. As wettability alteration of the surface is caused by the continuing adsorption of nanoparticles (see above), longer contact time led to lower  $\theta$ . However, after 180 min, no more incremental reduction in  $\theta$  was noticed implying that the surface reached its adsorption capacity (Al-Anssari et al. 2016).

It was proposed that temperature influences the drop behaviour (de Ruijter et al. 1998), and surface properties (Hamouda and Gomari 2006) which potentially influence the adsorption of silica nanoparticle on a calcite surface (Israelachvili 2011). Thus, to distinguish between the two effects, another set of experiments was performed (Figure 6-8) where both immersion and contact angle measurement conducted at the

same elevated temperature. The difference in  $\theta$  values between the two sets refers to the influence of temperature on nano-silica adsorption.

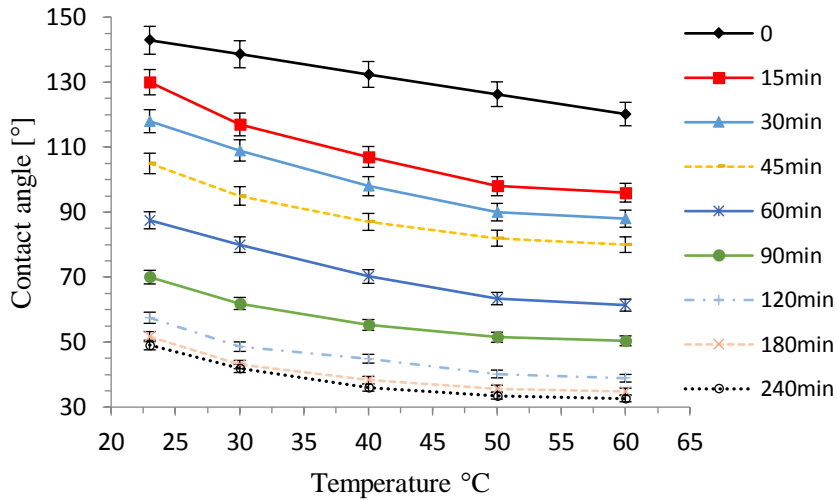


Figure 6-8 Set B: advancing water contact angle on oil-wet calcite surface in n-decane as a function of exposure time to nanofluid (0.2 wt% SiO<sub>2</sub>, 2 wt% NaCl brine) and temperature. Immersion temperature was the same as the temperature for contact angle measurements.

A clear difference is evident between the two temperatures exposure scenarios (Figure 6-7 and Figure 6-8) showing more reduction in set B. For instance, after 2 h treatment,  $\theta$  values measured at 40 °C were 49° and 41° for set A and set B, respectively. Similarly, for each contact angle measurement temperature, all  $\theta$  values in set B were smaller than those in set A; this difference indicates an increased in particle adsorption with increasing temperature. However, the effect of increasing temperature on contact angle (even up to 60°C) is less considerable as compared to the impact of immersing time for both scenarios (Figure 6-7 and Figure 6-8). It is evident that the maximum reduction in contact angle with increasing temperature was at low immersing time (reduction of 20° in  $\theta$ ) and the decrease in  $\theta$  was less significant at higher immersing times (Figure 6-8). However, increased immersing time has a more dramatic impacts on contact angle reduction ( $\theta$  reduced by around 55° and 85° after 1 and 2 hr respectively) consistent with the reported data about the dominant effect of immersing time on nano-treatment efficiency (Roustaei and Bagherzadeh 2014, Zhang et al. 2015, Al-Anssari et al. 2016, Nwidae et al. 2016a). Mechanistically, the increased temperature effects the surface modification in two different ways: a) it can support nanoparticles adhesion on surface due to increase in surface roughness (Israelachvili 2011), and b) it leads to a reduction in decrease the adsorption of nanoparticles particularly at temperatures  $\geq 50^{\circ}\text{C}$  due to a reduction in positive charges on calcite surface. Hamouda and Gomari (2006) reported that the rise in temperature from 20 °C to 50 °C changed the zeta potential of calcite to a less positive value by 2.5 mV ( from 3 mV to 0.5 mV respectively), which in turn decreased the electromotive force (charge difference) for silica particle adsorption; which cause the lower  $\theta$  in set B.

## 6.4 Conclusions

A wettability change from oil-wet to water-wet can enhance oil recovery, particularly in fractured oil-wet limestone (Ju and Fan 2009, Onyekonwu and Ogolo 2010, Alotaibi et al. 2011, Karimi et al. 2012a, Hendraningrat et al. 2013, Al-Anssari et al. 2016, Zhang et al. 2016, Nwidee et al. 2016a), and it can enhance CO<sub>2</sub> geo-storage capacities (Iglauer et al. 2015b, Arif et al. 2016a, Rahman et al. 2016).

It has been previously shown that nanofluids can achieve such a wettability modification (Hendraningrat et al. 2013, Roustaei and Bagherzadeh 2014, Zhang et al. 2014, Bayat et al. 2015, Al-Anssari et al. 2016, Nwidee et al. 2016a, Zhang et al. 2016). However, there is a series lack of information in terms of how temperature and nanoparticles size influences such a wettability alteration. We thus tested the efficiency of various silica nanofluids in this respect.

Moreover, as a crucial parameter for nanofluid stability, zeta potentials (Tantra et al. 2010, Metin et al. 2011, Bayat et al. 2014a) of the different nanofluids were measured at different pH value, particle loads, and salinities.

The results showed that a temperature increase reduces the required immersion time to achieve the same  $\theta$  reduction. However, at relatively longer immersion periods ( $\geq 60$  min),  $\theta$  converged to a minimum, independent of temperature. This is caused by an increased adsorption of silica nanoparticles on the calcite surface with increasing temperature, consistent with measurement for Zirconium Oxide nanoparticles (Karimi et al. 2012a).

Nanoparticle size (5 or 25 nm), however, had no effect on nanofluid wettability alteration efficiency. All tested nanofluids were stable against agglomeration and sedimentation when the pH of the fluid was kept between 5-6, consistent with Franks (2002), Costa et al. (2006), and Amiri et al. (2009).

Overall, we conclude that nanofluids are very efficient wettability modifiers, especially at higher temperatures; nanofluids thus have a high potential in the area of enhanced oil recovery and improved CO<sub>2</sub> geo-storage. However, we point out that a comprehensive investigation for zeta potentials of silica nanofluid, oil emulsion, and calcite dispersion at different temperatures is required for much broader understanding of the electrostatic interactions between charged interfaces.

## Chapter 7 Wettability of nanofluid-modified oil-wet calcite at reservoir conditions

### Abstract

Nanofluids, liquid suspensions of nanoparticles (Np), are an effective agent to alter the wettability of oil-wet reservoirs to water-wet thus promoting hydrocarbon recovery. It can also have an application to more efficient carbon storage. We present a series of contact angle ( $\theta$ ) investigations on initially oil-wet calcite surfaces to quantify the performance of hydrophilic silica nanoparticles for wettability alteration. These tests are conducted at typical in-situ high pressure (CO<sub>2</sub>), temperature and salinity conditions. A high pressure-temperature (P/T) optical cell with a regulated tilted surface was used to measure the advancing and receding contact angles at the desired conditions. The results showed that silica nanofluids can alter the wettability of oil-wet calcite to strongly water-wet at all operational conditions. Although limited desorption of silica nanoparticles occurred after exposure to high pressure (20 MPa), nanoparticle adsorption on the oil-wet calcite surface was mainly irreversible. The nanofluid concentration and immersion time played crucial roles in improving the efficiency of diluted nanofluids while salinity was less significant at high pressure and temperature.

The findings provide new insights into the potential for nanofluids being applied for improved enhanced oil recovery and carbon sequestration and storage.

**Keywords:** nanoparticle, silicon dioxide, nanofluid, wettability, calcite, carbon storage, enhanced oil recovery (EOR).

### 7.1 Introduction

Nanofluids or liquid suspensions of nanoparticles dispersed in deionized (DI) water, brine, or surfactant micelles, have become an elegant solution for many industrial applications including enhanced oil recovery (EOR) (Wong and De Leon 2010, Sharma et al. 2014b, Nwidee et al. 2016a, Al-Anssari et al. 2016, Al-Anssari et al. 2017e) and potentially carbon geostorage (Al-Anssari et al. 2017b). Various enhanced oil recovery processes have been tested to either accelerate the oil production or improve the recovery factor (e.g. EOR by CO<sub>2</sub> injection, Ameri et al. (2013)) from carbonate reservoirs. In this context, the wettability of the fluids/rock system plays a vital role in EOR effectiveness, where water-wet reservoirs are generally more favourable for accelerating oil production (Wu et al. 2008, Gupta and Mohanty 2010). One mechanism, which can significantly improve oil production from fractured limestone reservoirs, is to render the oil- (or intermediate-) wet carbonate surfaces water-wet, so that water spontaneously imbibes into the rock and displaces the oil from the matrix pore space (Rostami Ravari et al. 2011, Strand et al. 2016). Some of these results were supported by Micro-CT images that show the change in the oil clusters size and locations before and after the changes in wettability. Moreover, water-wet

formations are also considered more suitable for CO<sub>2</sub> storage (in terms of structural and residual trapping, Iglauer et al. (2015b), Iglauer et al. (2015c)). In certain circumstances it may be commercially beneficial to alter the wettability of oil-wet reservoirs to water-wet in order to improve oil production (Wu et al. 2008, Gupta and Mohanty 2010).

In this context, many studies have observed a significant shift in mineral surface wettability after treatment with nanofluids. Reported data showed that strongly oil-wet surfaces transformed after nano-treatment into strongly water-wet surfaces, e.g. for sandstone (Ju et al. 2006, Ju and Fan 2009, Hendraningrat et al. 2013, Zhang et al. 2014, Zhang et al. 2015) and for carbonate (Karimi et al. 2012a, Hendraningrat et al. 2013, Hendraningrat and Torsæter 2014, Kaveh et al. 2014, Roustaei and Bagherzadeh 2014, Al-Anssari et al. 2016). In addition, a comparison studies (Bayat et al. 2014b, Moghaddam et al. 2015, Nwidee et al. 2017a) between several types (ZrO<sub>2</sub>, CaCO<sub>3</sub>, TiO<sub>2</sub>, SiO<sub>2</sub>, MgO, Al<sub>2</sub>O<sub>3</sub>, CeO<sub>2</sub>, and CNT) of nanoparticles have previously proved that silica dioxide and, with less degree, zirconium oxide are more efficient in terms of wettability alteration laboratory coreflooding and contact angle experiments.

In this context, several studies reported reduction in contact angle ( $-\Delta\theta^\circ$ ) of mineral surfaces at ambient conditions after nano-treatment with silica nanoparticles. However, only limited amount of literature data have been reported for more relevant conditions (high pressure, temperature and salinity). Table 7-1 presents a summary of the major experimental variables considered in previous studies, and this work.

Al-Anssari et al. (2016) recently observed the variation of the contact angle with the composition and exposure time of calcite samples to nanofluids. Energy destructive spectroscopy (EDS) and scanning electron microscopy (SEM) verify the adsorption of silica nanoparticles on the calcite samples and the formation of nanotextured surfaces. Their results revealed that all the significant changes in contact angle were happened during the first hour of treatment and no more probable reduction was achieved after 3 hours of exposure to the nanofluid. Moreover, the efficiency of nanofluid increased with nanoparticles concentration until reach a minimum  $\theta$  at 2 wt% SiO<sub>2</sub>, where no more reduction were observed with increased concentrations.

Although efforts in studying the influence of nano-treatment on surface wettability, the fundamental aspects related to nanoparticle adsorption characteristics, optimal concentration and effect of exposure time on wettability alteration have not been tested at reservoir conditions before.

Thus, in this work we investigate the wettability of decane/brine and CO<sub>2</sub>/brine systems on an oil-wet calcite surface as a function of nanoparticle concentration, exposure time, surfactant addition, salinity and reservoir pressure to understand the influences of nanofluid-treatment on oil reservoirs and other subsurface formations. The results lead to a broader understanding of the potential for application of nanoparticles to enhanced oil recovery and CO<sub>2</sub> storage.

Table 7-1 Highest contact angle reduction ( $-\Delta\theta^\circ$ ) of minerals after treatment with nanoparticles

Reference	SiO <sub>2</sub> conce. wt%	Base fluid	Mineral	Condition	environment	Highest $\Delta\theta$ (°)
Moghaddam et al. (Moghaddam et al. 2015)	5	Ethanol and brine	carbonate	Ambient	Decane	-87°
Roustaei and Bagherzadeh (2014)	0.1- 0.6	5 wt% brine	carbonate	Ambient	Crude oil	-115°
Hendraningrat et al. (2013)	0.01-0.1	3 wt% brine	sandstone	Ambient	Crude oil	-32°
Bayat et al. (2014b)	0.005	DI water	limestone	Up to 333 K, and 0.1 MPa	Crude oil	-72°
Al-Anssari et al. (2016)	0.01-4	0-20wt% brine	Calcite	Ambient	Decane	-110°
Al-Anssari et al. (Al-Anssari et al. 2017b)	0.01-0.2	0-20wt% brine	Calcite	Up to 343 K and 20 MPa	CO <sub>2</sub>	-93°
Al-Anssari et al. (2017f)	0.01-0.2	0-20wt% brine	Calcite	Up to 343 K and ambient pressure	Decane	-104°
This work	0.05-0.5	Surfactant-brine (0-20 wt%)	Calcite	Up to 343 K and 20 MPa	Decane	

## 7.2 Materials and Experimental methodology

In this study, to mimic carbonate oil reservoirs, pure calcite samples were treated first with organic materials to achieve oil-wet surfaces. Silica nanofluids were then used to render the wettability of these oil-wet sample water-wet at reservoir conditions. Contact angle measurement for a drop of water on calcite substrate that immersed in decane at elevated pressure and temperature were used to investigate the efficiency of nanofluid in terms of in-suit wettability alteration.

### 7.2.1 Materials

Pure calcite (Iceland spar, from Ward's Natural Science) was used as a representative for carbonate reservoir rocks. Deionized (DI) water (Ultrapure from David Gray; conductivity = 0.02 mS/cm) and sodium chloride ( $\geq 99.5$  mol%, Scharlan) were used to prepare brine solutions (1-20 wt% NaCl, 0.17- 4.43 M). The dissolved air was removed from brine by vacuuming for 24 hours.

N-decane ( $>99$  mol%, from Sigma-Aldrich) was used as model oil similar to other published studies (Civan and Rasmussen 2012, Al-Anssari et al. 2016). Different cleaning agents, toluene (99 mol%, Chem-supply), n-hexane ( $>95$  mol%, Sigma-Aldrich), acetone and methanol (99.9 mol%, Rowe Scientific) were used to wash pure calcite samples. Nitrogen ( $>99.99$  mol%, BOC) was used as the ultrapure drying gas.  $CO_2$  (99.9 mol% from BOC, gas code-082) was used to achieve the desired pressure (Arif et al. 2016b) for nano-modification and contact angle measurements processes.

Stearic acid ( $\geq 98.5\%$ , Sigma Aldrich) was used to render the original calcite surface as oil-wet. A stearic acid solution (0.01M) was initially prepared by dissolving 0.285 g of stearic acid in 100 mL of n-decane ( $>99$  mol%, Sigma-Aldrich).

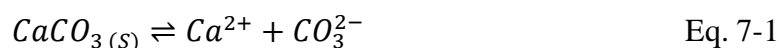
Silicon dioxide ( $SiO_2$ ) hydrophilic nanoparticles (porous spherical, Sigma Aldrich) were used to prepare different nanofluids.

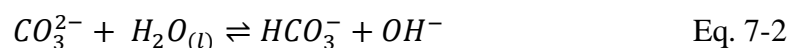
An anionic surfactant [Sodium Dodecylsulfate, SDS, Sigma Aldrich,  $\geq 98.5$  mol%, Mol.wt= 288.38 g.mol<sup>-1</sup>, the critical micelles concentration, CMC= 2450 mg.L<sup>-1</sup> (8.49x10<sup>-3</sup> mol.L<sup>-1</sup>)] was used to improve the stability of nanoparticle suspension in a brine (Ahualli et al. 2011, Iglesias et al. 2011, Sharma et al. 2015b).

### 7.2.2 Equilibration between calcite and brine

In carbonate reservoirs of the geological subsurface, the formation brine is in equilibrium with both calcite and any in-situ  $CO_2$  (Stumm and Morgan 1995). Thus, it is essential to ensure an equilibrium between calcite, water, and atmospheric  $CO_2$  to avoid calcite dissolution and associated change in surface charge during measurements.

Experimentally, the equilibrium between calcite and water in the presence of  $CO_2$  is reached when all carbonate ions are turned into bicarbonates (Alroudhan et al. 2016). Mechanistically, carbonate minerals are soluble in water and the dissolution yields carbonate ions ( $CO_3^{2-}$ ) which are likely to react with water to form bicarbonate ( $HCO_3^-$ ) and hydroxide ( $OH^-$ ) ions, and this leads to an increase in pH of the solution according to the equilibrium reactions:





Also, CO<sub>2</sub> dissolves into brine and directly reacts with hydroxide ions to form bicarbonate (HCO<sub>3</sub><sup>-</sup>) and thus reduces the pH according to the equilibrium reaction.



All brine solutions used in this study were equilibrated with calcite. To achieve equilibrium, the pH of the solution was continuously monitored during immersion of offcuts of calcite in brine solutions. The initial increase in pH is attributed to the formation of hydroxide ions and thus the dissolution of calcite (eq. 7-1 and 7-2). However, the later decrease in pH indicates the subsequent formation of bicarbonate (eq. 7-3). Eventually, a stabilized pH (≈8.35) was achieved reflecting the equilibrium condition (with no further calcite dissolution occurring, Venkatraman et al. (2014)).

### 7.2.3 Calcite surface preparations

The calcite surfaces were then washed with DI water and rinsed with toluene to remove any organic and inorganic contaminants. Subsequently, the samples were dried for 60 min at 90 °C and then exposed to air plasma for 10 min (using a Diemer Yocto instrument) to further remove any contaminants. This cleaning procedure is crucial in the contact angle measurements as residual contaminations can lead to systematic errors and biased results (Iglauer et al. 2014).

The surface roughness of each sample was measured using atomic force microscopy (AFM DSE 95-200, Semilab) and the samples were found to be smooth with surface roughness ranging between 18.2 to 37.6 nm (Al-Anssari et al. 2016). The calcite surface was measured for air/water contact angle at ambient condition showing that  $\theta$  was 0 +3° (Mc Caffery and Mungan 1970, Farokhpoor et al. 2013, Al-Anssari et al. 2016, Nwidee et al. 2016a).

Previously, fluorinated ethylene propylene (FEP) was used to represent oil-wet pores in many studies (Espinoza and Santamarina 2010, Jung and Wan 2012, Ameri et al. 2013, Kaveh et al. 2014). However, in this study, we prepared an oil-wet substrate by treating pure calcite plates with stearic acid for better simulation of an oil-wet carbonate reservoir (Hansen et al. 2000, Mihajlovic et al. 2009, Shi et al. 2010). The cleaned substrates were first submerged for 30 min in 2 wt% NaCl brine (pH=4). Then, after drying with ultrapure nitrogen, the samples were immersed into 0.01M stearic acid and aged at ambient condition for 7 days (Al-Anssari et al. 2017f).

#### 7.2.4 Nanofluid preparations

Various nanofluids were investigated to evaluate their stability and efficiency to alter oil-wet calcite surfaces to water-wet under reservoir pressure and temperature. These fluids were prepared by homogenizing silicon dioxide nanoparticles (properties are listed in Table 4-1) in base-fluid (e.g. DI water, brine, and SDS-brine solution) with an ultrasonic homogenizer (300 VT Ultrasonic Homogenizer/ BIOLOGICS) for 40 min. We note that magnetic stirring is insufficient to disperse nanoparticles in the base fluid to formulate a homogenized suspension (Mahdi Jafari et al. 2006).

Further, it is known that high salinity has a screening effect on the electrostatic repulsion forces between nanoparticles (Li and Cathles 2014) which leads to an accelerated coalescence and sedimentation of nanoparticles (Al-Anssari et al. 2016). Thus, anionic surfactant (SDS) was added to the nano-formulation to super charge the nanoparticles and enhance the repulsive force (Ahualli et al. 2011, Sharma et al. 2015b). Experimentally, a titanium micro tip with a 9.5 mm diameter was used to prepare 20 mL batches of nanofluid using sonication power of 240W. To avoid overheating, each batch was sonicated for 4 periods of 10 min with 5 min rest periods (Al-Anssari et al. 2017e). The required power and time of sonication are mainly dependent on nanofluid volume and nanoparticles load (Shen and Resasco 2009).

In this work, to analyse the impact of nanofluid composition on the stability and efficiency of treatment, different nanoparticle concentrations (0.05-0.2 wt%), surfactant (SDS) concentration (0, 0.5, 1 and 2 CMC), and brine salinities (0-10 wt% NaCl) were tested.

#### 7.2.5 Nanofluid stability and phase behaviour

Stability of nanofluid is an essential parameter that can limit the nanofluid application. The zeta potential of nanofluid suspension has a direct relationship with suspension stability; nanoparticles with lower Absolute value of zeta potentials (around the isoelectric point (IEP); the point at which zeta potential equal zero) are electrically more unstable and thus flocculate and precipitate more rapidly (El-Sayed et al. 2012). Further, electrolyte can dramatically reduce the repulsive forces between nanoparticles and thus accelerate particle flocculation and coagulation. Surfactants such as SDS can decrease zeta potential ( $\leq -25$  mV) of silica nanofluids through the adsorption on the surface of the nanoparticle to form a supercharging particle (Ahualli et al. 2011).

The phase behaviour of the nanofluids was monitored by electrostatic measurements. Zeta potential ( $\zeta$ ) of nanoparticles were measured using a Zetasizer Nano ZS instrument (Malvern Instruments, UK).

### 7.2.6 Nano-modification of oil-wet calcite surface at high pressure and temperature

In order to test the efficiency of the nanofluids in terms of wettability alteration, nano-modified samples were prepared by immersing the oil-wet sample in a nanofluid for prescribed exposure time, temperature, and pressure. Experimentally, each clean oil-wet calcite substrate was vertically rested (to avoid the effect of nanoparticle deposition by gravity) in a treatment vessel and submerged in a specific nanofluid (0.05, 0.1, 0.2, and 0.5 wt% SiO<sub>2</sub> dispersed in SDS-brine solution) for specific a period of time (1, 2, 3, 4, and 5 h) at a particular temperature (23, 50, 70 °C) and pressure (0.1, 10, 20 MPa). The modification vessel was designed to work under reservoir conditions. A constant immersion ratio of 5g nanofluid and 1g of calcite was used. Experimentally, the temperature of the system was set at fixed value (296, 323, or 343 K) using digital thermocouple, and the pressure inside the vessel was increased via a high precision syringe pump (Teledyne D-500, pressure accuracy of 0.1% FS) to the desired value (0.1, 10, 20 MPa).

### 7.2.7 Contact angle measurements

Wettability of calcite in n-decane-brine and CO<sub>2</sub>-brine systems were measured by means of tilted plate contact angle technique (Lander et al. 1993, Al-Anssari et al. 2016) using a high-P/T goniometric setup. The measurement unit was designed to work under typical reservoir conditions (high pressure, temperature, and salinity). The detail of the cell and other measurement units (Figure 7-1) was reported in our previous works (Arif et al. 2016c, d).

A calcite sample was placed inside the pressure cell on the tilted plate (tilted at angle = 17°). Temperature of the system was set at fixed values (23, 50, and 70°C), and pressure inside the measurement cell was increased using a high precision syringe pump (Teledyne D-500, pressure accuracy of 0.1% FS) to the desired values (0.1 MPa, 10 MPa, and 20 MPa) by injecting CO<sub>2</sub> into the cell. For decane-brine contact angle measurements, the sample and the end of needle were totally submerged in decane prior to increase the pressure via CO<sub>2</sub> injection. After pressure stabilization, a droplet of de-gassed liquid (DI water or brine) at an average volume of 6 μL ± 1 μL was allowed to flow at 0.4 mL/min to dispense onto the substrate via a needle.

Advancing ( $\theta_a$ ) and receding ( $\theta_r$ ) contact angles were measured simultaneously (Lander et al. 1993, Al-Anssari et al. 2016) from the leading and trailing edges of the droplet, respectively, exactly before the droplet started to move. A high-resolution video camera (Basler scA 640–70 fm, pixel size = 7.4 μm; frame rate = 71 fps; Fujinon CCTV lens: HF35HA-1B; 1:1.6/35 mm) was used to record the movement of the whole process, and  $\theta_a$  and  $\theta_r$  were measured on the taken images. Initially, the pure calcite surface was tested,  $\theta_a = \theta_r = 0^\circ$ . For the modified samples, all the measurements were carried out at the stable conditions.

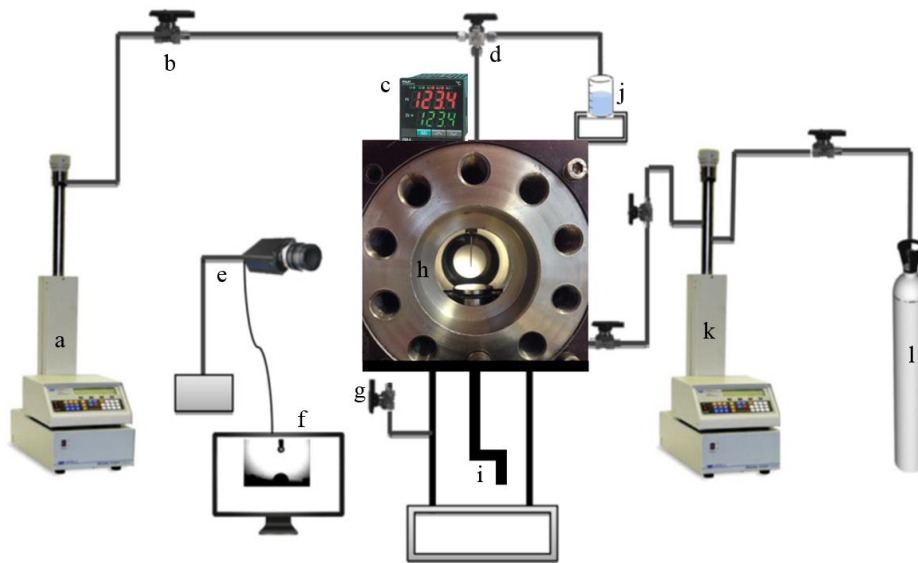


Figure 7-1 Experimental configuration for contact angle measurements; (a) syringe pump-brine, (b) two way valve, (c) temperature controller connected to the heating source, (d) three way valve, (e) high resolution camera, (f) visualization software, (g) pressure relief valve, (h) high P/T cell, (i) joystick controls the surface tilting, (j) feed/drain system, (k) syringe pump-gas, (l) compressing gas (CO<sub>2</sub>)-source.

For nano-treated samples, the measurements were done on the irreversible modified surfaces after treating with several washing liquids (Al-Anssari et al. 2016). Moreover, It was not necessary to thermodynamically equilibrate the fluids (CO<sub>2</sub> and brine or DI water) during  $\theta$  measurement since earlier studies revealed that mass transfer has no significant effect on contact angle during the first 60s (Sarmadivaleh et al. 2015, Al-Yaseri et al. 2016) and during this time all measurements were completed. In addition, at the leading edge of the CO<sub>2</sub> plume, non-equilibrated fluids are more relevant (Sarmadivaleh et al. 2015). The standard deviation of the measurements was  $\pm 3^\circ$  based on repeated measurements.

### 7.3 Results and discussion

Precise characterization of the wettability of rocks, before and after nano-treatment at representative operation conditions is essential to understand the implication of using nanoparticles to alter the wettability of rock for subsurface applications including EOR (Al-Anssari et al. 2016, Nwidee et al. 2016a, Zhang et al. 2016) and carbon geo-storage (Iglauer et al. 2015b, Iglauer et al. 2015c). To accomplish this, it is essential to formulate a stable nanosuspension which can work effectively at reservoir conditions.

### 7.3.1 Effect of salinity on nanofluids stability

It is well known that the electrolyte (which can vary in subsurface formations, Dake (1978)) can significantly influence nanofluid properties (Winkler et al. 2011, Li and Cathles 2014). It is thus essential to investigate the effect of salinity on nanofluid stability and formation of stable nanosuspension by adding a proper amount of oppositely charged ionic surfactant (Ahualli et al. 2011).

In this context, we systematically measured zeta potential ( $\zeta$ ) as a function of ionic strength (wt% NaCl) and surfactant concentration (SDS) (Figure 7-2).

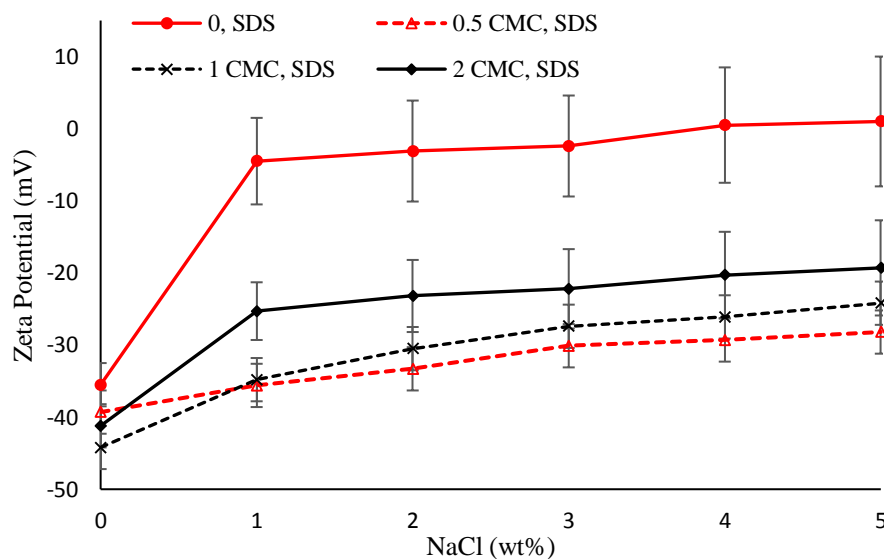


Figure 7-2 Effect of electrolyte, and surfactant concentration (in terms of CMC) on zeta potential of nanoparticles/brine/surfactant system (0.1wt% SiO<sub>2</sub> at pH= 6).

Figure 7-2 presents the measured zeta potential of a nanoparticle/brine/surfactant system at different salinities and surfactant concentration measured at 25°C. Results demonstrate that adding 0.5 CMC of SDS (Sodium Dodecylsulfate) in the nanosuspension can keep zeta potential as low as -28.2 mV even at high salinity (5 wt% NaCl). This result is very important in nanofluid preparations since earlier studies confirmed that nanofluid can be stable when zeta potential of the nano-suspension is  $\leq -25$  mV (Mondragon et al. 2012). Mechanistically, surfactant monomers adsorb onto the nanoparticle surface by their hydrophilic tail and not the head group due to identical charge between the hydrophilic nanoparticle and the head group of the anionic surfactant (Ahualli et al. 2011, Iglesias et al. 2011). The zeta potential increases and the stability improved owing to the higher repulsive forces between supercharged nanoparticles resulting from surfactant monomers adsorption. Thus, it is clearly possible to formulate a stable nanofluid even at high salinity by adding the right amount ( $<$  CMC) of SDS surfactant. Note that CMC value of SDS depends on suspensions salinity (Al-Anssari et al. 2017e).

It was also found that increased surfactant concentration ( $\geq$  CMC) has negative effects on the surfactant performance to improve nanofluid stability. Results showed that relatively high surfactant concentration ( $\geq$  CMC) was less efficient at keeping

nanoparticles with high surface charge; at such high SDS concentrations, more surfactant monomer will be crowded per unit area and thus joined up from their hydrophilic tail forming micelles rather than being adsorbed as monomers on a similarly charged nanoparticle surface (Tadros 2006). The repulsion forces between the free heads group of micelles and similarly charged hydrophilic nanoparticles will likely push nanoparticles to flocculate. Further, this phenomenon increases with salinity since CMC value decreases with the increase in electrolyte concentration leading to a similar influence as surfactant concentration increases (Dutkiewicz and Jakubowska 2002, Zhang et al. 2002, Zhao et al. 2006).

### 7.3.2 AFM and SEM analyses

The effect of irreversibly adsorbed nanoparticles on the surface roughness was measured using atomic force microscopy (AFM instruments model DME 95-200, Semilab). Two different surfaces were measured after modification with the same nanofluid but at two different pressures (0.1 MPa and 10 MPa). Moreover, scanning electron microscopy (SEM, Zeiss Neon 40EsB FIBSEM) was used to probe the adsorption/desorption behaviour of the nanoparticles. After nano-treatment, the samples were exposed to different fluids at ambient conditions to remove the excess adsorbed nanoparticles.

The root-mean-square (RMS) measurements of these tests showed that nanofluid-treatment has a significant impact on the surface roughness owing to the adsorption of the nanoparticles as nano-clusters on the surface (Al-Anssari et al. 2016) and we found that surface roughness increased after the nano-treatment. Moreover, it was also found that the pressure of nano-modification did not show any distinctive influence on the degree of surface roughens change. For instance, the RMS surface roughness of the sample increased from 78 nm (for the oil-wet case) to 838 nm after nano-modification at 0.1 MPa pressure while it increased from 71 to 704 nm for the sample modified at 20 MPa (Figure 7-3).

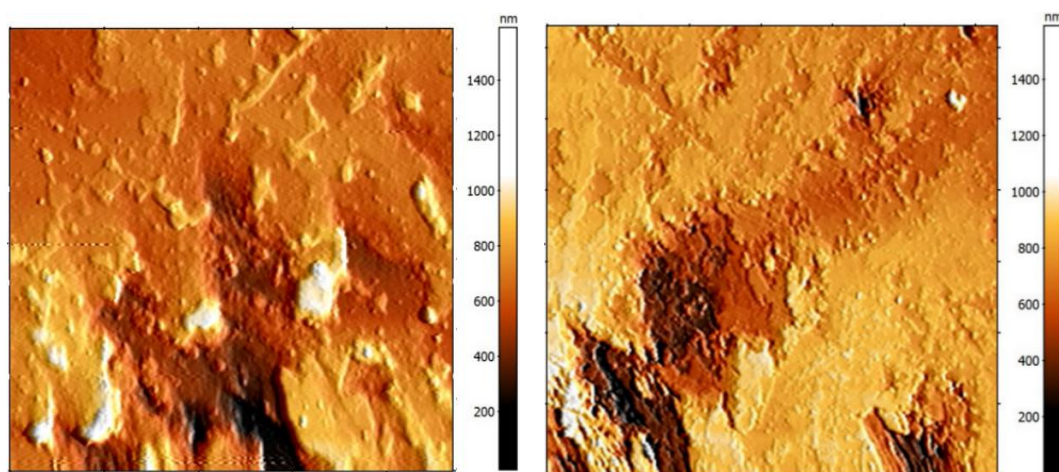


Figure 7-3 Atomic force microscopy images of a nano-modified calcite surface with nanofluid (0.2 wt% SiO<sub>2</sub> in 2 wt% brine, 0.5 CMC of SDS at 50°C for 4 h) after exposure at 20 MPa (left) and 0.1 MPa (right). The RMS surface roughness was 838 nm at 0.1 MPa, and 704 nm at 20 MPa pressure.

SEM images confirmed the similar adsorption of silica nanoparticles as an agglomerated clusters on calcite surface under different applying pressure (Zhang et al. 2011, Al-Anssari et al. 2016, Nwidee et al. 2016a). Thus, exposure of the surface to high pressure during nano-treatment did not change the surface morphology of the sample and the irregular spread coating of silica was visible (Figure 7-4). This is consistent with Al-Anssari et al. (2016) who investigate nanoparticle adsorption on oil-wet calcite surface using energy dispersive X-ray spectroscopy (EDS) to prove the existence of nanoparticles all along the nano-treated surface.

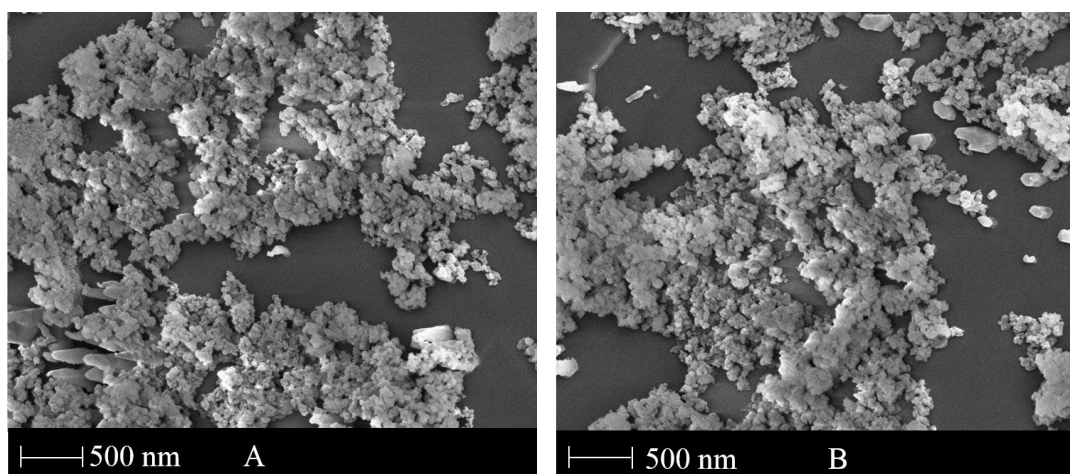


Figure 7-4 SEM images of an oil-wet calcite surface after treatment with the same nanofluid (0.2 wt% SiO<sub>2</sub> in 2 wt% brine, 0.5 CMC of SDS at 50°C for 4 h) after exposure at A) 20 MPa and B) 0.1 MPa.

### 7.3.3 Adsorption characteristics: reversible versus irreversible adsorption

Adsorption characteristics of the nanoparticles on the rock surface are key parameters for optimum nanofluid performance (Zargartalebi et al. 2015, Zhang et al. 2015). The stability of nano-adsorption is of particular interest, and thus the ratio between reversibly and irreversibly bound silica at different operational conditions is useful to be determined. In this section, after nano-modification of samples at the same conditions (50°C, 12 MPa, 1 h immersing time) with different nanofluids (0.01, 0.10, and 0.50 wt% Np in 0.5CMC SDS, 5 wt% NaCl), each sample was subjected to different elevated pressures prior to the exposure to different solvents (DI water, brine, and acetone) at ambient conditions. Eventually, the contact angle of decane-brine was measured at the ambient conditions (Figure 7-5) to compare with reported data. This test helps to mimic all the possible scenarios in oil reservoirs where a wide range of pressures are recorded.

For surface modification with a low SiO<sub>2</sub> concentration nanofluids ( $\leq 0.01$  wt%), most of the nanoparticles were bound irreversibly even after being exposed to high pressures (Figure 7-5). Meanwhile, the rate of nanoparticle desorption increased with exposure pressure, particularly at the pressures of 7 to 15 MPa, when the surface was treated with concentrated nanofluid ( $\geq 0.1$  wt% Np). However, no further significant desorption was observed above 15 MPa. The total difference in decane-brine advancing contact angles after desorption of the reversibly bound nanoparticles was  $\approx 12^\circ$  for 0.2 wt% SiO<sub>2</sub> and  $28^\circ$  for 0.5 wt% SiO<sub>2</sub>, which is still small considering the drastic reduction caused by nano-treatment ( $\approx 98^\circ$ , after treatment with 0.5 wt% SiO<sub>2</sub> for 1 h). A similar trend was observed for decane-brine receding contact angle. The increase in desorption with nanoparticle concentration is likely due to the larger silica clusters on the surface, owing to the faster agglomeration of nanoparticles at concentrated nanofluids (Bayat et al. 2014a, Bayat et al. 2014b), which are more pronounced at elevated pressures. On the other hand, for diluted nanofluids, nanoparticles adhere to the surface as mono or limited multi-layers (Zhang et al. 2014, Zhang et al. 2015), which are irreversible and less affected by exposure to a high pressure or different solvents. Al-Anssari et al. (2016) demonstrated that, at ambient condition, most nanoparticles were bound irreversibly onto the oil-wet calcite surface.

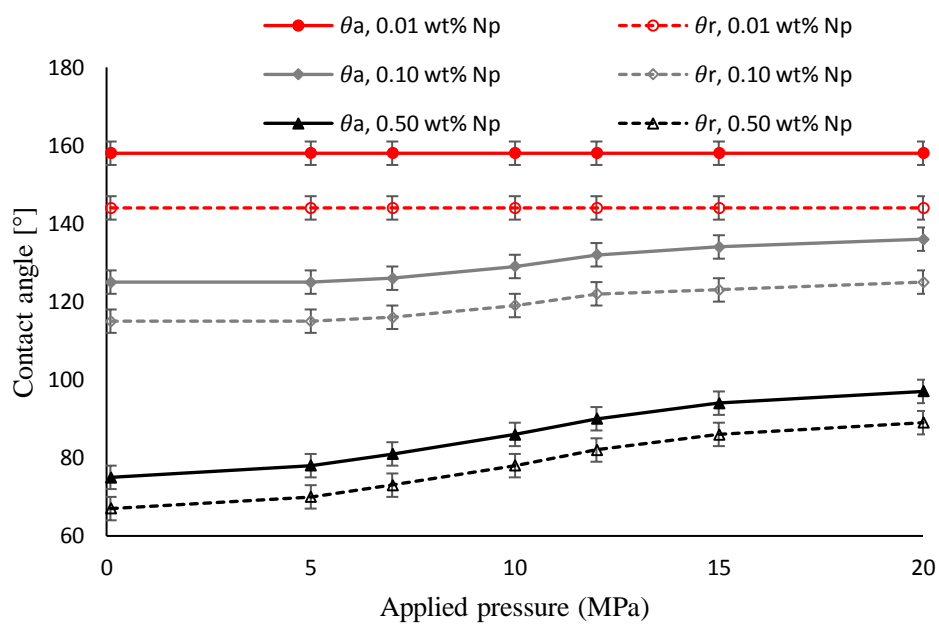


Figure 7-5 Water advancing ( $\theta_a$ ) and receding ( $\theta_r$ ) contact angle on different nano-treated oil-wet calcite surfaces in decane at ambient condition after treating each sample with a different nanofluid (0.01, 0.10, and 0.50 wt% Np in 0.5CMC of SDS, 5 wt% NaCl) for 1 hour and subjected to different pressures prior to the exposure to DI water, and acetone.

Technically, it is likely that the silica nanoparticles are chemisorbed onto the surface (Zhuravlev 2000, Al-Anssari et al. 2016). Moreover, the SEM images (Figure 7-4) revealed that adsorbed nanoparticles are in multilayers over the surface; thus, the elevated pressure is likely to break up nanocluster into smaller ones on the surface.

Based on the above observation, all nanofluid-modified samples were exposed to 20 MPa pressure for 120 min to avoid any possible nano-impurities resulting from nanoparticles desorption that can dramatically impact the accuracy of contact angle measurements (Iglauer et al. 2014).

### 7.3.4 Effect of nanoparticle (Np) concentration on the wettability

The nanoparticle concentration must be evaluated to determine optimum nanofluid formula considering the fact that higher nanoparticles concentrations (typically  $\geq 2$  wt%), despite being efficient to reduce  $\theta$  (Roustaei and Bagherzadeh 2014, Al-Ansari et al. 2016, Nwideo et al. 2016a), may determinately reduce reservoir permeability (ShamsiJazeyi et al. 2014). Moreover, a higher nanoparticle content can significantly reduce the stability of nanosuspension (Tantra et al. 2010, Metin et al. 2011) even with the presence of surfactants (Sharma et al. 2015b), which can limit the desired efficiency. Thus, it is vital to determine the lowest effective nanoparticle concentration (at reservoir conditions) that is commercially optimal from an economic perspective too (Iglauer et al. 2010).

To accomplish this, both surface modification and contact angle measurement were conducted at the same operational conditions (50°C, and 12 MPa, Figure 7-6). The modification period was 4 h. Note that: at 0 wt% Np (SiO<sub>2</sub>), the samples were treated with the base fluid (0.5CMC SDS, in 5 wt% NaCl) to allow systematic study of the impact of nanoparticles concentration on  $\theta$ .

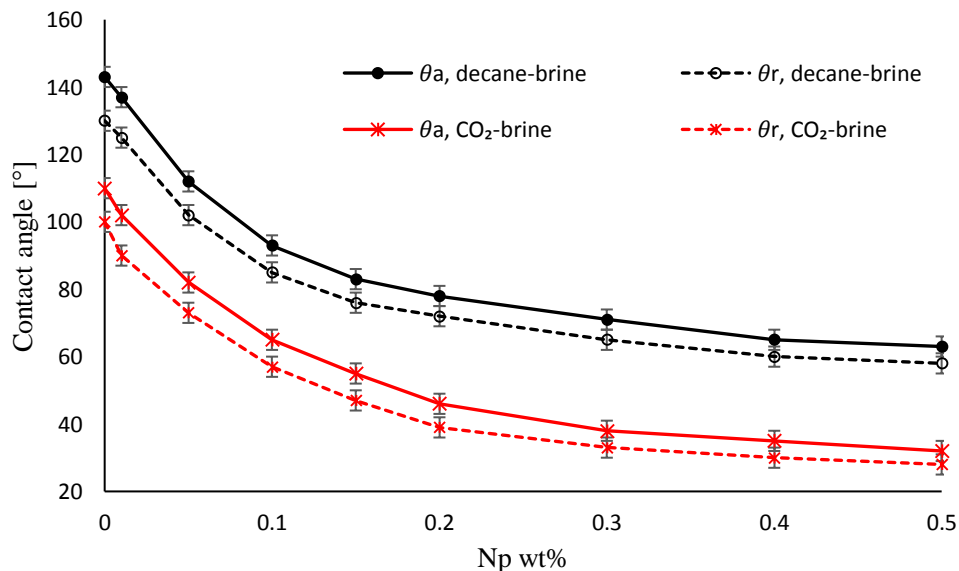


Figure 7-6 Water advancing ( $\theta_a$ ) and receding ( $\theta_r$ ) contact angle on nano-modified calcite surface in decane and CO<sub>2</sub> as a function nanoparticle (Np, SiO<sub>2</sub>) concentration in the base fluid (0.5CMC SDS in 5% NaCl).

Advancing and receding contact angles for both CO<sub>2</sub>/brine/mineral and decane/brine mineral systems clearly decreased with nanoparticle concentration (Figure 7-6). Moreover, the reduction in  $\theta$  was sharper till ~0.2 wt% Np after which it gradually flattened out. For instance,  $\theta_a$  reduced from 143° to 78° ±3° for decane-brine and from 110° to 46° ±3° for CO<sub>2</sub>/brine systems implying a sharp decline. For a concentration change from 0.2 to 0.5 wt% SiO<sub>2</sub>,  $\theta_a$  decreased from 78° to 63° ±3° for decane-brine and 46° to 32° ±3° for CO<sub>2</sub>-brine system employing (a small reduction in  $\theta_a$ ). Similar trends were observed for the decline in both advancing and receding contact angles (Figure 7-6).

The sharp reduction in  $\theta$  at low concentration nanofluids (up to 0.2 wt%) is likely due to the long immersing time (4h) used in this test, which is consistent with the reported data at ambient conditions (Zhang et al. 2014, Al-Ansari et al. 2016, Zhang et al. 2016). Meanwhile, the slight change in  $\theta$  at high Np concentration was due to reach the adsorption capacity of the surface (Zhang et al. 2015).

### 7.3.5 Effect of brine salinity on wettability of nano-modified surfaces

The salinity of reservoirs varies significantly and can reach very high levels (e.g. up to 30 wt% brine) (Dake 1978, Krevor et al. 2016). Moreover, formations salinity can directly impact the stability of the injected nanofluids. Thus, the concentration of nanofluids, after injection into oil reservoirs, can vary due to the precipitation (Tantra et al. 2010) and adsorption of nanoparticles on the rock surfaces (Zhang et al. 2015). It is thus important to investigate the effect of droplet salinity on  $\theta$  of nano-modified surfaces with different nanofluids at reservoir conditions (15 MPa and 70°C). To accomplish this, we investigated the effect of salinity on wettability of calcite for a broad range of salinity (from 0 – 30 wt% NaCl) and three nanofluid concentrations (0.05, 0.2, and 0.5 wt% Np). This was examined for both decane/brine (Figure 7-7) and CO<sub>2</sub>/brine systems (Figure 7-8). The initial advancing and receding contact angles at these operating conditions before nano-treatment were 165° and 147° in decane, while they were 149° and 135° in CO<sub>2</sub>, respectively (within ±3° of experimental error).

In general,  $\theta_a$  and  $\theta_r$  decreased with increasing salinity for decane/brine systems (Figure 7-7) and increased with salinity for CO<sub>2</sub>/brine systems (Figure 7-8) for all nanofluid concentrations analysed. After surface treatment with 0.5 wt% SiO<sub>2</sub> nanofluid for 1 h,  $\theta_a$  decreased from 60° to 38° when salinity increased from 0 to 30 wt% NaCl for decane/brine system (Figure 7-7). And for the same salinity increment,  $\theta_a$  increased from 32 to 41 for CO<sub>2</sub>/brine system (Figure 7-8).

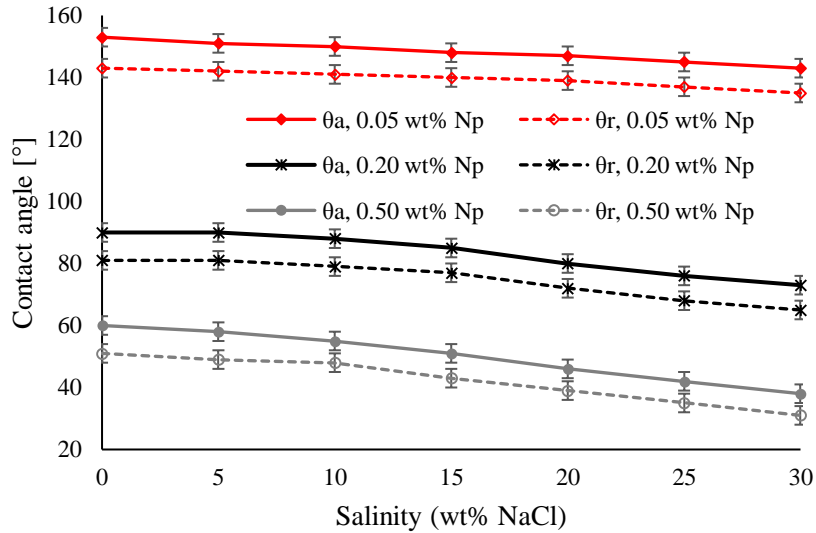


Figure 7-7 Impact of salinity and SiO<sub>2</sub> concentration (wt% Np) on advancing and receding contact angle of decane-brine system at reservoirs condition (15 MPa and 70°C) after 1 h of nano-treatment.

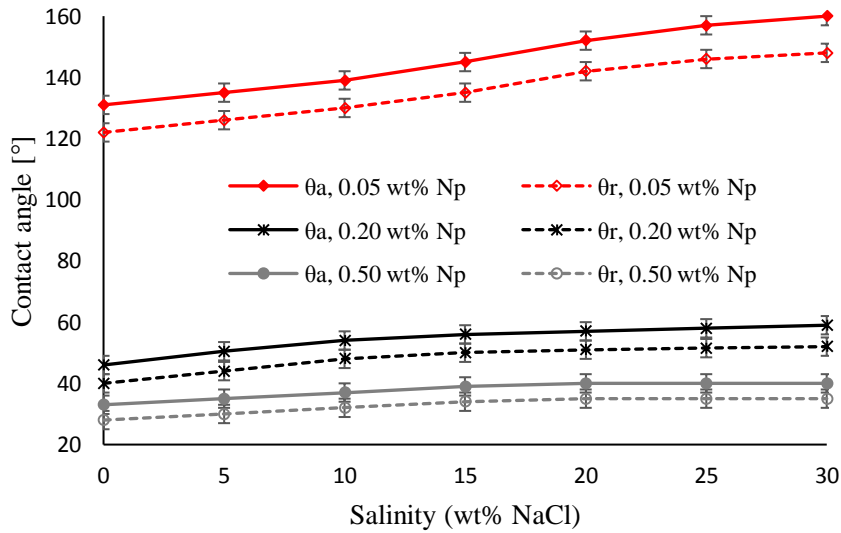


Figure 7-8 Impact of salinity and SiO<sub>2</sub> concentration (wt% Np) on advancing and receding contact angle of CO<sub>2</sub>-brine system at reservoirs condition (15 MPa and 70°C) after 1 h of nano-treatment.

Specifically, brine salinity only slightly influenced  $\theta$  of the decane-brine system on oil-wet calcite (at lower nanoparticle concentration, 0.05 wt% Np) owing to the strong adhesion between the oil film on the solid surface and surrounding decane. Increased nanoparticles concentrations in treatment fluids alter the wettability of oil-wet surfaces to water-wet removing the oil film from the surface and leading to a direct contact between salt and carbonate surfaces thus reducing  $\theta$ . At the same temperature and

pressure, increased droplet salinity and nanoparticle concentration enhances  $\theta$  reduction of the decane-brine system.

The more significant effect of salinity was observed for CO<sub>2</sub>-brine contact angle, at the oil-wet substrate (Figure 7-8). The trend of  $\theta$  in this case totally different from that reported for decane, and  $\theta$  significantly increased with salinity by around 23% to reach 160°. However, droplet salinity has no effect on the wettability of water-wet surfaces (surfaces treated with concentrated nanofluid having  $\geq 0.2$  wt% Np) and  $\theta$  only slightly increased with NaCl concentration. These differences in  $\theta$  trends between the two measurement mediums (decane and CO<sub>2</sub>) are related to the supercritical condition of carbon dioxide at this operational conditions and the dependence of calcite solubility on temperature, CO<sub>2</sub> pressure and salinity (Weyl 1959, Saaltink et al. 2013).

It is interesting to note that even at high salinity conditions, silica nanoparticles still have a drastic ability to alter the wettability of the surfaces to water-wet (Figure 7-7, and Figure 7-8). This suggests that nanoparticles have a great potential application in carbon storage as well as EOR where high salinities are likely.

### 7.3.6 Effect of exposure time on wettability alteration

It has been proved that nanoparticles adsorption is responsible for wettability changes of solid surfaces (Moghaddam et al. 2015, Zhang et al. 2015, Zhang et al. 2016). Consequently, the exposure time of the substrate to the nanofluid as well as a load of nanoparticles are thought to control the extent of surface modification (Al-Anssari et al. 2016). We thus investigated the relationship between nanoparticle concentration and immersion time on the wettability of a decane/brine/calcite system at typical reservoir conditions (20 MPa, 60°C, and 20% NaCl) to formulate a more efficient nanosuspension.

We found a strong relationship between  $\theta$  and immersing time at reservoir conditions for all the different nanofluid concentrations analysed (Figure 7-9). Essentially, longer exposure of the surface to the nanofluid resulted in much stronger resulting water-wet surfaces (lower  $\theta$ ; Figure 7-9). For all nanofluids analysed, contact angle decreased with exposure time. However, for nanoparticle concentration of 0 wt% (sole SDS effect),  $\theta$  continually decreased for 1 hour of exposure time and then there was no significant reduction in  $\theta$  for further exposure ( $\theta$  reduced by  $\sim 25^\circ$  after 1 hour and by additional  $5^\circ$  after further 4 hours, black lines in Figure 7-9). This reduction in  $\theta$  during the first hour was solely due to the effect of surfactant molecules in the base fluid (Zargartalebi et al. 2015). Such limited reduction in  $\theta$  is mainly related to the low surfactant concentration (0.5 CMC). It is also due to the structure of SDS surfactant which contains a large number of hydrophobic side chain group (Kundu et al. 2013) leading to increased hydrophobicity when adsorbed at carbonate surface (Ma et al. 2013).

For high nanoparticle concentration ( $> 0.5$  wt% Np), the major changes in surface wettability ( $\theta$  reduction) occurred during the first hour of exposure ( $\theta$  reduced by  $98^\circ$ ). Upon further surface exposure to nanofluid, the reduction in  $\theta$  was relatively flat (Figure 7-9). For instance, when  $\theta$  reduced by  $98^\circ$  after 1 h (a significant reduction) and by only  $35^\circ$  after further 4 h. In contrast, exposure time was found to be more crucial for low concentration nanofluids (0.05 wt% Np) as we found a sharp decrease in contact angle till 5 hours of exposure. For instance,  $\theta$  reduced by  $25^\circ$  after 1 h and by further  $47^\circ$  for 4 h further exposure. Moreover, treating an oil-wet calcite sample in 0.1 wt% nanofluid for 5 h gives a similar  $\theta$  reduction ( $-96 \pm 3^\circ$ ) to that result from 0.5 wt% nanofluid after only 1 h. Several reports have shown that, at ambient condition, wettability alteration of oil-wet surface occurs rapidly at concentrated silica nanoparticles (Roustaei and Bagherzadeh 2014, Al-Anssari et al. 2016, Zhang et al. 2016). We believe that the surface reached the adsorption capacity in a longer time for lower nanofluid concentrations (Al-Anssari et al. 2016) while at a relatively high concentration ( $\geq 0.2$  wt% Np), the adsorption capacity was reached much earlier (Roustaei and Bagherzadeh 2014). This is consistent with the observation by Zhang et al. (2015) who found that higher adsorption rate of nanoparticles can achieve by increasing the contact time between solid surface and silica nanoparticles. Our results showed another important finding, that at low nanoparticle concentration (0.05),  $\theta$  was higher than the measured value at zero nanoparticle load (0 wt% Np) during the first hour. This phenomenon is related to the consumption of surfactant molecules due to rapid adsorption on nanoparticles surface (Ahmadi and Sheng 2016) which eliminate the sole effect of the anionic surfactant, SDS, on surface wettability.

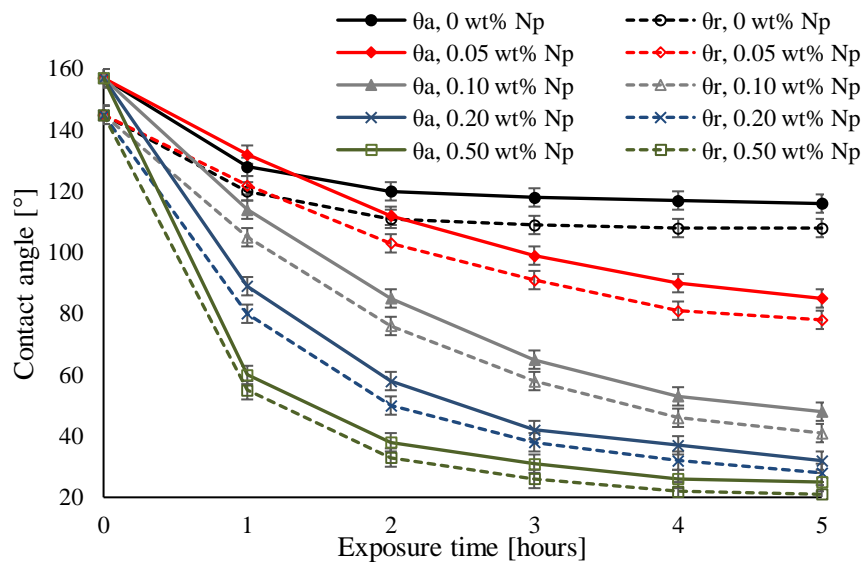


Figure 7-9 Effect of nanoparticle concentration ( $\text{SiO}_2$  wt%) in the base fluid (0.5cmc SDS, 4wt% NaCl) and immersing time (h) at reservoir conditions (20 MPa and  $60^\circ\text{C}$ ) on advancing and receding contact angles of decane-brine system. The droplet salinity was 20% NaCl.

## 7.4 Implications

Fractured carbonate reservoirs that contain more than half of the discovered remaining hydrocarbon reserves in the world are typically intermediate-wet and oil-wet (Gupta and Mohanty 2010). Thus, conventional waterflooding techniques are inefficient leading to low productivity (Wu et al. 2008). In this context, water does not spontaneously imbibe into the oil-wet matrix, which contains most of the stored oil, and hydrocarbon is mainly produced from fractures. As a result, only 10-30% of the hydrocarbon is recovered. On the other hand, the reported wettability data establish that oil-wet formations are CO<sub>2</sub>-wet at typical reservoir conditions (Al-Anssari et al. 2017b) reporting a direct negative impact on residual and structural trapping capacities for carbon geo-storage projects (Iglauer et al. 2015b, Iglauer et al. 2015c). It is well established that the decrease in structural and trapping can significantly increase risks of project failure.

The proposed mechanism, which can significantly enhance hydrocarbon production and improve carbon storage capacity and containment security, is to alter the oil-wet or intermediate-wet limestone rocks to water-wet. Several studies have been investigated the use of nanofluids and particularly silica nanofluid as a wettability alteration agent at laboratory conditions. However, only limited data is available at reservoirs high salinity (Al-Anssari et al. 2016), pressure (Al-Anssari et al. 2017b), and temperature (Al-Anssari et al. 2017f) and no available study has systematically combined and study all these factors for carbonate surface, oil, and brine system.

The suggested nanofluid treatment affectedly enhanced oil recovery, which attributed to a complete wettability alteration from strongly oil-wet to strongly water-wet at hydrocarbon production conditions. Fundamentally, with nano-priming, water can spontaneously imbibe to the rock matrix displacing a large amount of stored hydrocarbon into the liquid phase in the porous medium. Moreover, nanofluid treatment can considerably increase structural and residual storage capacities in carbon storage projects when CO<sub>2</sub> is injected into depleted oil reservoirs for storage and incremental hydrocarbon production.

In this work, the most interesting finding is that nanoparticles (e.g. 0.2 wt% SiO<sub>2</sub>) that dispersed efficiently in surfactant formulation (0.5 CMC) are stable against coagulation and agglomeration (zeta potential  $\leq -35$  mV) despite the high salinity (5wt% NaCl) and can significantly reduce the contact angle ( $\theta$ ) of decane/brine (e.g. from 151° to 82°) and CO<sub>2</sub>/brine (e.g. from 112° to 49°) systems at oil production conditions (50°C, and 12 MPa). These findings can significantly support the implementation of nanofluids injection in EOR and other subsurface projects. Also, the other important finding is that increased exposure time (from 1 to 5 h) reduces the required nanoparticles load (from 0.5 to 0.1 wt% SiO<sub>2</sub>) to achieve the same  $\theta$  reduction. This can improve the economic viability of nanofluid injection technique concerning crude oil prices and carbon tax since the flooding process can extend for a very long periods.

## 7.5 Conclusions

In this work, contact angle measurements were conducted on oil-wet calcite surfaces to evaluate the wettability alteration efficiency of nanofluids as a function of nanofluid concentration, exposure time and surfactant addition at typical reservoir conditions. Moreover, impacts of salinity and pressure were also investigated thoroughly.

We found that silica nanofluids can change the wettability of an oil-wet calcite surface to strongly water-wet at reservoir condition consistent with studies conducted at ambient condition (Zhang et al. 2015, Al-Anssari et al. 2016, Zhang et al. 2016). The nanoparticle adsorption was mainly found to be irreversible at high pressure (20 MPa) and temperature (50 °C). Nano-modification period (exposure time) played a crucial role in nanofluid efficiency particularly for dilute nanofluids. For instance, treating dilute nanofluid (0.1 wt% SiO<sub>2</sub>), 5 h of exposure time to achieve the same  $\theta$  reduction that can be obtained after 1 h exposure to a concentrated nanofluid (0.5 wt% SiO<sub>2</sub>). Moreover, for high concentration nanofluids ( $\geq 0.2$  wt% SiO<sub>2</sub>), all significant changes in wetting behaviour occurred only during the early period (the first and with less extend the 2<sup>nd</sup> h of exposure) consistent with reported data (Roustaei and Bagherzadeh 2014, Al-Anssari et al. 2016, Nwidee et al. 2016a) at ambient condition. In addition, we found that adding proper amount of anionic surfactant (SDS, Sodium Dodecylsulfate) can significantly improve nanofluid stability despite salt concentrations in the base fluid (Ahualli et al. 2011, Sharma et al. 2015b).

Finally, we found that contact angle increased with pressure at all conditions analysed consistent with (Arif et al. 2016a, Arif et al. 2016d). Moreover, we found that contact angle increases with salinity for CO<sub>2</sub>/brine systems consistent with Arif et al. (2016c) while decreases with salinity for decane/brine systems.

Overall, nanofluids demonstrate significant potential of wettability alteration at reservoir conditions which can lead to enhanced oil recovery and efficient CO<sub>2</sub> geo-storage.

## Chapter 8 **CO<sub>2</sub> geo-storage capacity enhancement via nanofluid priming**

### **Abstract**

CO<sub>2</sub> geo-storage efficiency is strongly influenced by the wettability of the CO<sub>2</sub>-brine-mineral system. With decreasing water-wetness, both, structural and residual trapping capacities are substantially reduced. This constitutes a serious limitation for CO<sub>2</sub> storage particularly in oil-wet formations (which are CO<sub>2</sub>-wet).

To overcome this, we treated CO<sub>2</sub>-wet calcite surfaces with nanofluids (nanoparticles dispersed in base fluid) and found that the systems turned strongly water-wet state, indicating a significant wettability alteration and thus a drastic improvement in storage potential. We thus conclude that CO<sub>2</sub> storage capacity can be significantly enhanced by nanofluid priming.

**Keywords:** Silica nanoparticles, carbon capture and storage, contact angle

### **8.1 Introduction**

CO<sub>2</sub> storage in depleted oil and gas reservoirs or deep saline aquifers has been considered as a practical approach to store anthropogenic CO<sub>2</sub> and thus provide a cleaner environment (Lackner 2003, Metz et al. 2005, Orr 2009). Once depleted, hydrocarbon reservoirs offer a large potential for CO<sub>2</sub> storage, and CO<sub>2</sub> injection can be combined with incremental oil recovery (CO<sub>2</sub>-enhanced oil recovery (EOR), Emberley et al. (2004); Ahr (2011). However, oil reservoirs are typically oil-wet or intermediate-wet (Gupta and Mohanty 2010), which drastically reduces structural (Iglauer et al. 2015b, Iglauer et al. 2015c) and residual (Chaudhary et al. 2013, Al-Menhali et al. 2016, Rahman et al. 2016) trapping capacities. This effect is caused by the fact that oil-wet surfaces are CO<sub>2</sub>-wet at storage conditions (i.e. at high pressure and elevated temperature), e.g. compare Dickson et al. (2006), Yang et al. (2007), Iglauer et al. (2015c), Arif et al. (2016d).

This reduced water-wettability thus constitutes a serious constraint for structural and residual trapping capacities in oil-wet reservoirs, which however, are most important economically due to CO<sub>2</sub>-EOR. To overcome this limitation we propose the injection of nanofluids; and we demonstrate here that nanofluids can be very efficient and render even strongly CO<sub>2</sub>-wet surfaces strongly water-wet.

### **8.2 Experimental methodology**

#### **8.2.1 Materials**

Pure calcite (Iceland spar, from WARD'S Natural Science), sample size (1cm x 1cm x 0.3cm) was used as a representative for limestone. Deionized (DI) water (Ultrapure from David Gray; electrical conductivity = 0.02 mS/cm) and Sodium chloride ( $\geq 99.5$  mol%, Scharlan) were used to prepare brine solutions (1-20 wt% NaCl in DI water). This range was selected to investigate the influence of salinity comprehensively. Brine solutions were prepared by mixing the components rigorously with a magnetic stirrer for more than 2 hrs to ensure complete dissolution and a homogeneous phase, followed by vacuuming for 12 hours to de-gas the brine. DI-water/brines were equilibrated with calcite by immersing calcite pieces and rigorously mixing while continuously monitoring the pH (Alroudhan et al. 2016). The formation of hydroxide ions is indicated by the initial increase in pH due to calcite dissolution and the subsequent decrease in pH indicates the formation of bicarbonate ions. Phase equilibrium was achieved when the constant pH value was stabilised (Venkatraman et al. 2014), under such conditions no more calcite dissolution occurs.

Surface cleaning agents used were toluene (99 mol%, Chem-supply), n-hexane ( $> 95$  mol%, Sigma-Aldrich), nitrogen ( $> 99.99$  mol%, BOC), acetone and methanol (both 99.9 mol%, Rowe Scientific). 99.9 mol% CO<sub>2</sub> (from BOC, gas code-082) was used as gas, liquid, and supercritical fluid (depending on the experimental condition).

The calcite surfaces were rendered oil-wet by treatment with stearic acid ( $\geq 98.5$  mol%, Sigma Aldrich). Specifically, 0.01 M stearic acid in n-decane was used for aging (prepared by dissolving 0.285 g of stearic acid in 100 mL of n-decane ( $>99$  mol%, Sigma-Aldrich) (Hansen et al. 2000, Mihajlovic et al. 2009, Shi et al. 2010); details of all investigated surfaces are tabulated in Table 8-1.

Silicon dioxide (SiO<sub>2</sub>) nanoparticles (porous spherical, 5 nm, purity = 99.5 wt%, Sigma Aldrich) were used to prepare nanofluid. 0.04 g silicon dioxide nanoparticles were sonicated (using a 300 VT Ultrasonic Homogenizer/ BIOLOGICS) with 20 mL base fluid to prepare a 0.2 wt% silica nano-dispersion; a detailed preparation procedure and nanoparticle-treatment of calcite surfaces can be found elsewhere (Al-Anssari et al. 2016, Mahbubul et al. 2016, Nwideo et al. 2016b, Nwideo et al. 2016a). Low concentration (490 mg.L<sup>-1</sup>, 0.2 CMC (critical micelle concentration)) of sodium Dodecylsulfate [SDS, Sigma Aldrich,  $\geq 98.5$  mol%, Mol.wt= 288.38 g.mol<sup>-1</sup>, CMC = 2450 mg.L<sup>-1</sup>] was dissolved in 2 wt% brine to formulate the base fluid. The presence of low SDS concentration can actively stabilize the nanosuspension (Ahualli et al. 2011, Sharma et al. 2015b).

Nanoparticle-surface interaction was investigated at nanoscale via atomic force microscopy [AFM; Zhang et al. (2011)]; the surface roughness of all four surfaces were measured via AFM (AFM instrument model DSE 95-200, Semilab)]. While the natural and oil-wet calcite surfaces were smooth, the nanoparticle-treated surfaces showed increased roughness (Figure 8-1 and Table 8-1), see further discussion below. The increase in surface roughness was mainly due to the permanent deposition of nanoparticle clusters on the surface.

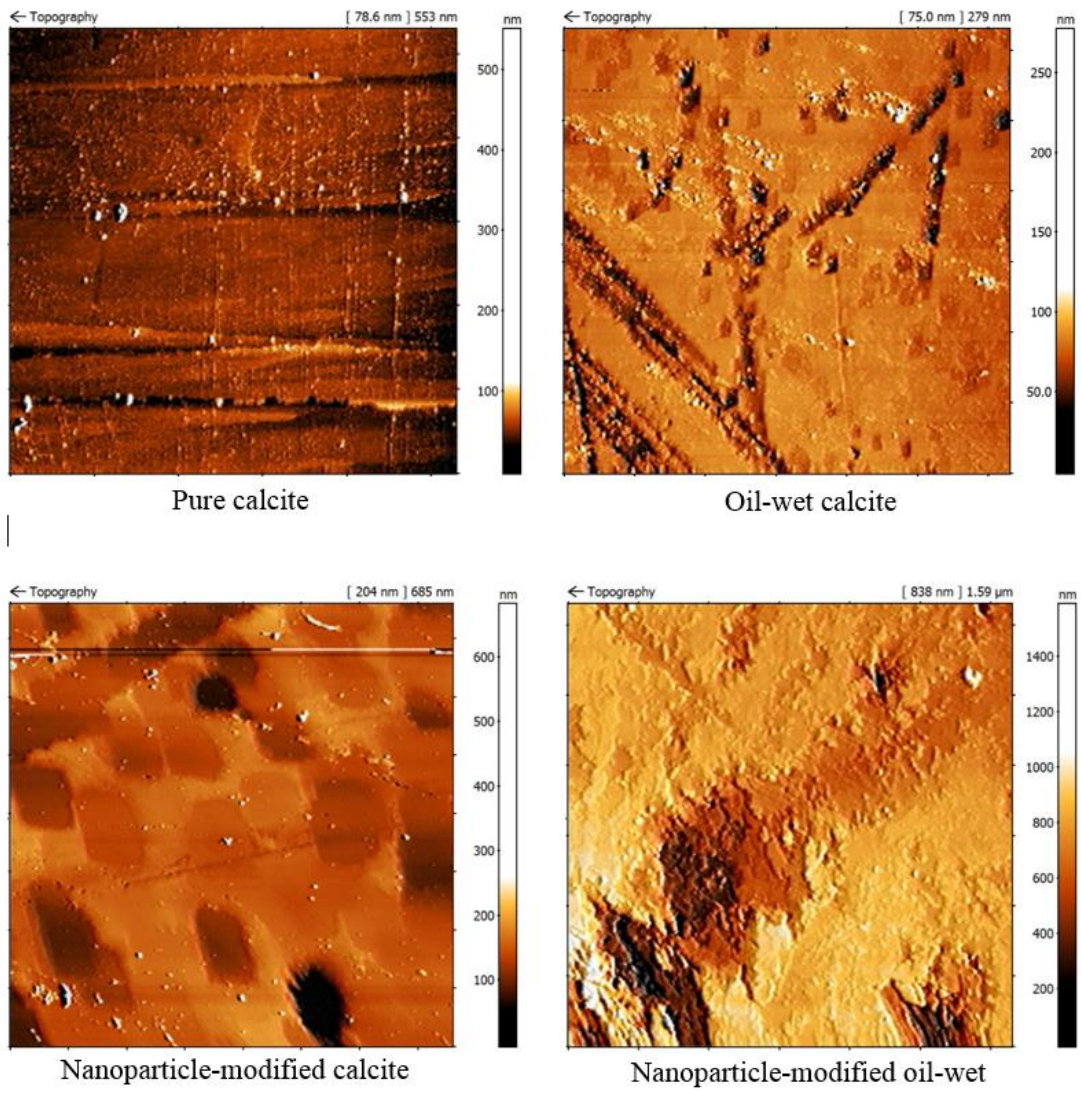


Figure 8-1 Atomic force microscopy images of a calcite surfaces used in the experiments.

Table 8-1 Sample treatment and original wettability state.

Surface	Treated with	Surface state	RMS* surface roughness (nm)	Ambient air/DI water contact angle (°)**	
				Advancing	Receding
natural calcite	(no treatment)	Hydrophilic	79	0	0
Artificially tailored Oil- wet calcite	0.01M stearic acid	Hydrophobic	75	119	111
Nanoparticle- treated natural calcite	silica nanofluid	Hydrophilic	204	0	0
Nanoparticle- treated oil-wet calcite	silica nanofluid after modification with 1M stearic acid	Hydrophilic	838	18	15

## 8.2.2 Contact angle measurements

CO<sub>2</sub>-wettability was measured directly by contact angle measurements using a tilted plate goniometric setup (Lander et al. 1993). The detailed experimental setup is described elsewhere (Arif et al. 2016c). The samples were first blown with pure nitrogen to remove any loose calcite, followed by washing with equilibrated DI-water and rinsing with toluene to remove any organic and inorganic contaminants. Subsequently, the samples were dried for 60 min at 100 °C and then exposed to air plasma for 5 min to further remove residual organic contaminants (removal of these organic contaminants is crucial otherwise the measurements will be highly biased (Love et al. 2005, Iglauer et al. 2014)). The nanoparticle-treated samples, however, were cleaned with DI-water to remove any reversibly adsorbed nanoparticle from the surface and then dried with ultra-pure nitrogen gas.

The clean samples were then placed inside the pressure cell on the tilted plate and the cell was set to the desired temperature (23, 40, 50, and 70 °C). Subsequently, the CO<sub>2</sub> pressure in the cell was raised to desired measurement values (0.1 MPa, 5 MPa, 10 MPa, 15 MPa and 20 MPa). Fluids used (CO<sub>2</sub>, and water pre-equilibrated with calcite) were thermodynamically equilibrated using an equilibrium reactor (Parr 4848 reactor, John Morris Scientific) according to the procedure described by El-Maghraby et al. (2012).

A droplet of de-gassed liquid (DI water or brine) with an average volume of 6 μL (± 1 μL) was then dispensed onto the substrate via a needle. Subsequently, advancing ( $\theta_a$ ) and receding ( $\theta_r$ ) water contact angles were measured simultaneously (Lander et al.

1993, Al-Anssari et al. 2016) at the leading and trailing edge of the droplet, exactly before the droplet started to move. A high-resolution video camera (Basler scA 640–70 fm, pixel size = 7.4  $\mu\text{m}$ ; frame rate = 71 fps; Fujinon CCTV lens: HF35HA-1B; 1:1.6/35 mm) was used to record movies of these processes, and  $\theta_a$  and  $\theta_r$  were measured on images extracted from the movie files (Nwidee et al. 2016b). The standard deviation of the measurements was  $\pm 3^\circ$  based on replicated measurements.

### 8.3 Results and Discussion

#### 8.3.1 Effect of nanoparticle-treatment on wettability as a function of pressure

We investigate the influence of CO<sub>2</sub> pressure on  $\theta_a$  and  $\theta_r$  for four calcite surfaces, i) pure (natural) calcite, ii) oil-wet calcite, iii) pure nanoparticle-treated calcite, and iv) oil-wet nanoparticle-treated calcite. A broad pressure range was tested to account for the pressure variation with injection depth (Dake 1978).

Both,  $\theta_a$  and  $\theta_r$ , increased with pressure for all surfaces (Figure 8-2). While natural calcite was strongly water-wet at ambient conditions ( $\theta_a \approx 0^\circ$ ) it turned weakly water-wet ( $\theta_a = 60^\circ$ ) at 20 MPa and 50°C. Such an increase in contact angle is also evident from previous work on carbonate rock (Yang et al. 2007, Broseta et al. 2012), and calcite (Bikkina 2011) samples and consistent with published contact angle data on other geological materials such as quartz (Saraji et al. 2014, Shojai Kaveh et al. 2014, Al-Yaseri et al. 2016), and mica (Arif et al. 2016a) minerals; and coal (Arif et al. 2016c) and inorganic shales (Iglauer et al. 2015b, Shojai Kaveh et al. 2016). The reason for the increased  $\theta$  is an increase in CO<sub>2</sub>-calcite intermolecular interactions, which significantly increase with increasing CO<sub>2</sub> density (and thus with increasing pressure, Iglauer et al., 2012; Al-Yaseri et al., 2016; Arif et al., 2016b). The result implies that structural and residual trapping capacities are significantly reduced at reservoir conditions, (e.g. Krevor et al. (2012), Chaudhary et al. (2013), Iglauer et al. (2015b), Iglauer et al. (2015c), Al-Menhali et al. (2016), Rahman et al. (2016)). Moreover, the oil-wet calcite was weakly CO<sub>2</sub>-wet even at ambient conditions ( $\theta_a = 115^\circ$  at 0.1 MPa and 50°C); and it turned strongly CO<sub>2</sub>-wet at storage conditions ( $\theta_a = 148^\circ$  at 20 MPa and 50°C). These results are consistent with Yang et al. (2008) who identified CO<sub>2</sub>-wet conditions for oil-wet carbonates at storage conditions and with additional literature data for various other oil-wet surfaces (e.g. Dickson et al. (2006), Siemons et al. (2006), Espinoza and Santamarina (2010), Shojai Kaveh et al. (2014), Arif et al. (2016d)). Importantly, such high  $\theta$  values imply that an upwards directed suction force is created, which dramatically increases the probability of CO<sub>2</sub> leakage, i.e. project failure. It is thus highly desirable to identify methods which can lower  $\theta$  to  $< 50^\circ$ , i.e. into a strongly water-wet state.

We thus tested the efficiency of nanoparticle-treatment, and we indeed found a massive reduction in  $\theta$  for the nano-treated calcite surfaces. Specifically, at 15 MPa and 50°C, weakly water-wet natural calcite ( $\theta_a = 56^\circ$ ) turned into strongly water-wet calcite after treatment with nanoparticles ( $\theta_a = 32^\circ$ ), and at the same conditions, the

oil-wet calcite (which was strongly CO<sub>2</sub>-wet;  $\theta_a = 147^\circ$ ) turned strongly water-wet ( $\theta_a = 41^\circ$ ), indicating a complete wettability reversal. Note that; the pure, and oil-wet calcite samples were treated with the base fluid (490 mg.L<sup>-1</sup> SDS in 2 wt% NaCl brine, 0 wt% nanoparticles) before  $\theta$  measurements. Thus the difference in  $\theta$  after nanoparticle-treatment are totally related to the impact of nanoparticles rather than the very small concentration (0.2 CMC) of SDS in the base fluid.

We conclude that nanofluid treatment is very efficient in terms of rendering CO<sub>2</sub>-wet surfaces strongly water-wet; and we propose to prime oil-wet reservoirs with nanofluids to improve storage capacities and containment security.

Mechanistically, the wettability alteration is attributed to the formation of mono- and multilayers of hydrophilic silica clusters, which strongly adhere to the calcite surface (as evidenced by SEM imaging; Figure 8-3) (Nikolov et al. 2010, Winkler et al. 2011, Al-Ansari et al. 2016, Zhang et al. 2016, Nwidae et al. 2016b). This nanoparticle-rock adhesion is caused by electrostatic interactions between the negatively charged silica nanoparticles and the positively charged calcium ions in the calcite surface (Wolthers et al. 2008, Ma et al. 2013, Zhang et al. 2015); thus, once injected, nanoparticles will permanently shift the wettability towards a water-wet state.

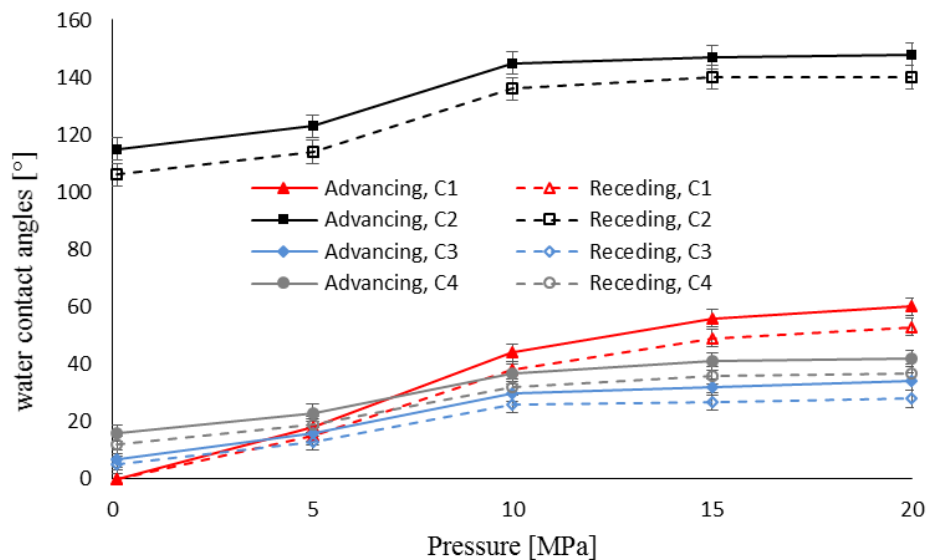


Figure 8-2 Water advancing and receding contact angles measured on natural calcite (C1), oil-wet calcite (C2), and nanoparticle-treated natural (C3) and oil-wet (C4) calcite as a function of pressure at 50°C for CO<sub>2</sub>/DI-water system.

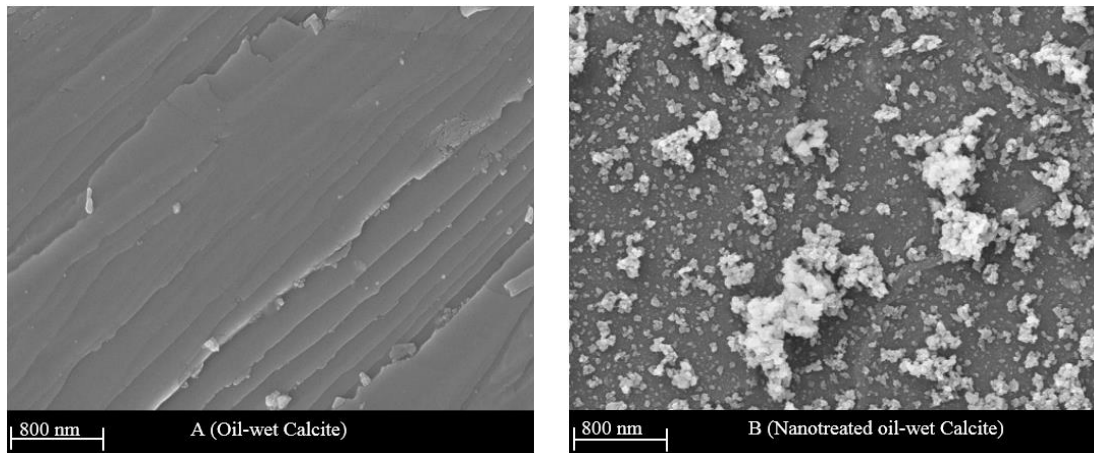


Figure 8-3 SEM images of A) oil-wet calcite and B) nanoparticle-treated oil-wet calcite; the silica nano-clusters are shown in white.

### 8.3.2 Effect of temperature and salinity

We furthermore investigated the effects of temperature and salinity as these variables are also expected to vary considerably even within the same storage formation (Tiab and Donaldson 2011, Krevor et al. 2016). We found that  $\theta$  (at a constant pressure of 15 MPa) decreased with temperature (Figure 8-4) and increased with salinity (Figure 8-5). These effects were strongest for oil-wet calcite.

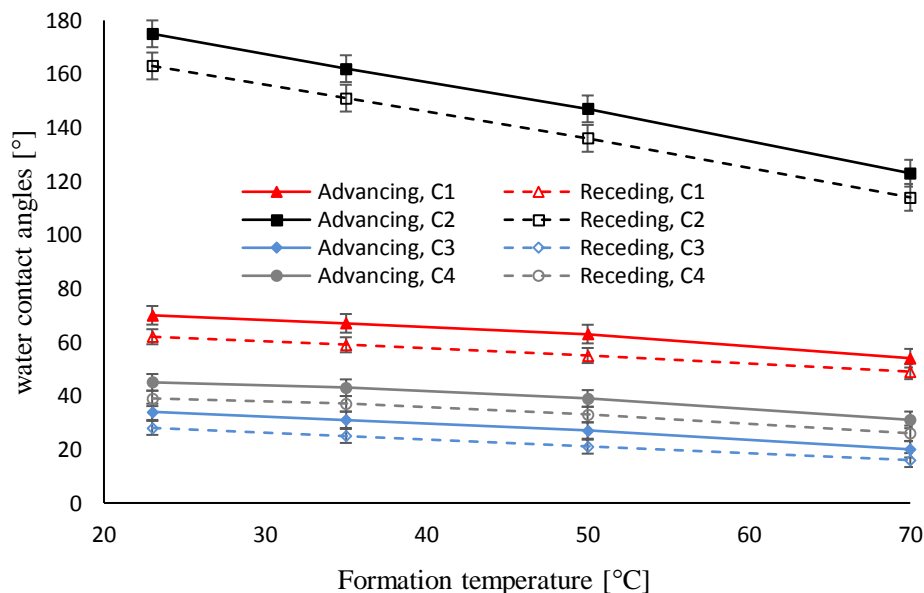


Figure 8-4 Water advancing and receding contact angles measured on natural calcite (C1), oil-wet calcite (C2), and nano-treated natural (C3) and oil-wet (C4) calcite surfaces as a function of temperature at 15 MPa for CO<sub>2</sub>/DI water systems.

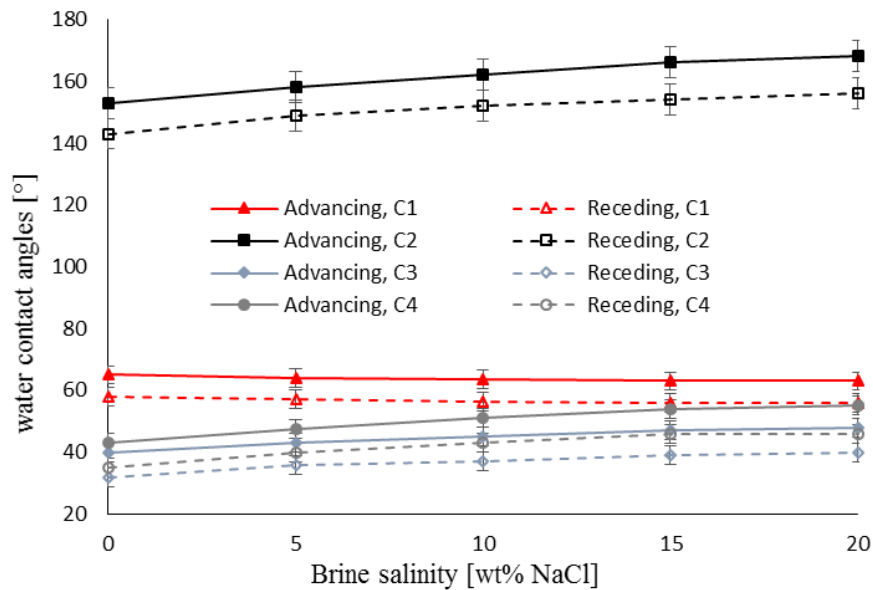


Figure 8-5 Water advancing and receding contact angles measured on natural calcite (C1), oil-wet calcite (C2), and nanoparticle-treated natural (C3) and oil-wet (C4) calcite surfaces as a function of salinity at 50°C and 15 MPa.

This is consistent with literature data, where an increase in contact angle with increasing salinity (Broseta et al. 2012, Al-Yaseri et al. 2016, Roshan et al. 2016) and decreasing temperature (Yang et al. 2007, Broseta et al. 2012, Arif et al. 2016a) was reported. In all cases tested, nanoparticle-treatment was effective over a wide range of salinities and temperatures, and in all cases rendered the CO<sub>2</sub>-wet surfaces strongly water-wet.

## 8.4 Implications

The measured wettability data demonstrate that oil-wet formations are CO<sub>2</sub>-wet at typical storage conditions indicating a direct negative impact on structural ( $\theta > 90^\circ$  potentially leads to leakage, and  $\theta > 0^\circ$  leads to reduced storage heights; Iglauer et al. (2015b)) and residual trapping capacities, and associated overall significantly increased risk of project failure. We note that in this work calcite is considered as a representative of caprock as well as storage rock. Both, structural and residual trapping are strongly influenced by the rock wettability (Iglauer et al. 2015b, Iglauer et al. 2015c, Krevor et al. 2015, Al-Menhali et al. 2016, Arif et al. 2016b, Rahman et al. 2016, Arif et al. 2017); and both (structural and residual) trapping capacities are significantly higher when calcite is water-wet (Arif et al. 2016d, Arif et al. 2017). Thus, the proposed nano-fluid priming dramatically improves storage efficiency, which is attributed to a complete wettability reversal from strongly CO<sub>2</sub>-wet to strongly water-wet. Essentially, with nanoparticle-treatment, structural and residual storage capacities are considerably higher due to strongly reduced  $\theta$ . Consequently, nanoparticle injection as a part of a CO<sub>2</sub> geo-storage scheme can significantly de-risk storage

projects and thus have a positive impact on mitigating anthropogenic greenhouse gas emissions.

## 8.5 Conclusions

We demonstrated that oil-wet rock surface are strongly CO<sub>2</sub>-wet at storage conditions, and this imposes a serious risk for CO<sub>2</sub> storage in oil reservoirs, which are typically oil-wet (Gupta and Mohanty 2010). We thus proposed the application of nanofluids for enhancing CO<sub>2</sub> geo-storage potentials, and evaluated their wettability alteration efficiency as a function of pressure, temperature and salinity, which are expected to vary widely in storage formations (Krevor et al. 2016). The nanofluid was very efficient and rendered strongly CO<sub>2</sub>-wet calcite ( $\theta_a = 148^\circ$  at 20 MPa and 50°C) strongly water-wet ( $\theta_a = 41^\circ$ ); and even natural calcite, which was weakly water-wet ( $\theta_a = 60^\circ$  at 20 MPa and 50°C) turned strongly water-wet ( $\theta_a = 34^\circ$ ) after nano-treatment.

We conclude that nanoparticle-treatment can significantly improve structural and residual trapping capacities and de-risk containment security, particularly in oil-wet formations.

### **Abstract**

Nanofluids (i.e. nanoparticles dispersed in a fluid) have tremendous potential in a broad range of applications, including pharmacy, medicine, water treatment, soil decontamination, or oil recovery and CO<sub>2</sub> geo-sequestration. In these applications nanofluid stability plays a key role, and typically robust stability is required. However, the fluids in these applications are saline, and no stability data is available for such salt-containing fluids. We thus measured and quantified nanofluid stability for a wide range of nanofluid formulations, as a function of salinity, nanoparticle content and various additives, and we investigated how this stability can be improved. Zeta sizer and dynamic light scattering (DLS) principles were used to investigate zeta potential and particle size distribution of nanoparticle-surfactant formulations. Also scanning electron microscopy was used to examine the physicochemical aspects of the suspension.

We found that the salt drastically reduced nanofluid stability (because of the screening effect on the repulsive forces between the nanoparticles), while addition of anionic surfactant improved stability. Cationic surfactants again deteriorated stability. Mechanisms for the different behaviour of the different formulations were identified and are discussed here.

We thus conclude that for achieving maximum nanofluid stability, anionic surfactant should be added.

**Keywords:** Silica, nanoparticle, surfactant, cationic, anionic, stability, zeta potential.

### **9.1 Introduction**

Nanoparticles (NPs) have been widely investigated for many scientific and industrial applications, spanning from drug delivery (Tong et al. 2012), medicine (Baeckkyoung et al. 2015, Lohse and Murphy 2012), polymer composites (ShamsiJazeyi et al. 2014), lubrication (Lu et al. 2014), and metal ion removal (Wang et al. 2012) to carbon geosequestration (Al-Anssari et al. 2017b) and enhanced oil recovery (Al-Anssari et al. 2016, Nwidee et al. 2016a, Al-Anssari et al. 2017e, Al-Anssari et al. 2017f). Typically, thermodynamic properties of the base fluids are significantly modified by the suspended nanoparticles; thus specific and attractive properties can be tailored, including viscosity, rheology (Lu et al. 2014), thermal conductivity (Chakraborty and Padhy 2008, Branson et al. 2013) and interfacial tension (Wu et al. 2013a).

The successful application of NPs in saline environments (e.g. subsurface operations) requires dispersible, stable, inexpensive and injectable nano-suspensions to facilitate a uniform transport and migration of nanofluids in porous medium. However, in subsurface formations, many factors including temperature, pressure, heterogeneity,

and complexity of reservoirs can dramatically impact the effectiveness of nanofluids. Increased temperature, for example, increases the kinetic energy of nanoparticles and consequently the collision rate between nanoparticles and eventually reducing nanofluid stability (Liu et al. 2013b). Another important pertinent challenge is the nanofluid stability is saline brine. It is well established that the brine salinity in subsurface formations and deep saline aquifers varies significantly and can reach very high levels (Dake 1978, Krevor et al. 2016). Under such saline environments, electrolytes (e.g. NaCl) can dramatically reduce the repulsive forces between NPs and consequently accelerate particles flocculation and coagulation due to the increased rate of collision and coalescences of NPs in the suspension (El-Sayed et al. 2012) leading to phase separation. In addition, it is known that the dispersion and stability of NPs in the base fluid can be improved by adding surface active agents such as surfactants (Ahualli et al. 2011, Al-Anssari et al. 2017e), polymers (ShamsiJazeyi et al. 2014), or surfactant-polymer combination (Sharma et al. 2015b) to the base fluid to adjust their properties for a specific application through the formation of surfactant coated nanoparticles.

A number of studies investigated the adsorption of surfactants onto NPs that were dispersed in DI water or dilute brine using contact angle measurements, adsorption isotherms of surfactant on nanoparticles, zeta potential measurements and dispersion stability in terms of nanoparticles and surfactant concentrations (Binks et al. 2008, Cui et al. 2010a, Limage et al. 2010, Ahualli et al. 2011, Sharma et al. 2015b, Zargartalebi et al. 2015). Despite the published data in the previous studies, there is no reported data about surfactant-nanosuspension dispersibility and stability at high salinity condition which is, nevertheless, very important. Thus in this study, we investigate the ability of anionic and cationic surfactants to disperse and stabilize silica NPs at high salinity conditions by measuring zeta potential and particle size of various nanofluid suspensions as a function of brine salinity (ranging from 0 wt% NaCl – 5 wt% NaCl). Sodium Dodecylsulfate (SDS) and Hexadecyltrimethylammonium Bromide (CTAB) are used as anionic and cationic surfactants respectively. The results demonstrate that anionic surfactants lead to better stability of nanofluids in comparison to cationic surfactants. This work thus leads to recognition of suitable conditions which promote better stability of nanofluids in saline environments which in turn lead to better transport of nanoparticles in porous media.

## **9.2 Experimental methodology**

### **9.2.1 Materials**

SiO<sub>2</sub> nanoparticles (porous spheres,  $\rho = 2.2 - 2.6 \text{ g cm}^{-3}$ ) with a purity of 99 mol% and a primary particle diameter of 5-10 nm were supplied as nano-powder by SIGMA-ALDRICH, Australia. Two surfactants, a) anionic [Sodium Dodecylsulfate, SDS, Sigma-Aldrich,  $\geq 98.5 \text{ mol}\%$ , Mol.wt=  $288.38 \text{ g.mol}^{-1}$ , CMC = 2450 mg/l] and, b) cationic [Hexadecyltrimethylammonium Bromide, CTAB, Sigma-Aldrich,  $\geq 98 \text{ mol}\%$ , Mol.wt=  $364.45 \text{ g.mol}^{-1}$ , CMC = 350 mg/l] were used in this study. These two

surfactants were chosen for their commercial availability and the widely known properties. Binks and Rodrigues (2009) reported that the particular structure of ionic surfactants have no effect on the electrical properties of silica particles and thus the adsorption of mono or di-chain ionic surfactant on silica surface gives similar effects on nanoparticles surface charge.

Deionized (DI) water (Ultrapure from David Gray; conductivity =  $0.02 \text{ mS}\cdot\text{cm}^{-1}$ ) was used to prepare NaCl ( $\geq 99.5 \text{ mol}\%$  purity, from Scharlan) solutions, nanofluids, and surfactant solutions.

### **9.2.2 Nanofluid formulation**

Surfactant coated nanoparticles were prepared by sonicating NPs in surfactants formulation with appropriate ratios. Various 100 mL surfactant solutions with varying surfactant concentrations (0, 245, 735, 980, 1125, 2450, 4900, and 7350 mg/l) and NaCl concentrations (0, 0.1, 0.5, 1.0, 1.5, 2.0, 2.5, 3.0 and 5.0 wt%) were prepared by adding the surfactant powder to brine and mixing with magnetic stirrer for 2 hours (Al-Anssari et al. 2017e). Note that the measured critical micelles concentrations (CMCs) with DI water were 2380 and 355 mg/l for SDS (Atkin et al. 2003, Zargartalebi et al. 2015) and CTAB (Lan et al. 2007), respectively.

Subsequently, various nano-suspensions were prepared by mixing a range of silica dioxide NPs concentrations (0.05 g, 0.10 g, 0.50 g, 1.00 g, 1.25 g, 1.50 g and 2.00 g) with the aqueous phase (brine, DI water or surfactant solution) and sonicating (with a 300 VT Ultrasonic Homogenizer/ BIOLOGICS instrument) for 15 min to homogenize the dispersion (Mahdi Jafari et al. 2006, Petzold et al. 2009, Shen and Resasco 2009, Mondragon et al. 2012). Such homogenisation is crucial for chemical stability as it is required for the zeta potential measurements, otherwise results may be biased (Vinogradov and Jackson 2015). The appearance of the dispersion was photographed at varied times when required to check the phase stability (further information in Supplementary material).

### **9.2.3 Particle size, zeta potential and SEM measurements**

The physicochemical characteristics of NPs were studied using scanning electron microscopy (SEM, Zeiss Neon 40EsB FIBSEM), particles size distribution (PSD), and zeta potential ( $\zeta$ ) measurements. A dynamic light scattering (DLS), Zetasizer Nano ZS (Malvern Instruments, UK), was used to determine particles size distribution and the zeta potential of the nano-suspension. The direct observation is the intensity fluctuation due to the diffusion of particles undergoing Brownian motion by a laser beam (Kaszuba et al. 2008), and this diffusion coefficient is then interpreted to a hydrodynamic diameter. Meanwhile, the surface electric charge can be estimated by zeta potential which is the measurable parameter related to the charge and electrical double layer of a solid surface in aqueous solution (Kirby and Hasselbrink 2004) and

it is totally based on displacement of the charge in the electrical double layer due to a tangential shifting of liquid phase against the solid using external force (Nakamura et al. 2003).

In this study we kept the pH of the suspension at pH = 6.25 for all tested formulations. Three measurements were taken for each test, and the average value was evaluated. The standard deviation of measurements was  $\pm 3$  mV however at relatively high salinity ( $> 1$  wt% NaCl) or around the isoelectric point (IEP), the standard deviation was higher (e.g.  $\pm 6$  mV).

### **9.3 Result and discussion**

Improving the stability of silica nanodispersion at high salinity conditions is a key in subsurface applications. Ionic surfactant can significantly affect the surface charges of NPs and its aggregation process, and in turn the stability of nanofluids. Thus, despite the potential changes in nanofluids compositions upon injection into the treated medium in the particle field, we investigated the influence of cationic and anionic surfactants in an attempt to address the effectiveness of surfactants to improve the nanofluids stability in a saline environment.

#### **9.3.1 Characterization of SiO<sub>2</sub> nanoparticles**

Silica nanoparticles can get dispersed in DI water owing to their inherent hydrophilicity. SiO<sub>2</sub> nanoparticles have a porous, spherical structure. However, the scanning electron microscopy (SEM) image of a dried aqueous dispersion of NPs (0.1 wt% SiO<sub>2</sub> dispersed in DI water) depict the non-spherical nature of NPs due to the formation of aggregates from primary particles (Figure 9-1). Further, size distribution measurements of the same nanofluid using dynamic light scattering (Figure 9-2) confirms the formation of these aggregates since the average particle diameter was 84 nm with a considerable ratio of significantly bigger aggregates  $\approx 0.75$   $\mu\text{m}$ .

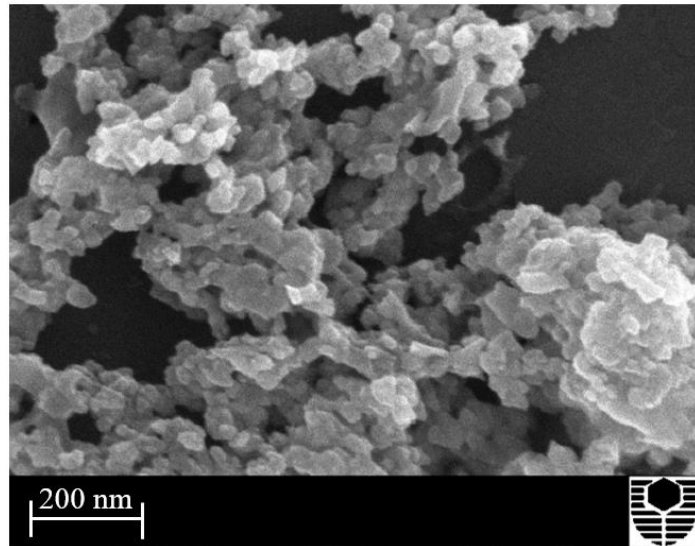


Figure 9-1 SEM profile of SiO<sub>2</sub> nanoparticles, ultrasonically dispersed in DI water, after drying.

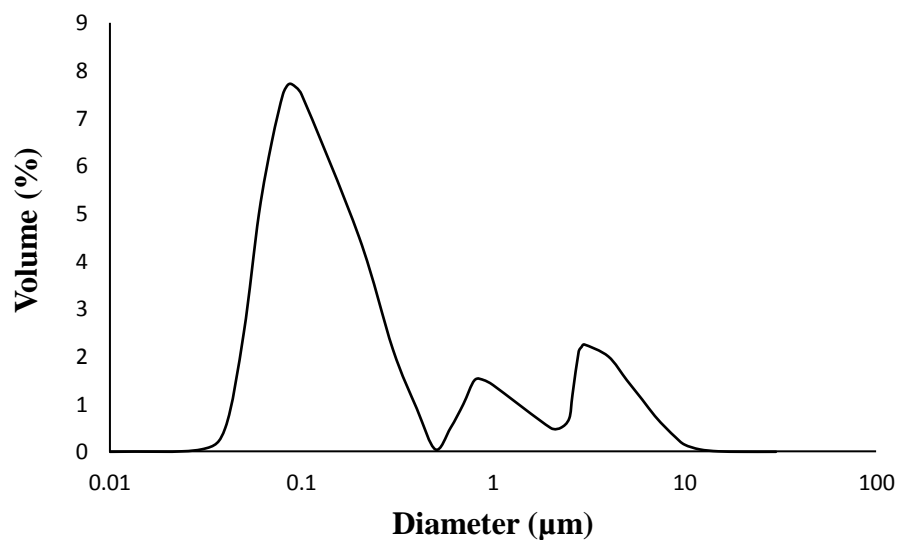


Figure 9-2 Size distribution of 0.1 wt% SiO<sub>2</sub> NPs ultrasonically dispersed in DI water (pH= 6.2) measured by dynamic light scattering (DLS) at ambient conditions.

Although, the efficient sonication process, both SEM image and size distribution measurements revealed the instability and the potential aggregation of silica NPs in DI water, yet the repulsive force between similarly charged NPs, the Brownian motion causes particles collision (Metin et al. 2011) and more collisions increase the possibility of NPs to stick with each other and forms small aggregates. Further, the dispersion condition are potentially more severe at higher NP load and in the presence of electrolyte.

### 9.3.2 Zeta potential as a function of salinity

Salts including NaCl can destabilize particle dispersions by compressing the electrical double layer and screening the electrostatic repulsion force among NPs. Moreover, NP concentration (wt% NP) can impact the stability of the colloid due to the increase in particles number per unit area which increase the collision rate between particles and thus the possibility of aggregates formation. As a consequence, it is essential to investigate the effect of suspension composition on the zeta potential of the nanofluid which is a stability scale for the colloid.

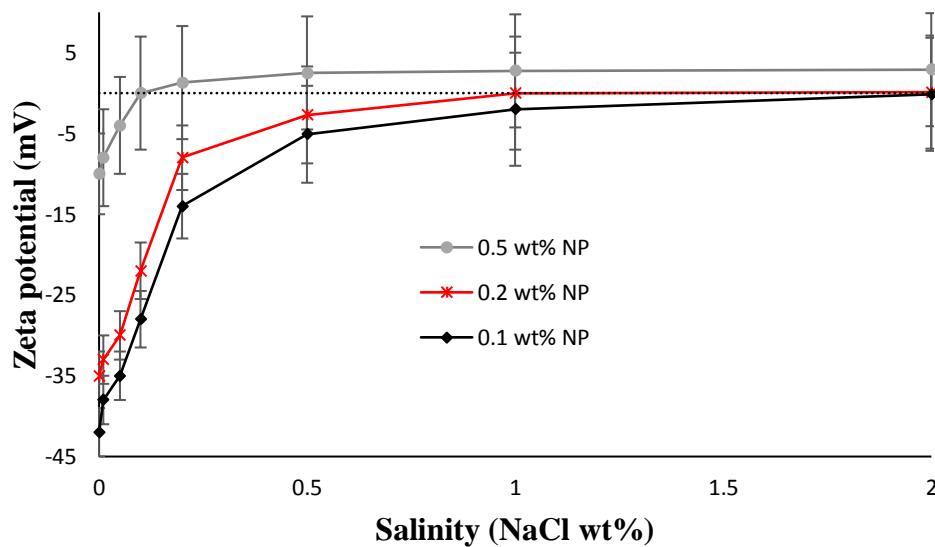


Figure 9-3 Zeta potential of SiO<sub>2</sub> NP dispersion as function of base fluid salinity and NP concentration (at 23°C and a constant pH = 6.25).

Our results of zeta potential measurements (Figure 9-3) demonstrated that both salt and NP concentrations had significant impact on zeta potential of nanofluids. A dramatic shift in zeta potential towards zero was observed with salinity increase for all NP loads (e.g.  $\xi$  was changed from -35 mV to -8 mV when the salinity of 0.2 wt% NP dispersion increased from 0 wt% NaCl to 0.2 wt% NaCl). This is principally important since nanosuspension can only be stable when  $|\pm\xi| \geq 30$  mV (Mondragon et al. 2012, Al-Anssari et al. 2017f). Further, the inversion of surface charge (from negative to positive) was recorded for the 0.5 wt% NP fluid as NaCl concentration increased ( $\geq 0.1$  wt% NaCl) due to the screening of surface charges of particles. These observations are consistent with the reported data at lower salt and nanoparticle concentrations (Tantra et al. 2010, Li and Cathles 2014).

Mechanistically, the increase of NP concentration increases the number of particles per unit area leading to the formation of agglomerates due to the increase in collisions rate between particles which forms a charge depletion region on particles surface (Tsai et al. 2005) and consequently support the formation of aggregates.

### 9.3.3 Surface activation of SiO<sub>2</sub> NPs by cationic surfactant

The CTAB surfactant was used to study the effect of cationic surfactant on the stability of oppositely charged hydrophilic silica NPs. Despite the ability of CTAB to invert the negative surface charge of silica NPs to positive, a significant sediment was observed at the bottom side of the samples referring to an accelerated aggregation and sedimentation process in the suspension. The sediment height versus CTAB concentration (Figure 9-4) was used to ascertain suspension instability.

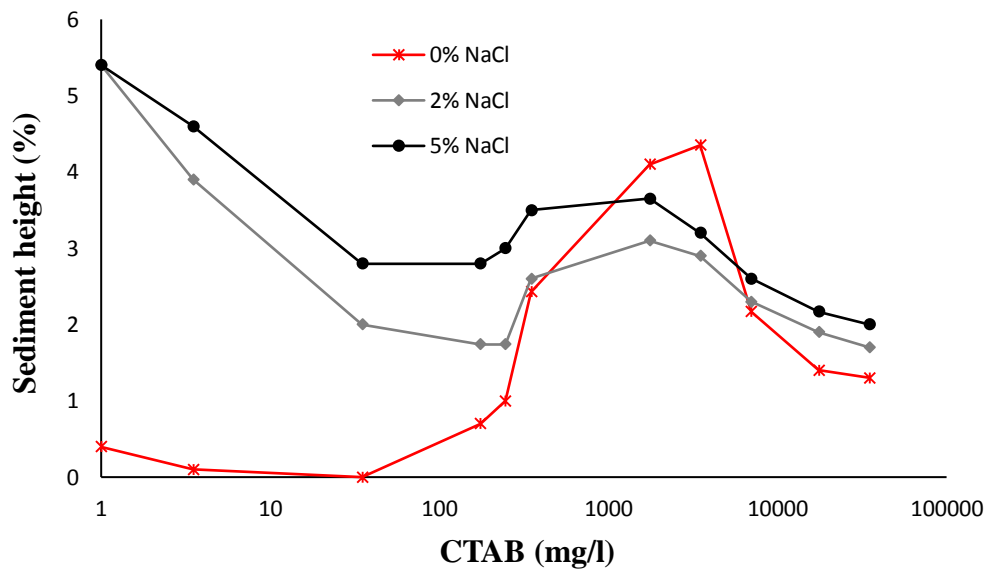


Figure 9-4 Sediment height versus CTAB concentration after 72 h, at different base fluid salinity for 0.1 wt% NP nanofluid at pH=7.

It was found that concentration of cationic surfactant had dramatic impact on aggregation processes of silica NPs at different salinities (Figure 9-4). For nano-suspensions with saline base fluid (2 wt% NaCl and 5 wt% NaCl), a significant sediment height ratios were recorded after 48 h at very low CTAB concentrations ( $\leq 40$  mg/l  $\approx 0.01$  CMC). Mechanistically, salts including NaCl can screen the electrostatic repulsion forces between NPs and thus cause the NPs to stick to each other forming larger aggregates (Bayat et al. 2014b, Bayat et al. 2014a). These aggregates are heavier than NPs and easy to sediment rapidly by gravity. The increase of CTAB concentration (up to 200 mg/l) reduced silica sediment height; however, further increase in cationic surfactant concentration ( $\geq 350$  mg/l, which is equivalent to CMC) leads to an increase and then a decrease in the sediment height when CTAB concentration become  $\geq 1750$  mg/l (5 CMC; Figure 9-4). This fluctuation in sediment height is potentially related to the change in surface charges of NPs and thus particle hydrophobicity as CTAB concentration increases which consequently leads to the formation of rigid network of NPs.

For nano-suspension with DI water base fluid, no sedimentation was recorded at low CTAB concentrations ( $\leq 35$  mg/l  $\approx 0.1$  CMC; Figure 9-4). However, with the absence of surfactant (0 mg/l CTAB), precipitation of slight amount of silica NP was recorded. Mechanistically, the aggregation of silica NPs dispersed in water is controlled by the density of silanol groups (SiOH) at particle surface. As a results, at pH = 6.25, the particle surfaces are appreciably negatively charged owing to dissociation of surface silanol (SiOH) groups (Binks et al. 2007) and the repulsive forces between negatively charged NPs are strong enough to keep these NPs separated from each other.

#### **9.3.4 Interaction between NPs surface and cationic surfactant**

The adsorption of single chain cationic surfactant (CTAB) molecules on the hydrophilic silica NP can invert the surface charge form the initial negative to neutral and then positive values. Further, the positivity increases with cationic surfactant concentration (Figure 9-5). This transition of surface charge explains the change in sedimentation height which refers to the interaction between NPs (Figure 9-4). Typically, the highest sedimentation height represents the condition of neutral charge when zeta potential is close to the iso-electric point (IEP).

Figure 9-5 proposed that a monolayer of adsorbed CTAB molecules is gradually form on the particle surface due to the electrostatic attraction between the positive head groups and the negative particle surface which neutralises the negative charges of the (SiO<sup>-</sup>) groups. Most of silica particles at this initial stage of cation adsorption are uncharged and thus remain relatively hydrophobic. Further increase in cation concentration forms a second layer of surfactant owing to the hydrophobic attraction between chains of adsorbed surfactant molecules in the monolayer and free monomers. The formation of the second layer produces totally positively charged nanoparticles owing to the coating with bilayer of cationic surfactant. Mechanistically, the positively charged CTAB groups adsorb on the negatively charged silica surface, thus neutralizing and subsequently positively charging the silica surface (Cui et al. 2010b, Liu et al. 2013a).

Overall, the cationic surfactant demonstrated a potential ability to destabilize silica nanofluid particularly with the presence of electrolyte (Figure 9-4 and Figure 9-5).

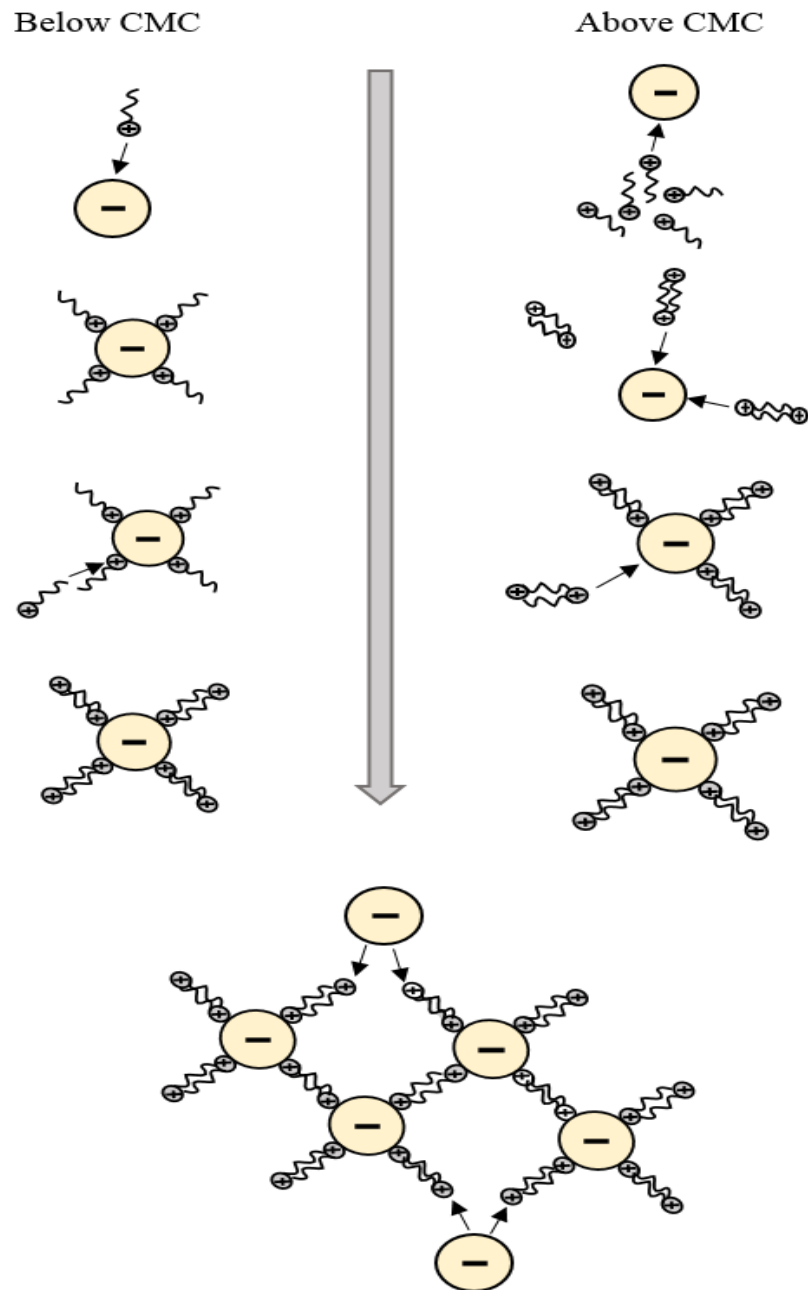


Figure 9-5 Mechanisms of cationic molecules adsorption with surfactant concentration before and after reaching the critical micelles concentration (CMC).

### 9.3.5 Surface activation of SiO<sub>2</sub> NPs by anionic surfactant

The SDS surfactant was used to study the effect of anionic surfactant on the stability of similarly charged hydrophilic silica NPs. Although previous studies reported that the addition of SDS to the nanofluid can supercharge the surface of silica particles leading to stronger negative charge and thus higher repulsive forces between NPs (Ahualli et al. 2011), our results demonstrated different agglomeration and sedimentation scenarios particularly with increased SDS and salt concentrations (Figure 9-6).

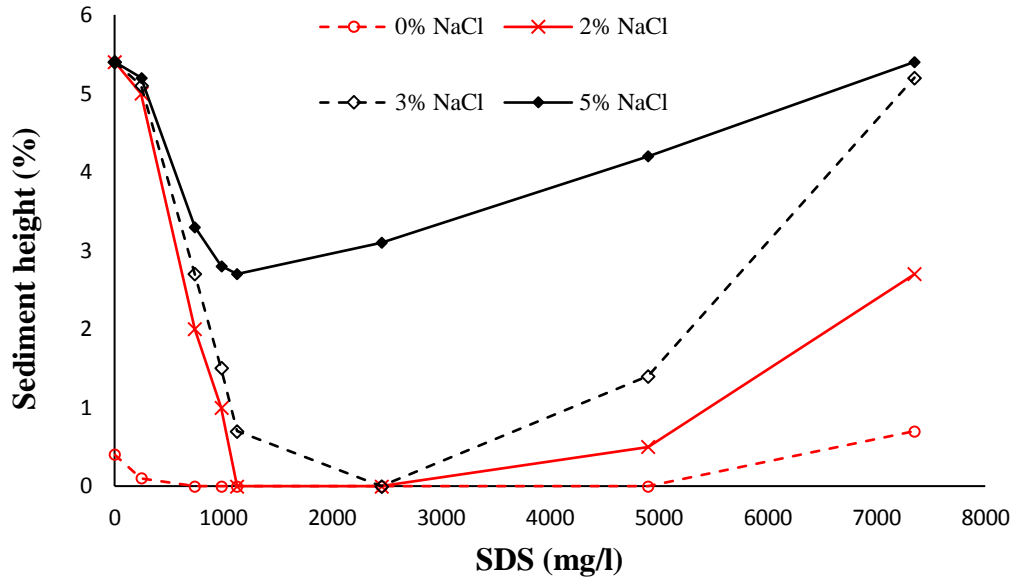


Figure 9-6 Sediment height versus SDS concentration after 72 h, at different base fluid salinity for 0.2 wt% NP nanofluid at pH=7.

Figure 9-6 provides the sedimentation trend of silica NPs at different base fluid composition. It is interesting to note that using appropriate concentration of SDS surfactant ( $\approx 2450$  mg/l, 1 CMC) in the base fluid can stabilize silica NPs even at relatively high salinity ( $\approx 3$  wt% NaCl). However, higher SDS concentration can lead to dramatic increase in particles precipitation referring to unstable nano-suspension. Also it is important to mention that even with the absence of electrolyte (DI water), there was a slight precipitation process of silica NPs with 0 mg/l SDS.

### 9.3.6 Interaction between NPs surface and anionic surfactant

It is of key importance to understand the role and behaviour of anionic surfactant monomers on NP surface before analysing the zeta potential as a function of brine and SDS concentrations.

Figure 9-7 suggests the potential behaviour of surfactant monomers at different concentrations. Typically, owing to the high surface area of NP, SDS monomers can be attached to NPs surface by the tail group since the head group of surfactant and the nanoparticles have the similar charge. The number of attached monomers increase with SDS concentration leading to supercharged nanoparticles which drastically increase the repulsive force between these negatively supercharged NPs (Ahualli et al. 2011). However, further increase in SDS concentration ( $\geq$  CMC) increases the number of monomers per unit area and leads to the generation of micelles (Iglesias et al. 2011). In this case, it is easy for surfactant monomers to join up together via the hydrophilic tail group instead of being adsorbed to a similarly charged NP. These strongly charged micelles have the ability to repel the negative NPs and forcing them to flocculate

gradually (Figure 9-7) after the creation of depleted zone around each of them (Tadros 2006).

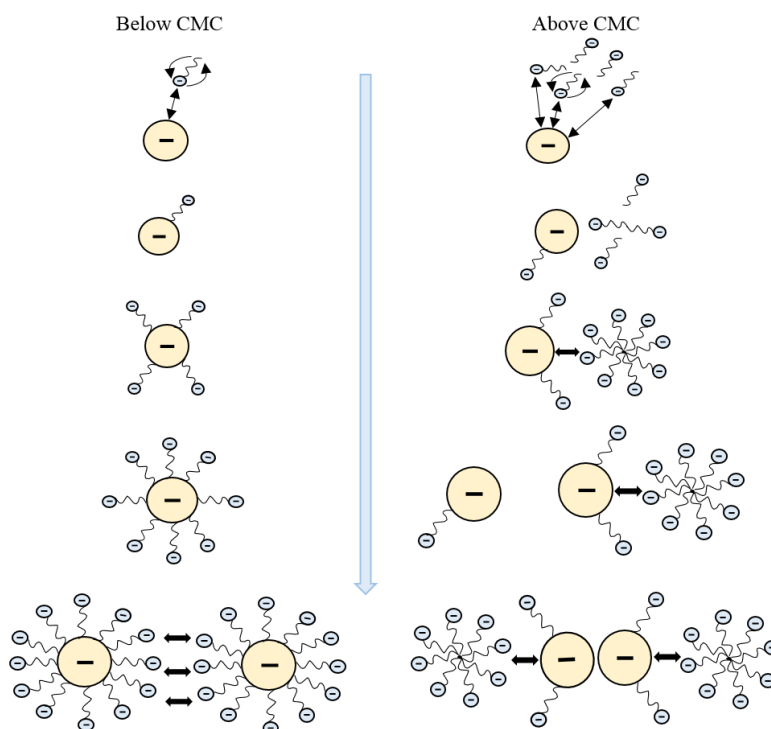


Figure 9-7 Mechanisms of anionic molecules adsorption with surfactant concentration before and after reaching the critical micelles concentration (CMC).

### 9.3.7 Zeta potential of SDS surfactant-brine-NPs formulation

Zeta potential of NP/brine/surfactant system at different salinities and surfactant concentration was measured at 298 K and constant NPs load (0.1 wt%) and acidity of the suspensions (pH = 6.25).

Figure 9-8 depict that at pH = 6.25, and SDS concentration = 0 mg/l, the zeta potential of silica NPs/DI water system was around  $-35 \pm 3$  mV which corresponds to a stable nano-suspension even with the absence of surfactant. The stability of such suspension is attributed to the efficient repulsive forces between NPs, consistent with Mondragon et al. (2012). However, it is found that zeta potential of the NP/DI-water/surfactant system first decreased (more negativity) with the increase in SDS concentration (up to SDS concentration  $\approx 2500$ mg/l) and afterwards, zeta potential of the system again increased with SDS concentration. For instance,  $\zeta$  decreased to -43 mV when SDS concentration was 2450 mg/l then increased gradually with SDS concentration to -28 mV at 7350 mg/l, SDS

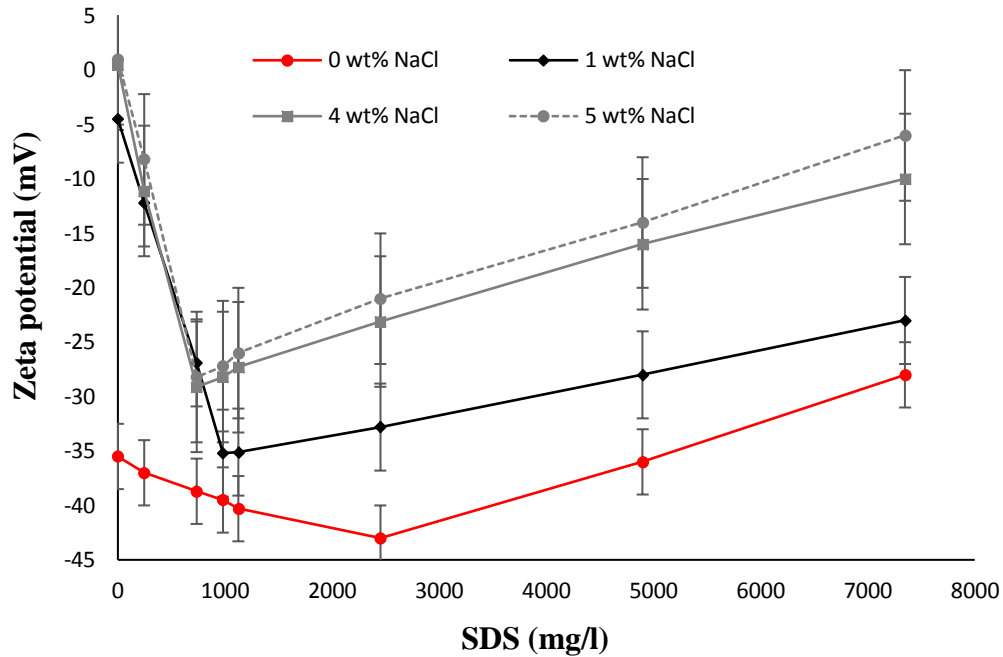


Figure 9-8 Effect of electrolyte, and surfactant (SDS) concentration on zeta potential of NPs /brine/surfactant system (0.1wt% SiO<sub>2</sub> at pH= 6.25).

Different minimum points were recorded depending on the salinity of the base fluid. The dependence of the minimum zeta potential on electrolyte concentration of the nanofluid is related to the effect of salt concentration on CMC value of surfactant (Al-Anssari et al. 2017e). Thus, the increase in surfactant concentration higher than CMC decreases the effect of such anionic surfactant on nanofluid stability.

### 9.3.8 Particle size distribution of surface treated NPs

The potential of SDS surfactant to limit NPs aggregation was tested via particle size distribution. To accomplish this, we formulated a nano-suspension with 0.1 wt% SiO<sub>2</sub> NPs dispersed in a base fluid of 1 wt% NaCl with two different surfactant concentrations (980 mg/l and 4900 mg/l of SDS dissolved in 1 wt% NaCl). The particle size was measured using a Zetasizer Nano ZS (Malvern Instruments, UK).

It is clear from Figure 9-9 that the addition of a particular amount of anionic surfactant (e.g. 0.4 CMC; 980 mg/l, Figure 9-9) prevents the rapid growth of NPs size and narrows the particle size distribution. This trend is attributed to the formation of a monolayer of surfactant monomers on the particle surface which increases the repulsive force between particles and thus increase the degree of dispersity (see Figure 9-7). In contrast, using high concentration of anionic surfactant (2 CMC; 4900 mg/l) decreases the dispersity of nanofluid leading to the formation of large aggregates.

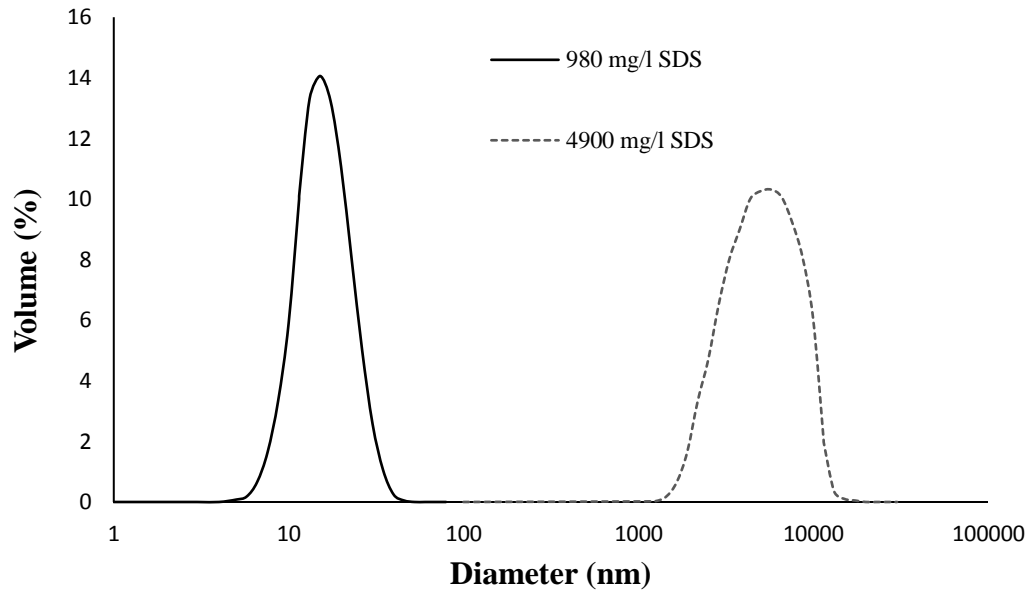


Figure 9-9 Compression of particle size distribution of NPs (0.1 wt%) with different surfactant concentrations (980 mg/l and 4900 mg/l of SDS) in the same base fluid (1 wt% NaCl).

These results confirm the positive effect of low concentration surfactant on zeta potential (Figure 9-8) and the effect of NP and NaCl concentrations on CMC of surfactant in the base fluid (Al-Anssari et al. 2017e). This is consistent with ShamsiJazeyi et al. (2014) who revealed the sensitivity of nano-dispersions (with DI water) stability to anionic surfactant concentration.

#### 9.4 Conclusions

The use of nanotechnology in many industries particularly subsurface applications is currently an active area of investigation (Al-Anssari et al. 2016, Zhang et al. 2016, Nwidae et al. 2017a, Al-Anssari et al. 2017f). Stability of nanofluid formulations is the key for the success of nanofluid application in high salinity environments (Sharma et al. 2015b, Al-Anssari et al. 2017b). In this study, the influence of anionic and cationic surfactants on the dispersion stability of saline silica nanofluids was investigated. However, we point out that the results of this study provide a basic framework of optimum surfactant concentration. But, in some practical field applications (e.g. soil decontamination, drilling, carbon geostorage, and enhanced oil recovery), other factors (e.g. temperature, rock type, rock mineralogy, adsorption of surfactant on rock surface) must be taken into account before decision making. Prior to sedimentation measurements, the zeta potentials for different silica nanoparticle (NP)-brine-surfactant formulations were measured. Clearly both cationic (CTAB) and anionic (SDS) surfactants had a significant influence on nanofluid stability due to their

effect on NP surface charges. Anionic surfactant (SDS), at concentrations below the critical micelles concentration (CMC), stabilized the nanofluid even at high salinity (5 wt% NaCl) which is explained by the increase in zeta potentials consistent with literature (Iglesias et al. 2011). In contrast, cationic surfactants (CTAB) accelerated nanoparticle agglomeration at all salinities. Two different mechanisms were highlighted to explain the behavior of cationic and anionic surfactant on the hydrophilic surface of NPs based on charges of hydrophilic silica nanoparticles and the head group of the cationic and anionic surfactant. We thus conclude that addition of low concentrations of anionic surfactants strongly enhances nanofluid stability and enables nanofluid application in saline environments.

## Chapter 10 Overall Discussion

This study aimed to assess the implementation of nanotechnology—particularly SiO<sub>2</sub> nanoparticles—in chemical enhanced oil recovery (CEOR), and carbon capture and storage (CCS). As mentioned in the literature review (Chapter 2), altering the wettability of naturally fractured oil-wet carbonate formations to a water-wet state, as well as reducing the interfacial tension (IFT) of oil/aqueous phase systems are key issues for incremental oil recovery. What is more, the oil-wet status of rock has a dramatically negative impact on both residual and structural trapping capacities for carbon geosequestration projects. It is well known that decreased structural and trapping capacities significantly increase the risk of project failure. Consequently, it is vital to render the wettability of oil-wet rocks to water-wet. Several reports have shown that nanofluids—a dispersion of nanoparticles in a base fluid—are potential wettability modifiers. Further, in prior studies it has been noted that nanoparticles alone have no significant effect on oil/water interfacial tension. However, very little has been reported in the literature about the effect of formation salinity on the ability of nanoparticles to render oil-wet surfaces water-wet.

Consequently, the initial objective of this research was to identify the most effective composition of nanofluid with respect to nanoparticle load and salinity. The first question concerned the influence of nanoparticles on the IFT of oil/water systems at high salinity, with and without the presence of surface-active materials. Moreover, the study was also designed to determine the effect of other reservoir conditions, including temperature and pressure, on the nano-treatment of oil-wet surfaces. In reviewing the literature, no data was found on the association between pressure, temperature and salinity on surface treatment with nanofluids. However, a strong relationship between salinity and suspended nanoparticle instability has been reported. Thus, determining whether a stable nanosuspension can be formulated in high salinity conditions was the other key question in this research.

The results of this study confirmed the limited influence of bare nanoparticles on the IFT of oil/water systems. This was related to the hydrophilic nature of nanoparticles, which keeps the majority of particles in the bulk of the water phase away from the interfaces. However, significant effects of nanoparticles on IFT were noticed with the presence of surfactants, particularly similarly charged anionic surfactant (SDS). Another important finding was the impact of nanoparticles on the critical micelles concentration (CMC) of both anionic and, with to a lesser degree, cationic surfactant (CTAB). Adding silica nanoparticles can drastically reduce the CMC of surfactants and, thus, the concentration of surfactant required to achieve the highest reduction of IFT. Moreover, the current study found that increased salinity tends to eliminate the effects of nanoparticles on CMC and IFT reduction. Briefly, the optimal synergistic effects of anionic surfactant and nanoparticles can be achieved at low electrolyte, surfactant and nanoparticle concentrations. Although no synergistic effects were reported at high salinities, high surfactant concentrations and high nanoparticle loads,

all the measured IFT values were equal to or below those measured in the absence of nanoparticles. Accordingly, silica nanoparticles have no negative impact on CEOR processes in terms of IFT reduction, which makes it a promising agent for use in oil recovery industries.

The most interesting finding was the drastic ability of nanofluids to alter the wettability of strongly oil-wet surfaces to a strongly water-wet state, which answers the key question about using nanoparticles in oil production industries. Starting with a very wide range of nanoparticle loads, base fluid salinities, exposure times and particle adsorption reversibility, the results revealed a dramatic reduction in the contact angle of oil-wet calcite samples after treatment with different nanofluids at ambient conditions. Surprisingly, no substantial differences were found in nanofluid density with increased nanoparticle load. Furthermore, EDS, SEM and AFM analyses indicated that silica nanoparticles coated the surfaces of the porous media in a way that was sufficient to change the wetting properties of the rocks. The size of silica nanoparticles, which is ten orders of magnitude smaller than the throats of the pores, enables these fine particles to penetrate deeply into the smallest porous structures. It was also interesting to note that the majority of nanoparticles were adsorbed irreversibly on carbonate surfaces, leading to permanent modification of surface wettability. Another important finding, particularly from the feasibility point of view, was that even dilute nanofluids exhibited the same significant effects with longer exposure periods. These results are consistent with recently published data on the influence of various nanoparticles on different rocks at ambient pressures and temperatures. However, up to this point, the crucial question concerned whether these nanoformulations exhibited similar efficiency at reservoir pressures and temperatures.

All potential scenarios for nanofluid treatment were considered in this study. Both salinity and nanoparticle load can dramatically impact the zeta potential of nanofluids and, thus, particle stability. Very little was found in the literature about these effects. The results of this study indicate that zeta potential and, consequently, nanoparticle stability, decrease with increasing salinity and nanoparticle concentration. Practically, it is impossible to control the salinity of subsurface formations. However, formulating diluted nanofluids with a relatively low concentration of nanoparticles can enhance the stability of nanoparticles in suspension. Nevertheless, nanoparticle aggregation is still an expected scenario after injection of nanofluid into subsurface formations, which can form a larger aggregates compared to the initial nanoparticle size. Surprisingly, within the tested nanoparticle sizes (5–25 nm), initial size had no significant influence on the efficiency of nanoparticles as wettability alteration agents. This confirms that all nanoparticles smaller than 30–50 nm display the same physical and chemical properties. On the key question of the influence of temperature on the nanotreatment process, this study found that surface treatment with nanofluids is more effective at high temperatures (23–70 °C). In the experiments, at higher temperatures, treated surfaces could be exposed to nanofluid for shorter durations to achieve the same change in surface wetness. Mechanistically, the rate of silica nanoparticle adsorption

on carbonate surfaces increases with temperature, leading to faster alteration of wettability. Accordingly, nanoparticles are very promising wettability alteration agents at relatively high temperatures, which makes them strong candidates for application in enhanced oil recovery and carbon storage projects. However, the other vital question concerns the effect of high pressure on the influence of nanoparticles on surface wetness.

With respect to this question, this study found that high pressures (up to 20 MPa), had limited effects on nanoparticle adsorption on treated surfaces. The results revealed that a minor desorption of silica nanoparticles could occur when the nanotreatment was conducted at 20 MPa. Further, nanoparticle adsorption on the treated surfaces was mostly irreversible at all tested temperatures, pressures and salinities. In general, at high pressures and temperatures, the nanofluid concentration and immersion time played crucial roles in improving the efficiency of diluted nanofluids, while salinity was less significant. The proposed nanoparticle treatment can enhance the efficiency oil recovery. This is related to an alteration of wettability from strongly-wet and intermediate-wet to water-wet. Essentially, with nano-treatment, water can spontaneously imbibe into the rock matrix, displacing a huge amount of trapped crude oil into the liquid phase in the porous medium.

Typically, enhanced oil recovery (EOR) processes can be combined with injection of CO<sub>2</sub> gas for incremental hydrocarbon recovery in a process known as *CO<sub>2</sub>-enhanced oil recovery*. In this process, carbon dioxide is injected into the injecting well to fix the pressure of the reservoir and be stored in the subsurface formations. However, the oil-wet nature of depleted reservoirs dramatically reduces the trapping capacities of subsurface formations, which imposes a severe risk to CO<sub>2</sub> storage in oil reservoirs. Therefore, injection of nanofluids prior to CO<sub>2</sub> injection can potentially improve carbon storage via shifting the oil-wet nature of the rocks to water-wet. Despite the vital importance of this application to EOR and carbon storage projects, no data was found in the literature about the influence of nanoparticles and surface wetness on CO<sub>2</sub> storage conditions. The current study found that oil-wet calcite surfaces are CO<sub>2</sub>-wet. These results are consistent with data on oil-wet sandstone and limestone surfaces. The most interesting finding was that nanofluid is very capable of rendering the strongly CO<sub>2</sub>-wet carbonate samples as strongly water-wet. Further, to mimic all the possible scenarios in carbonate reservoirs, which exhibit a diverse range of wetness states, the effect of nanoparticles on the CO<sub>2</sub>-wetness of natural calcite was investigated. Results show that pure calcite was weakly water-wet at high CO<sub>2</sub> pressure conditions. However, priming the surface with nanoparticles efficiently renders the surface wetness as strongly water-wet. This finding raises the possibility of improving structural and residual trapping capacities and lowering risks to containment security. It can thus be suggested that priming of oil-wet and water-wet formations with nanoparticles is useful for low-risk carbon storage projects.

In the oil industry, once primary and secondary oil recovery techniques no longer produce oil economically; enhanced oil recovery (EOR) methods can be utilized to produce 5 – 15% additional oil. While low-cost primary and secondary hydrocarbon

production processes depend upon pressures, costly enhanced oil recovery methods work by altering the properties of the hydrocarbons, formations water, and pore media. One of the suggested EOR techniques is chemical enhanced oil recovery (CEOR). Surfactant flooding is one of the chemical enhanced oil recoveries, which utilizes to reduce the interfacial tension of oil/water system and altering the wettability of oil-wet surface and thus facilitates the displacement of oil from the pores media. However, loss of these expensive chemicals due to adsorption of rock surfaces reduces the feasibility of the process particularly at the time of low oil prices. Any techniques or materials that can act as an alternative to the high-cost surfactant or work synergistically to reduce the loss and the required amount of these surface-active materials can be implemented successfully in EOR techniques. Nanofluids; dispersion of nanoparticles in liquid phase, with their unique and engineered properties may utilize as smart agent in EOR projects.

Despite the promising results reported by this study, the successful implementation of nanofluids in subsurface industries requires the formulation of low-cost and stable nanosuspensions. In these projects, nanosuspension stability plays a key role, and usually, robust stability is essential. Yet, subsurface fluids are briny and no stability data has been reported for such salt-containing fluids. In this study, salt was found to destabilise nanoparticles in suspension. This is mainly related to the screening effect of the salt on the repulsive forces between nanoparticles. Zeta potential measurements demonstrated that increased salinity, particularly at higher nanoparticle loads, shifts the zeta potential toward the isoelectric point (the point of zero surface charge). At this point, the repulsive forces between nanoparticles are zero and an accelerated aggregation process is expected. Characteristically, nanofluids can only be stable when  $|\zeta| \geq 30$  mV. Thus, the addition of surface-active materials such as surfactants is essential for stable nanosuspensions.

Several reports have shown that using an anionic surfactant can enhance the stability of nanofluids; however, only low salt and nanoparticle concentrations were investigated. This study investigated the effect of anionic and cationic surfactants on nanoparticle stability at relatively high salt concentrations. One interesting finding is that choosing the best surfactant depends on the initial surface charge of the nanoparticles. The results indicated a dramatic process of silica nanoparticle aggregation after the addition of cationic surfactant (CTAB) at all salinities. Typically, adsorption of the positive head group of CTAB on the negative surface of the nanoparticles gradually neutralises the surface charge of that particle. Subsequently, adjacent particles will tend to stick to each other under the effect of van der Waals attraction forces. It is possible to hypothesise that cationic surfactant can only be used with initially positively charged nanoparticles and not bare silica. These results suggest that different ionic surfactants should also be tested.

Prior studies have noted the importance of sodium dodecylsulfate (SDS) as an anionic surfactant in the oil industry. In the current study, SDS was used to test the influence of anionic surfactant on silica nanofluid stability. In this context, the most important finding was that using accurate concentrations of anionic surfactants ( $< \text{CMC}$ ) in the

base fluid of initially hydrophilic silica nanoparticles can produce an exceptionally stable nanofluid even at relatively high salinities. Mechanistically, due to the repulsive forces between similarly charged nanoparticle surfaces and the head groups of SDS monomers, the tail groups of SDS monomers attach to the nanoparticle surfaces. This continuous attachment of SDS monomers to the surface of nanoparticles extensively supercharges the particles, leading to very strong repulsive forces between them. Further increases in surfactant concentration, on the other hand, reduces the efficiency of SDS as a stability modifier. In such a case, surfactant monomers will tend to join up together via their tail groups to form micelles, and few or no monomers will reach the surface of nanoparticles. These scenarios were confirmed via zeta potential and particle-size distribution measurements of various surfactant-nanoparticle dispersions at various salinities. The outcomes of this study have demonstrated that bare nanoparticles are not recommended for subsurface industries where salinity can reach very high levels. An exact amount of anionic surfactant should be added to achieve maximum stability in silica nanofluids.

Overall, the proposed nanofluid treatment for EOR and carbon storage projects proved to be feasible under real operating conditions. These findings will encourage the implementation of nanofluid injection in all subsurface projects, including geothermal extraction, soil decontamination, carbon storage and EOR.

## Chapter 11 Conclusions, Recommendations and Perspectives for Future Work

This chapter comprises the conclusions and recommendations of the thesis. The conclusions are drawn from the chapters of this study, while the recommendations outline potential future studies.

### 11.1 Conclusions

Nanofluids—dispersions of nanoparticles in base fluids—have demonstrated superior performance in rendering oil-wet surfaces water-wet for easier displacement of hydrocarbons from porous media. Nanoparticles such as silicon dioxide—solely or in combination with a surfactant—are excellent agents for enhancing oil recovery by altering surface wettability and reducing the interfacial tension of oil/water systems. This thesis reports experimental data on the effects of nanofluid on reducing interfacial tension and altering the wettability of carbonate substrates. Advancing and receding contact angle measurements were made for a range of nanofluid compositions and operational conditions. An extensive series of experiments was conducted to investigate the potential of SiO<sub>2</sub> nanoparticles in reducing interfacial tension and altering the wettability of hydrophobic carbonate reservoirs. Various nanosuspensions were formulated, which contained nanoparticle concentrations of 0.001–4 wt% in DI water, brine, and anionic surfactant base fluids. Moreover, a wide range of operating conditions was investigated (brine salinity: 0–20 wt% NaCl, temperature: 23–70 °C, pressure: 0.1–20 MPa). The influences of nanoparticles on wettability and interfacial tension and, thus, oil displacement mechanisms, were carefully addressed. Further, potential interaction scenarios and the synergistic effects of nanoparticles and surfactant were also analysed. Overall, the results of the study lead to a better understanding of nanofluid behaviour and efficiency in saline media, and nanofluids' effects on surface wettability and, consequently, hydrocarbon production and carbon geo-storage. The major conclusions are briefly discussed below:

#### 1. *Interfacial tension (IFT) of nanofluid/oil systems*

A detailed investigation was conducted to study the synergistic effects of nanoparticles and ionic surfactants as they relate to the interfacial properties of oil-aqueous phase systems. Consequently, the effects of silica nanoparticles on the IFT of decane-water, decane-brine, decane-surfactant-water, and decane-surfactant-brine systems were studied. Generally, reductions in IFT were related to adsorption of surface-active materials at the fluid/fluid interface. Particularly, hydrophilic nanoparticles by themselves probably have no effect on IFT. Their hydrophilic nature traps these fine particles in the fluid bulk away from the interface. On the other hand, all surfactants efficiently reduce IFT until reaching the critical micelle concentration (CMC). The capability of ionic surfactants to

reduce IFT is related to their charged head groups. Subsequently, adsorption of ionic surfactant into the interface forms a charged monolayer at the interface, leading to lower IFT. Typically, the presence of salt in the surfactant solution significantly reduces the IFT. Mechanistically, salt has a strong ability to promote the accumulation of surface-active materials near the interface. Remarkably, the addition of nanoparticles can improve the ability of anionic surfactants to reduce IFT. Therefore, lower values of IFT were measured at an optimum nanoparticle concentration. A decreasing trend of IFT was observed with limited increases in nanoparticle concentration until reaching a minimum. However, an opposite (increasing) IFT trend was recorded with further increases in nanoparticle concentration until reaching a value that was equivalent to the IFT obtained in the absence of nanoparticles (no synergistic effects). This complicated behaviour was observed for both cationic and anionic surfactant formulations in combination with silica nanoparticles, and it was more complex for the cationic surfactant-nanoparticle system due to the opposite charges of nanoparticle surfaces and surfactant head groups. Moreover, the CMC of surfactant was also influenced by nanoparticles, but to a lesser degree than by salt.

Temperature also significantly reduced IFT. High temperatures significantly reduced IFT for all formulations due to its effect on the solubility of decane in water.

Overall, relatively small nanoparticle concentrations can improve the efficiency of diluted surfactant formulations (below the CMC) in reducing IFT. In this case, both nanoparticles and surfactant monomers can migrate to the oil-water interface, leading to synergistic effects in terms of IFT reduction. However, in highly concentrated surfactant formulations, the oil-water interface is dominated by surfactant molecules and no synergistic effects are observed.

## 2. *Chemistry of nanofluids*

Nanofluid stability is a key parameter for the efficient implementation of nanoparticles as wettability alteration agents in subsurface industries. Generally, salts have a screening effect on the repulsive forces between suspended nanoparticles, leading to increased agglomeration. Supercharging the surfaces of nanoparticles with surface-active materials can reduce the effect of salts on nanoparticle behaviour. Both cationic and anionic surfactants have a significant influence on nanoparticle surface charges and, thus, nanofluid stability. Addition of a limited amount of anionic surfactant can increase the absolute value of the zeta potential, leading to stabilised nanosuspensions even at relatively high salinities. Cationic surfactant, in contrast, accelerates nanoparticle agglomeration at all salinities by neutralising the negative surface charges of the nanoparticle. Thus, cationic surfactants are not beneficial for stabilising hydrophilic silica nanoparticles. Consequently, the merging of silica nanoparticles in saline

environments requires the addition of anionic surfactant, which significantly supercharges the negative surfaces of nanoparticles and provides a stable nanoformulation.

### 3. *Wettability of calcite/oil/brine systems:*

Pure calcite was strongly water-wet at ambient conditions. The advancing and receding contact angles were  $0^\circ$  for the calcite/air/brine system. Meanwhile, for the calcite/oil/brine system, advancing and receding contact angles were slightly higher; however, the surface was still strongly water-wet (maximum  $\theta \leq 45^\circ$ ). However, carbonate reservoirs are known to be naturally fractured oil-wet formations. Consequently, prior to the nanotreatment study, pure carbonate samples were modified with chemicals (silane or stearic acid) following a specific procedure to achieve oil-wet surfaces. This modification step was essential to simulate the conditions of solid surfaces inside oil reservoirs. The modified surfaces were intermediate-wet to oil-wet in the air and strongly oil-wet in decane at ambient conditions. However, both advancing and receding contact angles increased with pressure and increased slightly with salinity, but significantly decreased with temperature. Atomic force microscopy (AFM) measurements showed that both pure and oil-wet calcite had smooth surfaces. Scanning electron microscope (SEM) analysis confirmed the smoothness of calcite samples. Moreover, the surface elements of the samples were specified by energy dispersive microscope (EDS) analysis, which showed that the calcite surfaces were mainly composed of calcium and carbonate.

### 4. *Factors controlling wettability alteration:*

#### a. *Nanofluid composition*

Dilute nanofluid containing low concentration of sole nanoparticles dispersed in DI water or brine is less effective in altering the wettability of strongly oil-wet surfaces than concentrated nanofluids. Nanoparticle disjoining pressure, which is key to wettability alteration, is quite low on oil-wet surfaces. The minimum effective nanoparticle concentration, in this case, was 1 wt%, which is relatively high for achieving stable nanofluids. However, the presence of ionic surfactant will significantly reduce the effective nanoparticle concentration to less than 0.1 wt% due to the synergistic effects of the two agents. Mechanistically, surfactants act to shift wettability to intermediate-wet ( $\theta \leq 90^\circ$ ) and at this point, the structural disjoining pressure of nanoparticles will act synergistically with the surfactant to alter the wettability to strongly water-wet.

Salinity also has a vital effect on nanoparticle adsorption on solid surfaces. It affects the surface charges of suspended nanoparticles and the CMC of

surfactant in surfactant-nanoparticle-brine formulations. High salinity increases the deposition of nanoparticles on solid surfaces, leading to efficient alteration of surface wettability.

*b. Modification conditions*

- Exposure time plays a major role in nanofluid surface treatment. For concentrated nanofluids (e.g. 1 wt% SiO<sub>2</sub> nanoparticles in brine), most of the wettability change was achieved during the early period of treatment ( $\leq 60$  min). However, dilute nanofluids required longer treatment periods to achieve significant reductions in contact angle.
- Temperature increases, on the other hand, accelerate wettability alteration by nanofluids. Our results showed that at higher temperatures, less nanotreatment time is required to achieve the same reduction in contact angle. This is related to the increased adsorption of nanoparticles on oil-wet surfaces. However, further increases in temperature ( $\geq 60$  °C) had no significant effects on wettability alteration.
- The size of the initial nanoparticles in the suspensions, within the range tested (5–25 nm), had no obvious impact on the efficiency of wettability alteration via nanofluid treatment. This is a very important point, since the potential for limited agglomeration of nanoparticles in nanofluid, which can result in increased nanoparticle sizes, had no dramatic effect on the efficiency of wettability alteration.
- Increased pressures caused only slight effects on wettability alteration by nanofluid treatment. In this context, nanoparticles were mainly bounded irreversibly at calcite surfaces despite the pressure applied during nanotreatment processes. However, the effect of pressure on the irreversibility of nanoparticle adsorption increased with nanoparticle concentration. Thus, dilute nanofluids are efficient for wettability alteration applications in high-pressure conditions.

*c. Surface chemistry*

The efficiency of nanofluids as wettability alteration agents is likely affected by the surface composite, which influences nanoparticle transport within the solid matrix. Basically, the heterogeneity of carbonate reservoirs at various lengths scales adds significant complexity to nanoparticle mobilisation. Typically, carbonate surfaces may contain significant amounts of silica and clay in the porous medium. These impurities reduce the positive charges on carbonate surfaces due to the formation of negatively charged sites. Consequently, the repulsive forces between these negative sites and negatively charged nanoparticles are expected to decrease nanoparticle adoption on carbonate surfaces and, accordingly, the efficiency of wettability alteration.

## 11.2 Recommendations and Outlook for Future Work

Despite the fact that silica nanoparticles have demonstrated great potential for altering the wettability of oil-wet surfaces and reducing the interfacial tension of oil/water systems, nanofluids are still costly in practical applications and have relatively low stability in high salinity fields. Consequently, it is critical to design a cheap nano-suspension with a controlled structure and stable formulation. Moreover, although this study investigated a comprehensive range of variables (IFT, stability behaviour, wettability alteration), various nano-suspensions, interactions (nanoparticle-fluid, nanoparticle-surfactant, nanoparticle-solid) and wettability alteration mechanisms, there remain significant areas that this study did not cover. These gaps and limitations guide the outlook for future work, as follows:

- The wettability alteration of calcite—an electrochemically active material—via nanoparticle adsorption is quite complex and needs further investigation.
- Despite the use of equilibrated water with calcite in all experiments, significant dissolving was noticed in many calcite samples after treatment with nanofluid. This unfavourable desolution might have affected subsequent wettability measurements. Thus, modifying a reactor for water equilibration with calcite at nano-treatment conditions (pressure, temperature, salinity) would be useful to avoid surface desolution.
- The complex effect of surface chemical heterogeneity on wettability has not been adequately described. Fractional characterisation of wettability must be individually evaluated for each mineral forming the samples. Then, to establish a realistic characterisation for overall substrate wettability, a sum of the individual mineral wettabilities is required, using the following equation (Iglauer et al. 2015c).

$$\gamma_{i,cw} \cos \theta^* = \sum_{n=1}^N f_i (\gamma_{i,sc} - \gamma_{i,sw}) \quad \text{Equation 11-1}$$

Where  $i$  is the number of components forming the surface,  $\theta^*$  is the contact angle on the heterogeneous surface,  $f$  is the fraction of material on the substrate, and  $\gamma_{i,cw}$ ,  $\gamma_{i,sc}$  and  $\gamma_{i,sw}$  are the solid/oil, solid/water and oil/brine interfacial tensions of the  $i^{\text{th}}$  component, respectively. Thus, our observations, which were made on flat, single-crystal calcite, only act as a preliminary investigation into nanofluid/rock interactions. Upscaling of this promising approach is yet to be performed.

- Changes in surface roughness due to nanoparticle adsorption might be responsible for changes in contact angle, rather than changes in surface interfacial properties. Thus, the effect of nanotreatment on surface roughness must be carefully addressed.

- The zeta potential measurements of silica nanosuspensions in this study were conducted at atmospheric pressure. This was mainly due to the limitations of commercially-available Zetasizer instruments. Technical improvement of these instruments may allow zeta potential measurements to be conducted at high pressures, leading to a broader experimental matrix for studies on nanofluid behaviour and stability.
- High salinity has dramatic impacts on nanofluid zeta potential and, consequently, the stability of nanosuspensions; however, only relatively low salt concentrations were used in the zeta potential measurements due to the limitations of the Zetasizer instruments. The development of a sophisticated facility that allows high salinity zeta potential measurements will lead to a wider experimental matrix for studies of nanofluid behaviour
- The composite effect of different minerals on nanofluid stability is an important aspect of silica nanoparticle adsorption behaviour and stability in porous media. Potential interactions (side reactions) between silica nanoparticles and minerals can have diverse effects on nanofluids' stability and efficiency as wettability agents. Conducting zeta potential measurements for nanofluid samples pre-equilibrated with rocks will allow a better understanding of nanoparticle tendencies.
- The dynamic light scattering (DLS) technique used in this study to measure hydrodynamic particle diameters, particles sizes and particle size distributions is a laser-based technique and, hence, is very sensitive to the opacity of the tested solution. However, increased nanoparticle concentration can dramatically increase the opacity of nanofluids. Consequently, all particle size measurements were limited to dilute nanofluids. Using other measurement techniques such as transmission electron microscopy (TEM) can allow concentrated nanofluids to be analysed and help to confirm the results of DLS measurements.
- Advanced characterisation techniques such as scanning electron microscopy (SEM) and atomic force microscope (AFM) can qualitatively describe the adsorption of nanoparticles onto surfaces at ambient conditions. However, such characterisation at reservoir conditions (e.g. high pressure) is still a challenge. The development of a sophisticated facility that allows characterisation of nanoparticle adsorption in porous media under subsurface conditions will certainly advance future nanotreatment applications.

## References

- Abdallah, W., J. S. Buckley, A. Carnegie, J. Edwards, B. Herold, E. Fordham, A. Graue, T. Habashy, N. Seleznev, C. Signer, H. Hussain, B. Montaron, and M. Ziauddin. 2007. "Fundamentals of wettability." *Oilfield Review* 19 (2):44-61.
- Adamson, Arthur W, and Alice Petry Gast. 1967. *Physical chemistry of surfaces*. Sixth Edition ed: John Wiley.
- Ahmadall, Tabatabal, Marla V. Gonzalez, Jeffrey H. Harwell, and John F. Scamehorn. 1993. "Reducing Surfactant Adsorption in Carbonate Reservoirs." *SPE Reservoir Engineering* 8 (02):117-122. doi: 10.2118/24105-PA.
- Ahmadi, Mohammad Ali, and James Sheng. 2016. "Performance improvement of ionic surfactant flooding in carbonate rock samples by use of nanoparticles." *Petroleum Science*:1-12. doi: 10.1007/s12182-016-0109-2.
- Ahr, Wayne M. 2011. *Geology of carbonate reservoirs: the identification, description and characterization of hydrocarbon reservoirs in carbonate rocks*: John Wiley & Sons.
- Ahualli, S., G. R. Iglesias, W. Wachter, M. Dulle, D. Minami, and O. Glatter. 2011. "Adsorption of Anionic and Cationic Surfactants on Anionic Colloids: Supercharging and Destabilization." *Langmuir* 27 (15):9182-9192. doi: 10.1021/la201242d.
- Al-Anssari, Sarmad. 2009. "Study on Absorption of Ozone in Water Using Perforated Sieve Tray Column " *Journal of Engineering* 15:4438 -4446
- Al-Anssari, Sarmad, Muhammad Arif, Shaobin Wang, Ahmed Barifcani, and Stefan Iglauer. 2017a. "Stabilising nanofluids in saline environments." *Journal of Colloid and Interface Science* 508:222-229. doi: <https://doi.org/10.1016/j.jcis.2017.08.043>.
- Al-Anssari, Sarmad, Muhammad Arif, Shaobin Wang, Ahmed Barifcani, Maxim Lebedev, and Stefan Iglauer. 2017b. "CO<sub>2</sub> geo-storage capacity enhancement via nanofluid priming." *International Journal of Greenhouse Gas Control* 63:20-25. doi: 10.1016/j.ijggc.2017.04.015
- Al-Anssari, Sarmad, Muhammad Arif, Shaobin Wang, Ahmed Barifcani, Maxim Lebedev, and Stefan Iglauer. 2017c. "Wettability of nano-treated calcite/CO<sub>2</sub>/brine systems: Implication for enhanced CO<sub>2</sub> storage potential." *International Journal of Greenhouse Gas Control* 66:97-105. doi: <https://doi.org/10.1016/j.ijggc.2017.09.008>.
- Al-Anssari, Sarmad, Muhammad Arif, Shaobin Wang, Ahmed Barifcani, Maxim Lebedev, and Stefan Iglauer. 2018. "Wettability of nanofluid-modified oil-wet calcite at reservoir conditions." *Fuel* 211:405-414. doi: <https://doi.org/10.1016/j.fuel.2017.08.111>.

- Al-Anssari, Sarmad, Ahmed Barifcani, Shaobin Wang, Maxim Lebedev, and Stefan Iglauer. 2016. "Wettability alteration of oil-wet carbonate by silica nanofluid." *Journal of Colloid and Interface Science* 461:435-442. doi: <http://dx.doi.org/10.1016/j.jcis.2015.09.051>.
- Al-Anssari, Sarmad, Lezorgia. N. Nwideo, Muhammad Arif, Shaobin Wang, Ahmed Barifcani, Lebedev Maxim, and Stefan Iglauer. 2017d. "Wettability alteration of carbonate rocks via nanoparticle-anionic surfactant flooding at reservoirs conditions " SPE Symposium: Production Enhancement and Cost Optimisation, Kuala Lumpur, Malaysia, 7-8 November 2017.
- Al-Anssari, Sarmad, Shaobin Wang, Ahmed Barifcani, and Stefan Iglauer. 2017e. "Oil-water interfacial tensions of silica nanoparticle-surfactant formulations." *Tenside Surfactants Detergents* 54 (4):334-341. doi: <https://doi.org/10.3139/113.110511>.
- Al-Anssari, Sarmad, Shaobin Wang, Ahmed Barifcani, Maxim Lebedev, and Stefan Iglauer. 2017f. "Effect of temperature and SiO<sub>2</sub> nanoparticle size on wettability alteration of oil-wet calcite." *Fuel* 206:34-42. doi: 10.1016/j.fuel.2017.05.077.
- Al-Hadhrami, Hamed S., and Martin J. Blunt. 2000. "Thermally Induced Wettability Alteration to Improve Oil Recovery in Fractured Reservoirs." SPE/DOE Improved Oil Recovery Symposium, Tulsa, Oklahoma 2000/1/1/.
- Al-Lawati, Shabir, and Saad Saleh. 1996. "Oil Recovery in Fractured Oil Reservoirs by Low IFT Imbibition Process." SPE Annual Technical Conference and Exhibition, Denver, Colorado 1996/1/1/.
- Al-Manasir, Nodar, Anna-Lena Kjøniksen, and Bo Nyström. 2009. "Preparation and characterization of cross-linked polymeric nanoparticles for enhanced oil recovery applications." *Journal of Applied Polymer Science* 113 (3):1916-1924. doi: 10.1002/app.30176.
- Al-Menhali, Ali S., Hannah P. Menke, Martin J. Blunt, and Samuel C. Krevor. 2016. "Pore Scale Observations of Trapped CO<sub>2</sub> in Mixed-Wet Carbonate Rock: Applications to Storage in Oil Fields." *Environmental Science & Technology* 50 (18):10282–10290. doi: 10.1021/acs.est.6b03111.
- Al-Sahhaf, T., A. Elkamel, A. Suttar Ahmed, and A. R. Khan. 2005. "The Influence of Temperature, Pressure, Salinity, and Surfactant Concentration on the Interfacial Tension of the N-Octane-Water System." *Chemical Engineering Communications* 192 (5):667-684. doi: 10.1080/009864490510644.
- Al-Sulaimani, Hanaa, Yahya Al-Wahaibi, Saif Al-Bahry, Abdulkadir Elshafie, Ali Al-Bemani, and Sanket Joshi. 2012. "Residual-Oil Recovery Through Injection of Biosurfactant, Chemical Surfactant, and Mixtures of Both Under Reservoir Temperatures: Induced-Wettability and Interfacial-Tension Effects." *SPE Reservoir Evaluation & Engineering* 15 (02):210-217. doi: 10.2118/158022-PA.

- Al-Yaseri, Ahmed, Mohammad Sarmadivaleh, Ali Saeedi, Maxim Lebedev, Ahmed Barifcani, and Stefan Iglauer. 2015a. "N<sub>2</sub>+CO<sub>2</sub>+NaCl brine interfacial tensions and contact angles on quartz at CO<sub>2</sub> storage site conditions in the Gippsland basin, Victoria/Australia." *Journal of Petroleum Science and Engineering* 129 (0):58-62. doi: <http://dx.doi.org/10.1016/j.petrol.2015.01.026>.
- Al-Yaseri, Ahmed Z., Maxim Lebedev, Ahmed Barifcani, and Stefan Iglauer. 2016. "Receding and advancing (CO<sub>2</sub> + brine + quartz) contact angles as a function of pressure, temperature, surface roughness, salt type and salinity." *The Journal of Chemical Thermodynamics* 93:416-423. doi: <http://dx.doi.org/10.1016/j.jct.2015.07.031>.
- Al-Yaseri, Ahmed Z., Maxim Lebedev, Sarah J. Vogt, Michael L. Johns, Ahmed Barifcani, and Stefan Iglauer. 2015b. "Pore-scale analysis of formation damage in Bentheimer sandstone with in-situ NMR and micro-computed tomography experiments." *Journal of Petroleum Science and Engineering* 129 (0):48-57. doi: <http://dx.doi.org/10.1016/j.petrol.2015.01.018>.
- Al Mahrouqi, Dawoud, Jan Vinogradov, and Matthew D. Jackson. 2017. "Zeta potential of artificial and natural calcite in aqueous solution." *Advances in Colloid and Interface Science* 240:60-76. doi: <http://dx.doi.org/10.1016/j.cis.2016.12.006>.
- Alam, Md. Amirul, Abdul Shukor Juraimi, M. Y. Rafii, and Azizah Abdul Hamid. 2015. "Effect of Salinity on Biomass Yield and Physiological and Stem-Root Anatomical Characteristics of Purslane (*Portulaca oleracea* L.) Accessions." *BioMed Research International* 2015:15. doi: 10.1155/2015/105695.
- Ali, Imran. 2012. "New Generation Adsorbents for Water Treatment." *Chemical Reviews* 112 (10):5073-5091. doi: 10.1021/cr300133d.
- Alotaibi, Mohammed B., Ramez A. Nasralla, and Hisham A. Nasr-El-Din. 2011. "Wettability Studies Using Low-Salinity Water in Sandstone Reservoirs." *SPE Reservoir Evaluation & Engineering* 14 (06):713-725. doi: 10.2118/149942-PA.
- Alroudhan, A., J. Vinogradov, and M. D. Jackson. 2016. "Zeta potential of intact natural limestone: Impact of potential-determining ions Ca, Mg and SO<sub>4</sub>." *Colloids and Surfaces A: Physicochemical and Engineering Aspects* 493:83-98. doi: <http://dx.doi.org/10.1016/j.colsurfa.2015.11.068>.
- Alvarez, Nicolas J., Lynn M. Walker, and Shelley L. Anna. 2009. "A non-gradient based algorithm for the determination of surface tension from a pendant drop: Application to low Bond number drop shapes." *Journal of Colloid and Interface Science* 333 (2):557-562. doi: <http://dx.doi.org/10.1016/j.jcis.2009.01.074>.
- Amedi, Hamidreza, and Mohammad-Ali Ahmadi. 2016. "Experimental investigation the effect of nanoparticles on the oil-water relative permeability." *The*

*European Physical Journal Plus* 131 (5):125. doi: 10.1140/epjp/i2016-16125-4.

- Ameri, A., N. Shojai Kaveh, E. S. J. Rudolph, K-H Wolf, R. Farajzadeh, and J. Bruining. 2013. "Investigation on Interfacial Interactions among Crude Oil–Brine–Sandstone Rock–CO<sub>2</sub> by Contact Angle Measurements." *Energy & Fuels* 27 (2):1015-1025. doi: 10.1021/ef3017915.
- Amiri, Asal, Gisle Øye, and Johan Sjöblom. 2009. "Influence of pH, high salinity and particle concentration on stability and rheological properties of aqueous suspensions of fumed silica." *Colloids and Surfaces A: Physicochemical and Engineering Aspects* 349 (1–3):43-54. doi: <http://dx.doi.org/10.1016/j.colsurfa.2009.07.050>.
- Amott, Earl. 1959. "Observations relating to the wettability of porous rock." *Trans.* 2016:156-162.
- Amraei, A., Zahra Fakhroueian, and Alireza Bahramian. 2013. "Influence of New SiO<sub>2</sub> Nanofluids on Surface Wettability and Interfacial Tension Behaviour between Oil-Water Interface in EOR Processes." *Journal of Nano Research* 26:1-8. doi: <http://dx.doi.org/10.4028/www.scientific.net/JNanoR.26.1>.
- Anderson, William G. 1987a. "Wettability literature survey-part 4: Effects of wettability on capillary pressure." *Journal of Petroleum Technology* 39 (10):1,283-1,300.
- Anderson, William G. 1987b. "Wettability literature survey part 5: the effects of wettability on relative permeability." *Journal of Petroleum Technology* 39 (11):1,453-1,468.
- Anderson, William G. 1986. "Wettability Literature Survey- Part 1: Rock/Oil/Brine Interactions and the Effects of Core Handling on Wettability." *Journal of Petroleum Technology* 38 (10):1125-1144. doi: 10.2118/13932-PA.
- Andreas, Solga, Cerman Zdenek, F. Striffler Boris, Spaeth Manuel, and Barthlott Wilhelm. 2007. "The dream of staying clean: Lotus and biomimetic surfaces." *Bioinspiration & Biomimetics* 2 (4):S126.
- Andrew, Matthew, Branko Bijeljic, and Martin J. Blunt. 2014. "Pore-scale imaging of trapped supercritical carbon dioxide in sandstones and carbonates." *International Journal of Greenhouse Gas Control* 22:1-14. doi: <http://dx.doi.org/10.1016/j.ijggc.2013.12.018>.
- Antia, David D. J. 2011. "Modification of Aquifer Pore-Water by Static Diffusion Using Nano-Zero-Valent Metals." *Water* 3 (1):79.
- Arif, Muhammad, Ahmed Z. Al-Yaseri, Ahmed Barifcani, Maxim Lebedev, and Stefan Iglauer. 2016a. "Impact of pressure and temperature on CO<sub>2</sub>–brine–mica contact angles and CO<sub>2</sub>–brine interfacial tension: Implications for carbon

- geo-sequestration." *Journal of Colloid and Interface Science* 462:208-215. doi: <http://dx.doi.org/10.1016/j.jcis.2015.09.076>.
- Arif, Muhammad, Ahmed Barifcani, and Stefan Iglauer. 2016b. "Solid/CO<sub>2</sub> and solid/water interfacial tensions as a function of pressure, temperature, salinity and mineral type: Implications for CO<sub>2</sub>-wettability and CO<sub>2</sub> geo-storage." *International Journal of Greenhouse Gas Control* 53:263-273. doi: <http://dx.doi.org/10.1016/j.ijggc.2016.08.020>.
- Arif, Muhammad, Ahmed Barifcani, Maxim Lebedev, and Stefan Iglauer. 2016c. "CO<sub>2</sub>-wettability of low to high rank coal seams: Implications for carbon sequestration and enhanced methane recovery." *Fuel* 181:680-689. doi: <http://dx.doi.org/10.1016/j.fuel.2016.05.053>.
- Arif, Muhammad, Ahmed Barifcani, Maxim Lebedev, and Stefan Iglauer. 2016d. "Structural trapping capacity of oil-wet caprock as a function of pressure, temperature and salinity." *International Journal of Greenhouse Gas Control* 50:112-120. doi: <http://dx.doi.org/10.1016/j.ijggc.2016.04.024>.
- Arif, Muhammad, Franca Jones, Ahmed Barifcani, and Stefan Iglauer. 2017. "Electrochemical investigation of the effect of temperature, salinity and salt type on brine/mineral interfacial properties." *International Journal of Greenhouse Gas Control* 59:136-147.
- Arns, Christoph H., Fabrice Bauguet, Ajay Limaye, Arthur Sakellariou, Timothy Senden, Adrian Sheppard, Robert Martin Sok, Val Pinczewski, Stig Bakke, Lars Inge Berge, Paul E. Oren, and Mark A. Knackstedt. 2005. "Pore Scale Characterization of Carbonates Using X-Ray Microtomography." *SPE Journal* 10 (4):475-484. doi: 10.2118/90368-PA.
- Atkin, R., V. S. J. Craig, E. J. Wanless, and S. Biggs. 2003. "Mechanism of cationic surfactant adsorption at the solid–aqueous interface." *Advances in Colloid and Interface Science* 103 (3):219-304. doi: [http://dx.doi.org/10.1016/S0001-8686\(03\)00002-2](http://dx.doi.org/10.1016/S0001-8686(03)00002-2).
- Austad, T., S. F. Shariatpanahi, S. Strand, C. J. J. Black, and K. J. Webb. 2012. "Conditions for a Low-Salinity Enhanced Oil Recovery (EOR) Effect in Carbonate Oil Reservoirs." *Energy & Fuels* 26 (1):569-575. doi: 10.1021/ef201435g.
- Austad, Tor, and Dag C. Standnes. 2003. "Spontaneous imbibition of water into oil-wet carbonates." *Journal of Petroleum Science and Engineering* 39 (3–4):363-376. doi: [http://dx.doi.org/10.1016/S0920-4105\(03\)00075-5](http://dx.doi.org/10.1016/S0920-4105(03)00075-5).
- Babadagli, Tayfun. 2003. "Selection of proper enhanced oil recovery fluid for efficient matrix recovery in fractured oil reservoirs." *Colloids and Surfaces A: Physicochemical and Engineering Aspects* 223 (1–3):157-175. doi: [http://dx.doi.org/10.1016/S0927-7757\(03\)00170-5](http://dx.doi.org/10.1016/S0927-7757(03)00170-5).

- Baeckkyoung, Sung, Kim Se Hoon, Lee Sungwoo, Lim Jaekwan, Lee Jin-Kyu, and Soh Kwang-Sup. 2015. "Nanofluid transport in a living soft microtube." *Journal of Physics D: Applied Physics* 48 (34):345402. doi: doi:10.1088/0022-3727/48/34/345402.
- Balaji, Tatineni, Basova Yulia, Rahman Atikur, Islam Saiful, Rahman Mizanur, Islam Azharul, Perkins Joslyn, King James, Taylor Jasmine, Kumar Dhananjay, Ilias Shamsuddin, and Kuila Debasish. 2011. "Development of Mesoporous Silica Encapsulated Pd-Ni Nanocatalyst for Hydrogen Production." In *Production and Purification of Ultraclean Transportation Fuels*, 177-190. American Chemical Society.
- Bard, Allen J, Larry R Faulkner, Johna Leddy, and Cynthia G Zoski. 1980. *Electrochemical methods: fundamentals and applications*. Vol. 2: Wiley New York.
- Bayat, AliEsfandyari, Radzuan Junin, FarshadDaraei Ghadikolaei, and Ali Piroozian. 2014a. "Transport and aggregation of Al<sub>2</sub>O<sub>3</sub> nanoparticles through saturated limestone under high ionic strength conditions: measurements and mechanisms." *Journal of Nanoparticle Research* 16 (12):1-12. doi: 10.1007/s11051-014-2747-x.
- Bayat, AliEsfandyari, Radzuan Junin, Rahmat Mohsin, Mehrdad Hokmabadi, and Shahaboddin Shamsirband. 2015. "Influence of clay particles on Al<sub>2</sub>O<sub>3</sub> and TiO<sub>2</sub> nanoparticles transport and retention through limestone porous media: measurements and mechanisms." *Journal of Nanoparticle Research* 17 (5):1-14. doi: 10.1007/s11051-015-3031-4.
- Bayat, Esfandyari Ali, Radzuan Junin, Ariffin Samsuri, Ali Piroozian, and Mehrdad Hokmabadi. 2014b. "Impact of Metal Oxide Nanoparticles on Enhanced Oil Recovery from Limestone Media at Several Temperatures." *Energy & Fuels* 28 (10):6255-6266. doi: 10.1021/ef5013616.
- Bera, Achinta, T. Kumar, Keka Ojha, and Ajay Mandal. 2013. "Adsorption of surfactants on sand surface in enhanced oil recovery: Isotherms, kinetics and thermodynamic studies." *Applied Surface Science* 284:87-99. doi: <http://dx.doi.org/10.1016/j.apsusc.2013.07.029>.
- Bera, Achinta, Ajay Mandal, and B. B. Guha. 2014. "Synergistic Effect of Surfactant and Salt Mixture on Interfacial Tension Reduction between Crude Oil and Water in Enhanced Oil Recovery." *Journal of Chemical & Engineering Data* 59 (1):89-96. doi: 10.1021/je400850c.
- Berg, S., A. W. Cense, E. Jansen, and K. Bakker. 2010. "Direct Experimental Evidence of Wettability Modification By Low Salinity." *Petrophysics* 51 (05):314-322.
- Bikkina, Prem Kumar. 2011. "Contact angle measurements of CO<sub>2</sub>-water-quartz/calcite systems in the perspective of carbon sequestration." *International Journal of Greenhouse Gas Control* 5 (5):1259-1271. doi: <http://dx.doi.org/10.1016/j.ijggc.2011.07.001>.

- Binks, Bernard P, Mark Kirkland, and Jhonny A Rodrigues. 2008. "Origin of stabilisation of aqueous foams in nanoparticle–surfactant mixtures." *Soft Matter* 4 (12):2373-2382.
- Binks, Bernard P., and Jhonny A. Rodrigues. 2009. "Influence of surfactant structure on the double inversion of emulsions in the presence of nanoparticles." *Colloids and Surfaces A: Physicochemical and Engineering Aspects* 345 (1–3):195-201. doi: <http://dx.doi.org/10.1016/j.colsurfa.2009.05.001>.
- Binks, Bernard P., Jhonny A. Rodrigues, and William J. Frith. 2007. "Synergistic Interaction in Emulsions Stabilized by a Mixture of Silica Nanoparticles and Cationic Surfactant." *Langmuir* 23 (7):3626-3636. doi: 10.1021/la0634600.
- Biswal, Nihar Ranjan, Naveen Rangera, and Jayant K. Singh. 2016. "Effect of Different Surfactants on the Interfacial Behavior of the n-Hexane–Water System in the Presence of Silica Nanoparticles." *The Journal of Physical Chemistry B* 120 (29):7265-7274. doi: 10.1021/acs.jpccb.6b03763.
- Blute, Irena, Robert J. Pugh, John van de Pas, and Ian Callaghan. 2009. "Industrial manufactured silica nanoparticle sols. 2: Surface tension, particle concentration, foam generation and stability." *Colloids and Surfaces A: Physicochemical and Engineering Aspects* 337 (1–3):127-135. doi: <http://dx.doi.org/10.1016/j.colsurfa.2008.12.009>.
- Bonu, Venkataramana, Niranjana Kumar, Arindam Das, Sitaram Dash, and Ashok Kumar Tyagi. 2016. "Enhanced Lubricity of SnO<sub>2</sub> Nanoparticles Dispersed Polyolester Nanofluid." *Industrial & Engineering Chemistry Research* 55 (10):2696-2703. doi: 10.1021/acs.iecr.5b03506.
- Branson, Blake T., Paul S. Beauchamp, Jeremiah C. Beam, Charles M. Lukehart, and Jim L. Davidson. 2013. "Nanodiamond Nanofluids for Enhanced Thermal Conductivity." *ACS Nano* 7 (4):3183-3189. doi: 10.1021/nm305664x.
- Broseta, D., N. Tonnet, and V. Shah. 2012. "Are rocks still water-wet in the presence of dense CO<sub>2</sub> or H<sub>2</sub>S?" *Geofluids* 12 (4):280-294. doi: 10.1111/j.1468-8123.2012.00369.x.
- Buckley, J. S., G. J. Hirasaki, Y. Liu, S. Von Drasek, J. X. Wang, and B. S. Gill. 1998a. "Asphaltene Precipitation and Solvent Properties of Crude Oils." *Petroleum Science and Technology* 16 (3-4):251-285. doi: 10.1080/10916469808949783.
- Buckley, J. S., Y. Liu, and S. Monsterleet. 1998b. "Mechanisms of Wetting Alteration by Crude Oils." *SPE Journal* 3 (01):54-61. doi: 10.2118/37230-PA.
- Buckley, J. S., K. Takamura, and N. R. Morrow. 1989. "Influence of Electrical Surface Charges on the Wetting Properties of Crude Oils." *SPE Reservoir Engineering* 4 (03):332-340. doi: 10.2118/16964-PA.

- Buckley, Jill S. 1999. "Predicting the Onset of Asphaltene Precipitation from Refractive Index Measurements." *Energy & Fuels* 13 (2):328-332. doi: 10.1021/ef980201c.
- Buenaventura, JE, RS Alvarez, JG Flores, and IE Martinez. 2014. "Gas Injection Enhanced Oil Recovery Application in a Mature Naturally-Fractured-Carbonate Reservoir." SPE Latin America and Caribbean Petroleum Engineering Conference.
- Cai, Bi-Yu, Ji-Tao Yang, and Tian-Min Guo. 1996. "Interfacial Tension of Hydrocarbon + Water/Brine Systems under High Pressure." *Journal of Chemical & Engineering Data* 41 (3):493-496. doi: 10.1021/je950259a.
- Campelo, Juan M, Diego Luna, Rafael Luque, José M Marinas, and Antonio A Romero. 2009. "Sustainable Preparation of Supported Metal Nanoparticles and Their Applications in Catalysis." *ChemSusChem* 2 (1):18-45. doi: 10.1002/cssc.200800227.
- Castro Dantas, T. N., P. J. Soares A, A. O. Wanderley Neto, A. A. Dantas Neto, and E. L. Barros Neto. 2014. "Implementing New Microemulsion Systems in Wettability Inversion and Oil Recovery from Carbonate Reservoirs." *Energy & Fuels* 28 (11):6749-6759. doi: 10.1021/ef501697x.
- Chakraborty, Suman, and Sourav Padhy. 2008. "Anomalous Electrical Conductivity of Nanoscale Colloidal Suspensions." *ACS Nano* 2 (10):2029-2036. doi: 10.1021/nm800343h.
- Chaudhary, Kuldeep, M. Bayani Cardenas, William W. Wolfe, Jessica A. Maisano, Richard A. Ketcham, and Philip C. Bennett. 2013. "Pore-scale trapping of supercritical CO<sub>2</sub> and the role of grain wettability and shape." *Geophysical Research Letters* 40 (15):3878-3882. doi: 10.1002/grl.50658.
- Chen, Peila, and Kishore K. Mohanty. 2014. "Wettability Alteration in High Temperature Carbonate Reservoirs." SPE Improved Oil Recovery Symposium, Tulsa, Oklahoma, USA 2014/4/12/.
- Chen, Zehua, and Xiutai Zhao. 2015. "Enhancing Heavy-Oil Recovery by Using Middle Carbon Alcohol-Enhanced Waterflooding, Surfactant Flooding, and Foam Flooding." *Energy & Fuels* 29 (4):2153-2161. doi: 10.1021/ef502652a.
- Chilingar, George V., and T. F. Yen. 1983. "Some Notes on Wettability and Relative Permeabilities of Carbonate Reservoir Rocks, II." *Energy Sources* 7 (1):67-75. doi: 10.1080/00908318308908076.
- Chol, SUS. 1995. "Enhancing thermal conductivity of fluids with nanoparticles." *ASME-Publications-Fed* 231:99-106.
- Chu, Yan-Ping, Yong Gong, Xiao-Li Tan, Lu Zhang, Sui Zhao, Jing-Yi An, and Jia-Yong Yu. 2004. "Studies of synergism for lowering dynamic interfacial tension in sodium  $\alpha$ -(n-alkyl) naphthalene sulfonate/alkali/acidic oil systems." *Journal*

*of Colloid and Interface Science* 276 (1):182-187. doi:  
<http://dx.doi.org/10.1016/j.jcis.2004.03.007>.

- Civan, Faruk, and Maurice L. Rasmussen. 2012. "Parameters of Matrix/Fracture Immiscible-Fluids Transfer Obtained by Modeling of Core Tests." *SPE Journal* 17 (2):540-554. doi: 10.2118/104028-PA.
- Cook, P. 2014. *Geologically Storing Carbon: Learning from the Otway Project Experience*: CSIRO PUBLISHING.
- Costa, Carlos A. R., Carlos A. P. Leite, and Fernando Galembeck. 2006. "ESI-TEM Imaging of Surfactants and Ions Sorbed in Stöber Silica Nanoparticles." *Langmuir* 22 (17):7159-7166. doi: 10.1021/la060389p.
- Craig, Forrest F. 1971. *The reservoir engineering aspects of waterflooding*. Vol. 3: Society of Petroleum Engineers.
- Cui, Z. G., Y. Z. Cui, C. F. Cui, Z. Chen, and B. P. Binks. 2010a. "Aqueous Foams Stabilized by in Situ Surface Activation of CaCO<sub>3</sub> Nanoparticles via Adsorption of Anionic Surfactant." *Langmuir* 26 (15):12567-12574. doi: 10.1021/la1016559.
- Cui, Z. G., L. L. Yang, Y. Z. Cui, and B. P. Binks. 2009. "Effects of Surfactant Structure on the Phase Inversion of Emulsions Stabilized by Mixtures of Silica Nanoparticles and Cationic Surfactant." *Langmuir* 26 (7):4717-4724. doi: 10.1021/la903589e.
- Cui, Z. G., L. L. Yang, Y. Z. Cui, and B. P. Binks. 2010b. "Effects of Surfactant Structure on the Phase Inversion of Emulsions Stabilized by Mixtures of Silica Nanoparticles and Cationic Surfactant." *Langmuir* 26 (7):4717-4724. doi: 10.1021/la903589e.
- Curbelo, Fabíola D. S., Vanessa C. Santanna, Eduardo L. Barros Neto, Tarcílio Viana Dutra Jr, Tereza N. Castro Dantas, Afonso A. Dantas Neto, and Alfredo I. C. Garnica. 2007. "Adsorption of nonionic surfactants in sandstones." *Colloids and Surfaces A: Physicochemical and Engineering Aspects* 293 (1-3):1-4. doi: <http://dx.doi.org/10.1016/j.colsurfa.2006.06.038>.
- Dake, L. P. 1978. *Fundamentals of Reservoir Engineering*. Elsevier.
- Das, Sarit K., and Stephen U. S. Choi. 2009. "A Review of Heat Transfer in Nanofluids." In *Advances in Heat Transfer*, edited by Thomas F. Irvine and James P. Hartnett, 81-197. Elsevier.
- De, Mrinmoy, Partha S. Ghosh, and Vincent M. Rotello. 2008. "Applications of Nanoparticles in Biology." *Advanced Materials* 20 (22):4225-4241. doi: 10.1002/adma.200703183.
- de Ruijter, M., P. Kölsch, M. Voué, J. De Coninck, and J. P. Rabe. 1998. "Effect of temperature on the dynamic contact angle." *Colloids and Surfaces A*:

*Physicochemical and Engineering Aspects* 144 (1–3):235-243. doi: [http://dx.doi.org/10.1016/S0927-7757\(98\)00659-1](http://dx.doi.org/10.1016/S0927-7757(98)00659-1).

- Denekas, M. O., C. C. Mattax, and G. T. Davis. 1959. "Effects of Crude Oil Components on Rock Wettability." *SPE Journal* 2016:330-333.
- Dickson, Jasper L., Gaurav Gupta, Tommy S. Horozov, Bernard P. Binks, and Keith P. Johnston. 2006. "Wetting Phenomena at the CO<sub>2</sub>/Water/Glass Interface." *Langmuir* 22 (5):2161-2170. doi: 10.1021/la0527238.
- Ding, Baodong, Guicai Zhang, Jijiang Ge, and Xiaoling Liu. 2010. "Research on Mechanisms of Alkaline Flooding for Heavy Oil." *Energy & Fuels* 24 (12):6346-6352. doi: 10.1021/ef100849u.
- Dishon, Matan, Ohad Zohar, and Uri Sivan. 2009. "From Repulsion to Attraction and Back to Repulsion: The Effect of NaCl, KCl, and CaCl on the Force between Silica Surfaces in Aqueous Solution." *Langmuir* 25 (5):2831-2836. doi: 10.1021/la803022b.
- Dong, Lichun, and Duane Johnson. 2003. "Surface Tension of Charge-Stabilized Colloidal Suspensions at the Water–Air Interface." *Langmuir* 19 (24):10205-10209. doi: 10.1021/la035128j.
- Dutkiewicz, E., and A. Jakubowska. 2002. "Effect of electrolytes on the physicochemical behaviour of sodium dodecyl sulphate micelles." *Colloid and Polymer Science* 280 (11):1009-1014. doi: 10.1007/s00396-002-0723-y.
- Eastman, J. A., S. U. S. Choi, S. Li, W. Yu, and L. J. Thompson. 2001. "Anomalously increased effective thermal conductivities of ethylene glycol-based nanofluids containing copper nanoparticles." *Applied Physics Letters* 78 (6):718. doi: doi.org/10.1063/1.1341218.
- Ehrlich, Robert, and Robert J Wygal Jr. 1977. "Interrelation of crude oil and rock properties with the recovery of oil by caustic waterflooding." *Society of Petroleum Engineers Journal* 17 (04):263-270.
- Ehtesabi, Hamide, M. Mahdi Ahadian, Vahid Taghikhani, and M. Hossein Ghazanfari. 2014. "Enhanced Heavy Oil Recovery in Sandstone Cores Using TiO<sub>2</sub> Nanofluids." *Energy & Fuels* 28 (1):423-430. doi: 10.1021/ef401338c.
- Eide, O., G. Ersland, B. Brattekas, A. Haugen, A. Graue, and M. A. Ferno. 2015. "CO<sub>2</sub> EOR by Diffusive Mixing in Fractured Reservoirs." *SPE Journal* 56 (1):23-31.
- El-Maghraby, R. M., C. H. Pentland, S. Iglauer, and M. J. Blunt. 2012. "A fast method to equilibrate carbon dioxide with brine at high pressure and elevated temperature including solubility measurements." *The Journal of Supercritical Fluids* 62:55-59. doi: <http://dx.doi.org/10.1016/j.supflu.2011.11.002>.

- El-Sayed, Galila M., M. M. Kamel, N. S. Morsy, and F. A. Taher. 2012. "Encapsulation of nano Disperse Red 60 via modified miniemulsion polymerization. I. Preparation and characterization." *Journal of Applied Polymer Science* 125 (2):1318-1329. doi: 10.1002/app.35102.
- Elaissari, A., and E. Pefferkorn. 1991. "Aggregation modes of colloids in the presence of block copolymer micelles." *Journal of Colloid and Interface Science* 143 (2):343-355. doi: [http://dx.doi.org/10.1016/0021-9797\(91\)90268-D](http://dx.doi.org/10.1016/0021-9797(91)90268-D).
- Emberley, S., I. Hutcheon, M. Shevalier, K. Durocher, W. D. Gunter, and E. H. Perkins. 2004. "Geochemical monitoring of fluid-rock interaction and CO<sub>2</sub> storage at the Weyburn CO<sub>2</sub>-injection enhanced oil recovery site, Saskatchewan, Canada." *Energy* 29 (9–10):1393-1401. doi: <http://dx.doi.org/10.1016/j.energy.2004.03.073>.
- Esmaeilzadeh, Pouriya, Negahdar Hosseinpour, Alireza Bahramian, Zahra Fakhroueian, and Sharareh Arya. 2014. "Effect of ZrO<sub>2</sub> nanoparticles on the interfacial behavior of surfactant solutions at air–water and n-heptane–water interfaces." *Fluid Phase Equilibria* 361 (0):289-295. doi: <http://dx.doi.org/10.1016/j.fluid.2013.11.014>.
- Espinoza, D. Nicolas, and J. Carlos Santamarina. 2010. "Water-CO<sub>2</sub>-mineral systems: Interfacial tension, contact angle, and diffusion--Implications to CO<sub>2</sub> geological storage." *Water Resources Research* 46 (7). doi: 510.1002/nag.1610100506. <http://dx.doi.org/10.1029/2009WR008634>.
- Extrand, Charles W., and Y. Kumagai. 1995. "Liquid Drops on an Inclined Plane: The Relation between Contact Angles, Drop Shape, and Retentive Force." *Journal of Colloid and Interface Science* 170 (2):515-521. doi: <http://dx.doi.org/10.1006/jcis.1995.1130>.
- Fan, Heng, Daniel E. Resasco, and Alberto Striolo. 2011. "Amphiphilic Silica Nanoparticles at the Decane–Water Interface: Insights from Atomistic Simulations." *Langmuir* 27 (9):5264-5274. doi: 10.1021/la200428r.
- Fan, Xiaojiang, Yi Tao, Lingyun Wang, Xihui Zhang, Ying Lei, Zhuo Wang, and Hiroshi Noguchi. 2014. "Performance of an integrated process combining ozonation with ceramic membrane ultra-filtration for advanced treatment of drinking water." *Desalination* 335 (1):47-54. doi: <https://doi.org/10.1016/j.desal.2013.12.014>.
- Farokhpoor, Raheleh, Bård J. A. Bjørkvik, Erik Lindeberg, and Ole Torsæter. 2013. "CO<sub>2</sub> Wettability Behavior During CO<sub>2</sub> Sequestration in Saline Aquifer -An Experimental Study on Minerals Representing Sandstone and Carbonate." *Energy Procedia* 37 (0):5339-5351. doi: <http://dx.doi.org/10.1016/j.egypro.2013.06.452>.
- Fathi, Alimi, Tlili Mohamed, Gabrielli Claude, Georges Maurin, and Ben Amor Mohamed. 2006. "Effect of a magnetic water treatment on homogeneous and heterogeneous precipitation of calcium carbonate." *Water Research* 40 (10):1941-1950. doi: <https://doi.org/10.1016/j.watres.2006.03.013>.

- Fathi, S. Jafar, T. Austad, and S. Strand. 2011. "Water-Based Enhanced Oil Recovery (EOR) by "Smart Water": Optimal Ionic Composition for EOR in Carbonates." *Energy & Fuels* 25 (11):5173-5179. doi: 10.1021/ef201019k.
- Fedele, Laura, Laura Colla, Sergio Bobbo, Simona Barison, and Filippo Agresti. 2011. "Experimental stability analysis of different water-based nanofluids." *Nanoscale Research Letters* 6 (1):300. doi: 10.1186/1556-276x-6-300.
- Feng, L., S. Li, Y. Li, H. Li, L. Zhang, J. Zhai, Y. Song, B. Liu, L. Jiang, and D. Zhu. 2002. "Super-Hydrophobic Surfaces: From Natural to Artificial." *Advanced Materials* 14 (24):1857-1860. doi: 10.1002/adma.200290020.
- Fischer, Arnout R.H., Heleen van Dijk, Janneke de Jonge, Gene Rowe, and Lynn J. Frewer. 2013. "Attitudes and attitudinal ambivalence change towards nanotechnology applied to food production." *Public Understanding of Science* 22 (7):817-831. doi: 10.1177/0963662512440220.
- Franks, George V. 2002. "Zeta Potentials and Yield Stresses of Silica Suspensions in Concentrated Monovalent Electrolytes: Isoelectric Point Shift and Additional Attraction." *Journal of Colloid and Interface Science* 249 (1):44-51. doi: <http://dx.doi.org/10.1006/jcis.2002.8250>.
- Gaonkar, Anilkumar G. 1992. "Effects of salt, temperature, and surfactants on the interfacial tension behavior of a vegetable oil/water system." *Journal of Colloid and Interface Science* 149 (1):256-260. doi: [http://dx.doi.org/10.1016/0021-9797\(92\)90412-F](http://dx.doi.org/10.1016/0021-9797(92)90412-F).
- Garner, KendraL, and ArturoA Keller. 2014. "Emerging patterns for engineered nanomaterials in the environment: a review of fate and toxicity studies." *Journal of Nanoparticle Research* 16 (8):1-28. doi: 10.1007/s11051-014-2503-2.
- Georgiadis, Apostolos, Geoffrey Maitland, J. P. Martin Trusler, and Alexander Bismarck. 2010. "Interfacial Tension Measurements of the (H<sub>2</sub>O + CO<sub>2</sub>) System at Elevated Pressures and Temperatures." *Journal of Chemical & Engineering Data* 55 (10):4168-4175. doi: 10.1021/jc100198g.
- Ghadimi, A., R. Saidur, and H. S. C. Metselaar. 2011. "A review of nanofluid stability properties and characterization in stationary conditions." *International Journal of Heat and Mass Transfer* 54 (17-18):4051-4068. doi: <http://dx.doi.org/10.1016/j.ijheatmasstransfer.2011.04.014>.
- Gharbi, Oussama, and Martin J. Blunt. 2012. "The impact of wettability and connectivity on relative permeability in carbonates: A pore network modeling analysis." *Water Resources Research* 48 (12). doi: 10.1029/2012WR011877.
- Giraldo, Juliana, Pedro Benjumea, Sergio Lopera, Farid B. Cortés, and Marco A. Ruiz. 2013. "Wettability Alteration of Sandstone Cores by Alumina-Based Nanofluids." *Energy & Fuels* 27 (7):3659-3665. doi: 10.1021/ef4002956.

- Glover, Paul W.J., and Matthew D. Jackson. 2010. "Borehole electrokinetics." *The Leading Edge* 29 (6):724-728. doi: 10.1190/1.3447786.
- Gogate, Parag R., and Aniruddha B. Pandit. 2004. "A review of imperative technologies for wastewater treatment I: oxidation technologies at ambient conditions." *Advances in Environmental Research* 8 (3):501-551. doi: [https://doi.org/10.1016/S1093-0191\(03\)00032-7](https://doi.org/10.1016/S1093-0191(03)00032-7).
- Gomari, Rezaei K. A., and A. A. Hamouda. 2006. "Effect of fatty acids, water composition and pH on the wettability alteration of calcite surface." *Journal of Petroleum Science and Engineering* 50 (2):140-150. doi: <http://dx.doi.org/10.1016/j.petrol.2005.10.007>.
- Grate, Jay W., Karl J. Dehoff, Marvin G. Warner, Jonathan W. Pittman, Thomas W. Wietsma, Changyong Zhang, and Mart Oostrom. 2012. "Correlation of Oil–Water and Air–Water Contact Angles of Diverse Silanized Surfaces and Relationship to Fluid Interfacial Tensions." *Langmuir* 28 (18):7182-7188. doi: 10.1021/la204322k.
- Greenlee, Lauren F., Desmond F. Lawler, Benny D. Freeman, Benoit Marrot, and Philippe Moulin. 2009. "Reverse osmosis desalination: Water sources, technology, and today's challenges." *Water Research* 43 (9):2317-2348. doi: <https://doi.org/10.1016/j.watres.2009.03.010>.
- Guo, Ziqiang, Mingzhe Dong, Zhangxin Chen, and Jun Yao. 2013. "Dominant Scaling Groups of Polymer Flooding for Enhanced Heavy Oil Recovery." *Industrial & Engineering Chemistry Research* 52 (2):911-921. doi: 10.1021/ie300328y.
- Gupta, Robin, and Kishore Mohanty. 2010. "Temperature Effects on Surfactant-Aided Imbibition Into Fractured Carbonates." *SPE Journal* 25 (1):80-88. doi: 10.2118/110204-PA.
- Gurkov, Theodor D., Dora T. Dimitrova, Krastanka G. Marinova, Christine Bilke-Crause, Carsten Gerber, and Ivan B. Ivanov. 2005. "Ionic surfactants on fluid interfaces: determination of the adsorption; role of the salt and the type of the hydrophobic phase." *Colloids and Surfaces A: Physicochemical and Engineering Aspects* 261 (1–3):29-38. doi: <http://dx.doi.org/10.1016/j.colsurfa.2004.11.040>.
- Hamedi Shokrlu, Yousef, and Tayfun Babadagli. 2014. "Kinetics of the In-Situ Upgrading of Heavy Oil by Nickel Nanoparticle Catalysts and Its Effect on Cyclic-Steam-Stimulation Recovery Factor." *SPE Reservoir Evaluation & Engineering* 17 (03):355-364. doi: 10.2118/170250-PA.
- Hamouda, Aly Anis, and Rezaei Karam Ali Gomari. 2006. "Influence of Temperature on Wettability Alteration of Carbonate Reservoirs." SPE/DOE Symposium on Improved Oil Recovery, Tulsa, Oklahoma, USA 22-26 April.

- Hamouda, Aly, and Omid Karoussi. 2008. "Effect of Temperature, Wettability and Relative Permeability on Oil Recovery from Oil-wet Chalk." *Energies* 1 (1):19-34. doi: 10.3390/en1010019.
- Handy, Lyman L., Mokhtar El-Gassier, and Iraj Ershaghi. 1983. "A Modified Spinning Drop Method for High-Temperature Applications." *Society of Petroleum Engineers Journal* 23 (01):155-164. doi: 10.2118/9003-PA.
- Hansen, G., A. A. Hamouda, and R. Denoyel. 2000. "The effect of pressure on contact angles and wettability in the mica/water/n-decane system and the calcite+stearic acid/water/n-decane system." *Colloids and Surfaces A: Physicochemical and Engineering Aspects* 172 (1–3):7-16. doi: [http://dx.doi.org/10.1016/S0927-7757\(99\)00498-7](http://dx.doi.org/10.1016/S0927-7757(99)00498-7).
- Hart, Abarasi. 2014. "The novel THAI–CAPRI technology and its comparison to other thermal methods for heavy oil recovery and upgrading." *Journal of Petroleum Exploration and Production Technology* 4 (4):427-437. doi: 10.1007/s13202-013-0096-4.
- Hashemi, Rohallah, Nashaat N. Nassar, and Pedro Pereira Almao. 2014. "Nanoparticle technology for heavy oil in-situ upgrading and recovery enhancement: Opportunities and challenges." *Applied Energy* 133 (Supplement C):374-387. doi: <https://doi.org/10.1016/j.apenergy.2014.07.069>.
- Hendraningrat, Luky, Shidong Li, and Ole Torsæter. 2013. "A coreflood investigation of nanofluid enhanced oil recovery." *Journal of Petroleum Science and Engineering* 111 (0):128-138. doi: <http://dx.doi.org/10.1016/j.petrol.2013.07.003>.
- Hendraningrat, Luky, and Ole Torsæter. 2014. "Effects of the Initial Rock Wettability on Silica-Based Nanofluid-Enhanced Oil Recovery Processes at Reservoir Temperatures." *Energy & Fuels* 28 (10):6228-6241. doi: 10.1021/ef5014049.
- Henke, Kevin. 2009. *Arsenic: Environmental Chemistry, Health Threats and Waste Treatment*. 1 ed ed: Wiley.
- Hernández Battez, A., R. González, J. L. Viesca, J. E. Fernández, J. M. Díaz Fernández, A. Machado, R. Chou, and J. Riba. 2008. "CuO, ZrO<sub>2</sub> and ZnO nanoparticles as antiwear additive in oil lubricants." *Wear* 265 (3-4):422-428. doi: citeulike-article-id:1267284510.1016/j.wear.2007.11.013.
- Hirasaki, George, and Danhua Leslie Zhang. 2004. "Surface Chemistry of Oil Recovery From Fractured, Oil-Wet, Carbonate Formations." *SPE Journal* 9 (02):151-162. doi: 10.2118/88365-PA.
- Hjelmeland, O. S., and L. E. Larrondo. 1986. "Experimental Investigation of the Effects of Temperature, Pressure, and Crude Oil Composition on Interfacial Properties." *SPE Journal* 1 (04):321-328. doi: 10.2118/12124-PA.
- Hoeiland, S., T. Barth, A. M. Blokhus, and A. Skauge. 2001. "The effect of crude oil acid fractions on wettability as studied by interfacial tension and contact

- angles." *Journal of Petroleum Science and Engineering* 30 (2):91-103. doi: [http://dx.doi.org/10.1016/S0920-4105\(01\)00106-1](http://dx.doi.org/10.1016/S0920-4105(01)00106-1).
- Hoff, Erlend, Bo Nyström, and Björn Lindman. 2001. "Polymer–Surfactant Interactions in Dilute Mixtures of a Nonionic Cellulose Derivative and an Anionic Surfactant." *Langmuir* 17 (1):28-34. doi: 10.1021/la001175p.
- Høgnesen, Eli J., Martin Olsen, and Tor Austad. 2006. "Capillary and Gravity Dominated Flow Regimes in Displacement of Oil from an Oil-Wet Chalk Using Cationic Surfactant." *Energy & Fuels* 20 (3):1118-1122. doi: 10.1021/ef050297s.
- Iglauer, S., M. S. Mathew, and F. Bresme. 2012. "Molecular dynamics computations of brine–CO<sub>2</sub> interfacial tensions and brine–CO<sub>2</sub>–quartz contact angles and their effects on structural and residual trapping mechanisms in carbon geo-sequestration." *Journal of Colloid and Interface Science* 386 (1):405-414. doi: <http://dx.doi.org/10.1016/j.jcis.2012.06.052>.
- Iglauer, S., A. Paluszny, and M. J. Blunt. 2015a. "Corrigendum to “Simultaneous oil recovery and residual gas storage: A pore-level analysis using in situ X-ray micro-tomography”" *Fuel* 139:780: 905–914. doi: <http://dx.doi.org/10.1016/j.fuel.2014.09.031>.
- Iglauer, Stefan, Ahmed Zarzor Al-Yaseri, Reza Rezaee, and Maxim Lebedev. 2015b. "CO<sub>2</sub> wettability of caprocks: Implications for structural storage capacity and containment security." *Geophysical Research Letters* 42 (21):9279-9284. doi: 10.1002/2015GL065787.
- Iglauer, Stefan, Adriana Paluszny, Christopher H. Pentland, and Martin J. Blunt. 2011a. "Residual CO<sub>2</sub> imaged with X-ray micro-tomography." *Geophysical Research Letters* 38 (21). doi: 10.1029/2011GL049680.
- Iglauer, Stefan, C. H. Pentland, and A. Busch. 2015c. "CO<sub>2</sub> wettability of seal and reservoir rocks and the implications for carbon geo-sequestration." *Water Resources Research* 51 (1):729-774. doi: 10.1002/2014WR015553.
- Iglauer, Stefan, Abdulsalam Salamah, Mohammad Sarmadivaleh, Keyu Liu, and Chi Phan. 2014. "Contamination of silica surfaces: Impact on water–CO<sub>2</sub>–quartz and glass contact angle measurements." *International Journal of Greenhouse Gas Control* 22 (0):325-328. doi: <http://dx.doi.org/10.1016/j.ijggc.2014.01.006>.
- Iglauer, Stefan, Yongfu Wu, Patrick Shuler, Yongchun Tang, and William A. Goddard Iii. 2009. "Alkyl polyglycoside surfactant–alcohol cosolvent formulations for improved oil recovery." *Colloids and Surfaces A: Physicochemical and Engineering Aspects* 339 (1–3):48-59. doi: <http://dx.doi.org/10.1016/j.colsurfa.2009.01.015>.
- Iglauer, Stefan, Yongfu Wu, Patrick Shuler, Yongchun Tang, and William A. Goddard Iii. 2010. "New surfactant classes for enhanced oil recovery and their tertiary

oil recovery potential." *Journal of Petroleum Science and Engineering* 71 (1–2):23-29. doi: <http://dx.doi.org/10.1016/j.petrol.2009.12.009>.

Iglauer, Stefan, Wolfgang Wüiling, Christopher H. Pentland, Saleh K. Al-Mansoori, and Martin J. Blunt. 2011b. "Capillary-Trapping Capacity of Sandstones and Sandpacks." 16 (04):778-783. doi: 10.2118/120960-PA.

Iglesias, Guillermo Ramon, Wolfgang Wachter, Silvia Ahualli, and Otto Glatter. 2011. "Interactions between large colloids and surfactants." *Soft Matter* 7 (10):4619-4622. doi: 10.1039/C1SM05177F.

IPCC, 2005. 2005. Intergovernmental Panel on Climate Change (IPCC) (2005), IPCC special report on

carbon dioxide capture and storage, prepared by Working Group III of the Intergovernmental Panel on Climate Change, Cambridge University Press. In *Cambridge, United Kingdom and New York, NY, USA*.

Israelachvili, Jacob N. 2011. "17 - Adhesion and Wetting Phenomena." In *Intermolecular and Surface Forces (Third Edition)*, 415-467. San Diego: Academic Press.

Jadhunandan, P. P., and N. R. Morrow. 1995. "Effect of Wettability on Waterflood Recovery for Crude-Oil/Brine/Rock Systems." *SPE Journal* 10 (1):40-46. doi: 10.2118/22597-PA.

Jarrell, PM, CE Fox, MH Stein, and SL Webb. 2002. "Practical aspects of CO2 flooding: SPE Monograph v. 22, Henry L." *Doherty Series, Richardson, Texas*.

Jarvie, Helen P., Hisham Al-Obaidi, Stephen M. King, Michael J. Bowes, M. Jayne Lawrence, Alex F. Drake, Mark A. Green, and Peter J. Dobson. 2009. "Fate of Silica Nanoparticles in Simulated Primary Wastewater Treatment." *Environmental Science & Technology* 43 (22):8622-8628. doi: 10.1021/es901399q.

Jennings Jr, Harley Y. 1967. "The effect of temperature and pressure on the interfacial tension of benzene-water and normal decane-water." *Journal of Colloid and Interface Science* 24 (3):323-329. doi: [http://dx.doi.org/10.1016/0021-9797\(67\)90257-3](http://dx.doi.org/10.1016/0021-9797(67)90257-3).

Jones Jr, Frank O. 1964. "Influence of chemical composition of water on clay blocking of permeability." *Journal of Petroleum Technology* 16 (04):441-446.

Jones, Nicole, Binata Ray, Koodali T. Ranjit, and Adhar C. Manna. 2008. "Antibacterial activity of ZnO nanoparticle suspensions on a broad spectrum of microorganisms." *FEMS Microbiology Letters* 279 (1):71-76. doi: 10.1111/j.1574-6968.2007.01012.x.

- Ju, Binshan, and Tailiang Fan. 2009. "Experimental study and mathematical model of nanoparticle transport in porous media." *Powder Technology* 192 (2):195-202. doi: <http://dx.doi.org/10.1016/j.powtec.2008.12.017>.
- Ju, Binshan, Tailiang Fan, and Mingxue Ma. 2006. "Enhanced oil recovery by flooding with hydrophilic nanoparticles." *China Particuology* 4 (1):41-46. doi: [http://dx.doi.org/10.1016/S1672-2515\(07\)60232-2](http://dx.doi.org/10.1016/S1672-2515(07)60232-2).
- Jung, Jong-Won, and Jiamin Wan. 2012. "Supercritical CO<sub>2</sub> and Ionic Strength Effects on Wettability of Silica Surfaces: Equilibrium Contact Angle Measurements." *Energy & Fuels* 26 (9):6053-6059. doi: 10.1021/ef300913t.
- Kallury, Krishna M. R., Peter M. Macdonald, and Michael Thompson. 1994. "Effect of Surface Water and Base Catalysis on the Silanization of Silica by (Aminopropyl)alkoxysilanes Studied by X-ray Photoelectron Spectroscopy and <sup>13</sup>C Cross-Polarization/Magic Angle Spinning Nuclear Magnetic Resonance." *Langmuir* 10 (2):492-499. doi: 10.1021/la00014a025.
- Karimi, Ali, Zahra Fakhroueian, Alireza Bahramian, Nahid Pour Khiabani, Jabar Babae Darabad, Reza Azin, and Sharareh Arya. 2012a. "Wettability Alteration in Carbonates using Zirconium Oxide Nanofluids: EOR Implications." *Energy & Fuels* 26 (2):1028-1036. doi: 10.1021/ef201475u.
- Karimi, Mahvash, Maziyar Mahmoodi, Ali Niazi, Yahya Al-Wahaibi, and Shahab Ayatollahi. 2012b. "Investigating wettability alteration during MEOR process, a micro/macro scale analysis." *Colloids and Surfaces B: Biointerfaces* 95:129-136. doi: <http://dx.doi.org/10.1016/j.colsurfb.2012.02.035>.
- Kaszuba, Michael, David McKnight, Malcolm T. Connah, Fraser K. McNeil-Watson, and Ulf Nobbmann. 2008. "Measuring sub nanometre sizes using dynamic light scattering." *Journal of Nanoparticle Research* 10 (5):823-829. doi: 10.1007/s11051-007-9317-4.
- Kaveh, N. Shojai, E. S. J. Rudolph, P. van Hemert, W. R. Rossen, and K. H. Wolf. 2014. "Wettability Evaluation of a CO<sub>2</sub>/Water/Bentheimer Sandstone System: Contact Angle, Dissolution, and Bubble Size." *Energy & Fuels* 28 (6):4002-4020. doi: 10.1021/ef500034j.
- Kewen, Li, and Firoozabadi Abbas. 2000. "Experimental Study of Wettability Alteration to Preferential Gas-Wetting in Porous Media and Its Effects." *SPE Journal* 3 (02):139-149. doi: 10.2118/62515-PA.
- Kim, Wun-gwi, Hyun Uk Kang, Kang-min Jung, and Sung Hyun Kim. 2008. "Synthesis of Silica Nanofluid and Application to CO<sub>2</sub> Absorption." *Separation Science and Technology* 43 (11-12):3036-3055. doi: 10.1080/01496390802063804.
- Kirby, Brian J., and Ernest F. Hasselbrink. 2004. "Zeta potential of microfluidic substrates: 1. Theory, experimental techniques, and effects on separations." *Electrophoresis* 25 (2):187-202. doi: 10.1002/elps.200305754.

- Krevor, Samuel, Martin J. Blunt, Sally M. Benson, Christopher H. Pentland, Catriona Reynolds, Ali Al-Menhali, and Ben Niu. 2015. "Capillary trapping for geologic carbon dioxide storage – From pore scale physics to field scale implications." *International Journal of Greenhouse Gas Control* 40:221-237. doi: <http://dx.doi.org/10.1016/j.ijggc.2015.04.006>.
- Krevor, Samuel C. M., Ronny Pini, Lin Zuo, and Sally M. Benson. 2012. "Relative permeability and trapping of CO<sub>2</sub> and water in sandstone rocks at reservoir conditions." *Water Resources Research* 48 (2):n/a-n/a. doi: 10.1029/2011WR010859.
- Krevor, Samuel, Catriona Reynolds, Ali Al-Menhali, and Ben Niu. 2016. "The Impact of Reservoir Conditions and Rock Heterogeneity on CO<sub>2</sub>-Brine Multiphase Flow in Permeable Sandstone." *Petrophysics* 57 (1):12-18.
- Kulak, Alexander, Simon R. Hall, and Stephen Mann. 2004. "Single-step fabrication of drug-encapsulated inorganic microspheres with complex form by sonication-induced nanoparticle assembly." *Chemical Communications* (5):576-577. doi: 10.1039/B314465H.
- Kumar, Suresh, Rahul R. Nair, Premlal B. Pillai, Satyendra Nath Gupta, M. A. R. Iyengar, and A. K. Sood. 2014. "Graphene Oxide–MnFe<sub>2</sub>O<sub>4</sub> Magnetic Nanohybrids for Efficient Removal of Lead and Arsenic from Water." *ACS Applied Materials & Interfaces* 6 (20):17426-17436. doi: 10.1021/am504826q.
- Kundu, Partha, Akanksha Agrawal, Haaris Mateen, and Indra M. Mishra. 2013. "Stability of oil-in-water macro-emulsion with anionic surfactant: Effect of electrolytes and temperature." *Chemical Engineering Science* 102:176-185. doi: <http://dx.doi.org/10.1016/j.ces.2013.07.050>.
- Kunieda, Hironobu, and Reiko Aoki. 1996. "Effect of Added Salt on the Maximum Solubilization in an Ionic-Surfactant Microemulsion." *Langmuir* 12 (24):5796-5799. doi: 10.1021/la960472k.
- Kvítek, Libor, Aleš Panáček, Jana Soukupová, Milan Kolář, Renata Večeřová, Robert Prucek, Mirka Holecová, and Radek Zbořil. 2008. "Effect of Surfactants and Polymers on Stability and Antibacterial Activity of Silver Nanoparticles (NPs)." *The Journal of Physical Chemistry C* 112 (15):5825-5834. doi: 10.1021/jp711616v.
- Lackner, Klaus S. 2003. "Climate change. A guide to CO<sub>2</sub> sequestration." *Science* 300 (5626):1677-1678. doi: 10.1126/science.1079033.
- Lager, A, KJ Webb, and CJJ Black. 2007. "Impact of brine chemistry on oil recovery." IOR 2007-14th European Symposium on Improved Oil Recovery.
- Lan, Qiang, Fei Yang, Shuiyan Zhang, Shangying Liu, Jian Xu, and Dejun Sun. 2007. "Synergistic effect of silica nanoparticle and cetyltrimethyl ammonium bromide on the stabilization of O/W emulsions." *Colloids and Surfaces A:*

*Physicochemical and Engineering Aspects* 302 (1–3):126-135. doi: <http://dx.doi.org/10.1016/j.colsurfa.2007.02.010>.

- Lander, Lorraine M., Lisa M. Siewierski, William J. Brittain, and Erwin A. Vogler. 1993. "A systematic comparison of contact angle methods." *Langmuir* 9 (8):2237-2239. doi: 10.1021/la00032a055.
- Leach, R. O., O. R. Wagner, H. W. Wood, and C. F. Harpke. 1962. "A Laboratory and Field Study of Wettability Adjustment in Water Flooding." *Journal of Petroleum Technology* 14 (02):206-212. doi: 10.2118/119-PA.
- Lee, Sang Soo, Frank Heberling, Neil C. Sturchio, Peter J. Eng, and Paul Fenter. 2016. "Surface Charge of the Calcite (104) Terrace Measured by Rb<sup>+</sup> Adsorption in Aqueous Solutions Using Resonant Anomalous X-ray Reflectivity." *The Journal of Physical Chemistry C* 120 (28):15216-15223. doi: 10.1021/acs.jpcc.6b04364.
- Legens, Christelle, Herve Toulhoat, Louis Cuiec, Frederic Villieras, and Thierry Palermo. 1999. "Wettability Change Related to Adsorption of Organic Acids on Calcite: Experimental and Ab Initio Computational Studies." *SPE Journal* 4 (04):328-333. doi: 10.2118/57721-PA.
- Leong, T. S. H., T. J. Wooster, S. E. Kentish, and M. Ashokkumar. 2009. "Minimising oil droplet size using ultrasonic emulsification." *Ultrasonics Sonochemistry* 16 (6):721-727. doi: <http://dx.doi.org/10.1016/j.ultsonch.2009.02.008>.
- Li, Kewen, and Roland N. Horne. 2006. "Generalized Scaling Approach for Spontaneous Imbibition: An Analytical Model." *SPE Reservoir Evaluation & Engineering* 9 (03):251-258. doi: 10.2118/77544-PA.
- Li, Wei, Jian-hua Zhu, and Jian-hua Qi. 2007. "Application of nano-nickel catalyst in the viscosity reduction of Liaohe extra-heavy oil by aqua-thermolysis." *Journal of Fuel Chemistry and Technology* 35 (2):176-180. doi: [http://dx.doi.org/10.1016/S1872-5813\(07\)60016-4](http://dx.doi.org/10.1016/S1872-5813(07)60016-4).
- Li, Xingxun, and Xianfeng Fan. 2015. "Effect of CO<sub>2</sub> phase on contact angle in oil-wet and water-wet pores." *International Journal of Greenhouse Gas Control* 36:106-113. doi: <http://dx.doi.org/10.1016/j.ijggc.2015.02.017>.
- Li, Yan Vivian, and Lawrence M. Cathles. 2014. "Retention of silica nanoparticles on calcium carbonate sands immersed in electrolyte solutions." *Journal of Colloid and Interface Science* 436 (0):1-8. doi: <http://dx.doi.org/10.1016/j.jcis.2014.08.072>.
- Limage, Stéphanie, Jurgen Krägel, Murielle Schmitt, Christian Dominici, Reinhard Müller, and Mickael Antoni. 2010. "Rheology and Structure Formation in Diluted Mixed Particle–Surfactant Systems." *Langmuir* 26 (22):16754-16761. doi: 10.1021/la102473s.

- Lin, M. Y., H. M. Lindsay, D. A. Weitz, R. Klein, R. C. Ball, and P. Meakin. 1990. "Universal diffusion-limited colloid aggregation." *Journal of Physics: Condensed Matter* 2 (13):3093.
- Liu, Kuan-Liang, Kirtiprakash Kondiparty, Alex D. Nikolov, and Darsh Wasan. 2012a. "Dynamic Spreading of Nanofluids on Solids Part II: Modeling." *Langmuir* 28 (47):16274-16284. doi: 10.1021/la302702g.
- Liu, Y., M. Tourbin, S. Lachaize, and P. Guiraud. 2013a. "Silica nanoparticles separation from water: Aggregation by cetyltrimethylammonium bromide (CTAB)." *Chemosphere* 92 (6):681-687. doi: <http://dx.doi.org/10.1016/j.chemosphere.2013.03.048>.
- Liu, Yanping, Mallorie Tourbin, Sébastien Lachaize, and Pascal Guiraud. 2012b. "Silica Nanoparticle Separation from Water by Aggregation with AlCl<sub>3</sub>." *Industrial & Engineering Chemistry Research* 51 (4):1853-1863. doi: 10.1021/ie200672t.
- Liu, Yi, Chengjun Sun, Trudy Bolin, Tianpin Wu, Yuzi Liu, Michael Sternberg, Shouheng Sun, and Xiao-Min Lin. 2013b. "Kinetic Pathway of Palladium Nanoparticle Sulfidation Process at High Temperatures." *Nano Letters* 13 (10):4893-4901. doi: 10.1021/nl402768b.
- Lohse, Samuel E., and Catherine J. Murphy. 2012. "Applications of Colloidal Inorganic Nanoparticles: From Medicine to Energy." *Journal of the American Chemical Society* 134 (38):15607-15620. doi: 10.1021/ja307589n.
- London, Gabor, Gregory T. Carroll, and Ben L. Feringa. 2013. "Silanization of quartz, silicon and mica surfaces with light-driven molecular motors: construction of surface-bound photo-active nanolayers." *Organic & Biomolecular Chemistry* 11 (21):3477-3483. doi: 10.1039/C3OB40276B.
- Love, J. Christopher, Lara A. Estroff, Jennah K. Kriebel, Ralph G. Nuzzo, and George M. Whitesides. 2005. "Self-Assembled Monolayers of Thiolates on Metals as a Form of Nanotechnology." *Chemical Reviews* 105 (4):1103-1170. doi: 10.1021/cr0300789.
- Lu, Gui, Yuan-Yuan Duan, and Xiao-Dong Wang. 2014. "Surface tension, viscosity, and rheology of water-based nanofluids: a microscopic interpretation on the molecular level." *Journal of Nanoparticle Research* 16 (9):1-11. doi: 10.1007/s11051-014-2564-2.
- Ma, Huan, Mingxiang Luo, and Lenore L. Dai. 2008. "Influences of surfactant and nanoparticle assembly on effective interfacial tensions." *Physical Chemistry Chemical Physics* 10 (16):2207-2213. doi: 10.1039/B718427C.
- Ma, Kun, Leyu Cui, Yezi Dong, Tianlong Wang, Chang Da, George J. Hirasaki, and Sibani Lisa Biswal. 2013. "Adsorption of cationic and anionic surfactants on natural and synthetic carbonate materials." *Journal of Colloid and Interface Science* 408:164-172. doi: <http://dx.doi.org/10.1016/j.jcis.2013.07.006>.

- Maerker, JM, and WW Gale. 1992. "Surfactant flood process design for Loudon." *SPE reservoir engineering* 7 (01):36-44.
- Maghzi, Ali, Ali Mohebbi, Riyaz Kharrat, and MohammadHossein Ghazanfari. 2011. "Pore-Scale Monitoring of Wettability Alteration by Silica Nanoparticles During Polymer Flooding to Heavy Oil in a Five-Spot Glass Micromodel." *Transport in Porous Media* 87 (3):653-664. doi: 10.1007/s11242-010-9696-3.
- Mahadevan, Jagan. 2012. "Comments on the paper titled "Contact angle measurements of CO<sub>2</sub>-water-quartz/calcite systems in the perspective of carbon sequestration": A case of contamination?" *International Journal of Greenhouse Gas Control* 7 (0):261-262. doi: <http://dx.doi.org/10.1016/j.ijggc.2011.09.002>.
- Mahbubul, I. M., Tet Hien Chong, S. S. Khaleduzzaman, I. M. Shahrul, R. Saidur, B. D. Long, and M. A. Amalina. 2014. "Effect of Ultrasonication Duration on Colloidal Structure and Viscosity of Alumina-Water Nanofluid." *Industrial & Engineering Chemistry Research* 53 (16):6677-6684. doi: 10.1021/ie500705j.
- Mahbubul, I. M., R. Saidur, M. A. Amalina, and M. E. Niza. 2016. "Influence of ultrasonication duration on rheological properties of nanofluid: An experimental study with alumina-water nanofluid." *International Communications in Heat and Mass Transfer*. doi: <http://dx.doi.org/10.1016/j.icheatmasstransfer.2016.05.014>.
- Mahdi Jafari, Seid, Yinghe He, and Bhesh Bhandari. 2006. "Nano-Emulsion Production by Sonication and Microfluidization—A Comparison." *International Journal of Food Properties* 9 (3):475-485. doi: 10.1080/10942910600596464.
- Mandal, Ajay, and Achinta Bera. 2012a. "Surfactant Stabilized Nanoemulsion: Characterization and Application in Enhanced Oil Recovery." *World Academy of Science, Engineering and Technology* 67:21-26.
- Mandal, Ajay, and Achinta Bera. 2012b. "Surfactant stabilized nanoemulsion: characterization and application in enhanced oil recovery." *World Academy of Science, Engineering and Technology, International Journal of Chemical, Molecular, Nuclear, Materials and Metallurgical Engineering* 6 (7):537-542.
- Marcolongo, Juan P., and Martín Mirenda. 2011. "Thermodynamics of Sodium Dodecyl Sulfate (SDS) Micellization: An Undergraduate Laboratory Experiment." *Journal of Chemical Education* 88 (5):629-633. doi: 10.1021/ed900019u.
- Marmur, Abraham. 2006. "Soft contact: measurement and interpretation of contact angles." *Soft Matter* 2 (1):12-17. doi: 10.1039/B514811C.
- Mason, Geoffrey, and Norman R. Morrow. 2013. "Developments in spontaneous imbibition and possibilities for future work." *Journal of Petroleum Science*

- Mayer, E. H., R. L. Berg, J. D. Carmichael, and R. M. Weinbrandt. 1983. "Alkaline Injection for Enhanced Oil Recovery - A Status Report." *Journal of Petroleum Technology* 35 (01):209-221. doi: 10.2118/8848-PA.
- Mc Caffery, Frank G., and Necmettin Mungan. 1970. "Contact Angle And Interfacial Tension Studies of Some Hydrocarbon-Water-Solid Systems." doi: 10.2118/70-03-04.
- McKenna, Caroline E., Mona Marie Knock, and Colin D. Bain. 2000. "First-Order Phase Transition in Mixed Monolayers of Hexadecyltrimethylammonium Bromide and Tetradecane at the Air–Water Interface." *Langmuir* 16 (14):5853-5855. doi: 10.1021/la000675f.
- Metin, Cigdem O., Jimmie R. Baran, and Quoc P. Nguyen. 2012a. "Adsorption of surface functionalized silica nanoparticles onto mineral surfaces and decane/water interface." *Journal of Nanoparticle Research* 14 (11):1246. doi: 10.1007/s11051-012-1246-1.
- Metin, Cigdem O., Roger T. Bonnecaze, Larry W. Lake, Caetano R. Miranda, and Quoc P. Nguyen. 2012b. "Aggregation kinetics and shear rheology of aqueous silica suspensions." *Applied Nanoscience* 4 (2):169-178. doi: 10.1007/s13204-012-0185-6.
- Metin, CigdemO, LarryW Lake, CaetanoR Miranda, and QuocP Nguyen. 2011. "Stability of aqueous silica nanoparticle dispersions." *Journal of Nanoparticle Research* 13 (2):839-850. doi: 10.1007/s11051-010-0085-1.
- Metz, Bert, Ogunlade Davidson, HC De Coninck, Manuela Loos, and LA Meyer. 2005. IPCC, 2005: IPCC special report on carbon dioxide capture and storage. Prepared by Working Group III of the Intergovernmental Panel on Climate Change. In *Cambridge, United Kingdom and New York, NY, USA*.
- Mihajlovic, Slavica, Živko Sekulic, Aleksandra Dakovic, Dusica Vucinic\*, Vladimir Jovanovic, and Jovica Stojanovic. 2009. "Surface Properties of Natural Calcite Filler Treated with Stearic Acid." *Ceramics – Silikáty* 53 (4):268-275.
- Mirkin, Chad A. 2005. "The Beginning of a Small Revolution." *Small* 1 (1):14-16. doi: 10.1002/smll.200400092.
- Moghaddam, Nazari, Rasoul, Alireza Bahramian, Zahra Fakhroueian, Ali Karimi, and Sharareh Arya. 2015. "Comparative Study of Using Nanoparticles for Enhanced Oil Recovery: Wettability Alteration of Carbonate Rocks." *Energy & Fuels* 29 (4):2111-2119. doi: 10.1021/ef5024719.
- Mohammed, Mohammedalmojtaba, and Tayfun Babadagli. 2014. "Alteration of Matrix Wettability During Alternate Injection of Hot-water/Solvent into

Heavy-oil Containing Fractured Reservoirs." SPE Heavy Oil Conference-Canada, Calgary, Alberta, Canada 2014/6/10/.

- Mondragon, Rosa, J. Enrique Julia, Antonio Barba, and Juan Carlos Jarque. 2012. "Characterization of silica–water nanofluids dispersed with an ultrasound probe: A study of their physical properties and stability." *Powder Technology* 224:138-146. doi: <http://dx.doi.org/10.1016/j.powtec.2012.02.043>.
- Morrow, Norman, and Jill Buckley. 2011. "Improved Oil Recovery by Low-Salinity Waterflooding." *Journal of Petroleum Technology* 63 (05):106-112. doi: 10.2118/129421-JPT.
- Morrow, Norman R., and Geoffrey Mason. 2001. "Recovery of oil by spontaneous imbibition." *Current Opinion in Colloid & Interface Science* 6 (4):321-337. doi: [http://dx.doi.org/10.1016/S1359-0294\(01\)00100-5](http://dx.doi.org/10.1016/S1359-0294(01)00100-5).
- Morse, John W., and Rolf S. Arvidson. 2002. "The dissolution kinetics of major sedimentary carbonate minerals." *Earth-Science Reviews* 58 (1–2):51-84. doi: [http://dx.doi.org/10.1016/S0012-8252\(01\)00083-6](http://dx.doi.org/10.1016/S0012-8252(01)00083-6).
- Mungan, Necmettin. 1965. "Permeability reduction through changes in pH and salinity." *Journal of Petroleum Technology* 17 (12):1,449-1,453.
- Munshi, A. M., V. N. Singh, Mukesh Kumar, and J. P. Singh. 2008. "Effect of nanoparticle size on sessile droplet contact angle." *Journal of Applied Physics* 103 (8). doi: <http://dx.doi.org/10.1063/1.2912464>.
- Murshed, S. M. Sohel, Tan Say-Hwa, and Nguyen Nam-Trung. 2008. "Temperature dependence of interfacial properties and viscosity of nanofluids for droplet-based microfluidics." *Journal of Physics D: Applied Physics* 41 (8):085502.
- Najafabadi, Nariman Fathi, Mojdeh Delshad, Kamy Sepehrnoori, Quoc Phuc Nguyen, and Jieyuan Zhang. 2008. "Chemical Flooding of Fractured Carbonates Using Wettability Modifiers." SPE Symposium on Improved Oil Recovery, Tulsa, Oklahoma, USA, 2008/1/1/.
- Nakamura, Akihiro, Hitoshi Furuta, Masayoshi Kato, Hirokazu Maeda, and Yasunori Nagamatsu. 2003. "Effect of soybean soluble polysaccharides on the stability of milk protein under acidic conditions." *Food Hydrocolloids* 17 (3):333-343. doi: [http://dx.doi.org/10.1016/S0268-005X\(02\)00095-4](http://dx.doi.org/10.1016/S0268-005X(02)00095-4).
- Nasralla, Ramez A., Mohammed A. Bataweel, and Hisham A. Nasr-El-Din. 2013. "Investigation of Wettability Alteration and Oil-Recovery Improvement by Low-Salinity Water in Sandstone Rock." *Journal of Canadian Petroleum Technology* 52 (02):144-154. doi: 10.2118/146322-PA.
- Nelson, RC, JB Lawson, DR Thigpen, and GL Stegemeier. 1984. "Cosurfactant-enhanced alkaline flooding." SPE Enhanced Oil Recovery Symposium.

- Nikolov, Alex, Kirti Kondiparty, and Darsh Wasan. 2010. "Nanoparticle Self-Structuring in a Nanofluid Film Spreading on a Solid Surface." *Langmuir* 26 (11):7665-7670. doi: 10.1021/la100928t.
- Nooney, Robert I., Angela White, Christy O'Mahony, Claire O'Connell, Susan M. Kelleher, Stephen Daniels, and Colette McDonagh. 2015. "Investigating the colloidal stability of fluorescent silica nanoparticles under isotonic conditions for biomedical applications." *Journal of Colloid and Interface Science* 456:50-58. doi: <http://dx.doi.org/10.1016/j.jcis.2015.05.051>.
- Nwideo, Lezorgia N., Sarmad Al-Ansari, Ahmed Barifcani, Mohammad Sarmadivaleh, and Stefan Iglauer. 2016a. "Nanofluids for Enhanced Oil Recovery Processes: Wettability Alteration Using Zirconium Oxide." Offshore Technology Conference Asia, Kuala Lumpur, Malaysia, 2016/3/22/.
- Nwideo, Lezorgia N., Sarmad Al-Ansari, Ahmed Barifcani, Mohammad Sarmadivaleh, Maxim Lebedev, and Stefan Iglauer. 2017a. "Nanoparticles influence on wetting behaviour of fractured limestone formation." *Journal of Petroleum Science and Engineering* 149:782-788. doi: <http://dx.doi.org/10.1016/j.petrol.2016.11.017>.
- Nwideo, Lezorgia N., Sarmad Al-Ansari, Ahmed Barifcani, Mohammad Sarmadivaleh, Lebedev Maxim, and Stefan Iglauer. 2016b. "Nanoparticles Influence on Wetting Behaviour of Fractured Limestone Formation." *Journal of Petroleum Science and Engineering*. doi: <http://dx.doi.org/10.1016/j.petrol.2016.11.017>.
- Nwideo, Lezorgia N., Maxim Lebedev, Ahmed Barifcani, Mohammad Sarmadivaleh, and Stefan Iglauer. 2017b. "Wettability alteration of oil-wet limestone using surfactant-nanoparticle formulation." *Journal of Colloid and Interface Science* 504:334-345. doi: <https://doi.org/10.1016/j.jcis.2017.04.078>.
- Okubo, T. 1995. "Surface Tension of Structured Colloidal Suspensions of Polystyrene and Silica Spheres at the Air-Water Interface." *Journal of Colloid and Interface Science* 171 (1):55-62. doi: <http://dx.doi.org/10.1006/jcis.1995.1150>.
- Onyekonwu, Mike O., and Naomi A. Ogolo. 2010. "Investigating the Use of Nanoparticles in Enhancing Oil Recovery." Nigeria Annual International Conference and Exhibition, Tinapa - Calabar, Nigeria 2010/1/1/.
- Orr, Franklin M. 2009. "Onshore Geologic Storage of CO<sub>2</sub>." *Science* 325 (5948):1656-1658. doi: 10.1126/science.1175677.
- Paik, Ungyu, Jang Yul Kim, and Vincent A. Hackley. 2005. "Rheological and electrokinetic behavior associated with concentrated nanosize silica hydrosols." *Materials Chemistry and Physics* 91 (1):205-211. doi: <http://dx.doi.org/10.1016/j.matchemphys.2004.11.011>.
- Pastrana-Martínez, Luisa M., Nuno Pereira, Rui Lima, Joaquim L. Faria, Helder T. Gomes, and Adrián M. T. Silva. 2015. "Degradation of diphenhydramine by

- photo-Fenton using magnetically recoverable iron oxide nanoparticles as catalyst." *Chemical Engineering Journal* 261:45-52. doi: <https://doi.org/10.1016/j.cej.2014.04.117>.
- Pedersen, Karen Schou, Peter L Christensen, and Jawad Azeem Shaikh. 2014. *Phase behavior of petroleum reservoir fluids*: CRC Press.
- Perez, J. Manuel. 2007. "Iron oxide nanoparticles: Hidden talent." *Nature Nanotechnology*; London 2 (9):535-536. doi: <http://dx.doi.org/dbgw.lis.curtin.edu.au/10.1038/nnano.2007.282>.
- Petosa, Adamo R., Deb P. Jaisi, Ivan R. Quevedo, Menachem Elimelech, and Nathalie Tufenkji. 2010. "Aggregation and Deposition of Engineered Nanomaterials in Aquatic Environments: Role of Physicochemical Interactions." *Environmental Science & Technology* 44 (17):6532-6549. doi: 10.1021/es100598h.
- Petzold, Gudrun, Rosana Rojas-Reyna, Mandy Mende, and Simona Schwarz. 2009. "Application Relevant Characterization of Aqueous Silica Nanodispersions." *Journal of Dispersion Science and Technology* 30 (8):1216-1222. doi: 10.1080/01932690802701887.
- Philippe Sciau, Claude Mirguet, Christian Roucau, Delhia Chabanne, Max Schvoerer. 2009. "Double nanoparticle layer in a 12th century lustreware decoration: accident or technological mastery." *Journal of Nano Research* 8:133-139. doi: 10.4028/www.scientific.net/JNanoR.8.133.
- Pokrovsky, O. S., and J. Schott. 2002. "Surface Chemistry and Dissolution Kinetics of Divalent Metal Carbonates." *Environmental Science & Technology* 36 (3):426-432. doi: 10.1021/es010925u.
- Ponmani, Swaminathan, R. Nagarajan, and Jitendra S. Sangwai. 2015. "Effect of Nanofluids of CuO and ZnO in Polyethylene Glycol and Polyvinylpyrrolidone on the Thermal, Electrical, and Filtration-Loss Properties of Water-Based Drilling Fluids." *SPE Journal* 21 (2):405-415. doi: 10.2118/178919-PA.
- Ponmani, Swaminathan, R. Nagarajan, and Jitendra S. Sangwai. 2016. "Effect of Nanofluids of CuO and ZnO in Polyethylene Glycol and Polyvinylpyrrolidone on the Thermal, Electrical, and Filtration-Loss Properties of Water-Based Drilling Fluids." *SPE Journal* 21 (02):405-415. doi: 10.2118/178919-PA.
- Prey, Du, and E Lefebvre. 1978. "Gravity and capillarity effects on imbibition in porous media." *Society of Petroleum Engineers Journal* 18 (03):195-206.
- Qiao, Weihong, Yingchun Cui, Youyi Zhu, and Hongyan Cai. 2012. "Dynamic interfacial tension behaviors between Guerbet betaine surfactants solution and Daqing crude oil." *Fuel* 102:746-750. doi: <http://dx.doi.org/10.1016/j.fuel.2012.05.046>.

- Quemada, Daniel, and Claudio Berli. 2002. "Energy of interaction in colloids and its implications in rheological modeling." *Advances in Colloid and Interface Science* 98 (1):51-85. doi: [http://dx.doi.org/10.1016/S0001-8686\(01\)00093-8](http://dx.doi.org/10.1016/S0001-8686(01)00093-8).
- Rahman, Taufiq, Maxim Lebedev, Ahmed Barifcani, and Stefan Iglauer. 2016. "Residual trapping of supercritical CO<sub>2</sub> in oil-wet sandstone." *Journal of Colloid and Interface Science* 469:63-68. doi: <http://dx.doi.org/10.1016/j.jcis.2016.02.020>.
- Rajauria, Sukumar, Christopher Axline, Claudia Gottstein, and Andrew N. Cleland. 2015. "High-Speed Discrimination and Sorting of Submicron Particles Using a Microfluidic Device." *Nano Letters* 15 (1):469-475. doi: 10.1021/nl503783p.
- Ramakoteswaa, Rao N., Gahane Leena, and S.V Ranganayakulu. 2014. "Synthesis, Applications and Challenges of Nanofluids – Review." *IOSR Journal of Applied Physics* 21:21-28.
- Rao, Dandina N. 1999. "Wettability Effects in Thermal Recovery Operations." *SPE Reservoir Evaluation & Engineering* 2 (05):420-430. doi: 10.2118/57897-PA.
- Ravera, Francesca, Michele Ferrari, Libero Liggieri, Giuseppe Loglio, Eva Santini, and Alessandra Zanobini. 2008. "Liquid–liquid interfacial properties of mixed nanoparticle–surfactant systems." *Colloids and Surfaces A: Physicochemical and Engineering Aspects* 323 (1–3):99-108. doi: <http://dx.doi.org/10.1016/j.colsurfa.2007.10.017>.
- Ravera, Francesca, Eva Santini, Giuseppe Loglio, Michele Ferrari, and Libero Liggieri. 2006. "Effect of Nanoparticles on the Interfacial Properties of Liquid/Liquid and Liquid/Air Surface Layers." *The Journal of Physical Chemistry B* 110 (39):19543-19551. doi: 10.1021/jp0636468.
- RezaeiDoust, A., T. Puntervold, S. Strand, and T. Austad. 2009. "Smart Water as Wettability Modifier in Carbonate and Sandstone: A Discussion of Similarities/Differences in the Chemical Mechanisms." *Energy & Fuels* 23 (9):4479-4485. doi: 10.1021/ef900185q.
- Roger, G. M., S. Durand-Vidal, O. Bernard, P. Turq, T. M. Perger, and M. Bešter-Rogač. 2008. "Interpretation of Conductivity Results from 5 to 45 °C on Three Micellar Systems below and above the CMC." *The Journal of Physical Chemistry B* 112 (51):16529-16538. doi: 10.1021/jp804971c.
- Rohrer, H. 1995. "The nanometer age: Challenge and chance." *Microelectronic Engineering* 27 (1):3-15. doi: [https://doi.org/10.1016/0167-9317\(94\)00045-V](https://doi.org/10.1016/0167-9317(94)00045-V).
- Roshan, H., A. Z. Al-Yaseri, M. Sarmadivaleh, and S. Iglauer. 2016. "On wettability of shale rocks." *Journal of Colloid and Interface Science* 475:104-111. doi: <http://dx.doi.org/10.1016/j.jcis.2016.04.041>.

- Rostami Ravari, Reza, Skule Strand, and Tor Austad. 2011. "Combined Surfactant-Enhanced Gravity Drainage (SEGD) of Oil and the Wettability Alteration in Carbonates: The Effect of Rock Permeability and Interfacial Tension (IFT)." *Energy & Fuels* 25 (5):2083-2088. doi: 10.1021/ef200085t.
- Roustaei, Abbas, and Hadi Bagherzadeh. 2014. "Experimental investigation of SiO<sub>2</sub> nanoparticles on enhanced oil recovery of carbonate reservoirs." *Journal of Petroleum Exploration and Production Technology*:1-7. doi: 10.1007/s13202-014-0120-3.
- Rubilar, Olga, Mahendra Rai, Gonzalo Tortella, MariaCristina Diez, AmedeaB Seabra, and Nelson Durán. 2013. "Biogenic nanoparticles: copper, copper oxides, copper sulphides, complex copper nanostructures and their applications." *Biotechnology Letters* 35 (9):1365-1375. doi: 10.1007/s10529-013-1239-x.
- Saaltink, Maarten W., Victor Vilarrasa, Francesca De Gaspari, Orlando Silva, Jesús Carrera, and Tobias S. Rötting. 2013. "A method for incorporating equilibrium chemical reactions into multiphase flow models for CO<sub>2</sub> storage." *Advances in Water Resources* 62, Part C:431-441. doi: <http://dx.doi.org/10.1016/j.advwatres.2013.09.013>.
- Sakuma, H., M. P. Andersson, K. Bechgaard, and S. L. S. Stipp. 2014. "Surface Tension Alteration on Calcite, Induced by Ion Substitution." *The Journal of Physical Chemistry C* 118 (6):3078-3087. doi: 10.1021/jp411151u.
- Salager, Jean-Louis, Nelson Marquez, Alain Graciaa, and Jean Lachaise. 2000. "Partitioning of Ethoxylated Octylphenol Surfactants in Microemulsion–Oil–Water Systems: Influence of Temperature and Relation between Partitioning Coefficient and Physicochemical Formulation." *Langmuir* 16 (13):5534-5539. doi: 10.1021/la9905517.
- Salathiel, R. A. 1973. "Oil Recovery by Surface Film Drainage In Mixed-Wettability Rocks." *Journal of Petroleum Technology* 25 (10):1216-1224. doi: 10.2118/4104-PA.
- Saleh, Navid, Traian Sarbu, Kevin Sirk, Gregory V. Lowry, Krzysztof Matyjaszewski, and Robert D. Tilton. 2005. "Oil-in-Water Emulsions Stabilized by Highly Charged Polyelectrolyte-Grafted Silica Nanoparticles†." *Langmuir* 21 (22):9873-9878. doi: 10.1021/la050654r.
- Saleh, TS, and RMY Graves. 1993. "Experimental investigation of linear scaling of micellar displacement in porous media." *SPE paper* 251 (72):2-5.
- Saraji, Soheil, Mohammad Piri, and Lamia Goual. 2014. "The effects of SO<sub>2</sub> contamination, brine salinity, pressure, and temperature on dynamic contact angles and interfacial tension of supercritical CO<sub>2</sub>/brine/quartz systems." *International Journal of Greenhouse Gas Control* 28:147-155. doi: <http://dx.doi.org/10.1016/j.ijggc.2014.06.024>.

- Saravanan, P., R. Gopalan, and V. Chandrasekaran. 2008. "Synthesis and Characterisation of Nanomaterials." *Defence Science Journal* 58 (4):504.
- Sarkheil, Hamid, and Javad Tavakoli. 2015. "Oil-Polluted Water Treatment Using Nano Size Bagasse Optimized- Isotherm Study." *European Online Journal of Natural and Social Sciences* 4 (2):392-400.
- Sarmadivaleh, Mohammad, Ahmed Z. Al-Yaseri, and Stefan Iglauer. 2015. "Influence of temperature and pressure on quartz–water–CO<sub>2</sub> contact angle and CO<sub>2</sub>–water interfacial tension." *Journal of Colloid and Interface Science* 441 (0):59-64. doi: <http://dx.doi.org/10.1016/j.jcis.2014.11.010>.
- Schechter, D. S., D. Zhou, and F. M. Orr. 1994. "Low IFT drainage and imbibition." *Journal of Petroleum Science and Engineering* 11 (4):283-300. doi: [http://dx.doi.org/10.1016/0920-4105\(94\)90047-7](http://dx.doi.org/10.1016/0920-4105(94)90047-7).
- Schembre, Josephina M., Guo-Qing Tang, and Anthony R. Kovalick. 2006. "Interrelationship of Temperature and Wettability on the Relative Permeability of Heavy Oil in Diatomaceous Rocks (includes associated discussion and reply)." *SPE Reservoir Evaluation & Engineering* 9 (03):239-250. doi: 10.2118/93831-PA.
- Schramm, Laurier L. 2000. *Surfactants: fundamentals and applications in the petroleum industry*: Cambridge University Press.
- Schramm, Laurier L., Karin Mannhardt, and Jerry J. Novosad. 1991. "Electrokinetic properties of reservoir rock particles." *Colloids and Surfaces* 55:309-331. doi: [http://dx.doi.org/10.1016/0166-6622\(91\)80102-T](http://dx.doi.org/10.1016/0166-6622(91)80102-T).
- Seethepalli, Anita, Bhargaw Adibhatla, and Kishore K. Mohanty. 2004. "Physicochemical Interactions During Surfactant Flooding of Fractured Carbonate Reservoirs." *SPE Journal* 9 (04):411-418. doi: 10.2118/89423-PA.
- Shah, DO, KS Chan, and VK Bansal. 1977. "The Importance of Interfacial Charge vs Interfacial Tension in Secondary and Tertiary Oil Recovery Processes." Proc. of AIChE 83 rd National Meeting, Houston, Texas.
- ShamsiJazeyi, Hadi, Clarence A. Miller, Michael S. Wong, James M. Tour, and Rafael Verduzco. 2014. "Polymer-coated nanoparticles for enhanced oil recovery." *Journal of Applied Polymer Science* 131 (15):1-13. doi: 10.1002/app.40576.
- Shanshool, Haider Abbsa, Sarmad Foad Al-Anssari, and Sawsan A. M. Mohammed. 2011. "Treatment of high strength acidic industrial chemical wastewater using expanded bed adsorber." *Journal of Engineering* 17 (1):103-115.
- Sharma, Gaurav, and Kishore Mohanty. 2013. "Wettability Alteration in High-Temperature and High-Salinity Carbonate Reservoirs." *SPE Journal* 18 (4):646-655. doi: 10.2118/147306-PA.

- Sharma, MM, and YC Yortsos. 1987. "Fines migration in porous media." *AIChE Journal* 33 (10):1654-1662.
- Sharma, Tushar, Stefan Iglauer, and Jitendra S. Sangwai. 2016. "Silica Nanofluids in an Oilfield Polymer Polyacrylamide: Interfacial Properties, Wettability Alteration, and Applications for Chemical Enhanced Oil Recovery." *Industrial & Engineering Chemistry Research* 55 (48):12387-12397. doi: 10.1021/acs.iecr.6b03299.
- Sharma, Tushar, G. Suresh Kumar, Bo Hyun Chon, and Jitendra S. Sangwai. 2014a. "Thermal stability of oil-in-water Pickering emulsion in the presence of nanoparticle, surfactant, and polymer." *Journal of Industrial and Engineering Chemistry* (0). doi: <http://dx.doi.org/10.1016/j.jiec.2014.07.026>.
- Sharma, Tushar, G. Suresh Kumar, Bo Hyun Chon, and Jitendra S. Sangwai. 2015a. "Thermal stability of oil-in-water Pickering emulsion in the presence of nanoparticle, surfactant, and polymer." *Journal of Industrial and Engineering Chemistry* 22:324-334. doi: <http://dx.doi.org/10.1016/j.jiec.2014.07.026>.
- Sharma, Tushar, G. Suresh Kumar, and Jitendra S. Sangwai. 2015b. "Comparative effectiveness of production performance of Pickering emulsion stabilized by nanoparticle–surfactant–polymer over surfactant–polymer (SP) flooding for enhanced oil recovery for Brownfield reservoir." *Journal of Petroleum Science and Engineering* 129:221-232. doi: <http://dx.doi.org/10.1016/j.petrol.2015.03.015>.
- Sharma, Tushar, G. Suresh Kumar, and Jitendra S. Sangwai. 2014b. "Enhanced oil recovery using oil-in-water (o/w) emulsion stabilized by nanoparticle, surfactant and polymer in the presence of NaCl." *Geosystem Engineering* 17 (3):195-205. doi: 10.1080/12269328.2014.959622.
- Shen, Min, and Daniel E. Resasco. 2009. "Emulsions Stabilized by Carbon Nanotube–Silica Nanohybrids." *Langmuir* 25 (18):10843-10851. doi: 10.1021/la901380b.
- Sheppard, Adrian P, Ji-Youn Arns, Mark A Knackstedt, and W. Val Pinczewski. 2005. "Volume Conservation of the Intermediate Phase in Three-Phase Pore-Network Models." *Transport in Porous Media* 59 (2):155-173. doi: 10.1007/s11242-004-1488-1.
- Shi, Xuetao, Roberto Rosa, and Andrea Lazzeri. 2010. "On the Coating of Precipitated Calcium Carbonate with Stearic Acid in Aqueous Medium." *Langmuir* 26 (11):8474-8482. doi: 10.1021/la904914h.
- Shin, Donghyun, and Debjyoti Banerjee. 2011. "Enhancement of specific heat capacity of high-temperature silica-nanofluids synthesized in alkali chloride salt eutectics for solar thermal-energy storage applications." *International Journal of Heat and Mass Transfer* 54 (5):1064-1070. doi: <https://doi.org/10.1016/j.ijheatmasstransfer.2010.11.017>.

- Shojai Kaveh, N. , E. S. J. Rudolph, P. van Hemert, W. R. Rossen, and K. H. Wolf. 2014. "Wettability Evaluation of a CO<sub>2</sub>/Water/Bentheimer Sandstone System: Contact Angle, Dissolution, and Bubble Size." *Energy & Fuels* 28 (6):4002-4020. doi: 10.1021/ef500034j.
- Shojai Kaveh, N., A. Barnhoorn, and K. H. Wolf. 2016. "Wettability evaluation of silty shale caprocks for CO<sub>2</sub> storage." *International Journal of Greenhouse Gas Control* 49:425-435. doi: <http://dx.doi.org/10.1016/j.ijggc.2016.04.003>.
- Shushan, Debra, and Christopher Marcoux. 2011. "The Rise (and Decline?) of Arab Aid: Generosity and Allocation in the Oil Era." *World Development* 39 (11):1969-1980. doi: <http://dx.doi.org/10.1016/j.worlddev.2011.07.025>.
- Siemons, Nikolai, Hans Bruining, Hein Castelijns, and Karl-Heinz Wolf. 2006. "Pressure dependence of the contact angle in a CO<sub>2</sub>-H<sub>2</sub>O-coal system." *Journal of Colloid and Interface Science* 297 (2):755-761. doi: <http://dx.doi.org/10.1016/j.jcis.2005.11.047>.
- Skaug, Michael J., Liang Wang, Yifu Ding, and Daniel K. Schwartz. 2015. "Hindered Nanoparticle Diffusion and Void Accessibility in a Three-Dimensional Porous Medium." *ACS Nano* 9 (2):2148-2156. doi: 10.1021/acsnano.5b00019.
- Song, Xiaoyun, Zhiwen Qiu, Xiaopeng Yang, Haibo Gong, Shaohua Zheng, Bingqiang Cao, Hongqiang Wang, Helmuth Möhwald, and Dmitry Shchukin. 2014. "Submicron-Lubricant Based on Crystallized Fe<sub>3</sub>O<sub>4</sub> Spheres for Enhanced Tribology Performance." *Chemistry of Materials* 26 (17):5113-5119. doi: 10.1021/cm502426y.
- Spiteri, Elizabeth J., Ruben Juanes, Martin J. Blunt, and Franklin M. Orr. 2008. "A New Model of Trapping and Relative Permeability Hysteresis for All Wettability Characteristics." *SPE* 13 (03):277-288. doi: 10.2118/96448-PA.
- Srikant, R R, D N Rao, M S Subrahmanyam, and Vamsi P Krishna. 2009. "Applicability of cutting fluids with nanoparticle inclusion as coolants in machining." *Proceedings of the Institution of Mechanical Engineers, Part J: Journal of Engineering Tribology* 223 (2):221-225. doi: 10.1243/13506501jet463.
- Standnes, Dag C., and Tor Austad. 2000. "Wettability alteration in chalk: 2. Mechanism for wettability alteration from oil-wet to water-wet using surfactants." *Journal of Petroleum Science and Engineering* 28 (3):123-143. doi: [http://dx.doi.org/10.1016/S0920-4105\(00\)00084-X](http://dx.doi.org/10.1016/S0920-4105(00)00084-X).
- Stipp, S. L. S. 1999. "Toward a conceptual model of the calcite surface: hydration, hydrolysis, and surface potential." *Geochimica et Cosmochimica Acta* 63 (19-20):3121-3131. doi: [http://dx.doi.org/10.1016/S0016-7037\(99\)00239-2](http://dx.doi.org/10.1016/S0016-7037(99)00239-2).
- Stoll, Martin, Jan Hofman, Dick J. Ligthelm, Marinus J. Faber, and Paul van den Hoek. 2008. "Toward Field-Scale Wettability Modification—The Limitations of

Diffusive Transport." *SPE Reservoir Evaluation & Engineering* 11 (03):633-640. doi: 10.2118/107095-PA.

- Strand, S., T. Puntervold, and T. Austad. 2016. "Water based EOR from Clastic Oil Reservoirs by Wettability Alteration: A Review of Chemical Aspects." *Journal of Petroleum Science and Engineering*. doi: <http://dx.doi.org/10.1016/j.petrol.2016.08.012>.
- Strand, Skule, Tor Austad, Tina Puntervold, Eli J. Høgnesen, Martin Olsen, and Sven Michael F. Barstad. 2008. "'Smart Water' for Oil Recovery from Fractured Limestone: A Preliminary Study." *Energy & Fuels* 22 (5):3126-3133. doi: 10.1021/ef800062n.
- Strand, Skule, Eli J. Høgnesen, and Tor Austad. 2006. "Wettability alteration of carbonates—Effects of potential determining ions ( $\text{Ca}^{2+}$  and  $\text{SO}_4^{2-}$ ) and temperature." *Colloids and Surfaces A: Physicochemical and Engineering Aspects* 275 (1–3):1-10. doi: <http://dx.doi.org/10.1016/j.colsurfa.2005.10.061>.
- Stumm, Werner, and James J. Morgan. 1995. *Aquatic chemistry : chemical equilibria and rates in natural waters* 3rd ed. New York Wiley
- Suebsiri, Jitsopa, Malcolm Wilson, and Paitoon Tontiwachwuthikul. 2006. "Life-Cycle Analysis of  $\text{CO}_2$  EOR on EOR and Geological Storage through Economic Optimization and Sensitivity Analysis Using the Weyburn Unit as a Case Study." *Industrial & Engineering Chemistry Research* 45 (8):2483-2488. doi: 10.1021/ie050909w.
- Sui, Dan, Vebjørn Haraldstad Langåker, and Zhixin Yu. 2017. "Investigation of Thermophysical Properties of Nanofluids for Application in Geothermal Energy." *Energy Procedia* 105:5055-5060. doi: <https://doi.org/10.1016/j.egypro.2017.03.1021>.
- Suleimanov, B. A., F. S. Ismailov, and E. F. Veliyev. 2011. "Nanofluid for enhanced oil recovery." *Journal of Petroleum Science and Engineering* 78 (2):431-437. doi: <http://dx.doi.org/10.1016/j.petrol.2011.06.014>.
- Susnar, S. S., H. A. Hamza, and A. W. Neumann. 1994. "Pressure dependence of interfacial tension of hydrocarbon—water systems using axisymmetric drop shape analysis." *Colloids and Surfaces A: Physicochemical and Engineering Aspects* 89 (2–3):169-180. doi: [http://dx.doi.org/10.1016/0927-7757\(94\)80116-9](http://dx.doi.org/10.1016/0927-7757(94)80116-9).
- Syed, S., M. I. Alhazzaa, and M. Asif. 2011. "Treatment of oily water using hydrophobic nano-silica." *Chemical Engineering Journal* 167 (1):99-103. doi: <http://dx.doi.org/10.1016/j.cej.2010.12.006>.
- Tadros, Tharwat F. 2006. *Applied surfactants: principles and applications*: John Wiley & Sons.

- Takahashi, S., and A. R. Kovscek. 2010a. "Spontaneous countercurrent imbibition and forced displacement characteristics of low-permeability, siliceous shale rocks." *Journal of Petroleum Science and Engineering* 71 (1–2):47-55. doi: <http://dx.doi.org/10.1016/j.petrol.2010.01.003>.
- Takahashi, Satoru, and Anthony R. Kovscek. 2010b. "Wettability estimation of low-permeability, siliceous shale using surface forces." *Journal of Petroleum Science and Engineering* 75 (1–2):33-43. doi: <http://dx.doi.org/10.1016/j.petrol.2010.10.008>.
- Tang, GQ, and NR Morrow. 1996. Effect of temperature, salinity and oil composition on wetting behavior and oil recovery by waterflooding. Society of Petroleum Engineers (SPE), Inc., Richardson, TX (United States).
- Tang, Guo-Qing, and Norman R. Morrow. 1999. "Influence of brine composition and fines migration on crude oil/brine/rock interactions and oil recovery." *Journal of Petroleum Science and Engineering* 24 (2–4):99-111. doi: [http://dx.doi.org/10.1016/S0920-4105\(99\)00034-0](http://dx.doi.org/10.1016/S0920-4105(99)00034-0).
- Tang, Guoqing, and Norman R Morrow. 2002. "Injection of dilute brine and crude oil/brine/rock interactions." *Environmental Mechanics: Water, Mass and Energy Transfer in the Biosphere: The Philip Volume*:171-179.
- Tantra, Ratna, Philipp Schulze, and Paul Quincey. 2010. "Effect of nanoparticle concentration on zeta-potential measurement results and reproducibility." *Particuology* 8 (3):279-285. doi: <http://dx.doi.org/10.1016/j.partic.2010.01.003>.
- Täuber, Daniela, Ines Trenkmann, and Christian von Borczyskowski. 2013. "Influence of van der Waals Interactions on Morphology and Dynamics in Ultrathin Liquid Films at Silicon Oxide Interfaces." *Langmuir* 29 (11):3583-3593. doi: 10.1021/la3043796.
- Tavenas, F, P Jean, P Leblond, and S Leroueil. 1983. "The permeability of natural soft clays. Part II: Permeability characteristics." *Canadian Geotechnical Journal* 20 (4):645-660.
- Taylor, Robert, Sylvain Coulombe, Todd Otanicar, Patrick Phelan, Andrey Gunawan, Wei Lv, Gary Rosengarten, Ravi Prasher, and Himanshu Tyagi. 2013. "Small particles, big impacts: A review of the diverse applications of nanofluids." *Journal of Applied Physics* 113 (1):011301. doi: <http://dx.doi.org/10.1063/1.4754271>.
- Thomas, S. 2008. "Enhanced oil recovery-an overview." *Oil & Gas Science and Technology-Revue de l'IFP* 63 (1):9-19.
- Tiab, D, and E. C. Donaldson. 2011. *Petrophysics: theory and practice of measuring reservoir rock and fluid transport properties*: Gulf professional publishing.

- Tong, Rong, Houman D. Hemmati, Robert Langer, and Daniel S. Kohane. 2012. "Photoswitchable Nanoparticles for Triggered Tissue Penetration and Drug Delivery." *Journal of the American Chemical Society* 134 (21):8848-8855. doi: 10.1021/ja211888a.
- Treiber, L. E., and W. W. Owens. 1972. "A Laboratory Evaluation of the Wettability of Fifty Oil-Producing Reservoirs." *SPE Journal* 12 (06):531-540. doi: 10.2118/3526-PA.
- Tsai, De4Hao, SH Kim, TD Corrigan, Raymond J Phaneuf, and Michael R Zachariah. 2005. "Electrostatic-directed deposition of nanoparticles on a field generating substrate." *Nanotechnology* 16 (9):1856.
- van Dijk, Heleen, Arnout R. H. Fischer, Hans J. P. Marvin, and Hans C. M. van Trijp. 2015. "Determinants of stakeholders' attitudes towards a new technology: nanotechnology applications for food, water, energy and medicine." *Journal of Risk Research*:1-22. doi: 10.1080/13669877.2015.1057198.
- Vashisth, Charu, Catherine P. Whitby, Daniel Fornasiero, and John Ralston. 2010. "Interfacial displacement of nanoparticles by surfactant molecules in emulsions." *Journal of Colloid and Interface Science* 349 (2):537-543. doi: <http://dx.doi.org/10.1016/j.jcis.2010.05.089>.
- Vatanparast, H., A. H. Alizadeh, A. Bahramian, and H. Bazdar. 2011. "Wettability Alteration of Low-permeable Carbonate Reservoir Rocks in Presence of Mixed Ionic Surfactants." *Petroleum Science and Technology* 29 (18):1873-1884. doi: 10.1080/10916461003610389.
- Venkatraman, Ashwin, Larry W. Lake, and Russell T. Johns. 2014. "Gibbs Free Energy Minimization for Prediction of Solubility of Acid Gases in Water." *Industrial & Engineering Chemistry Research* 53 (14):6157-6168. doi: 10.1021/ie402265t.
- Vignati, Emanuele, Roberto Piazza, and Thomas P. Lockhart. 2003. "Pickering Emulsions: Interfacial Tension, Colloidal Layer Morphology, and Trapped-Particle Motion." *Langmuir* 19 (17):6650-6656. doi: 10.1021/la034264l.
- Vinogradov, Jan, and Matthew D. Jackson. 2015. "Zeta potential in intact natural sandstones at elevated temperatures." *Geophysical Research Letters* 42 (15):6287-6294. doi: 10.1002/2015GL064795.
- Vledder, Paul, Ivan Ernesto Gonzalez, Julio Cesar Carrera Fonseca, Terence Wells, and Dick Jacob Ligthelm. 2010. "Low Salinity Water Flooding: Proof Of Wettability Alteration On A Field Wide Scale." SPE Improved Oil Recovery Symposium, Tulsa, Oklahoma, USA 2010/1/1/.
- Wagner, O. R., and R. O. Leach. 1959. "Improving Oil Displacement Efficiency by Wettability Adjustment." *SPE Journal* 216:65-72. doi: 10.2118/1101-G.

- Wang, Hui, Nan Yan, Yan Li, Xuhui Zhou, Jian Chen, Binxing Yu, Ming Gong, and Qianwang Chen. 2012. "Fe nanoparticle-functionalized multi-walled carbon nanotubes: one-pot synthesis and their applications in magnetic removal of heavy metal ions." *Journal of Materials Chemistry* 22 (18):9230-9236. doi: 10.1039/C2JM16584H.
- Wang, Jun, Fei Yang, Caifu Li, Shangying Liu, and Dejun Sun. 2008. "Double Phase Inversion of Emulsions Containing Layered Double Hydroxide Particles Induced by Adsorption of Sodium Dodecyl Sulfate." *Langmuir* 24 (18):10054-10061. doi: 10.1021/la8001527.
- Wang, Leizheng, and Kishore Mohanty. 2014. "Enhanced Oil Recovery in Gasflooded Carbonate Reservoirs by Wettability-Altering Surfactants." *SPE Journal* 20 (01):60-69. doi: 10.2118/166283-PA.
- Wang, W, and A Gupta. 1995. "Investigation of the effect of temperature and pressure on wettability using modified pendant drop method." SPE Annual Technical Conference and Exhibition.
- Wasan, Darsh, Alex Nikolov, and Kirti Kondiparty. 2011. "The wetting and spreading of nanofluids on solids: Role of the structural disjoining pressure." *Current Opinion in Colloid & Interface Science* 16 (4):344-349. doi: <http://dx.doi.org/10.1016/j.cocis.2011.02.001>.
- Webb, KJ, CJJ Black, and IJ Edmonds. 2005. "Low salinity oil recovery—The role of reservoir condition corefloods." IOR 2005-13th European Symposium on Improved Oil Recovery.
- Weyl, P. K. 1959. "The change in solubility of calcium carbonate with temperature and carbon dioxide content." *Geochimica et Cosmochimica Acta* 17 (3):214-225. doi: [http://dx.doi.org/10.1016/0016-7037\(59\)90096-1](http://dx.doi.org/10.1016/0016-7037(59)90096-1).
- Whitby, Catherine P., Daniel Fornasiero, and John Ralston. 2009. "Effect of adding anionic surfactant on the stability of Pickering emulsions." *Journal of Colloid and Interface Science* 329 (1):173-181. doi: <http://dx.doi.org/10.1016/j.jcis.2008.09.056>.
- White, Curt M., Brian R. Strazisar, Evan J. Granite, James S. Hoffman, and Henry W. Pennline. 2003. "Separation and Capture of CO<sub>2</sub> from Large Stationary Sources and Sequestration in Geological Formations—Coalbeds and Deep Saline Aquifers." *Journal of the Air & Waste Management Association* 53 (6):645-715. doi: 10.1080/10473289.2003.10466206.
- White, Eliot J, Oren C Baptist, and Carlon Sanford Land. 1964. Formation damage estimated from water sensitivity tests, Patrick Draw area, Wyoming. Bureau of Mines, Laramie, Wyo.(USA). Petroleum Research Center.
- White, Robin J, Rafael Luque, Vitaliy L Budarin, James H Clark, and Duncan J Macquarrie. 2009. "Supported metal nanoparticles on porous materials.

- Methods and applications." *Chemical Society reviews* 38 (2):481-494. doi: 10.1039/b802654h.
- Williams, WC, IC Bang, E Forrest, LW Hu, and J Buongiorno. 2006. "Preparation and characterization of various nanofluids." Proceedings of the NSTI Nanotechnology Conference and Trade Show (Nanotech'06).
- Wilson, Gregory J., Aaron S. Matijasevich, David R. G. Mitchell, Jamie C. Schulz, and Geoffrey D. Will. 2006. "Modification of TiO<sub>2</sub> for Enhanced Surface Properties: Finite Ostwald Ripening by a Microwave Hydrothermal Process." *Langmuir* 22 (5):2016-2027. doi: 10.1021/la052716j.
- Winkler, Katarzyna, Maciej Paszewski, Tomasz Kalwarczyk, Ewelina Kalwarczyk, Tomasz Wojciechowski, Ewa Gorecka, Damian Pocięcha, Robert Holyst, and Marcin Fialkowski. 2011. "Ionic Strength-Controlled Deposition of Charged Nanoparticles on a Solid Substrate." *The Journal of Physical Chemistry C* 115 (39):19096-19103. doi: 10.1021/jp206704s.
- Wolthers, M., D. Di Tommaso, Z. Du, and N. H. de Leeuw. 2012. "Calcite surface structure and reactivity: molecular dynamics simulations and macroscopic surface modelling of the calcite-water interface." *Physical Chemistry Chemical Physics* 14 (43):15145-15157. doi: 10.1039/C2CP42290E.
- Wolthers, Mariëtte, Laurent Charlet, and Philippe Van Cappellen. 2008. "The surface chemistry of divalent metal carbonate minerals; a critical assessment of surface charge and potential data using the charge distribution multi-site ion complexation model." *American Journal of Science* 308 (8):905-941. doi: 10.2475/08.2008.02.
- Wong, Kaufui V., and Omar De Leon. 2010. "Applications of Nanofluids: Current and Future." *Advances in Mechanical Engineering* 2. doi: 10.1155/2010/519659.
- Wu, Stanley, Alex Nikolov, and Darsh Wasan. 2013a. "Cleansing dynamics of oily soil using nanofluids." *Journal of Colloid and Interface Science* 396:293-306. doi: <http://dx.doi.org/10.1016/j.jcis.2013.01.036>.
- Wu, W., H. Bostanci, L. C. Chow, Y. Hong, C. M. Wang, M. Su, and J. P. Kizito. 2013b. "Heat transfer enhancement of PAO in microchannel heat exchanger using nano-encapsulated phase change indium particles." *International Journal of Heat and Mass Transfer* 58 (1):348-355. doi: <https://doi.org/10.1016/j.ijheatmasstransfer.2012.11.032>.
- Wu, Yongfu, Patrick J. Shuler, Mario Blanco, Yongchun Tang, and William A. Goddard. 2008. "An Experimental Study of Wetting Behavior and Surfactant EOR in Carbonates With Model Compounds." *SPE Journal* 13 (1):26-34. doi: 10.2118/99612-PA.
- Xie, Quan, Shunli He, and Wanfeng Pu. 2010. "The effects of temperature and acid number of crude oil on the wettability of acid volcanic reservoir rock from the

- Hailar Oilfield." *Petroleum Science* 7 (1):93-99. doi: 10.1007/s12182-010-0011-2.
- Xie, Xina, William W. Weiss, Zhengxin J. Tong, and Norman R. Morrow. 2005. "Improved Oil Recovery from Carbonate Reservoirs by Chemical Stimulation." 10 (3):276-285. doi: 10.2118/89424-PA.
- Xu, Wei, Subhash C. Ayirala, and Dandina N. Rao. 2008. "Measurement of Surfactant-Induced Interfacial Interactions at Reservoir Conditions." *SPE Journal* 11 (01):83-94. doi: 10.2118/96021-PA.
- Yang, Daoyong, Yongan Gu, and Paitoon Tontiwachwuthikul. 2007. "Wettability Determination of the Reservoir Brine-Reservoir Rock System with Dissolution of CO<sub>2</sub> at High Pressures and Elevated Temperatures." *Energy & Fuels* 22 (1):504-509. doi: 10.1021/ef700383x.
- Yang, Daoyong, Yongan Gu, and Paitoon Tontiwachwuthikul. 2008. "Wettability Determination of the Crude Oil-Reservoir Brine-Reservoir Rock System with Dissolution of CO<sub>2</sub> at High Pressures and Elevated Temperatures." *Energy & Fuels* 22 (4):2362-2371. doi: 10.1021/ef800012w.
- Yavuz, C. T., J. T. Mayo, W. W. Yu, A. Prakash, J. C. Falkner, S. Yean, L. Cong, H. J. Shipley, A. Kan, M. Tomson, D. Natelson, and V. L. Colvin. 2006. "Low-field magnetic separation of monodisperse Fe<sub>3</sub>O<sub>4</sub> nanocrystals." *Science* 314 (5801):964-7. doi: 10.1126/science.1131475.
- Yildiz, Hasan O., and Norman R. Morrow. 1996. "Effect of brine composition on recovery of Moutray crude oil by waterflooding." *Journal of Petroleum Science and Engineering* 14 (3):159-168. doi: [http://dx.doi.org/10.1016/0920-4105\(95\)00041-0](http://dx.doi.org/10.1016/0920-4105(95)00041-0).
- Yotsumoto, Hiroki, and Roe-Hoan Yoon. 1993. "Application of Extended DLVO Theory: I. Stability of Rutile Suspensions." *Journal of Colloid and Interface Science* 157 (2):426-433. doi: <http://dx.doi.org/10.1006/jcis.1993.1205>.
- Yousef, Ali A, Jim Liu, Guy Blanchard, Salah Al-Saleh, Tareq Al-Zahrani, Rashad Al-Zahrani, Hasan Al-Tammar, and Nayef Al-Mulhim. 2012. "Smartwater flooding: industry's first field test in carbonate reservoirs." SPE Annual Technical Conference and Exhibition, San Antonio, Texas.
- Yu-Cheng, Chen, Huang Xin-Chun, Luo Yun-Ling, Chang Yung-Chen, Hsieh You-Zung, and Hsu Hsin-Yun. 2013. "Non-metallic nanomaterials in cancer theranostics: a review of silica- and carbon-based drug delivery systems." *Science and Technology of Advanced Materials* 14 (4):044407.
- Yu, Wenhua, David M. France, Jules L. Routbort, and Stephen U. S. Choi. 2008. "Review and Comparison of Nanofluid Thermal Conductivity and Heat Transfer Enhancements." *Heat Transfer Engineering* 29 (5):432-460. doi: 10.1080/01457630701850851.

- Zabalegui, Aitor, Dhananjay Lokapur, and Hohyun Lee. 2014. "Nanofluid PCMs for thermal energy storage: Latent heat reduction mechanisms and a numerical study of effective thermal storage performance." *International Journal of Heat and Mass Transfer* 78:1145-1154. doi: <https://doi.org/10.1016/j.ijheatmasstransfer.2014.07.051>.
- Zargartalebi, Mohammad, Nasim Barati, and Riyaz Kharrat. 2014. "Influences of hydrophilic and hydrophobic silica nanoparticles on anionic surfactant properties: Interfacial and adsorption behaviors." *Journal of Petroleum Science and Engineering* 119:36-43. doi: <http://dx.doi.org/10.1016/j.petrol.2014.04.010>.
- Zargartalebi, Mohammad, Riyaz Kharrat, and Nasim Barati. 2015. "Enhancement of surfactant flooding performance by the use of silica nanoparticles." *Fuel* 143 (0):21-27. doi: <http://dx.doi.org/10.1016/j.fuel.2014.11.040>.
- Zendehboudi, Sohrab, Mohammad Ali Ahmadi, Amin Reza Rajabzadeh, Nader Mahinpey, and Ioannis Chatzis. 2013. "Experimental study on adsorption of a new surfactant onto carbonate reservoir samples—application to EOR." *The Canadian Journal of Chemical Engineering* 91 (8):1439-1449. doi: 10.1002/cjce.21806.
- Zeppieri, Susana, Jhosgre Rodríguez, and A. L. López de Ramos. 2001. "Interfacial Tension of Alkane + Water Systems†." *Journal of Chemical & Engineering Data* 46 (5):1086-1088. doi: 10.1021/je000245r.
- Zhang, Hua, Alex Nikolov, and Darsh Wasan. 2014. "Enhanced Oil Recovery (EOR) Using Nanoparticle Dispersions: Underlying Mechanism and Imbibition Experiments." *Energy & Fuels* 28 (5):3002-3009. doi: 10.1021/ef500272r.
- Zhang, Hua, T. S. Ramakrishnan, Alex D. Nikolov, and Darsh Wasan. 2016. "Enhanced Oil Recovery (EOR) Driven by Nanofilm Structural Disjoining Pressure: Flooding Experiments and Microvisualization." *Energy & Fuels*. doi: 10.1021/acs.energyfuels.6b00035.
- Zhang, Jieyuan, Quoc Phuc Nguyen, Adam Flaaten, and Gary Arnold Pope. 2008. "Mechanisms of Enhanced Natural Imbibition with Novel Chemicals." SPE Symposium on Improved Oil Recovery, Tulsa, Oklahoma, USA 2008/1/1/.
- Zhang, Lingling, Yunhong Jiang, Yulong Ding, Malcolm Povey, and David York. 2007a. "Investigation into the antibacterial behaviour of suspensions of ZnO nanoparticles (ZnO nanofluids)." *Journal of Nanoparticle Research* 9 (3):479-489. doi: 10.1007/s11051-006-9150-1.
- Zhang, Lu, Lan Luo, Sui Zhao, and Jiayong Yu. 2002. "Studies of Synergism/Antagonism for Lowering Dynamic Interfacial Tensions in Surfactant/Alkali/Acidic Oil Systems, Part 2: Synergism/Antagonism in Binary Surfactant Mixtures." *Journal of Colloid and Interface Science* 251 (1):166-171. doi: <http://dx.doi.org/10.1006/jcis.2002.8293>.

- Zhang, Peimao, Medad T. Tweheyo, and Tor Austad. 2007b. "Wettability alteration and improved oil recovery by spontaneous imbibition of seawater into chalk: Impact of the potential determining ions  $\text{Ca}^{2+}$ ,  $\text{Mg}^{2+}$ , and  $\text{SO}_4^{2-}$ ." *Colloids and Surfaces A: Physicochemical and Engineering Aspects* 301 (1–3):199-208. doi: <http://dx.doi.org/10.1016/j.colsurfa.2006.12.058>.
- Zhang, Tiantian, Michael J. Murphy, Haiyang Yu, Hitesh G. Bagaria, Ki Youl Yoon, Bethany M. Nielson, Christopher W. Bielawski, Keith P. Johnston, Chun Huh, and Steven L. Bryant. 2015. "Investigation of Nanoparticle Adsorption During Transport in Porous Media." *SPE Journal* 20 (04):667-677. doi: 10.2118/166346-PA.
- Zhang, Wen, Andrew G. Stack, and Yongsheng Chen. 2011. "Interaction force measurement between E. coli cells and nanoparticles immobilized surfaces by using AFM." *Colloids and Surfaces B: Biointerfaces* 82 (2):316-324. doi: <http://dx.doi.org/10.1016/j.colsurfb.2010.09.003>.
- Zhang, Yang, Yongsheng Chen, Paul Westerhoff, and John Crittenden. 2009. "Impact of natural organic matter and divalent cations on the stability of aqueous nanoparticles." *Water Research* 43 (17):4249-4257. doi: <http://dx.doi.org/10.1016/j.watres.2009.06.005>.
- Zhao, Zhongkui, Chenguang Bi, Zongshi Li, Weihong Qiao, and Lübo Cheng. 2006. "Interfacial tension between crude oil and decylmethylnaphthalene sulfonate surfactant alkali-free flooding systems." *Colloids and Surfaces A: Physicochemical and Engineering Aspects* 276 (1–3):186-191. doi: <http://dx.doi.org/10.1016/j.colsurfa.2005.10.036>.
- Zheng, Xiuwen, Liying Zhu, Aihui Yan, Xinjun Wang, and Yi Xie. 2003. "Controlling synthesis of silver nanowires and dendrites in mixed surfactant solutions." *Journal of Colloid and Interface Science* 268 (2):357-361. doi: <http://dx.doi.org/10.1016/j.jcis.2003.09.021>.
- Zhu, Dingwei, Yugui Han, Jichao Zhang, Xiaolan Li, and Yujun Feng. 2014. "Enhancing rheological properties of hydrophobically associative polyacrylamide aqueous solutions by hybridizing with silica nanoparticles." *Journal of Applied Polymer Science* 131 (19). doi: 10.1002/app.40876.
- Zhuravlev, L. T. 2000. "The surface chemistry of amorphous silica. Zhuravlev model." *Colloids and Surfaces A: Physicochemical and Engineering Aspects* 173 (1–3):1-38. doi: [http://dx.doi.org/10.1016/S0927-7757\(00\)00556-2](http://dx.doi.org/10.1016/S0927-7757(00)00556-2).

*"Every reasonable effort has been made to acknowledge the owners of copyright material. I would be pleased to hear from any copyright owner who has been omitted or incorrectly acknowledged".*

# APPENDIX A

Inbox - sarmad.al-ansari@postgrad.curtin.edu.au - Outlook

Quick Steps: Reply, Reply All, Forward

**Schmitt Antje** <Antje.Schmitt@hanser.de>  
WG: Copyright

To: Sarmad Foad Jaber Al-Ansari

Action Items Get more apps

Dear Sir,  
we herewith grant you the right to use the figures cited below in your publication. Please make sure to publish a correct copyright note with the figure:  
"from the journal Tenside, Vol. ..., no. ...., 2017, by ... (authors name), © Carl Hanser Verlag GmbH & Co.KG, Muenchen".

If there are any further questions please let me know.

Best Regards  
Antje Schmitt

**Antje Schmitt**  
Assistant to the Managing Director  
Carl Hanser Verlag GmbH & Co. KG  
Kolbergerstrasse 22  
81679 Muenchen / Germany  
T +49 89 99830-200  
F +49 89 99830-225  
Mail: [Antje.Schmitt@hanser.de](mailto:Antje.Schmitt@hanser.de)

Carl Hanser Verlag GmbH & Co. KG  
Sitz und Registergericht: Muenchen HRA 49621  
Personlich haftende Gesellschafterin:  
Carl Hanser Verlagshandlungsgesellschaft mbH  
Sitz und Registergericht: Muenchen HRB 40463  
Geschaeftsfuehrung: Wolfgang Beisler, Stephan D. Joll, Jo Lesdke

---

**Von:** Sarmad Foad Jaber Al-Ansari [<mailto:sarmad.al-ansari@postgrad.curtin.edu.au>]  
**Gesendet:** Mittwoch, 17. Januar 2018 07:42  
**An:** onlinesupport  
**Cc:** [sarmadfoad@yahoo.com](mailto:sarmadfoad@yahoo.com)  
**Betreff:** Copyright

Dear Sir/ Madam  
I am the author of the paper <https://doi.org/10.3139/113.110511>

Schmitt Antje No Items



**Title:** Wettability alteration of oil-wet carbonate by silica nanofluid  
**Author:** Sarmad Al-Anssari,Ahmed Barifcani,Shaobin Wang,Lebedev Maxim,Stefan Iglauer  
**Publication:** Journal of Colloid and Interface Science  
**Publisher:** Elsevier  
**Date:** 1 January 2016

Copyright © 2015 Elsevier Inc. All rights reserved.

Logged in as:  
Sarmad Al-Anssari  
Curtin university  
Account #:  
3001238667

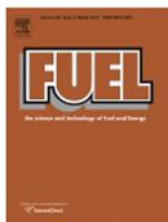
LOGOUT

Please note that, as the author of this Elsevier article, you retain the right to include it in a thesis or dissertation, provided it is not published commercially. Permission is not required, but please ensure that you reference the journal as the original source. For more information on this and on your other retained rights, please visit: <https://www.elsevier.com/about/our-business/policies/copyright#Author-rights>

BACK

CLOSE WINDOW

Copyright © 2018 Copyright Clearance Center, Inc. All Rights Reserved. [Privacy statement](#). [Terms and Conditions](#).  
Comments? We would like to hear from you. E-mail us at [customer@copyright.com](mailto:customer@copyright.com)



**Title:** Effect of temperature and SiO<sub>2</sub> nanoparticle size on wettability alteration of oil-wet calcite

**Author:** Sarmad Al-Anssari, Shaobin Wang, Ahmed Barifcani, Maxim Lebedev, Stefan Iglauer

**Publication:** Fuel

**Publisher:** Elsevier

**Date:** 15 October 2017

© 2017 Elsevier Ltd. All rights reserved.

Logged in as:

Sarmad Al-Anssari  
Curtin university

Account #:  
3001238667

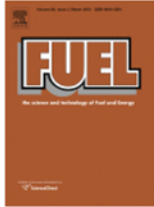
[LOGOUT](#)

Please note that, as the author of this Elsevier article, you retain the right to include it in a thesis or dissertation, provided it is not published commercially. Permission is not required, but please ensure that you reference the journal as the original source. For more information on this and on your other retained rights, please visit: <https://www.elsevier.com/about/our-business/policies/copyright#Author-rights>

[BACK](#)

[CLOSE WINDOW](#)

Copyright © 2018 Copyright Clearance Center, Inc. All Rights Reserved. [Privacy statement](#). [Terms and Conditions](#).  
Comments? We would like to hear from you. E-mail us at [customercare@copyright.com](mailto:customercare@copyright.com)



**Title:** Wettability of nanofluid-modified oil-wet calcite at reservoir conditions

**Author:** Sarmad Al-Anssari, Muhammad Arif, Shaobin Wang, Ahmed Barifcani, Maxim Lebedev, Stefan Iglauer

**Publication:** Fuel

**Publisher:** Elsevier

**Date:** 1 January 2018

© 2017 Elsevier Ltd. All rights reserved.

Logged in as:  
Sarmad Al-Anssari  
Curtin university  
Account #:  
3001238667

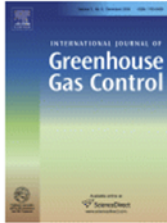
LOGOUT

Please note that, as the author of this Elsevier article, you retain the right to include it in a thesis or dissertation, provided it is not published commercially. Permission is not required, but please ensure that you reference the journal as the original source. For more information on this and on your other retained rights, please visit: <https://www.elsevier.com/about/our-business/policies/copyright#Author-rights>

BACK

CLOSE WINDOW

Copyright © 2018 Copyright Clearance Center, Inc. All Rights Reserved. [Privacy statement](#). [Terms and Conditions](#).  
Comments? We would like to hear from you. E-mail us at [customer@copyright.com](mailto:customer@copyright.com)



**Title:** CO2 geo-storage capacity enhancement via nanofluid priming  
**Author:** Sarmad Al-Anssari, Muhammad Arif, Shaobin Wang, Ahmed Barifcani, Maxim Lebedev, Stefan Iglauer  
**Publication:** International Journal of Greenhouse Gas Control  
**Publisher:** Elsevier  
**Date:** August 2017  
© 2017 Elsevier Ltd. All rights reserved.

Logged in as:  
Sarmad Al-Anssari  
Curtin university  
Account #:  
3001238667

LOGOUT

Please note that, as the author of this Elsevier article, you retain the right to include it in a thesis or dissertation, provided it is not published commercially. Permission is not required, but please ensure that you reference the journal as the original source. For more information on this and on your other retained rights, please visit: <https://www.elsevier.com/about/our-business/policies/copyright#Author-rights>

BACK

CLOSE WINDOW



**Title:** Stabilising nanofluids in saline environments  
**Author:** Sarmad Al-Anssari, Muhammad Arif, Shaobin Wang, Ahmed Barifcani, Stefan Iglauer  
**Publication:** Journal of Colloid and Interface Science  
**Publisher:** Elsevier  
**Date:** 15 December 2017

© 2017 Elsevier Inc. All rights reserved.

Logged in as:  
Sarmad Al-Anssari  
Curtin university  
Account #:  
3001238667

LOGOUT

Please note that, as the author of this Elsevier article, you retain the right to include it in a thesis or dissertation, provided it is not published commercially. Permission is not required, but please ensure that you reference the journal as the original source. For more information on this and on your other retained rights, please visit: <https://www.elsevier.com/about/our-business/policies/copyright#Author-rights>

BACK

CLOSE WINDOW

Copyright © 2018 Copyright Clearance Center, Inc. All Rights Reserved. [Privacy statement](#). [Terms and Conditions](#).  
Comments? We would like to hear from you. E-mail us at [customercare@copyright.com](mailto:customercare@copyright.com)